2013

Optimizing Light Requirements and Dilution Rates for Maximizing Algal Cell Growth and Lipid Content for Biofuel Feedstock Production

Beatrice Gabriela Terigar
Louisiana State University and Agricultural and Mechanical College, beatrice.terigar@gmail.com

OPTIMIZING LIGHT REQUIREMENTS AND DILUTION RATES FOR MAXIMIZING ALGAL CELL GROWTH AND LIPID CONTENT FOR BIOFUEL FEEDSTOCK PRODUCTION

A Dissertation

Submitted to the Graduate Faculty of the
Louisiana State University and
Agricultural and Mechanical College
in partial fulfillment of the
requirements for the degree of
Doctor of Philosophy

in

The Interdepartmental Program
In Engineering Science

by
Beatrice Gabriela Terigar
B.S., Aurel Vlaicu University of Arad, Romania, 2007
M.S., Louisiana State University, 2009
August 2013

This dissertation is dedicated to the two people who raised me into the person I am today:

my mother and father.

Thank you for giving me the chance to prove and improve myself through all my walks of life.

ACKNOWLEDGMENTS

My greatest accumulation of gratitude is owed to Dr. Chandra S. Theegala, who directed this dissertation. His teaching, scholarship, service to students as well as to the academy, and capacity for compassionate guidance together are a model of professional and personal investment. Properly expressed, I will be thanking you for the rest of my life for believing in me.

I would also like to express my gratitude to all members of my dissertation committee, namely Dr. Barbara C. Benson of Civil Engineering at ULL, Dr. Ronald F. Malone of Civil & Environmental Engineering, Dr. Michael G. Benton of Chemical Engineering and Dr. Lawrence J. Rouse of Oceanography and Coastal Sciences for their assistance rendered to me. Their suggestions and comments helped improve the quality of this research.

To all the people from our research group and all student workers, for their help and assistance during this project, I express a very special thank you!

This is a major milestone in my life for which I wish to thank my parents, Iolanda and Gavril Terigar, and all my family. There is absolutely no way I could have done this without the unconditional love and unending encouragement and support, which pushed me through the difficult times.

Finally yet importantly, I would like to thank all those who contributed remotely for my success. Along the way, I have received additional encouragement and votes of confidence, and I am lucky to have many true friends by my side. The friendship that they have freely given me is one of the greatest sources of comfort in my life.

Thank you all for helping me grow to become the person I am today!

TABLE OF CONTENTS

LIST OF TABLES

LIST OF FIGURES

LIST OF ACRONYMS

ATP - adenosine triphosphate
Chl - chlorophyll

D1 - the 32-kDa reaction-center protein of PSII, encoded by the chloroplast *psb A* gene

D2 - the 34-kDa reaction-center protein of PSII, encoded by the chloroplast *psb D* gene

HRT – Hydraulic Retention Time (h)

I_0 - PAR surface intensity (μmol/s/m^2)

I_a – average PAR in the reactor (μmol/s/m^2)

I_{opt} – optimum PAR level in the reactor (μmol/s/m^2) that provides μ_{max}

I_z – PAR at depth z (μmol/s/m^2)

k_a – the culture attenuation coefficient (L/mg/cm)

k_d – decay rate in the reactor (day^{-1})

k_{max} – maximum decay rate (day^{-1})

k_s – PAR in the culture at 1/2 μ_{max}

D/L – dark to light ratio

NADPH - reduced form of nicotinamide adenine dinucleotide phosphate (NADP)

Pa – areal productivity (g/m^3/day)

PAR - Photosynthetic Active Radiation (μmol/s/m^2)

PPFFR - Photosynthetic Photon Flux Fluence Rate (μmol/s/m^2)

PSI- photosystem I;

PSII - photosystem II

Pv – volumetric productivity (g/m^3/day)

Q – flow rate (m^3/h)

TSS -Total Suspended Solids (mg/L)

V – volume (m^3)

X - culture biomass density (mg/L)

z – depth (cm)

μ – growth rate (d^{-1})

μ_{max} – the maximum specific growth rate (day^{-1})

ABSTRACT

There is a rapidly growing interest in the potential of microalgae as feedstock for the next generation of biofuels. The current study was designed to meet the following objectives: (1) Investigate the interdependence among cell density, biomass and lipid productivity to maximize feedstock production from outdoor cultures; (2) Investigate the effect of cycling high-intensity lights to identify optimum Dark:Light (D/L) ratios, which can be effectively used by researchers to maximize aerial biomass productivities; (3) Develop a deterministic model to simulate the biomass productivity in continuous-flow bioreactor at various hydraulic retention times.

Results indicated that variation in HRTs has a major bearing on biomass and lipid productivities. In general, higher net biomass productivity was achieved at shorter HRTs. However, the maximum net lipid productivity was achieved at longest retention time for all algal species studied. Upon stopping the media flow, the lipid concentrations increased at the expense of proteins and to a lesser degree on carbohydrates. The study also indicated that cultures closer to their physiological cell density limit divert the incident energy more towards lipid production.

Results from experiments targeted at the second objective indicated that enhancement of the photosynthetic utilization of high intensity light due to light modulation can be achieved. Both growth rates and cell concentrations reached their maximum values under medium light cycle ratio (4/1 D/L) and medium frequencies (6.4-25.6 Hz), and progressively decreased with further increase in D/L ratio and frequency. Light efficiency measurements based on chlorophyll content were interrelated with the cell concentrations and growth rates. Outdoor culture-cycling studies suggested that aerial productivities could be significantly maximized by increasing the culture volume or depth for a given light exposed area if an optimum D/L ratio is maintained.

A deterministic mass balance model was developed to simulate microalgal productivities in outdoor continuous-flow systems. The productivity models were comparable to actual experimental data and statistically validated. Higher biomass cell concentrations was achieved at longer HRTs and declined with shortening the HRTs. Maximum volumetric and areal production was achieved at the shorter, 6 h HRT, producing 125 $g/m^3 \cdot day$ and 43 $g/m^2 \cdot day$, respectively. Growth variations due to fluctuations in available average light intensities and biomass concentrations were also simulated, concluding that productivity is directly dependent on light availability and biomass concentrations in algal bioreactors.

CHAPTER 1
INTRODUCTION

1.1. Overview

Volatile oil prices observed from 2000 to the present have renewed interest in alternative fuels. In addition, mounting evidence of global climate change has raised concern over the carbon footprint of burning fossil fuels (Chisti, 2007). These reasons, coupled with the desire to reduce reliance on foreign oil imports and to improve energy security, have spurred research in and development of alternative fuels, especially for replacing crude oil products like diesel.

Oils and lipids from both edible and non-edible sources like soybeans, sunflowers, rapeseed, jatropha, Chinese tallow seed, animal fat, and greases have been widely investigated as potential biodiesel feedstock (Patil et al., 2009; Boldor et al., 2010; Morais et al., 2010; Terigar et al., 2010; Jain and Sharma, 2011; Hoekman et al., 2012). However, attaining the large quantities of these lipid feedstocks required to displace even a small portion of the current fossil fuel demand appears to be a herculean task. Some challenges include: seasonal growth variation, slow growth rate of many traditional oilseed plants, low aerial productivity rates, competition with edible oils, extensive and costly oil extraction processes, and availability of prime agricultural land.

Microalgae have been extensively researched as a feedstock source for a wide variety of applications such as aquaculture, food production, cosmetics, pharmaceuticals, agriculture, and for many environmental remediation purposes (Grima et al., 1994; Chisti, 2007; Gonzalez Lopez et al., 2010; Greenwell et al., 2010; Ahmad et al., 2011). Today, microalgal biodiesel (Ahmad et al., 2011) and biohydrogen (Akkerman et al., 2002) production, and CO_2 removal from flue gas (de Morais and Costa, 2007) are receiving particular attention. Use of microalgae as a

prospective bio-oil feedstock is attractive due to its potential high oil content and fast generation of biomass, which can be harvested frequently over a long period of time. A comparative analysis of microalgal oil production with that from different oilseed plants indicates that the former can achieve 9-300 times higher oil production rate per hectare per year if their oil content is about 30 % dry weight (dw), and 21-800 times higher production for 70 % dw oil content (Chisti, 2007).

The scalability of microalgae growth systems is a primary research topic in anticipation of the commercialization of microalgae-based biofuels. However, one of the challenges for this technology is achieving high oil content while maintaining exponential or high growth of the organisms. Efforts were made through the years to demonstrate the feasibility of large-scale cultivation of algae in open ponds through "The Aquatic Species Program," which started in 1978 but was later terminated in 1996 by the Department of Energy. Since then, extensive research in the private and academic sectors was reported, with the focus on maximizing biomass and lipid productivity. Although several technologies were optimized, it has become more and more obvious that outdoor continuous systems will more likely make this technology affordable (Miron et al., 2000; Molina et al., 2001; Chisti, 2007).

Design and operational factors that influence the overall productivity and net specific growth rate include culture depth, mixing rate (cell light/dark ratio and cycling frequency), dilution rate, and incident light intensity. Although these factors were previously investigated, the lack of consistency and parameters that do not directly apply to real-world applications for algal biomass production were used. Therefore, previous efforts could not fully describe algal growth and productivity performances under real, existing conditions.

Current research was developed in an attempt to address these productivity limitations by using parameters that reflect direct correlations with outdoor growth environments for high algal biomass productivity.

1.2. Objectives

The current study was designed to meet the following objectives:

(1) Determine the optimal dilution rates for maximizing the net biomass production and lipid yields in a continuous, outdoor system for three different microalgae species, *Nannochloris sp.,* *Selenastrum capricornutum*, and *Scenedesmus dimorphus*. This objective is presented in Chapter 3 of this thesis. It involved subjecting outdoor continuous-flow systems to four hydraulic retention times in order to investigate the biomass and lipid productivities, and growth rates inside the reactors. A two-phase growth strategy was also employed to identify compositional changes in the cell under nutrient deprivation.

(2) Investigate the effect of cycling high-intensity lights in order to maximize aerial biomass productivity of a representative alga, *Nannochloris* sp. This study is presented in Chapter 4. Algal reactors were exposed to intermittent light with lengths ranging from 5 ms to 7.5 s, and dark/light ratios ranging from 1:3 to 30:1 D/L. Essential D/L effects on biomass cell concentration, growth rate and light harvesting efficiency (in terms of chlorophyll) is presented. Furthermore, the results were validated for an outdoor, direct sunlight-receiving bioreactor.

(3) Develop a deterministic model to simulate the biomass productivity in an bioreactor operated under continuous-flow at various hydraulic retention times. Chapter 5 presents a deterministic model that describes and investigates the growth and productivities of outdoor continuous-flow bioreactors under light-limited conditions.

1.3. References

Ahmad, A.L., Yasin, N.H.M., Derek, C.J.C., Lim, J.K., 2011. Microalgae as a sustainable energy source for biodiesel production: A review. Renewable & Sustainable Energy Reviews 15(1), 584-593.

Akkerman, I., Janssen, M., Rocha, J., Wijffels, R.H., 2002. Photobiological hydrogen production: photochemical efficiency and bioreactor design. International Journal of Hydrogen Energy 27(11-12), 1195-1208.

Boldor, D., Kanitkar, A., Terigar, B.G., Leonard, C., Lima, M., Breitenbeck, G.A., 2010. Microwave Assisted Extraction of Biodiesel Feedstock from the Seeds of Invasive Chinese Tallow Tree. Environmental Science & Technology 44(10), 4019-4025.

Chisti, Y., 2007. Biodiesel from microalgae. Biotechnology Advances 25(3), 294-306.

de Morais, M.G., Costa, J.A.V., 2007. Biofixation of carbon dioxide by Spirulina sp and Scenedesmus obliquus cultivated in a three-stage serial tubular photobioreactor. Journal of Biotechnology 129(3), 439-445.

Gonzalez Lopez, C.V., Ceron Garcia, M.d.C., Acien Fernandez, F.G., Bustos, C.S., Chisti, Y., Fernandez Sevilla, J.M., 2010. Protein measurements of microalgal and cyanobacterial biomass. Bioresource Technology 101(19), 7587-7591.

Greenwell, H.C., Laurens, L.M.L., Shields, R.J., Lovitt, R.W., Flynn, K.J., 2010. Placing microalgae on the biofuels priority list: a review of the technological challenges. Journal of the Royal Society Interface 7(46), 703-726.

Grima, E.M., Medina, A.R., Gimenez, A.G., Perez, J.A.S., Camacho, F.G., Sanchez, J.L.G., 1994. Comparison between Extraction of Lipids and Fatty-Acids from Microalgal Biomass. Journal of the American Oil Chemists Society 71(9), 955-959.

Hoekman, S.K., Broch, A., Robbins, C., Ceniceros, E., Natarajan, M., 2012. Review of biodiesel composition, properties, and specifications. Renewable & Sustainable Energy Reviews 16(1), 143-169.

Jain, S., Sharma, M.P., 2011. Long term storage stability of Jatropha curcas biodiesel. Energy 36(8), 5409-5415.

Morais, S., Mata, T.M., Martins, A.A., Pinto, G.A., Costa, C.A.V., 2010. Simulation and life cycle assessment of process design alternatives for biodiesel production from waste vegetable oils. Journal of Cleaner Production 18(13), 1251-1259.

Patil, P.D., Gude, V.G., Deng, S.G., 2009. Biodiesel Production from Jatropha Curcas, Waste Cooking, and Camelina Sativa Oils. Industrial & Engineering Chemistry Research 48(24), 10850-10856.

Terigar, B.G., Balasubramanian, S., Lima, M., Boldor, D., 2010. Transesterification of Soybean and Rice Bran Oil with Ethanol in a Continuous-Flow Microwave-Assisted System: Yields, Quality, and Reaction Kinetics. Energy & Fuels 24, 6609-6615.

CHAPTER 2
BACKGROUND AND LITERATURE REVIEW

2.1. Overview

The scalability of microalgae growth systems is a primary research topic in anticipation of the commercialization of microalgae-based biofuels. However, one of the challenges for this technology is achieving high oil content while maintaining exponential or high growth of the organisms (Amaro et al., 2012). An optimal design for a bioreactor for mass microalgal cultivation is an important factor governing the overall photosynthetic productivity. The design and some of the operational factors that influence the overall productivity and net specific growth rate include: light availability, nutrient addition rate, temperature, and algal species. This work approaches optimizations for all these parameters, so a good understanding of these concepts and knowledge of some previous work is described.

2.2. Cultivation methods

Different cultivation systems for microalgal biomass production have been developed, tested and used in laboratories and on an industrial scale over the years. However, microalgal culture systems are mainly characterized as open or closed systems.

Open systems, ponds or raceways ponds, consist of independent closed-loop recirculation shallow channels between 15 and 50 cm deep and incorporate low energy-consuming paddlewheels for gas/liquid mixing and circulation (Jorquera et al., 2010). The concentration of algal biomass is typically 0.5–1.0 g/L (Chisti, 2007), and the typical surface area of operation is 200 ha for extensive ponds or 0.5 to 1 ha for raceway ponds (Pienkos and Darzins, 2009; Brennan and Owende, 2010). Open systems are preferable due to lower material and construction costs and because they require less maintenance due to their simplicity (Benemann

and Weissman, 1985). Furthermore, open systems take advantage of the free solar energy source and CO_2 availability, significantly reducing the energy and resource consumption. They also have a long material-built lifetime. However, factors that could reduce productivity, such as culture contamination with unwanted strains and environmental conditions like temperature and rain, must be addressed to achieve optimal productivity. The current major disadvantage of raceway ponds is that they need large land areas, and this can become an issue if they displace areas currently dedicated to food crops. Currently, open systems are typically used for commercial-scale operations for the cultivation of microalgae and cyanobacteria, such as *Chlorella sp*., *Nannochloropsis*, *Dunaliella salina* and *Pleurochrysis carterae*, among others (Moreno et al., 2003; Moheimani and Borowitzka, 2006; Radmann et al., 2007).

Closed systems, also known as photobioreactors (PBRs), are currently designed in a variety of configurations, like tubular, flat panel and column photobioreactors (Eriksen, 2008). Most of the research carried out in photobioreactors is designed to overcome the major problems encountered with the open pond production systems, and has been carried out under artificial or natural lighting (Janssen et al., 2003). Tubes can be configured horizontally (Carlozzi and Torzillo, 1996; Molina et al., 2001), vertically (Miyamoto et al., 1988; Converti et al., 2006), inclined (Vunjak-Novakovic et al., 2005), or as a helix (Fernandez et al., 2003; Hall et al., 2003; Jiang and Zhu, 2010), while mechanical pumps or airlifts create the pumping force (Camacho et al., 1999; Miron et al., 2000; Fernandes et al., 2010). Typically, photobioreactors showed higher concentrations of algal biomass (between 5-15 g/L) than open ponds, with better capture of radiant energy, more optimal use of the cultivated area, and easier operational control (Tredici and Zittelli, 1998; Evens et al., 2000; Wijanarko et al., 2008).

Although photobioreactors are often considered the most suitable for commercial large-scale cultures of microalgae, the length of the tubes are limited by O_2 accumulation, CO_2 depletion, and pH control (Chisti, 2007). Therefore, photobioreactors cannot be scaled up infinitely, and large-scale production plants rely on multiplication of the reactor units (Janssen et al., 2003). The design failures of industrial-scale photobioreactors have been well described by Tredici (Tredici and Zittelli, 1998). The comparative energy life-cycle analyses (Jorquera et al., 2010; Dassey, 2013; Dassey et al., 2013) made it clear that the use of photobioreactors for biomass production becomes unfavorable when additional energy costs (such as those required for concentrating the microalgae from the culture medium and oil extraction) are considered, showing a smaller return of investment (ROI) compared to the open raceways for both biomass and oil production. It is becoming more and more obvious that the growth and harvest processes need better integration and synergies in order to make this technology affordable.

2.3. Light utilization

As with plants, light is the source of energy that drives photosynthetic reactions. Light intensity plays an important role, but requirements greatly vary with the culture depth and the density of the algal culture. Light intensity must be increased with higher depths and cell concentrations in order for light to penetrate through the entire culture; whereas high light intensity might result in photoinhibition. Photoinhibition of photosynthesis is caused by an excess of excitation energy due to increased light levels, or if the activity of the Calvin cycle and other energy-dissipative mechanisms (e.g. photorespiration) are diminished by unfavorable environmental conditions (Kyle et al., 1987).

Light in bioreactors is usually represented in terms of photosynthetically active radiation (PAR) (scalar or incident) and is expressed as the radiant energy (400-700 nm) incident on a unit

of surface per time, internationally expressed in moles of photons per unit time and per unit area ($\mu mol/s/m^2$), where 1μmol corresponds to 1 micromole of photons, that is, 6.02 x 10^{17} photons, at a given wavelength (Barsanti and Gualtieri, 2005). This is the fraction of the solar radiation spectrum that contains the appropriate wavelengths of light used in photosynthesis. The PAR range covers the visible spectrum of light, which includes red (700–635 nm), orange (635–590 nm), yellow (590–560 nm), green (560–490 nm), blue (490–450 nm), and violet (450–400 nm) wavelengths. However, not all of PAR wavelengths are used in photosynthesis. Plants obtain the majority of light energy from the red, blue, and violet portions of the spectrum because these wavelengths are the most readily absorbed by light-harvesting pigments (chlorophylls, carotenoid and xanthophyll) (Larkum et al., 2003). Different pigments absorb light energy at different wavelengths. All chlorophylls have two major absorption bands: blue or blue-green (430-475 nm) and red (630-675 nm), and reflect green light strongly, so they appear green to the human eye. Carotenoids and xanthophylls (oxidized carotenoids) absorb light maximally between 400 nm and 550 nm and appear red, orange, or yellow (Masojidek et al., 2004).

Overall, the solar energy absorbed by photosynthetic pigments is converted into the chemical energy of biomass. The reaction can be simply described as:

$$CO_2 + H_2O + \text{sunlight} \rightarrow CH_2O + O_2 + \text{waste heat} \qquad \text{(Eq. 2.1)}$$

Where, CH_2O represents a nominal carbohydrate molecule, the immediate end product of photosynthesis. The initial products of CO_2 fixation – sugars – are later converted to a selection of secondary products, like structural (cellulose) or energy-storage polymers (starch and fats) and functional molecules (enzymes, DNA, RNA, pigments, phospholipids) that are necessary for cell growth (Larkum et al., 2003).

Photosynthesis is also a redox reaction in which electrons are transferred from water to CO_2 (CO_2, the electron acceptor, is reduced, and water, the electron donor, is oxidized). Electron transfer occurs against the electrochemical gradient, and so the reaction is endothermic and requires a source of energy (light) to proceed (Barsanti and Gualtieri, 2005). Chlorophyll molecules initiate the photochemical reactions and have a double function: as light absorbers and, in the excited state, as sources of electrons. Special chlorophylls absorb light and eject strongly reducing electrons that are then transferred by several electron carriers to a final acceptor, NADP. The pigments are thus oxidized, and NADP is reduced to NADPH. The photo-oxidized chlorophyll is very reactive, forcing a molecule of water to split and the electron deficiency in the chlorophyll molecule to be replenished by water oxidation. The light-driven electron transport in the photosynthetic membrane also generates ATP, which, together with NADPH, is then used in the so-called dark reactions of the Calvin–Benson cycle to fix (reduce) CO_2 (Falkowski and Raven, 2007). During the cycle, 18 ATP and 12 NADPH molecules are required for every six molecules of CO_2 converted to one molecule of glucose. According to the now widely accepted "Z-scheme" of photosynthesis (which describes the oxidation/reduction changes during the light reactions of photosynthesis), first proposed in 1960 (Hill and Bendall, 1960), two different photochemical systems (containing special chlorophylls in the reaction center and several molecules of antenna pigments), are responsible for the electron transfer reactions from water to NADP: photosystem II (PSII) and photosystem I (PSI). These two systems operate in series, with several membrane and soluble complexes and molecules acting as intermediate carriers. Thus, two photons are necessary (one absorbed by PSII and one by PSI) to move one electron from water to NADP. Since the formation of one molecule of NADPH requires two electrons and, consequently, four photons to obtain the two moles of NADPH necessary to fix

one mole of CO_2, a minimum of eight moles of photons are required (Larkum et al., 2003). The absorption of eight photons also leads to the accumulation of 12 protons in the chloroplast lumen. With four protons required for the synthesis of one ATP, this is just sufficient to synthesize the three ATP necessary, together with the two NADPH, for reduction of one molecule of CO_2 to its sugar equivalent (CH_2O) in the Calvin cycle (Pessarakli, 1996).

The PSI and PSII complexes contain an internal antenna domain carrying light-harvesting chlorophylls and carotenoids, both non-covalently bound to a protein and a central core domain where biochemical reactions take place (Barsanti and Gualtieri, 2005). In the internal antenna complexes, chlorophylls do most of the light harvesting, while the carotenoids and other pigments (xanthophylls) mainly protect against excess light and possibly transfer the absorbed radiation (Seyedeh Fatemeh et al., 2012). PSI and PSII form a super complex because they are associated with an external antenna, called light-harvesting complex (LHC), whose main function is the absorption of solar radiation and the efficient transmission of excitation energy toward reaction center chlorophylls (Larkum et al., 2003).

Chlorophyll (Chl) molecules harvest light energy and drive electron transfer, thus playing a central role in photosynthesis (Nelson and Yocum, 2006). Chlorophyll is actively synthesized during the growth process when the photosynthetic apparatuses are formed and binds to proteins to form various Chl protein complexes. These complexes and subunit proteins assemble stoichiometrically to form photosystems, although the detailed mechanisms have not yet been elucidated (Osawa and Aiba, 1982; Shimoda et al., 2012). The photosynthetic coloration of algae led to the discovery and characterization of Chls. Thus, red algae are characterized by the presence of only Chl a; green algae are characterized by the presence of Chl a and b and a suite of characteristic carotenoids; brown algae are characterized by the presence of Chl a and Chl c

(Larkum et al., 2003). While it is known that Chl a is the principal and indispensable photochemically active pigment for the photochemistry in oxygenic photosynthetic organisms, the presence of Chl b in green algae is still under debate. It is believed that Chl b is a light-gathering efficiency enhancer (Satoh et al., 2001) because the absorption spectrum of Chl b (around 450 and 650) is different from that of Chl a (429 nm) (Satoh et al., 2001). This would enable the cells to harvest a wider range of light. Other studies suggest that Chl b is tightly linked with the turnover of LHC and that the metabolism of Chl b forms an essential part of light-acclimation mechanisms (Tanaka and Tanaka, 2011).

The amount and composition of the Chl protein complexes is variable in thylakoids and depend on the incident irradiance during plant growth. Photosynthetic organisms acclimate to the level of irradiance by adjusting the size of the antenna associated with each photosystem (Tanaka and Melis, 1997). In PSII, the Chl a-b light-harvesting complex (LHCII) is primarily responsible for the process of light absorption. Usually, when algae are grown under low light intensity, PSII contains large LHCII antennas and displays a low Chl a/Chl b ratio and a high LHCII to PSII core ratio. When grown under high light intensity, PSII contains a small LHCII antenna, and it displays a high Chl a/Chl b ratio and a low LHCII to PSII core ratio (Wood, 1979; Tanaka and Melis, 1997; Yang et al., 1998). Previous work has demonstrated that Chl antenna size of green algae such as *Chlorella vulgaris (*Ley and Mauzerall, 1982; Maxwell et al., 1987)*, Dunaliella salina* (Smith et al., 1990) and *Chlamydomonas reinhardtii* (Melis et al., 1996) were usually malleable, and that under high-light growth, the Chl antenna size was significantly smaller than that under low light.

The transient formation of strong oxidants, the abundance of oxygen, and exposure to high rates of excitation energy can lead to photo-oxidative damage. Such photodamage occurs

frequently within the reactor center of PSII, causing irreversible inhibition in the electron - transport function of the reactor center chlorophyll (P680) in the D1 protein and stops phohosynthesis (Melis, 1991; Hortensteiner and Krautler, 2011). However, an elaborate repair mechanism operates in organisms of oxygenic photosynthesis and restores the functional status of PSII. This phenomenon, known as the PSII damage and repair cycle (Guenther et al., 1990), operates in synergy with photosynthesis and appears to be conserved in cyanobacteria, algae, and crop plants (Park et al., 2007). A schematic sequence of events in PSII is presented in Fig. 2.1.

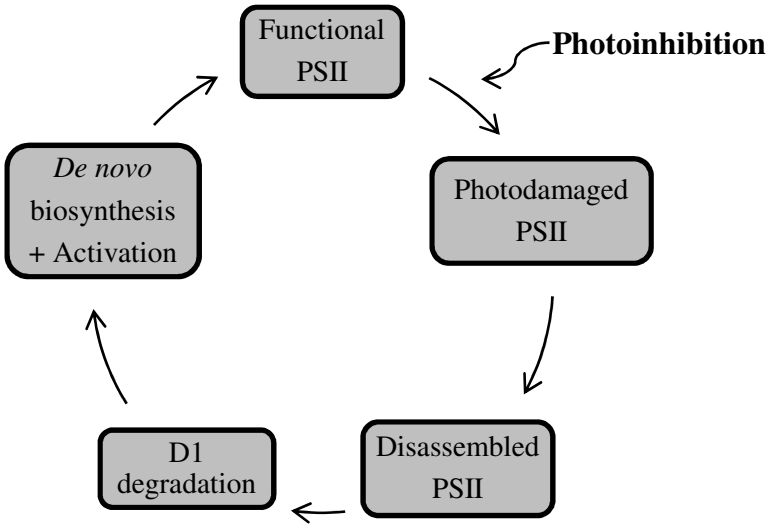

Figure 2.1. Photoinhibition of photosystem II (PSII) leads to loss of PSII electron transfer activity. PSII is continuously repaired via degradation and synthesis of the D1 protein. Adapted from Park et al., 2007.

In broad terms, photodamage to D1 is followed by prompt, partial disassembly of the PSII complex; exposure of the photodamaged PSII core to the stroma of the chloroplast; degradation of photodamaged D1; *de novo* biosynthesis and insertion in the thylakoid membrane; and reassembly of the PSII complex, followed by activation of the electron-transport process through the reconstituted D1/D2 heterodimer (Aro et al., 1993; Melis, 1999; Yokthongwattana et al., 2001; Park et al., 2007). There is a dynamic relationship between photodamage and repair,

which will define whether there is an adverse effect on photosynthesis. Whenever the rate of photodamage exceeds the capacity of chloroplast repair, the productivity of the photosynthetic apparatus declines and plant growth diminishes (Baroli and Melis, 1996; Raven, 2011).

2.4. Growth under circulation-induced intermittent lighting

Algal cultures in bioreactors can reach high optical densities, which leads to significant light attenuation. As a consequence, surface-exposed cells absorb most of the light, leaving only a residual part of the radiation for the cells underneath, which become limited in their growth. The surface layers that are exposed to excess light become very susceptible to photoinhibition; therefore, they must thermally dissipate up to 80% of their photons in order to avoid radiation damage. This greatly reduces their light-use efficiency (Sforza et al., 2012).

Several concepts were developed in trying to diminish this loss in efficiency. It has been shown that the overall efficiency of photobioreactors increases when the light path is diminished, reducing the inhomogeneity of light distribution (Richmond et al., 2003). However, very short light paths are difficult to implement in large-scale bioreactors due to practical and economic reasons. Another approach considered for lowering photoinhibition was rapidly mixing and moving the cells from darkness to full sunlight. These mixing cycles vary according to the cultivation system, and mixing rates of different time scales can be achieved (Carvalho et al., 2011). This idea led to research on light/dark periods (ratios) during active photosynthesis.

Alternation of light/dark periods has been suggested to be beneficial in terms of photosynthetic efficiency (Phillips and Myers, 1954; Nedbal et al., 1996; Kim et al., 2006; Grobbelaar, 2010; Xue et al., 2011). Multiple set-ups for measuring the efficiencies were also adopted, most of them including very small bioreactors (30 ml-60 ml) (Xue et al., 2011) and extremely sophisticated and uneconomical turbidostats (Merchuk et al., 1998; Janssen et al.,

1999; Janssen et al., 2000), and utilizing light emitting diodes (LED) systems as a light source (Lee and Palsson, 1994; Grobbelaar et al., 1996; Nedbal et al., 1996; Katsuda et al., 2006). However, a majority of the LED systems failed to approach the high light intensities of solar radiation. Only a few studies were found in which the light intensities reported potentially approached the solar intensity (Janssen et al., 2001; Kim et al., 2006; Sforza et al., 2012). The major issue in using LEDs as light source is their life span. Overdriving an LED light will increase the luminous output, but dramatically decrease life span if thermal management is not considered. Also, an LED is said to have reached the end of its life when its light output reaches 50% of the rated luminous output, not necessarily when it reaches zero. Therefore, not replacing an LED in a timely fashion can contribute to inaccuracies when measuring light intensities.

Experiments reported in the literature focused on very different ranges of flash frequencies and light intensities. Frequencies ranging from 100 Hz-1 kHz and light intensities varying from as low as 10 μmol/s/m^2 to 1200 μmol/s/m^2 make a complete comparison of results difficult. In earlier studies, most frequently, the D/L frequencies implemented were either too low (<0.1 Hz) or too high (>150 Hz) (Grobbelaar et al., 1996; Nedbal et al., 1996; Yoon et al., 2008; Marshall and Huang, 2010; Xue et al., 2011). Only a few studies focused more on medium D/L frequencies (Grobbelaar et al., 1992; Janssen et al., 2000). Moreover, the light intensities applied were much lower than that received from full sunlight during summer days (Merchuk et al., 1998; Janssen et al., 1999; Janssen et al., 2000; Park and Lee, 2000; Yoshimoto et al., 2005; Katsuda et al., 2006; Jiang and Zhu, 2010) and at randomly selected D/L ratios. It has been shown that faster mixing rates of algal cultures increases the yield of biomass on light energy (Laws et al., 1983; Hu and Richmond, 1996). The duration of the D/L cycles in these studies was in the range of 0.2-1 s in reactors developed with a short light path and fast mixing rates

provided by intense aeration. The influence of medium-duration D/L cycles is not clear. In short-term oxygen evolution experiments for *Chlorella* and *Scenedesmus,* no influence of fluctuating light of equal time-average irradiance (1-0.0038 Hz, 1-263 s cycle duration) was found on specific oxygen production and carbon fixation (Grobbelaar, 1991; Grobbelaar et al., 1992). These results were observed under light intensities oscillating from 10-750 μmol/s/m^2. Others observed a decrease in the specific growth rate of *Chlamydomonas, Oocystis, Dunaliella, Chlorella* and *Scenedesmus* at frequencies of 0.2-0.1 Hz (5-10 s cycles) in comparison with continuous illumination of the same time-average irradiance (at 630 μmol/s/m^2) (Nedbal et al., 1996; Janssen et al., 1999). On the contrary, evidence has been presented suggesting that cells were able to store enough ATP and reducing power to sustain maximal growth for 6 and 9 seconds in darkness (Pirt, 1986; Merchuk et al., 1998). Thus, previous efforts could not fully describe the growth and productivity performances under solar radiation conditions. This is essential, since most commercial bioreactors with high productivities are operated outdoors under natural lighting.

Very often it has been stated that at photo flux densities higher than 500 μmol/s/m^2, where photosaturation is believed to start, the probability of photodamage will increase and will result in a reduction of the photosynthetic capacity and efficiency (Melis, 1999). However, Richmond (Richmond, 2000) suggested that the photosynthetic rate vs. irradiance response curve, also called the PI curve, developed over the years (Goldman, 1980; Kirk, 1983) is very misleading (Fig. 2.2). The PI curve plays a central role in measuring, modeling, and predicting algal photosynthesis, and assessing both intra and interspecific variations in photosynthetic physiology. The PI curve represents a typical growth response to light, similar to the growth response to substrate availability. First, the initial rate of response to increased light availability

is highest (P_m), followed by a decrease signifying the initiation of the saturation process. Finally, there is no more net response with the photosynthetic machinery of the cells having become fully light saturated (E_k, saturating irradiance). If the light flux were to increase much above saturation, becoming excessive, photoinhibition would become evidently leading, if prolonged, to culture deterioration (Larkum et al., 2003) phenomenon termed light saturation or light photoinhibition. The plot also considers the relationship between the efficiency by which light is utilized in the cell. The efficiency (P/E_d on plot) is highest at very low light, decreasing as soon as the flux increases. At strong light, e.g. sunlight at midday, efficiency becomes 20% or less of its efficiency at low light. This information, utilized by a majority of researchers in measuring the light efficiency during different light intensities, is only valid for optically thin cultures where no mutual shading occurs and all cells receive light continuously. This situation is non-existent in mass cultures where cells receive light intermittently due to mixing, which would be the most practical way by which to dilute strong light, ensuring effective use of light by the culture (Richmond et al., 2003).

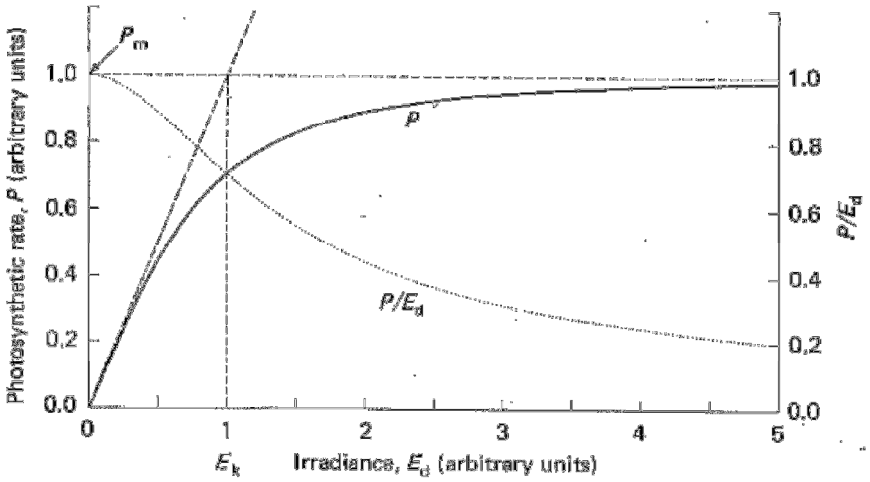

Figure 2.2. Idealized curve of specific photosynthetic rate (P) as a function of irradiance (Ed), illustrating the maximum photosynthetic rate (Pm) and the saturation onset parameter (Ek). The variation of P/Ed (a measure of the efficiency of utilization of incident light) with irradiance value is also indicated. (From Kirk, 1983).

Intermittent illumination, which results in diluted light for the average cell, is, therefore, mandatory for effective utilization of strong light, which can be maximized by optimizing the light regime of the reactor. The light intermittence is thus associated with the ratio between the light and the dark period in the cycle, the frequency of the D/L cycle, and the lengths of the light and that of the dark periods in a cycle.

2.5. Light-limited models

Mathematical modeling is a useful tool for design and optimization of bioprocesses. Developing a fundamental understanding of light dynamics within any reactor is critical to the proper establishment of design and operating criteria.

The light cannot be assumed to be distributed homogeneously along the depth of a reactor due to self-shading, which causes the incident light to be progressively dissipated as it passes through the culture. In moderate density cultures (<1000 mg/L biomass concentration), the irradiance at a given depth in a reactor can be calculated for a specified surface intensity using the Lambert-Beer Law (Camacho et al., 1999; Evens et al., 2000). Irradiance at any depth is a function of the intensity at the surface, multiplied by the antilog of the negative extinction coefficient at that depth:

$$I_z = I_0 e^{-k_c z} \qquad \text{(Eq. 2.2)}$$

where: I_z= PAR (μmol/s/m^2) at z depth

I_0 = the PAR surface intensity (μmol/s/m^2)

k_c = light attenuation coefficient (cm^{-1})

z = depth (cm)

The depth-integrated light I_a as a function of I_0 and biomass X (mg/L), can be calculated by integrating the Lambert-Beer equation (Eq. 2.3) over the depth of the reactor (d):

$$I_a = \frac{1}{d}\int_0^d I_z dz = \frac{I_0}{k_a X d}\left(1 - e^{-k_a X d}\right) \quad \text{(Eq. 2.3)}$$

where, Ia = average PAR (μmol/s/m^2) and k_a = the culture attenuation coefficient (L/mg/cm).

The mathematical model determines the distance travelled by an incident ray of light to any point inside the culture and estimates the local irradiance, taking into account the light attenuation due to biomass.

Since the photosynthetic process is photochemical in nature, it can be assumed that the photosynthetic growth is proportional to the amount of light energy absorbed by each cell (Ogbonna et al., 1995). Only a part of the absorbed energy is used for growth, while the rest is either lost (as heat energy, etc.) or used for cell maintenance and other non-growth related metabolic activities. Some classic growth models such as that of Monod (Eq. 2.4) are based on the specific growth rate and, consequently, in most of the growth kinetics and photosynthetic cell growth models, the specific growth rates during the exponential growth phase are used as growth parameters.

$$\mu = \mu_{max}\frac{I_a}{k_s + I_a} \quad \text{(Eq. 2.4)}$$

where: μ_{max} = the maximum specific growth rate (h^{-1})

μ = growth rate (h^{-1})

k_s = average PAR in the culture at 1/2 μ_{max} (μmol/s/m^2)

In an optimal system, where no other factors (temperature, nutrient addition rate, pH) are limiting, the light availability determines the rate of photosynthesis and productivity. However, as described in the previous subchapter, excessive light can be harmful and is known to produce

a photoinhibitory response. In continuous cultures, as typically used for microalgae, the biomass productivity is a function of the cell concentration and dilution rate (Grima et al., 1999). At steady state, the dilution rate equals the specific growth rate, which is governed by the amount of light, the rate controlling factor.

Many researchers have suggested various kinds of mathematical models of algal growth kinetics and/or photosynthesis over the years (Steele, 1965; Bannister, 1979; Aiba, 1982; Evers, 1991; Grima et al., 1994; Prokop et al., 1995; Fernandez et al., 1997; Rubio et al., 2003). The difference among these models is the fundamental hypotheses of the models based upon the expression of the light dependence of microalgal photosynthesis. In some models, the algal photosynthesis is assumed to be dependent on the average photon flux density obtained by volume-averaging the spatial distributed photon flux density inside the photobioreactor (Grima et al., 1994; Prokop et al., 1995). This implies that the average photon flux density could be a representative value of spatially distributed density within the reactor. Other models suggest a linear relationship between the average photon absorption rate by the whole algal culture and the specific growth rate, suggesting the use of averaged photon absorption rate for the kinetic analysis of microalgal culture (Aiba, 1982). However, Iehana (Iehana, 1983; Iehana, 1990) revealed non-linearity in this relationship at high concentrations. Therefore, the Monod-type expression suggested by Iehana would be a more adequate approach, able to cover a wide range of cell concentrations. Other models are based on more sophisticated theories that individual algal cells respond to the photon flux density at their local position (Evers, 1991; Cornet et al., 1992; Cornet et al., 1992). Table 2.1 presents the most popular growth models used in literature.

These models have μ as either a monotone increasing function of the incident intensity or a hyperbola-shaped relationship between μ and average intensity. The hyperbola function model

is usually used in high self-shading cultures where the relationship between μ and average intensity becomes very broad (Fernandez et al., 1997; Benson, 2003). Some exponential models have also been reported as the best description of growth as well (Cornet et al., 1992). Steel's model (Steele, 1965) is an exponential peak-shaped function that accounts for inhibition of growth at high light intensities (Fredrickson and Tsuchiya, 1977).

$$\mu = \mu_{max} \frac{I_a}{I_{opt}} e^{1 - \frac{I_a}{I_{opt}}} \quad \text{(Eq. 2.5)}$$

where: I_{opt} = the PPFFR at which μ achieves its maximum value.

Statistical comparison of the majority of the equations from Table 2.1 found that Steel and Molina Grima et al.'s models had a better accuracy in describing the growth kinetics (Grima et al., 1996; Yun and Park, 2003).

Table 2.1. Models for light-dependent specific growth rate

Equation	Reference
$\mu = \frac{\alpha \mu_{max} I}{\mu_{max} + \alpha I}$	(Tamiya et al., 1953)
$\mu = \mu_{max}(1 - e^{-\frac{I}{I_{max}}})$	(Van Oorschot, 1995)
$\mu = \mu_{max} \frac{I}{I_{opt}} e^{1-\frac{I}{I_{opt}}}$	(Steele, 1965)
$\mu = \frac{\mu_{max} I}{(K_i^n + I^n)^{\frac{1}{n}}}$	(Bannister, 1979)
$\mu = \frac{\mu_{max} I}{K_s + I + \frac{I^2}{K_i}}$	(Aiba, 1982)
$\mu = \frac{\mu_{max} I^n}{k_s^n + I^n}$	(Grima et al., 1994)

n = ratio I_0/I_a; K_i = photoinhibition factor; α = fitting parameter.

2.6. References

Aiba, S., 1982. Growth kinetics pf photosynthetic microorganisms. Advanced Biochemical Engineering 23, 85-156.

Amaro, H.M., Macedo, A.C., Malcata, F.X., 2012. Microalgae: An alternative as sustainable source of biofuels? Energy 44(1), 158-166.

Aro, E.M., Virgin, I., Andersson, B., 1993. Photoinhibition of Photosystem-2 - Inactivation, Protein Damage and Turnover. Biochimica et Biophysica Acta 1143(2), 113-134.

Bannister, T.T., 1979. Quantitative Description of Steady-State, Nutrient-Saturated Algal Growth, Including Adaptation. Limnology and Oceanography 24(1), 76-96.

Baroli, I., Melis, A., 1996. Photoinhibition and repair in Dunaliella salina acclimated to different growth irradiances. Planta (Heidelberg) 198(4), 640-646.

Barsanti, L., Gualtieri, P., 2005. Algae. Anatomy, Biochemistry, and Biotechnology. Taylor and Francis Group. Boca Raton, Fl.

Benemann, J.R., Weissman, J.C., 1985. Productivity of Microalgae Cultures in Outdoor Systems. Abstracts of Papers of the American Chemical Society 190(Sep), 147-MBD.

Benson, B., 2003. Optimization of the light dynamics in the hydraulically integrated serial turbidostat algal reactor (HISTAR). PhD Dissertation, Department of Civil and Environmental Engineering, Louisiana State University, Baton Rouge, LA.

Brennan, L., Owende, P., 2010. Biofuels from microalgae-A review of technologies for production, processing, and extractions of biofuels and co-products. Renewable & Sustainable Energy Reviews 14(2), 557-577.

Camacho, F.G., Gomez, A.C., Fernandez, F.G.A., Sevilla, J.F., Grima, E.M., 1999. Use of concentric-tube airlift photobioreactors for microalgal outdoor mass cultures. Enzyme and Microbial Technology 24(3-4), 164-172.

Carlozzi, P., Torzillo, G., 1996. Productivity of Spirulina in a strongly curved outdoor tubular photobioreactor. Applied Microbiology and Biotechnology 45(1-2), 18-23.

Carvalho, A.P., Silva, S.O., Baptista, J.M., Malcata, F.X., 2011. Light requirements in microalgal photobioreactors: an overview of biophotonic aspects. Applied Microbiology and Biotechnology 89(5), 1275-1288.

Chisti, Y., 2007. Biodiesel from microalgae. Biotechnology Advances 25(3), 294-306.

Converti, A., Lodi, A., Del Borghi, A., Solisio, C., 2006. Cultivation of Spirulina platensis in a combined airlift-tubular reactor system. Biochemical Engineering Journal 32(1), 13-18.

Cornet, J.F., Dussap, C.G., Cluzel, P., Dubertret, G., 1992. A Structured Model for Simulation of Cultures of the Cyanobacterium Spirulina-Platensis in Photobioreactors .2. Identification of Kinetic-Parameters under Light and Mineral Limitations. Biotechnology and Bioengineering 40(7), 826-834.

Cornet, J.F., Dussap, C.G., Dubertret, G., 1992. A Structured Model for Simulation of Cultures of the Cyanobacterium Spirulina-Platensis in Photobioreactors .1. Coupling between Light Transfer and Growth-Kinetics. Biotechnology and Bioengineering 40(7), 817-825.

Dassey, A.J., 2013. Designing a cost effective microalgae harvesting strategy for biodiesel production with electrofloculation and dissolved air flotation. PhD Dissertation, Department of Engineering Science, Louisiana State University, Baton Rouge, LA.

Dassey, A.J., Hall, S.G., Theegala, C.S. Algae biodiesel life cycle analysis for Louisiana: comparing literarture with current work. Submitted to Algal Research Journal.

Eriksen, N.T., 2008. The technology of microalgal culturing. Biotechnology Letters 30(9), 1525-1536.

Evens, T.J., Chapman, D.J., Robbins, R.A., D'Asaro, E.A., 2000. An analytical flat-plate photobioreactor with a spectrally attenuated light source for the incubation of phytoplankton under dynamic light regimes. Hydrobiologia 434(1-3), 55-62.

Evers, E.G., 1991. A model for light-limited continuous cultures - growth, shading, and maintenance. Biotechnology and Bioengineering 38(3), 254-259.

Falkowski, P.G., Raven, J.A., 2007. Aquatic photosynthesis. Princeton University Press.

Fernandes, B.D., Dragone, G.M., Teixeira, J.A., Vicente, A.A., 2010. Light Regime Characterization in an Airlift Photobioreactor for Production of Microalgae with High Starch Content. Applied Biochemistry and Biotechnology 161(1-8), 218-226.

Fernandez, F.G.A., Camacho, F.G., Perez, J.A.S., Sevilla, J.M.F., Grima, E.M., 1997. A model for light distribution and average solar irradiance inside outdoor tubular photobioreactors for the microalgal mass culture. Biotechnology and Bioengineering 55(5), 701-714.

Fernandez, F.G.A., Hall, D.O., Guerrero, E.C., Rao, K.K., Grima, E.M., 2003. Outdoor production of Phaeodactylum tricornutum biomass in a helical reactor. Journal of Biotechnology 103(2), 137-152.

Fredrickson, A.G., Tsuchiya, H.M. 1977, Microbial kinetics and dynamics. Chemical Reactor Theory. Lapidus, L., Amundson, N. Englewood Cliffs, NJ, Prentice-Hall**:** 405-483.

Goldman, J.C. 1980, Physiological aspects in algal mass cultures. Algae biomass. G, S., J., S.C., Elsevier/North-Holland Biomedical Press**:** 343-360.

Grima, E.M., Camacho, F.G., Perez, J.A.S., Sevilla, J.M.F., Fernandez, F.G.A., Gomez, A.C., 1994. A Mathematical-Model of Microalgal Growth in Light-Limited Chemostat Culture. Journal of Chemical Technology and Biotechnology 61(2), 167-173.

Grima, E.M., Fernandez, F.G.A., Camacho, F.G., Chisti, Y., 1999. Photobioreactors: light regime, mass transfer, and scaleup. Journal of Biotechnology 70(1-3), 231-247.

Grima, E.M., Sevilla, J.M.F., Perez, J.A.S., Camacho, F.G., 1996. A study on simultaneous photolimitation and photoinhibition in dense microalgal cultures taking into account incident and averaged irradiances. Journal of Biotechnology 45(1), 59-69.

Grobbelaar, J.U., 1991. The influence of light dark cycles in mixed algal cultures on their productivity Bioresource Technology 38(2-3), 189-194.

Grobbelaar, J.U., 2010. Microalgal biomass production: challenges and realities. Photosynthesis Research 106(1-2), 135-144.

Grobbelaar, J.U., Kroon, B.M.A., Burgerwiersma, T., Mur, L.R., 1992. Influence of medium frequency light dark cycles of equal duration on the photosynthesis and respiration of chlorella-pyrenoidosa. Hydrobiologia 238, 53-62.

Grobbelaar, J.U., Nedbal, L., Tichy, V., 1996. Influence of high frequency light/dark fluctuations on photosynthetic characteristics of microalgae photoacclimated to different light intensities and implications for mass algal cultivation. Journal of Applied Phycology 8(4-5), 335-343.

Guenther, J.E., Nemson, J.A., Melis, A., 1990. Development of Photosystem-Ii in Dark-Grown Chlamydomonas-Reinhardtii - a Light-Dependent Conversion of Ps-Ii-Beta, Qb-Nonreducing Centers to the Ps-Ii-Alpha, Qb-Reducing Form. Photosynthesis Research 24(1), 35-46.

Hall, D.O., Fernandez, F.G.A., Guerrero, E.C., Rao, K.K., Grima, E.M., 2003. Outdoor helical tubular photobioreactors for microalgal production: Modeling of fluid-dynamics and mass transfer and assessment of biomass productivity. Biotechnology and Bioengineering 82(1), 62-73.

Hill, R., Bendall, F.A.Y., 1960. Function of the Two Cytochrome Components in Chloroplasts: A Working Hypothesis. Nature 186(4719), 136.

Hortensteiner, S., Krautler, B., 2011. Chlorophyll breakdown in higher plants. Biochimica et Biophysica Acta 1807(8), 977-988.

Hu, Q., Richmond, A., 1996. Productivity and photosynthetic efficiency of Spirulina platensis as affected by light intensity, algal density and rate of mixing in a flat plate photobioreactor. Journal of Applied Phycology 8(2), 139-145.

Iehana, M., 1983. Kinetic-Analysis of the Growth of Spirulina Sp on Continuous Culture. Journal of Fermentation Technology 61(5), 457-466.

Iehana, M., 1990. Kinetic-Analysis of the Growth of Chlorella-Vulgaris. Biotechnology and Bioengineering 36(2), 198-206.

Janssen, M., de Winter, M., Tramper, J., Mur, L.R., Snel, J., Wijffels, R.H., 2000. Efficiency of light utilization of Chlamydomonas reinhardtii under medium-duration light/dark cycles. Journal of Biotechnology 78(2), 123-137.

Janssen, M., Kuijpers, T.C., Veldhoen, B., Ternbach, M.B., Tramper, J., Mur, L.R., Wijffels, R.H., 1999. Specific growth rate of Chlamydomonas reinhardtii and Chlorella sorokiniana under medium duration light dark cycles: 13-87 s. Journal of Biotechnology 70(1-3), 323-333.

Janssen, M., Tramper, J., Mur, L.R., Wijffels, R.H., 2003. Enclosed outdoor photobioreactors: Light regime, photosynthetic efficiency, scale-up, and future prospects. Biotechnology and Bioengineering 81(2), 193-210.

Jiang, J.-G., Zhu, Y.-H., 2010. Preliminary and comparative studies on the cultivations of dunaliella salina between outdoors and in the photobioreactor. Journal of Food Process Engineering 33(1), 104-114.

Jorquera, O., Kiperstok, A., Sales, E.A., Embirucu, M., Ghirardi, M.L., 2010. Comparative energy life-cycle analyses of microalgal biomass production in open ponds and photobioreactors. Bioresource Technology 101(4), 1406-1413.

Katsuda, T., Shimahara, K., Shiraishi, H., Yamagami, K., Ranjbar, R., Katoh, S., 2006. Effect of flashing light from blue light emitting diodes on cell growth and astaxanthin production of Haematococcus pluvialis. Journal of Bioscience and Bioengineering 102(5), 442-446.

Kim, Z.H., Kim, S.H., Lee, H.S., Lee, C.G., 2006. Enhanced production of astaxanthin by flashing light using Haematococcus pluvialis. Enzyme and Microbial Technology 39(3), 414-419.

Kirk, J.T.O., 1983. Light and photosynthesis in aquatic ecosystems. Cambridge University Press. Cambridge, Great Britain

Kyle, D.J., C.B., O., Arntzen, C.J., 1987. Topics in photosynthesis: Photoinhibition. Elsevier. Amsterdam-New York-Oxford.

Larkum, A., Douglas, S., Raven, J., 2003. Photosynthesys in algae. Kluwer Academics. Dordrecht, Nederland.

Larkum, A.W.D., Douglas, S.E., Raven, J.A., 2003. Photosynthesis in algae. Kluwer Academic. Dordrecht, Boston.

Laws, E.A., Terry, K.L., Wickman, J., Chalup, M.S., 1983. A simple algal production system designed to utilize the flashing light effect. Biotechnology and Bioengineering 25(10), 2319-2335.

Lee, C.G., Palsson, B.O., 1994. High-density algal photobioreactors using light-emitting-diodes. Biotechnology and Bioengineering 44(10), 1161-1167.

Ley, A.C., Mauzerall, D.C., 1982. Absolute Absorption Cross-Sections for Photosystem-Ii and the Minimum Quantum Requirement for Photosynthesis in Chlorella-Vulgaris. Biochimica et Biophysica Acta 680(1), 95-106.

Marshall, J.S., Huang, Y., 2010. Simulation of light-limited algae growth in homogeneous turbulence. Chemical Engineering Science 65(12), 3865-3875.

Maxwell, G.M., Allen, E.R., Freese, E., 1987. Immersible probe for continual monitoring of the population-density of microorganisms grown in liquid-media. Applied and Environmental Microbiology 53(3), 618-619.

Melis, A., 1991. Dynamics of Photosynthetic Membrane-Composition and Function. Biochimica et Biophysica Acta 1058(2), 87-106.

Melis, A., 1999. Review: Photosystem-II damage and repair cycle in chloroplasts: what modulates the rate of photodamage in vivo? Trends in Plant Science 4, 130-135.

Melis, A., Murakami, A., Nemson, J.A., Aizawa, K., Ohki, K., Fujita, Y., 1996. Chromatic regulation in Chlamydomonas reinhardtii alters photosystem stoichiometry and improves the quantum efficiency of photosynthesis. Photosynthesis Research 47(3), 253-265.

Merchuk, J.C., Ronen, M., Giris, S., Arad, S., 1998. Light/dark cycles in the growth of the red microalga Porphyridium Sp. Biotechnology and Bioengineering 59(6), 705-713.

Miron, A.S., Camacho, F.G., Gomez, A.C., Grima, E.M., Chisti, Y., 2000. Bubble-column and airlift photobioreactors for algal culture. Aiche Journal 46(9), 1872-1887.

Miyamoto, K., Wable, O., Benemann, J.R., 1988. Vertical Tubular Reactor for Microalgae Cultivation. Biotechnology Letters 10(10), 703-708.

Moheimani, N.R., Borowitzka, M.A., 2006. The long-term culture of the coccolithophore Pleurochrysis carterae (Haptophyta) in outdoor raceway ponds. Journal of Applied Phycology 18(6), 703-712.

Molina, E., Fernandez, J., Acien, F.G., Chisti, Y., 2001. Tubular photobioreactor design for algal cultures. Journal of Biotechnology 92(2), 113-131.

Moreno, J., Vargas, M.A., Rodriguez, H., Rivas, J., Guerrero, M.G., 2003. Outdoor cultivation of a nitrogen-fixing marine cyanobacterium, Anabaena sp ATCC 33047. Biomolecular Engineering 20(4-6), 191-197.

Nedbal, L., Tichy, V., Xiong, F.H., Grobbelaar, J.U., 1996. Microscopic green algae and cyanobacteria in high-frequency intermittent light. Journal of Applied Phycology 8(4-5), 325-333.

Nelson, N., Yocum, C.F., 2006. Structure and function of photosystems I and II. Annual Review of Plant Biology 57, 521-565.

Ogbonna, J.C., Yada, H., Tanaka, H., 1995. Kinetic-study on light-limited batch cultivation of photosynthetic cells Journal of Fermentation and Bioengineering 80(3), 259-264.

Osawa, Z., Aiba, M., 1982. Effect of Residual Solvent on the Photodegradation of Polyvinyl-Chloride). Polymer Photochemistry 2(5), 339-348.

Park, K.-H., Lee, C.-G., 2000. Optimization of algal photobioreactors using flashing lights. Biotechnology and Bioprocess Engineering 5(3), 186.

Park, S., Khamai, P., Garcia-Cerdan, J.G., Melis, A., 2007. REP27, a tetratricopeptide repeat nuclear-encoded and chloroplast- localized protein, functions in D1/32-kD reaction center protein turnover and photosystem II repair from photodamage. Plant Physiology 143(4), 1547-1560.

Pessarakli, M., 1996. Handbook of Photosynthesis. Marcel Dekker Inc. new York.

Phillips, J.N., Myers, J., 1954. Growth of *Chlorella* in flasing light. Plant Physiology 29(2), 152-161.

Pienkos, P.T., Darzins, A., 2009. The promise and challenges of microalgal-derived biofuels. Biofuels Bioproducts & Biorefining-Biofpr 3(4), 431-440.

Pirt, S.J., 1986. The thermodynamic efficiency (quantum demand) and dynamics of photosynthetic growth. New Phytologist 102(1), 3-37.

Prokop, R., Dostal, P., Bakosova, M., 1995. Control of continuous stirred tank reactors based on delta model representation. Hungarian Journal of Industrial Chemistry 23(4), 263-269.

Radmann, E.M., Reinehr, C.O., Costa, J.A.V., 2007. Optimization of the repeated batch cultivation of microalga Spirulina platensis in open raceway ponds. Aquaculture 265(1-4), 118-126.

Raven, J.A., 2011. The cost of photoinhibition. Physiologia Plantarum 142(1), 87-104.

Richmond, A., 2000. Microalgal biotechnology at the turn of the millennium: A personal view. Journal of Applied Phycology 12(3-5), 441-451.

Richmond, A., Zhang, C.W., Zarmi, Y., 2003. Efficient use of strong light for high photosynthetic productivity: interrelationships between the optical path, the optimal population density and cell-growth inhibition. Biomolecular Engineering 20(4-6), 229-236.

Rubio, F.C., Camacho, F.G., Sevilla, J.M.F., Chisti, Y., Grima, E.M., 2003. A mechanistic model of photosynthesis in microalgae. Biotechnology and Bioengineering 81(4), 459-473.

Satoh, S., Ikeuchi, M., Mimuro, M., Tanaka, A., 2001. Chlorophyll b expressed in cyanobacteria functions as a light harvesting antenna in photosystem I through flexibility of the proteins. Journal of Biological Chemistry 276(6), 4293-4297.

Seyedeh Fatemeh, M., Bryce, R., Nik, W., 2012. Spectral conversion of light for enhanced microalgae growth rates and photosynthetic pigment production. Bioresource Technology 125, 75-81.

Sforza, E., Simionato, D., Giacometti, G.M., Bertucco, A., Morosinotto, T., 2012. Adjusted Light and Dark Cycles Can Optimize Photosynthetic Efficiency in Algae Growing in Photobioreactors. Plos One 7(6).

Shimoda, Y., Ito, H., Tanaka, A., 2012. Conversion of chlorophyll b to chlorophyll a precedes magnesium dechelation for protection against necrosis in Arabidopsis. Plant Journal 72(3), 501-511.

Smith, B.M., Morrissey, P.J., Guenther, J.E., Nemson, J.A., Harrison, M.A., Allen, J.F., Melis, A., 1990. Response of the Photosynthetic Apparatus in Dunaliella-Salina (Green-Algae) to Irradiance Stress. Plant Physiology 93(4), 1433-1440.

Steele, J.H. 1965, Notes on some theoretical problems in production ecology. Primary production in Aquatic Environments. Goldman, C.R. Berkley, CA, University of Callifornia Press**:** 383-398.

Tamiya, H., Iwamura, T., Shibata, K., Hase, E., Nihei, T., 1953. Correlation between Photosynthesis and Light-Independent Metabolism in the Growth of Chlorella. Biochimica et Biophysica Acta 12(1), 23-40.

Tanaka, A., Melis, A., 1997. Irradiance-dependent changes in the size and composition of the chlorophyll a-b light-harvesting complex in the green alga Dunaliella salina. Plant and Cell Physiology 38(1), 17-24.

Tanaka, R., Tanaka, A., 2011. Chlorophyll cycle regulates the construction and destruction of the light-harvesting complexes. Biochimica Et Biophysica Acta-Bioenergetics 1807(8), 968-976.

Tredici, M.R., Zittelli, G.C., 1998. Efficiency of sunlight utilization: Tubular versus flat photobioreactors. Biotechnology and Bioengineering 57(2), 187-197.

Van Oorschot, J.L.P., 1995. Conversion of light energy in alagal cultures. Med van Lund. Wang.(55), 225-277.

Vunjak-Novakovic, G., Kim, Y., Wu, X.X., Berzin, I., Merchuk, J.C., 2005. Air-lift bioreactors for algal growth on flue gas: Mathematical modeling and pilot-plant studies. Industrial & Engineering Chemistry Research 44(16), 6154-6163.

Wijanarko, A., Dianursanti, Sendjaya, A.Y., Hermansyah, H., Witarto, A.B., Gozan, M., Sofyan, B.T., Asami, K., Ohtaguchi, K., Soemantojo, R.W., Song, S.K., 2008. Enhanced Chlorella vulgaris Buitenzorg growth by photon flux density alteration in serial photobioreactors. Biotechnology and Bioprocess Engineering 13(4), 476-482.

Wood, A.M., 1979. Chlorophyll a:b ratios in marine planktonic algae. Journal of Phycology 15(3), 330-332.

Xue, S., Su, Z., Cong, W., 2011. Growth of Spirulina platensis enhanced under intermittent illumination. Journal of Biotechnology 151(3), 271-277.

Yang, D.-H., Webster, J., Adam, Z., Lindahl, M., Andersson, B., 1998. Induction of acclimative proteolysis of the light-harvesting chlorophyll a/b protein of photosystem II in response to elevated light intensities. Plant Physiology (Rockville) 118(3), 827-834.

Yokthongwattana, K., Chrost, B., Behrman, S., Casper-Lindley, C., Melis, A., 2001. Photosystem II damage and repair cycle in the green alga Dunaliella salina: Involvement of a chloroplast-localized HSP70. Plant and Cell Physiology 42(12), 1389-1397.

Yoon, J.H., Shin, J.-H., Ahn, E.K., Park, T.H., 2008. High cell density culture of Anabaena variabilis with controlled light intensity and nutrient supply. Journal of Microbiology and Biotechnology 18(5), 918-925.

Yoshimoto, N., Sato, T., Kondo, Y., 2005. Dynamic discrete model of flashing light effect in photosynthesis of microalgae. Journal of Applied Phycology 17(3), 207-214.

Yun, Y.S., Park, J.M., 2003. Kinetic modeling of the light-dependent photosynthetic activity of the green microalga Chlorella vulgaris. Biotechnology and Bioengineering 83(3), 303-31.

CHAPTER 3
INVESTIGATING THE INTERDEPENDENCE AMONG CELL DENSITY, BIOMASS PRODUCTIVITY, AND LIPID PRODUCTIVITY TO MAXIMIZE BIOFUEL FEEDSTOCK PRODUCTION FROM OUTDOOR MICROALGAL CULTURES

3.1. Introduction

In recent years, increasing fossil fuel prices have accelerated the search for renewable, sustainable energy sources to meet the world's energy demand. Oils and lipids from both edible and non-edible sources like soybeans, sunflowers, rapeseed, jatropha, Chinese tallow seed, animal fat, and greases have been widely investigated as potential biodiesel feedstocks (Chisti, 2007; Patil et al., 2009; Terigar et al., 2010; Jain and Sharma, 2011; Hoekman et al., 2012). Unlike other forms of renewable energy like wind and solar, biodiesel contains chemical energy that can be used in engines "as-is" or after blending to various degrees with petrodiesel. However, obtaining the large quantities of these lipid feedstocks to displace even a small portion of the current fossil fuel demand appears to be a herculean task. Some challenges include: seasonal growth variation, slow growth rate of many traditional oilseed plants, low aerial productivity rates, competition with edible oils, extensive and costly harvesting and oil extraction processes, and availability of prime agricultural land.

Microalgae have been and still are extensively researched as a feedstock source for a wide variety of products such as polyunsaturated fatty acids, pigments, bio-hydrogen, human and animal protein sources, and for many environmental remediation purposes. Microalgae is also a favorable biodiesel source because of its advantages over higher plants in terms of oil productivity and fast generation of biomass, allowing frequent harvesting (Amaro et al., 2012). However, one of the challenges in microalgal technology is achieving high oil contents while maintaining exponential or high growth of the organisms.

To produce such products efficiently, the development of proficient algal bioreactors and mass cultivation techniques is necessary. The usual technique for producing microalgae consists of a multistep backup batch culture system involving several tanks that occupy a great deal of space and is labor intensive to operate. Continuous cultures require less labor, and considerably higher production is achieved than in conventional batch or semi-continuous culture methods (James and Aburezeq, 1989). Droop (1975) defines continuous culture as "steady-state continuous flow cultures in which the rate of growth is governed by the rate of supply of the limiting nutrient." Continuous culture systems are delicately balanced so that organisms are harvested continually and the nutrient-enriched media (containing nitrogen phosphorus and inorganic salts) is replenished continually, consistent with the growth rate of the culture. The net specific growth rates and productivity in continuous outdoor cultures are directly dependent on the nutrient addition rate, incident light, and dilution rate in the system.

Light and nutrients are two of the critical factors, among others, in culturing cells at high densities (Suh et al., 2003). Growth and production performance of a microalgal cell is directly dependent on the availability of light, which depends on the distance between the cell and the light source; the intensity and duration of light exposure; and the density of the culture (Day et al., 2012). At the surface of cultures, excessive levels of irradiance can result in photoinhibition, metabolic uncoupling, photo-oxidative damage, and the potential death of the cell (Richmond, 2004). Conversely, cells deep within the culture will be light-limited. Both phenomena often lead to a decline in cell growth and productivity (Yoon et al., 2008); therefore, a controlled supply of light energy is necessary for efficient growth.

In addition to light energy, the nutrient supply and availability is an important factor. Lack of sufficient amounts of essential nutrients, either organic or inorganic, produces stress that

can significantly affect cell growth (Mata et al., 2010). For this purpose, nitrogen and carbon sources can be added intermittently or continuously, or culture medium can be exchanged with fresh medium (Rao et al., 2007). The nutritional value of microalgae can vary considerably according to the culture conditions. Under a nutrient stress environment, microalgae proved to possess a huge metabolic plasticity and ability to change their original chemical composition. In nitrogen-deficient batch cultures in the stationary phase, for example, it has been shown that cells are halted just before cell division, with photosynthesis being directed toward highly reduced storage products, such as fat (Rai and Gaur, 2001). An actively growing population, on the other hand, consisting mostly of young cells, when deprived of nitrogen, can still mature and divide to produce second-generation cells, which fail to develop normally and with a metabolic pattern that is fixed in a state favoring synthesis of carbohydrates (Guschina and Harwood, 2006).

The average lipid content of algal cells varies between 1% and 70% but can reach 90% of dry weight under certain conditions (Metting, 1996). As the lipid content increases during culture growth, other cell components, including proteins and carbohydrates, decrease. This is generally coupled to a reduction in the growth rate as well (Brennan and Owende, 2010). Nitrogen levels, light intensity, temperature, salinity, and CO_2 concentration have all been demonstrated to have an impact on the lipid content of the algal cells (Chiu et al., 2009; Wagenen et al., 2012; Devi et al., 2012; Chen et al., 2011). Above all, nitrogen deficiency often was the trigger to induce the switch to lipid accumulation. When nitrogen deprivation is imposed during batch culture growth exposed to suitable irradiances, photosynthesis continues at a reduced rate, and the flow of fixed carbon is diverted from protein to either lipid or carbohydrate synthesis (Rodolfi et al., 2009). While carbohydrate content may reach above 70% of the dry mass without significant reduction in productivity, lipid accumulation is often associated with a reduction in biomass productivity

(Spolaore et al., 2006). Furthermore, the ability to accumulate lipids is species, or even intra-species specific, rather than genus specific (Hu et al., 2008).

To date, there is little published data on the influence of dilution rates on the productivity of microalgae in continuous outdoor growth systems. The present study is aimed at determining the optimal dilution rates for maximizing the net biomass production and lipid yields in a continuous, outdoor system for three different microalgae species, *Nannochloris* sp. (Cat. no. LB2291, UTEX, TX), *Selenastrum capricornutum* (Cat. no. 1648, UTEX, TX) and *Scenedesmus dimorphus* (Cat. no. 746, UTEX, TX).

3.2. Material and Methods

3.2.1. Experimental set-up

Experiments intended at maximizing biomass and lipid production in an outdoor continuous system were carried out during the months of June and July, at Louisiana State University (Baton Rouge, LA; latitude: 30°24*'32''N; longitude 91°10'W''*). The average day time high and night time low temperatures during the tested period were 38°C and 23°C. The outdoor experiments were conducted in twelve 75 L, 40 cm high plastic round containers, each with an overflow port at a height of 36 cm from the bottom. The total volumes of the cultures were 55 L.

Sterile media was added to each outdoor tank at pre-determined rates. Four different feed flows were maintained (152.8, 76.4, 50.9 and 38.2 ml/min), which correspond to four different hydraulic retention times (HRT) of 6, 12, 18 and 24 hrs. The flows were maintained from 8 am to 8 pm, approximately representing the summer sunrise and sunset times, and the HRTs were calculated based on these 12 hours of available natural light. The flows were stoped at the end of the day to avoid overnight flushout of the active algae cultures. The F/2 stock media (Guillard

media, item F2A1 and F2B1 Pentair Aquatic Eco-Systems Inc., Apopka, FL) required for the daily flow was stored in a 2,100 L aerated fiberglass tank and was renewed every two days. To minimize contamination, the tank was covered with a tarp and secured tightly with a strap. A 1/5 HP (Item # JGP12000 Jebao, World Pump, Tucson, AZ) pump was used to continuously circulate the water through a series of 3 UV sterilizers (Gamma Model #1400–8W, Current, Vista, CA). A schematic of the oudoor set-up is represented in Figure 3.1. Valves V1 and V2 were included to facilitate multiples passes through the UV filters and for 100% recirculation during the night times.

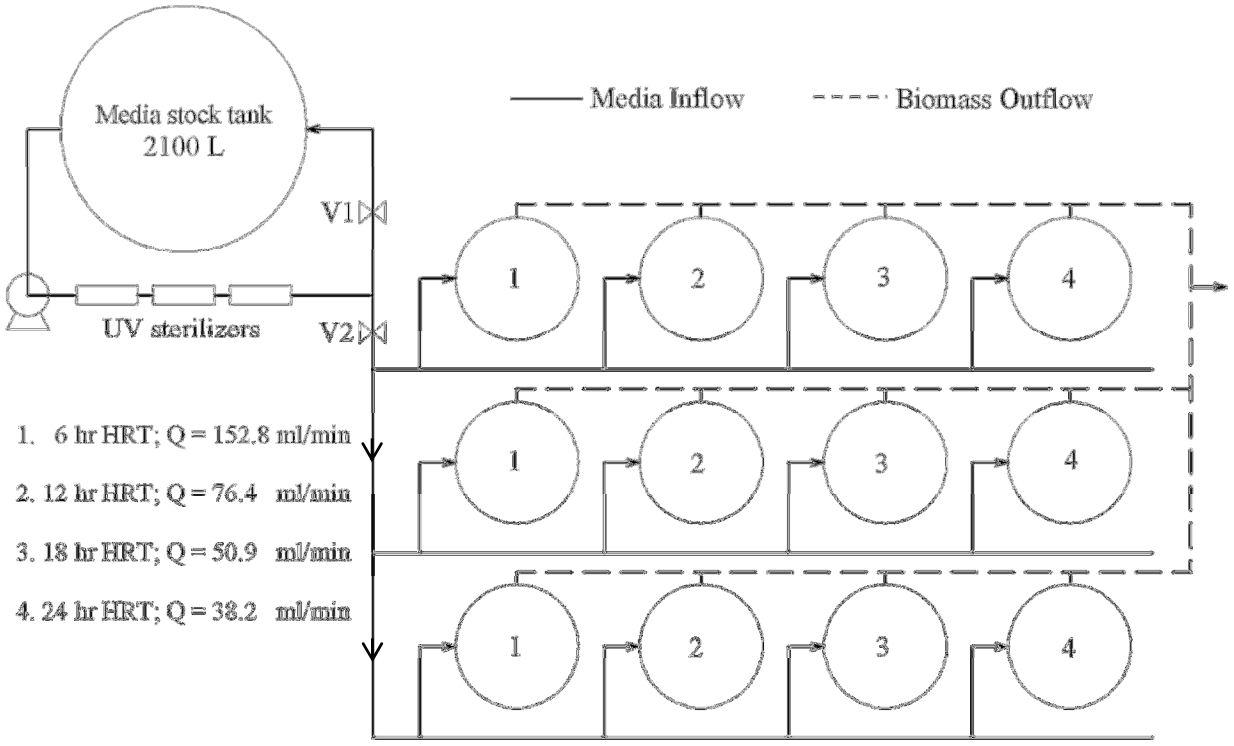

Figure 3.1. Schematic reprezentation of the outdoor culture set-up.
The solid lines represent the media inflow into the system, while the dashed lines represent the biomass mixture leaving the system. The same numerotation of the bioreactors indicates the biorecators with similar HRT's.

Aeration is important for microalgal cultures for various reasons: CO_2 in air is a source of carbon for the phototrophs; CO_2 provides essential pH stabilization; and physically mixing the

culture keeps nutrients and cells evenly distributed, which reduces self-shading and/or photoinhibition, and avoids thermal stratification inside the culture. For this study, algal cells were continuously mixed with airlift pumps. Once the cultures reached steady state densities, samples were collected and analyzed for lipid, protein, and carbohydrate contents.

During photosynthesis, plants use energy in the region of the electromagnetic spectrum from 400-700 nm. The radiation in this range, referred to as Photosynthetically Active Radiation (PAR), is typically measured as Photosynthetic Photon Flux Density (PPFD), which has units of quanta (photons) per unit time per unit surface area (µmol /s/m^2). A LI-190 Quantum Sensor (LI-COR, Lincoln, NE) was used to accurately and continuously measure this variable at the top surface of the culture surface. Temperatures of the algae cultures were continuously monitored with HOBO®Data Loggers (U12-008, Onset®, Bourne, MA). All experiments were performed in triplicate for further statistical validity.

3.2.2. Experimental analysis

Microalgal dry weight per liter (mg-dry/L) was determined using the Total Suspended Solids (TSS) method (American Public Health Association (APHA), 2012) and by measurement of the optical densities of the cultures. Samples for TSS determination were collected three times a day, at 8 AM, 1 PM, and 8 PM respectively, for the entire duration of the experiment.

Lipid extraction was performed using a modified method (Kumari et al., 2011) of the original Folch method (Folch et al., 1957). In short, lipids were extracted from 1 g of dry algae mass with 6 ml of chloroform/methanol (2/1, v/v) by vortexing (1 min) and centrifugation at a g-force of 2,057g for 15 min at room temperature. The supernatants were collected, residues were extracted thrice with 4 ml chloroform/methanol (1/1, v/v) by centrifugation and combined supernatants were washed with 4 ml of Milli-Q distilled water. The lower organic phase was

collected after centrifugation at 2,057g for 5 min at room temperature; thereafter, evaporated to dryness and total lipids content were determined gravimetrically.

Total nitrogen was quantified by CHN analysis. Dry samples were combusted in a CHN elemental analyzer (Elementar, Vario EL III). Helium was used as a carrier gas. Acetanilide (C = 71.09%; N = 10.36%; H = 6.71%) was used to calibrate the instrument. Nitrogen-to-protein conversion factor (N-Prot factor) was used to estimate the protein contents in microalgae biomass by measuring the total nitrogen contents (Bradford, 1976; Lourenço et al., 2002; Gonzalez Lopez et al., 2010). The latest conversion factor, N x 4.44 suggested by Gonzalez Lopez et al., (Gonzalez Lopez et al., 2010) was used to estimate the protein content in microalgal biomass in the current study.

3.3. Results and Discussion

3.3.1. Culture Growth

Temperatures in the outdoor bioreactors oscillated between 40°C during the day and 23°C during the night. The continuous flow of sterile fresh media provided the key nutrients for optimal growing. It is important to note that the HRTs shown here are computed based on flow during 8 AM-8 PM. Therefore the true HRTs computed on a per-day basis including nights will be twice the shown values (12, 24, 36 and 48 hrs).

Figure 3.2 shows the production of biomass in the culture systems for the three species studied. The steady state biomass densities increased with increase in the retention times. The biomass densities achieved at steady state for higher HRTs (24 hr HRT) were considerably higher than the ones achieved at lower HRTs. During the present investigation using a HRT of 24 hrs, it was possible to obtain a dry weight biomass density of of 212.6 mg/L of *Nannochloris* sp., 207.1 mg/L of *S. capricornutum*, and 250.7 mg/L of *S. dimorphus*. Lowering the retention

times led to significantly lower biomass densities in the system.

During the night, in absence of direct sunlight, the light intensity is too low to support cell growth. The existing cells will metabolize the cell components to obtain maintenance energy, thus leading to a slightly decrease in cell weight. This is represented at several instances (points A - 8PM, B - 8 AM, C – 2 PM) in Figure 3.2A, where the lower peaks on the curves are associated with the readings after the night period and the first reading of the day at 8 am, before active photosynthesis. Biomass losses during the night were also reported by other investigators when using photobioreactors to achieve a high algal yield (Ogbonna and Tanaka, 1996; Theegala et al., 1999; Theegala, 1997).

Despite the apparent light limitation in the algal cultures, light-limited models and kinetics are not considered for the present chapter. For this chapter, growth rates between two consecutive readings were computed assuming a linear first-order relationship. Specific growth rate (μ day $^{-1}$) was calculated as follows:

$$\mu=\ln(W_f/W_0)/\Delta t \qquad \text{(Eq. 3.1)}$$

where W_f and W_0 were the final and initial biomass concentration, respectively and Δt was the time between the two readings.

Specific growth rates, computed using Eq. (3.1), are plotted in Figure 3.3, along with their specific regression analysis results. The scattered symbols represent the growth rates of the algal cells during the day. The growth rates for the night period were excluded since they had negative values and interfered with performing an accurate nonlinear regression analysis. The growth rates follow an exponential decay with time tendency, attributed to biomass accumulation in the systems.

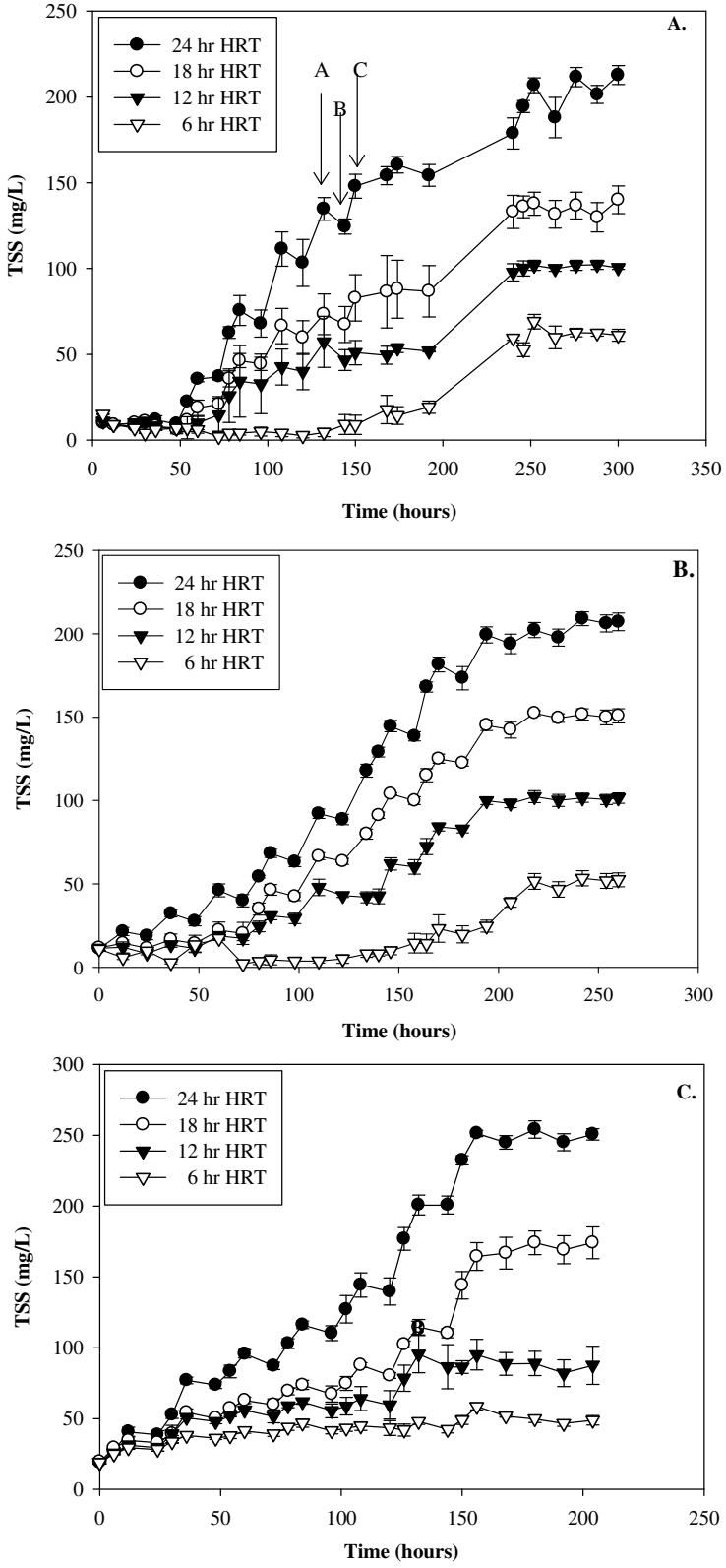

Figure 3.2. Dry biomass densities with time and standard error bars for A) *Nannochloris* sp., B) *S. capricornutum*, and C) *S. dimorphus* for 6, 12, 18 and 24 hr HRT.

At higher HRTs (24 hr HRT), due to high cellular densities, mutual shading occurs, and algal cells become shade-adapted and have a decreased light saturated photosynthetic capacity which leads to lower growth rates (Grima et al., 1999; Janssen et al., 2000). On the contrary, higher specific growth rates are achieved at shorter HRTs (6 hr HRT) due to lower steady-state biomass densities (Fig. 3.2) and greater light penetration into the culture. This phenomenon is distinctly visible at early stages after inoculation, where algal cells at lower HRT (6 hr HRT) have very low biomass densities.

3.3.2. Lipid content of microalgae at different HRTs

The lipid content in microalgae reported in literature varies from about 1-85% of the dry weight (Chisti, 2007; Rodolfi et al., 2009) and, together with other factors, is affected by the nutritional composition of the medium. Lipid accumulation in algae typically occurs during periods of environmental stress, where growth occurs under nutrient limited conditions. Many species are known to respond to nitrogen limited conditions by increasing lipid production (Takagi et al., 2000; Guevara et al., 2005; Xia et al., 2008; Chen et al., 2011). When nitrogen deprivation is imposed during culture growth exposed to suitable irradiances, photosynthesis continues, however at a reduced rate, and the flow of fixed carbon is diverted from protein to either lipid or carbohydrate synthesis (Rodolfi et al., 2009). While carbohydrate content may reach above 70% of the dry mass without significant reduction in productivity, lipid accumulation is often associated with a reduction in biomass productivity (Spolaore et al., 2006). Furthermore, the ability to accumulate lipids is species, or even intra-species specific, rather than genus specific (Hu et al., 2008).

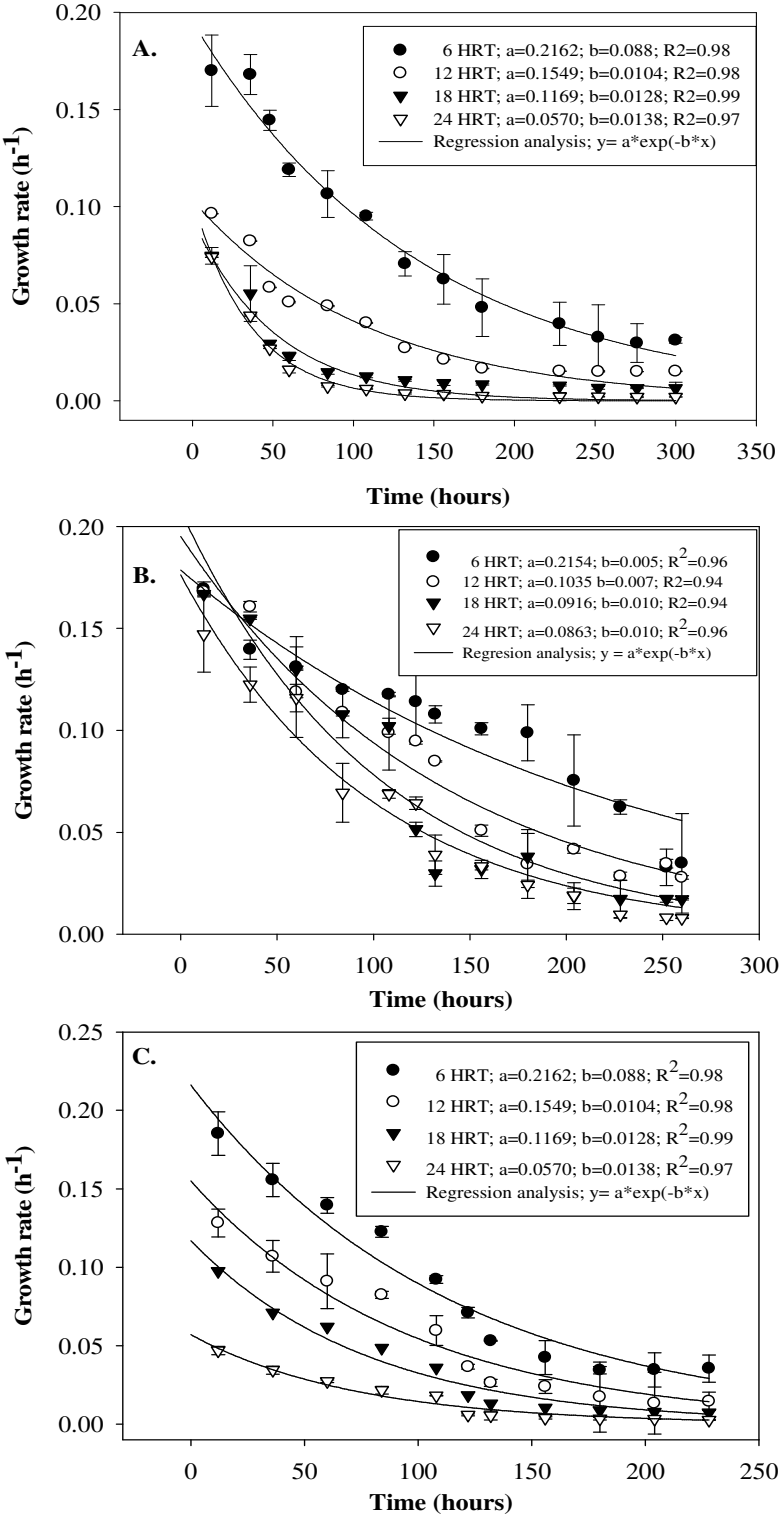

Figure 3.3. Growth rates with specific standard error bars for A) *Nannochloris* sp., B) *S. capricornutum*, and C) *S. dimorphus*. The curves represent the regression analysis and describe the function y=a·e-bx, where "y" represents the growth rate (h^{-1}) at time "x", "a" the maximum growth rate (h^{-1}) and "b" is the time based coefficient (h).

In the continuous culture system, cells were collected by centrifugation at steady state and lipid extraction was performed in order to determine the lipid concentrations at different HRTs. Results are tabulated in Table 3.1. For all three species, the lipid concentration linearly increased with increases in cell concentration, from lower HRT (6 hr HRT) to higher HRT (24 hr HRT). The lipid concentration ranged from 8.5 to 23.6 % for *Nannochloris* sp., 11.8 to 29.6% for *S. capricornutum* and 7.4 to 25.9% for *S. dimorphus* respectively. Since higher growth rates were observed at the fastest flow rates (shortest HRTs), the low accumulation of lipids at higher dilution rates is due to the growth mechanism of the algal cells, which under higher nutrients availability environment, allocate their carbon assimilation to cell synthesis (Rai and Gaur, 2001; Devi et al., 2012).

Table 3.1. Lipid content at steady state for the three algal species and different HRTs studied. Results are expressed in percentage of dry mass (% DM).

HRT (hr) / Species	6	12	18	24
Nannochloris sp.	8.45±0.27	12.49±0.28	16.20±0.37	23.62±0.70
S. capricornutum	11.77±0.59	18.21±1.20	22.77±0.25	29.57±0.34
S. dimorphus	7.37±0.84	11.94±0.31	18.05±0.67	25.91±0.78

At longer HRTs, the dilution rate is significantly smaller than the maximum net specific growth rate. When steady state is achieved for cultures with long HRTs (say 24 hr), the cell densities have reached their maximum culture density, as dictated by the physiology of that particular species. Therefore, the incident energy is directed towards lipid production and switching the carbon allocation from reproduction to lipid synthesis, bringing the ability of accumulating lipids at a full play (Rodolfi et al., 2009; Mata et al., 2010).

3.3.3. Net Biomass and Lipid Productivity

The efficiency of a continuous system is often expressed based on the net daily productivity. Figure 3.4 illustrates the net biomass and net lipid production of the system at the different HRTs studied. For *Nannochloris* sp. (Fig. 3.4A), the highest net biomass aerial production rate of 43.4 g/m^2/day was achieved at the shortest retention time (6 hr HRT). As the HRT increased, the culture density increased, dilution rate decreased and the net biomass aerial productivity decreased. Although the biomass productivity figures were significantly different ($P<0.05$) at 12, 18 and 24 hr HRTs, the difference is not substantial from a practical point-of-view. However, maximum net lipid productivity increased with reducing the feed flow. The maximum net lipid productivity occurred at 24 hr HRT (7.9 g/m^2/day), followed by 18 hr HRT (4.8 g/m^2/day), and lastly 12 hr HRT and 6 hr HRT (3.9 and 3.7 g/m^2/day), with no significant difference between the last two aerial lipid productivities.

S. capricornutum (Fig. 3.4B) showed similar results as *Nannochloris* sp. Biomass net productivity decreased with increasing the retention time up to 18 hours. No significant difference ($P>0.05$) was observed between 18 and 24 hr HRT in net biomass produced. Maximum net biomass produced was 37.6 g/m^2/day achieved at 6 hr HRT, while maximum net lipid produced was 9.6 g/m^2/day at 24 hr HRT. Lipid productivity was found to be significantly different among the HRTs ($P<0.05$).

S. dimorphus on the other hand exhibited slightly different results for the net biomass accumulated (Fig. 3.4C). The highest net biomass (40 g/m^2/day) and also the highest net lipid (10.4 g/m^2/day) productivity occurred at 24 hr HRT. A significant difference ($P<0.05$) was found between 24 and 6 hr HRT in biomass produced. This finding demonstrates that at 6 hr HRT, the dilution rate was higher than the optimum rates for *S. dimorphus*.

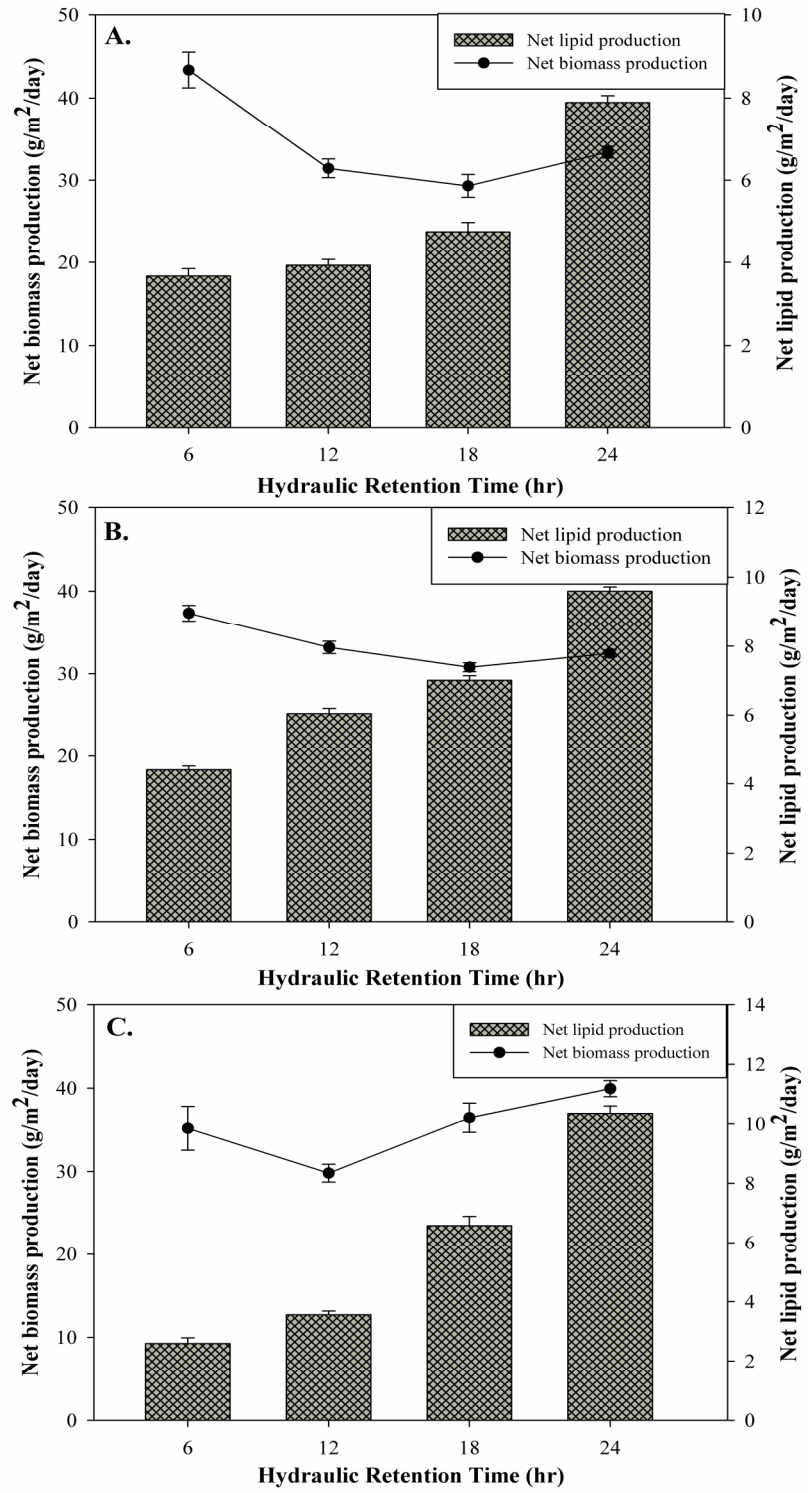

Figure 3.4. Net biomass (solid line, left axes) and net lipid production (solid bars, right axes) (± SD) for A) *Nannochloris* sp., B) *S. capricornutum*, and C) *S. dimorphus*. The four flows represent the four HRTs studied (6, 12, 18, 24 hrs).

This is a very important factor when dealing with a continuous system. If the growth rates of the cells are slower that the dilution rate, the cells will be eventually washed out from the system, reducing the biomass production. These findings are vital for producers who are focusing on either maximizing the biomass or lipid productivity. If biomass production is desired, in general, a shorter hydraulic retention time should be employed. However, as stated earlier special attention should be given not to exceed the cells growth rate and avoid washout of the culture. On the other hand, if the goal is higher lipid production, longer hydraulic retention time should be adopted, which leads to higher culture densities.

3.3.4. Biomass Composition

Some microalgal species are able to accumulate lipids under certain environmental conditions and stresses, and, among other factors, their growth is affected by the nutritional composition of the medium. However, little is known about the mechanism of lipid accumulation (Singh et al., 2002). Furthermore, a clearer understanding is needed to identify the most effective mode for maximum aerial daily lipid productivity. For example, should the cultures be stressed from the first day to induce lipid productivity? Or should cultures be first geared towards maximum biomass and later stressed to enhance lipid percentages? To identify an ideal strategy for maximizing daily aerial lipid productivities, a separate study was conducted and a two-phase growth strategy was employed. *S. capricornutum was* grown first in an excess-nutrient (Guillard F/2 with no nutrient limitation) mode in the continuous set-up previously described, followed by a lipid induction phase under nutrient deprivation (also called nutrient deficiency or starvation). Once the algal cultures reached steady state densities, samples were collected for analysis and the media flow was curtailed to induce nutrient starvation and stress. Algal biomass compositions at the steady state for each HRT were compared with the biomass composition of

the same cultures after two and six days after stopping the inflow.

When nutrient deprivation is imposed upon a culture exposed to suitable irradiances, photosynthesis continues, although at a possible reduced rate, and the cells switch the fixed carbon allocation from reproduction (protein synthesis) to either lipid or carbohydrate synthesis (Guschina and Harwood, 2006). Table 3.2 represents the changes in protein, lipid and carbohydrate as the cultures are kept under nutrient starvation for two and six days after reaching steady-state densities. The lipid content increased with the increased duration of nutrient deficiency at all HRTs studied. The percent lipid increase was least (~5%) at the longest HRT (24 hrs). At 18 and 12 hr HRTs the increase was 6.6% and 9%, respectively. At the fastest flow rate (shortest HRT; 6 hrs), the lipid accumulation almost doubled after 6 days from 11.7 % to 22.7 %. However, the increase in lipid composition during starvation was obtained at the expense of the other components, mainly proteins and carbohydrates, but to a smaller degree. Assimilation of lipids in favor of proteins during starvation was also noticed in previous literature work (Rodolfi et al., 2009). However, there are also indications that lipid accumulation during starvation stress may also derive from newly fixed carbon (Gaur, 2001).

Table 3.2. Biomass composition for *S. capricornutum*. Proteins, Lipids and Carbohydrates are expressed in percentage of dry biomass.

HRT		Protein %	Lipid %	Carbohydrate %
24 hr	SS	37.036	29.573	33.391
	2 DAY after	34.455	30.343	35.202
	6 DAY after	32.405	34.594	33.001
18 hr	SS	37.766	22.774	39.460
	2 DAY after	35.927	24.621	39.451
	6 DAY after	32.907	29.447	37.646
12 hr	SS	37.929	18.214	43.858
	2 DAY after	36.038	21.810	42.152
	6 DAY after	33.379	27.354	39.267
6 hr	SS	38.436	11.774	49.790
	2 DAY after	36.420	14.243	49.337
	6 DAY after	32.261	22.700	46.039

In terms of biomass densities, algal concentrations increased after 6 days with 6, 27, 77 and 181% for the cultures grown at 24, 18, 12 and 6 hr HRTs, respectively (Fig. 3.5). At the onset of the stress, the cultures that grew under different HRTs are more or less nutrient limited compared with each other. The biomass density increase in the 6 day-stress period (and no flow rate) was least at the longest HRT (24 hr). At shorter HRTs and just prior to curtailing the flow to induce stress, the biomass concentrations were still low and nutrients were readily available for growth synthesis rather than lipid synthesis (Table 3.3) (full table with all nutrients available presented in Appendix I). This led to increased biomass concentration with little increase in lipid accumulation after 2 days of undergoing stress. After two days, the nutrients were depleted and the cells were closer to their physiological maximum densities. The light energy received after this point was mostly diverted towards lipid accumulation.

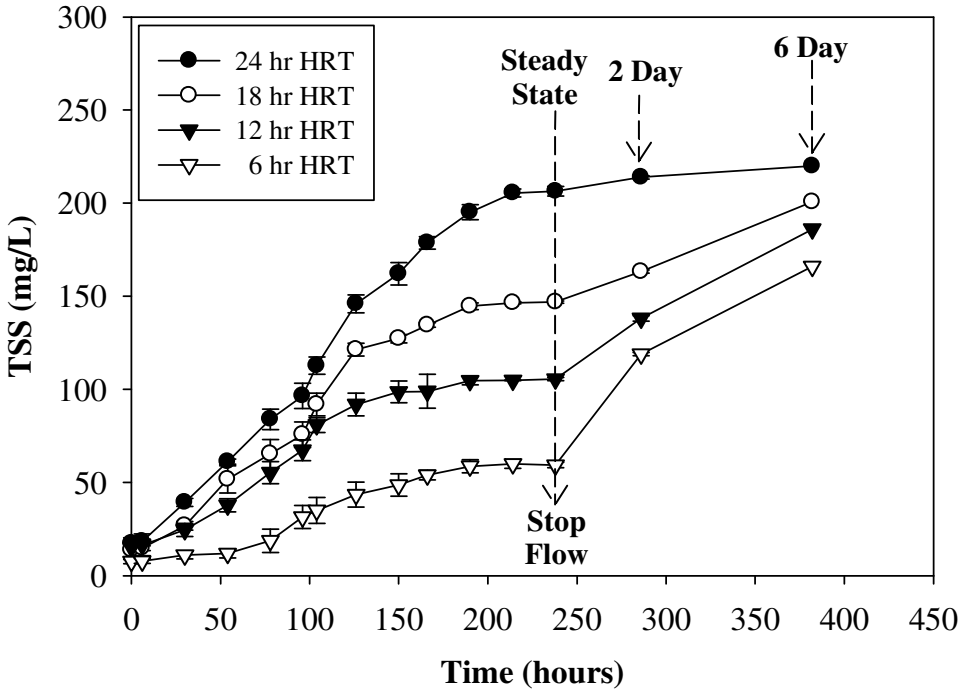

Figure 3.5. Dry biomass accumulation with time for *S. capricornutum*. The dashed arrows emphasize densities achieved at steady-state, two days and six days under nutrient stress.

Table 3.3. Nutrients availability for cultures grown at 24, 18, 12 and 6 HRT at steady-state (SS), two days (2D) and six days (6D) under nutrient stress. Nutrients expressed in mg/L.

Nutrient	F/2	24 HRT			18 HRT			12 HRT			6 HRT		
		SS	2D	6D	SS	2D	6D	SS	2D	6D	SS	2D	6D
NO_3-N	28.85	6.72	0.83	0.23	7.35	2.62	0.35	11.38	6.40	0.78	20.53	10.81	1.09
NO_2-N	38.24	20.62	11.68	2.55	24.84	12.01	6.52	29.41	14.41	9.00	33.45	20.60	11.01
Chloride	36.58	42.89	35.38	36.46	43.06	34.00	36.96	43.29	36.94	35.23	42.31	34.15	33.16
Fluoride	0.22	1.43	0.62	0.57	0.31	0.21	4.87	0.68	0.16	0.00	0.47	0.41	0.27
Sulfate	7.57	9.58	9.40	9.24	7.67	5.28	5.99	6.25	5.95	2.88	6.12	6.51	6.59
Phosphate	11.34	8.13	5.94	4.82	8.54	5.69	3.64	9.20	7.42	4.41	9.49	7.49	4.63

The maximum lipid percentage achieved in this study was 34.6 % under 24 hr HRT after 6 days of nutrient starvation. The increase in lipid accumulation also depends on the maximum lipid capacity of the algal strain. While *S. capricornutum* is not known for accumulating more than 37-40 % lipids, a strain that can attain higher lipid content would probably have a more substantial increase in lipid production.

3.4. Conclusions

Results indicated that variation in HRTs has a major bearing on biomass and lipid productivities. Although not valid for all tested species and HRTs, in general, higher net biomass productivity was achieved at shorter HRTs. However, the maximum net lipid productivity was achieved at longest retention time for all algal species studied. Upon stopping the media flow, the lipid concentrations increased at the expense of proteins and to a lesser extent at the expense of carbohydrates. The study also indicated that cultures that are closer to the physiological cell density limit and lower nutrient levels divert the incident energy more towards lipid production.

3.5. References

American Public Health Association (APHA), American Water Works Association (AWWA), (WEF), W.E.F., 2012. Standard Methods for the Examination of Water and Wastewater. Washington, DC.

Bradford, M.M., 1976. Rapid and sensitive method for quantitation of microgram quantities of protein utilizing principle of protein-dye binding. Analytical Biochemistry 72(1-2), 248-254.

Brennan, L., Owende, P.M.O., 2010. biofuels from microalgae - a review of technologies for production, procesing and extractions of biofuels and coproducts. Renewable and Sustainable Energy, 14, 557-577.

Chen, M., Tang, H., Ma, H., Holland, T.C., Ng, K.Y.S., Salley, S.O., 2011. Effect of nutrients on growth and lipid accumulation in the green algae *Dunaliella tertiolecta*. Bioresource Technology 102(2), 1649-1655.

Chisti, Y., 2007. Biodiesel from microalgae. Biotechnology Advances 25(3), 294-306.

Devi, M.P., Subhash, G.V., Mohan, S.V., 2012. Heterotrophic cultivation of mixed microalgae for lipid accumulation and wastewater treatment during sequential growth and starvation phases: Effect of nutrient supplementation. Renewable Energy 43(1), 276-283.

Droop, M.R., 1975. The chemostat in mariculture. 10th European Symposium on Marine Biology, Ostend, Belgium University Press.

Folch, J., Lees, M., Stanley, G.H.S., 1957. A simple method for the isolation and purification of total lipides from animal tissues. Journal of Biological Chemistry 226(1), 497-509.

Gonzalez Lopez, C.V., Ceron Garcia, M.d.C., Acien Fernandez, F.G., Bustos, C.S., Chisti, Y., Fernandez Sevilla, J.M., 2010. Protein measurements of microalgal and cyanobacterial biomass. Bioresource Technology 101(19), 7587-7591.

Grima, E.M., Fernandez, F.G.A., Camacho, F.G., Chisti, Y., 1999. Photobioreactors: light regime, mass transfer, and scaleup. Journal of Biotechnology 70(1-3), 231-247.

Guevara, M., Lodeiros, U., Gomez, O., Lemus, N., Nunez, P., Romero, L., Vasquez, A., Rosales, N., 2005. Carotenogenesis of five strains of the algae *Dunaliella sp* (*Chlorophyceae*) isolated from Venezuelan hypersaline lagoons. Revista De Biologia Tropical 53(3-4), 331-337.

Guschina, I.A., Harwood, J.L., 2006. Lipids and lipid metabolism in eukaryotic algae. Progress in Lipid Research 45(2), 160-186.

Hoekman, S.K., Broch, A., Robbins, C., Ceniceros, E., Natarajan, M., 2012. Review of biodiesel composition, properties, and specifications. Renewable & Sustainable Energy Reviews 16(1), 143-169.

Jain, S., Sharma, M.P., 2011. Long term storage stability of Jatropha curcas biodiesel. Energy 36(8), 5409-5415.

James, C.M., Aburezeq, T.S., 1989. An intensive chemostat culture system for the production of rotifers for aquaculture. Aquaculture 81(3-4), 291-301.

Janssen, M., de Bresser, L., Baijens, T., Tramper, J., Mur, L.R., Snel, J.F.H., Wijffels, R.H., 2000. Scale-up aspects of photobioreactors: effects of mixing-induced light/dark cycles. Journal of Applied Phycology 12(3-5), 225-237.

Kumari, P., Reddy, C.R.K., Jha, B., 2011. Comparative evaluation and selection of a method for lipid and fatty acid extraction from macroalgae. Analytical Biochemistry 415(2), 134-144.

Lourenço, S.O., Barbarino, E., De-Paula, J.C., Pereira, L.O., Marquez, U.M.L., 2002. Amino acid composition, protein content and calculation of nitrogen-to-protein conversion factors for 19 tropical seaweeds. Phycological Research 1(50), 233-241.

Mata, T.M., Martins, A.A., Caetano, N.S., 2010. Microalgae for biodiesel production and other applications: A review. Renewable & Sustainable Energy Reviews 14(1), 217-232.

Metting, F.B., Biodiversity and application of microalgae. Journal of Industrial Microbiology, 17(1) 477-489.

Ogbonna, J.C., Tanaka, H., 1996. Night biomass loss and changes in biochemical composition of cells during light/dark cyclic culture of Chlorella pyrenoidosa. Journal of Fermentation and Bioengineering 82(6), 558-564.

Patil, P.D., Gude, V.G., Deng, S.G., 2009. Biodiesel Production from Jatropha Curcas, Waste Cooking, and Camelina Sativa Oils. Industrial & Engineering Chemistry Research 48(24), 10850-10856.

Quinn, J., de Winter, L., Bradley, T., 2011. Microalgae bulk growth model with application to industrial scale systems. Bioresource Technology 102(8), 5083-5092.

Rai, L.C., Gaur, J.P., 2001. Algal adaptation to environmental stresses. Springer. New York.

Rao, R., Sarada, A.R., and Ravishankar, G.A., 2007. Influence of CO2 on growth and hydrocarbon production in *Botryococcus braunii*. Journal of Microbiology Biotechnology, 17, 414-419.

Rodolfi, L., Zittelli, G.C., Bassi, N., Padovani, G., Biondi, N., Bonini, G., Tredici, M.R., 2009. Microalgae for Oil: Strain Selection, Induction of Lipid Synthesis and Outdoor Mass Cultivation in a Low-Cost Photobioreactor. Biotechnology and Bioengineering, 102(1), 100-112.

Shifrin, N.S., Chisholm, S.W., 1981. Phytoplankton lipids - interspecific differences and effects of nitrate, silicate and light-dark cycles. Journal of Phycology 17(4), 374-384.

Singh, S.C., Sinha, R.P., Hader, D.P., 2002. Role of lipids and fatty acids in stress tolerance in cyanobacteria. Acta Protozoologica 41(4), 297-308.

Spolaore, P., Joannis-Carssan, C., Duran, E., Isambert, A., Comercial Applications of microalgae. Journal of Biosscience and Bioengineering, 101(2), 87-96.

Suh, I.S. and Lee, C, 2003. Photobioreactor engineering: Design and performance. Biotechnology Bioprocess Engineering 8, 313-321.

Takagi, M., Watanabe, K., Yamaberi, K., Yoshida, T., 2000. Limited feeding of potassium nitrate for intracellular lipid and triglyceride accumulation of *Nannochloris sp* UTEX LB1999. Applied Microbiology and Biotechnology 54(1), 112-117.

Taub, F.B. 1980, Use of continuous culture technique to control nutritional quality. Algae Biomass. Shelef, G., Soeder, C.J. Amsterdam, Elsevier/North-Holland Biomedical Press**:** 708-721.

Terigar, B.G., Balasubramanian, S., Boldor, D., 2010. Effect of Storage Conditions on the Oil Quality of Chinese Tallow Tree Seeds. Journal of the American Oil Chemists Society 87(5), 573-582.

Theegala, C.S., Malone, R.F., Rusch, K.A., 1999. Contaminant washout in a hydraulically integrated serial turbidostat algal reactor (HISTAR). Aquacultural Engineering 19(4), 223-241.

Wagenen, J., Miller, T.W., Hobbs, S., Hook, P., Huesemann, M., 2012. Effects of light and temperature on fatty acid production in *Nannochloris Salina*. Energies, 5,731-740.

Xia, X., Li, Z., Wang, P., Cribb, M., Chen, H., Zhao, Y., 2008. Analysis of photosynthetic photon flux density and its parameterization in Northern China. Agricultural and Forest Meteorology 148(6-7), 1101-1108.

Zijffers, J.W.F., Schippers, K.J., Zheng, K., Janssen, M., Tramper, J., Wijffels, R.H., 2010. Maximum Photosynthetic Yield of Green Microalgae in Photobioreactors. Marine Biotechnology 12(6), 708-718.

CHAPTER 4
CYCLING HIGH INTENSITY LIGHTS TO MAXIMIZE AERIAL BIOMASS PRODUCTIVITY OF MICROALGAL CULTURES

4.1. Introduction

Microalgae can serve as feedstocks for a variety of products including biodiesel, biohydrogen, pigments, and aquaculture feeds. It is also being used for environmental applications, such as capture of CO_2 from flue gases and remediation of environmental pollutants (Mata et al., 2010; Theegala et al., 2007). Studies on the mass culture of algae under outdoor conditions have demonstrated that the most important factor limiting the aerial yield is related to light saturation (Grima et al., 1999; Ogbonna and Tanaka, 2000). From literature, it is clear that the two parameters that are very useful to characterize the efficiency of a microalgal cultivation system are: 1) the volumetric productivity, which is the product of the biomass density (mg/L) and the specific growth rate (h^{-1}), and 2) the efficiency of light utilization. An increase in the efficiency of light utilization will lead to an increase of the volumetric productivity. For light limited cultures, light energy is analogous to the growth limiting substrate, therefore has to be used as efficiently as possible.

In algal bioreactors, optimal light requirements change during the growth cycle. At low culture densities, a high incident light intensity can cause photoinhibition in the upper layers. For dense algal cultures, light penetration can be limited and can create zones of dissimilar Photon Flux Densities, which can cause suboptimal algal growth (Suh and Lee, 2003; Zijffers et al., 2010). Photoinhibition occurs continuously when plants or cyanobacteria are exposed to light, and the photosynthesizing organism must, therefore, continuously repair the damage. Under the photoinhibitory conditions, when the rate of photodamage exceeds the rate of repair mechanism,

photoinactivated PSII reaction centers accumulate in the thylakoid membranes (Yokthongwattana et al., 2001). The PSII repair cycle, occurring in chloroplasts and in cyanobacteria, consists in synthesis of the degraded D1 protein of the PSII reaction center, followed by activation of the reaction center (Park et al., 2007). Studies suggested that, under conditions that accelerate damage to PSII, like high light intensities and under prolonged direct light applications, chloroplasts are unable to rapidly process photodamaged D1 and thus are unable to efficiently restore the function of PSII (Baroli and Melis, 1996; Melis, 1999).

In both practical and theoretical studies over the years, it has been shown that light of different intensity may be used with higher efficiency if presented in different light/dark periods (Weller and Franck, 1941; Grobbelaar, 1991; Baroli and Melis, 1996; Merchuk et al., 1998; Janssen et al., 2000; Rier et al., 2006; Wahal and Viamajala, 2010). Multiple set-ups for measuring the light utilization efficiencies were adopted. The majority include very small bioreactors (30 ml-60 ml) (Xue et al., 2011) and sophisticated turidostats (Merchuk et al., 1998; Janssen et al., 1999; Janssen et al., 2000), utilizing LED systems as a light source (Lee and Palsson, 1994; Grobbelaar et al., 1996; Nedbal et al., 1996; Katsuda et al., 2006). However, majority of the LED systems failed to approach the high light intensities of the solar radiation. Only few studies were found where the light intensities reported potentially approached the solar intensity (Janssen et al., 2001; Kim et al., 2006; Sforza et al., 2012). The major issue in using LED's as light source is their life span. Overdriving an LED light will increase the luminous output, but dramatically decrease life span if thermal management is not considered. An LED is said to have reached the end of its life when its light output reaches 50% of the rated luminous output, not necessarily when it reaches zero. Therefore, not replacing an LED in time can contribute to inaccuracies when measuring the intensities.

When mixed, algae will travel through zones of dissimilar flux densities or light/dark cycles (Miron et al., 2000; Fernandez et al., 2001). Depending on the mixing characteristics of the algal suspension, algal cells will be exposed to a series of dark/light cycles (D/L ratios). In earlier studies, most frequently, the D/L frequencies implemented were either too low (<0.1 Hz) or too high (>150 Hz) (Grobbelaar et al., 1996; Nedbal et al., 1996; Yoon et al., 2008; Marshall and Huang, 2010; Xue et al., 2011). Only a few studies focused more on medium D/L frequencies (Grobbelaar et al., 1992; Janssen et al., 2000). Moreover, the light intensities applied were much lower than that received from full sunlight during summer days (Merchuk et al., 1998; Janssen et al., 1999; Janssen et al., 2000; Park and Lee, 2000; Yoshimoto et al., 2005; Katsuda et al., 2006; Kim et al., 2006; Jiang and Zhu, 2010) and at randomly selected D/L ratios. Thus, previous efforts could not fully describe the growth and productivity performances under real existing considerations. Systematic assessment of the effect of D/L ratios at the full intensity (of sunlight) is essential since most commercial production facilities operate under natural light.

The present study focused on investigating the characteristics of growth of a representative alga, *Nannocloris sp.*, in intermittent light. Important information, which to the best of our knowledge presented for the first time, includes biomass cell concentration, growth rates and light harvesting efficiencies (in terms of chlorophyll) for an extensive range of D/L ratios and frequencies. Furthermore the results were validated for an outdoor bioreactor utilizing direct sunlight.

4.2. Materials and Methods

4.2.1. Experimental set-up

4.2.1.1. Bioreactor design

The bioreactor consisted of a cylindrical aluminum pipe, 4 x 9 (D x H) inch, with an open

top. A total of nine bioreactors were created. The interior walls of the bioreactor were lined with black paint (spray painted) to minimize internal light scattering emitted from the external source. The mixing in the bioreactor was kept at a minimum and was continuously provided by an air pump connected to an air stone (0.5"D x 1"H). The total volume of the reactor was 2 L. The volume used during the experiments was 1.9 L.

4.2.1.2. Light intensity

Experiments were performed at the Photon Flux Density of 2000 μmols/m^2/s, mimicking the peak intensity of the sun during a clear summer day. This intensity was achieved by four 6500K, 23W, instant-on micro-mini Compact Fluorescent lights (Osram Sylvania Products INC., Winchester, KY) mounted in a custom-built reflector assembly. The light reflector assembly was placed above the bioreactor, and had provisions to easily adjust the distance between the light source and top surface of bioreactor, in order to supply the desired PAR intensity. Light intensity (μmols/s/m^2) was measured in the PAR range (Photosynthetic Active Radiation, 400-700 nm) by a PAR quantum sensor (LI-190, LI-COR Inc., Lincoln, NE).

4.2.1.3. Intermittent illumination

Intermittency of illumination ranging from 7.5 s to 5 ms, with light/dark ratios from 3:1 to 1:30, was provided by a 40 cm diameter rotating disc with different sector openings to achieve the desired ratios. The D/L frequency was adjusted by varying the rotational speed of the disc. The frequency (Hz) is defined as the number of flashing per second and expressed by $(t_{Light} + t_{Dark})^{-1}$, where t_{Light} and t_{Dark} are the duration of light and dark periods in seconds (s) for each cycle, respectively. Rotation was facilitated using a motor powered by a high capacity regulated DC switching power supply (Mastech HY3010 EX, Acifica Inc., San Jose, CA). For lower speed rotations (< 48 rpm) (low frequencies) a Pittman (Harleysville, PA) DC gear motor was used,

while a DC Planetary gear motor (Anaheim Automation, Anaheim, CA) was used for high speed rotations (>48 rpm) (high frequencies). A complete table with the light and dark times, frequencies and disc physical characteristics is presented in (Appendix II). The rotating disc was placed approximately 1.5 cm above the bioreactor. The control photobioreactors received continuous lighting.

4.2.1.4. Temperature Control

Culture temperature was maintained constant at 26°C using a Neslab CFT-25 refrigerated recirculator (Neslab Instruments Inc., Newington, NH) connected to a water bath in which three bioreactors were placed. Temperatures were continuously monitored using a USB-TC data logger with type T thermocouples placed in the water bath.

One complete set-up consisted of three bioreactors (for simultaneous triplicate measurements). Each bioreactor included an identical light reflector assembly on the top, and an optical device and air stone located inside the bioreactor. The rotating disc (40 cm diameter) was placed on top of the bioreactors, in between the bioreactors top surface and the light reflector assembly, and provided consistent and identical D/L ratios and frequencies to each bioreactor (Figure 4.1). A total of three identical set-ups were assembled to facilitate three triplicate experiments simultaneously (see Appendix II for set-up pictures). Constant temperature (approx. 26°C) was maintained by the recirculating water bath, which simultaneously controlled the temperatures of the three set-ups.

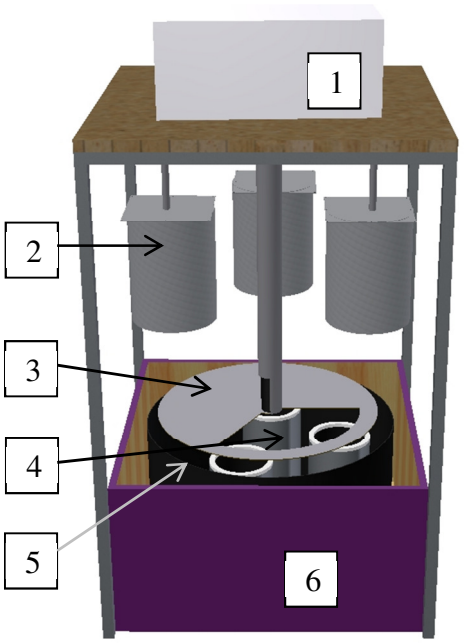

1. Power Supply
2. Adjustable light reflector assembly
3. Rotating disc with motor
4. Aluminum vessel with biomass measurement device (on top)
5. Water bath (20 L)
6. Frame box

Figure 4.1. Illustration of one out of three identical set-ups used for the light cycling study. One complete set-up consisted of three bioreactors, three optical devices, three adjustable light reflector assemblies, one rotating disc, one water bath and one power supply.

4.2.2. Analytical Methods

4.2.2.1. Immersible Device for Continuous Measurement of Biomass Concentration

Biomass concentrations were monitored every three hours by a custom built biomass optical-density measuring apparatus consisting of a matched pair of LED transmitter (665nm) and detector (550-980 nm). For this project wide-angle red LED's (RadioShack® No. 276-0309) were used, which have a typical luminous intensity of 800 mcd, and a spectral peak at 665 nm. The detector had a spectral bandwidth range of 550-980 nm. The emitters and detectors were inserted at the ends of two separate 'L' shaped 0.635 cm (¼ inch) diameter PEX tubing (Figure 4.2). Each end of the tubing was terminated with transparent round shaped Plexiglas to make the measuring probe submersible and waterproof. The distance between the emitter and detector was 4 cm. The opposite sides of the tubing were mounted vertically on a 1.3 cm H x 10.16 cm D PVC pipe (the ring). A total of 9 sets of optical devices were built. The emitters were powered by

a regulated DC power supply set at 2.6 V. The emitters, light source and air pump were controlled by USB –ERB08 relays (Measurement Computing Corporation, Norton, MA). The receiver LED leads were connected to USB-1208FS modules (Measurement Computing Corporation, Norton, MA) for measurement of the analog output (mV). The relays and modules wore connected to a laptop and LabVIEW^{TM} 9.0 software (National Instrument Corporation, Austin, TX) was used for data acquisition and process control (see Appendix II for control panel and block diagram).

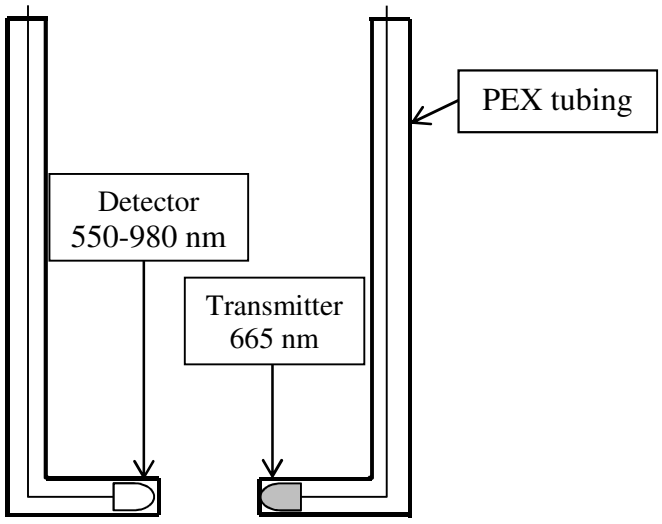

Figure 4.2. Immersible device for continuous measurement of biomass concentration. The device consisted in a pair of LED transmitter and detector inserted into two separate 'L' shaped PEX tubing. The device was inserted into the bioreactor to continuously monitor the biomass concentration during cell growth.

A data acquisition cycle consisted of three steps: (1) a pre-sampling step of 5 sec, which consisted of turning on the emitter LED's, turning off the fluorescent light source in order to avoid any receiving signals from stray light, and turning off the air pumps to permit air bubbles in the bioreactors to rise out from the light path of the detectors; (2) the sampling step, where the receiver LED's signals were taken at a sampling rate of 10 Hz for 10 sec, averaged then

outputted as a single reading; and (3) a post-sampling step of 5 sec during which the emitter LED's were turned off, and the fluorescent light source and air pumps were turned back on. The data acquisition cycle was repeated every three hours (three hours minus the 20 sec of the cycle period) for the entire duration of the experiment.

For calibration, concentrations of 0, 25, 50, 75 and 100% were prepared by dilution from a fully grown *Nannochloris* sp. algal culture. The 0% dilution (distillated water) was used as the blank for calibrating the biomass optical-density measuring LED's. For each concentration, the voltage output in mV from each individual receiver LED was recorded in triplicate. An individual calibration curve for each of the 9 sets of LED's was generated. The Total Suspended Solids (TSS) were determined following the standard Total Suspended Solids method (EPA, 2011) for each concentration in triplicate.

Calibration curves were obtained for each individual transmitter and detector LED set (total of 9 sets) by correlating the mV recorded response from the detector with the TSS (mg/L) results obtained. The calibration curves are shown in Appendix II (continuous line). A high R^2 (0.99) for the regression analysis performed showed that the data follows a polynomial second order fit. The individual generated equations were used for the experimental TSS calculations. Standard deviations between the readings were very low ($< 10^{-3}$ mg/L) showing the accuracy of the measurements between the sampling.

4.2.2.2. Specific growth rate

Growth rates between two consecutive readings were computed assuming a linear first-order relationship. Specific growth rate (h^{-1}) was calculated as follows:

$$\mu = \ln(W_2/W_1)/\Delta t \qquad \text{(Eq. 4.1)}$$

where W_2 and W_1 were the final and initial biomass concentration, respectively and Δt was the time interval between the two readings.

4.2.2.3. Determination of Chlorophyll a and b

Chlorophyll concentration was determined using the Standard Method of the Examination of Water and Wastewater for Chlorophyll determination (American Public Health Association (APHA), 2009) for spectroscopic measurements. Determination is based on the absorption of light by aqueous acetone (90%) extracts of chlorophyll from a predetermined volume of algae sample. Cultures samples were withdrawn and filtered onto glass fiber Whatman filters GF/F type, 47 mm in diameter. Chlorophyll extraction was carried out by grinding the filters in a three milliliter of 90% acetone in a glass homogenizer in an ice bath under low light condition for 1 min. After grinding the chlorophyll extracts were transferred to a graduated and stoppered centrifuge tube to which exactly 7 mL of 90% acetone was added (i.e. total volume was 10 mL + dead volume). The extract was centrifuged for 20 min at 500*g* (where *g* is the gravitational acceleration, 9.81 m/s^2). After completion of centrifugation, the absorbance of the supernatant (OD) was measured at 630, 647, 664, and 750 nm against a 90 % acetone blank using a Genesys 6 spectrophotometer (Thermo Electron Scientific Instruments LLC, Madison, WI). The concentration of Chlorophyll a, b and c was calculated according to the equations below, after Jeffery and Humphrey (Jeffrey and Humphrey, 1975) (Seyedeh Fatemeh et al., 2012):

Chl a, mg/L =

$$11.85*(OD664-OD750) - 1.54*(OD647-OD750) + 0.08*(OD630- OD750) \quad \text{(Eq. 4.2)}$$

Chl b, mg/L =

$$-5.43*(OD664-OD750) +21.03*(OD647-OD750) -2.66*(OD630- OD750) \quad \text{(Eq. 4.3)}$$

Chl c, mg/L =

-1.67*(OD664-OD750) -7.60*(OD647-OD750) +24.52*(OD630- OD750) (Eq. 4.4)

where, OD664, OD647 and OD630 are optical densities (with a 1 cm light path) at the respective wavelengths. The OD reading at 750 nm is a correction for turbidity. Because the optical density of the extract is very sensitive to changes in acetone:water proportions, it was important to use exactly a 90% acetone solution. The chlorophyll contents in the algal cells (mg/g) were calculated by dividing the concentration of the chlorophylls (mg/L) by the cell dry weight (g/L).

Growth media consisted of standard F/2 growth media (Guillard media, Pentair Aquatic Eco-Systems Inc., Apopka, FL), which was inoculated with 5% (v/v) of *Nannochloris* sp. (Cat. nr. LB2291, UTEX, TX) algal species. Data for each sample was averaged across each replicate measurement and replicate sample, and standard deviations of each sample and standard error across all samples were calculated. The results were imported into SigmaPlot ®10.0 (Systat Software Inc., San Jose, CA) for plotting graphs and conducting any further regression analysis. Statistical analyses were also performed using SigmaPlot®10.0.

4.3. Results and Discussions

4.3.1. Biomass concentration

The algal cells were grown at D/L ratios ranging from 1/1 to 10/1 and frequencies ranging from 0.1 to 102.4 Hz until they reached steady state. The plots in Figure 4.3 represent the maximum TSS achieved at the D/L ratios and frequencies studied. The highest cell concentration, expressed in mg/L, was observed at a ratio of 4/1 D/L for all frequencies studied. Highest cell concentration achieved for this study was 352.3 mg/L and it occurred at 4/1 D/L ratio and a frequency of 6.4 Hz. It was noticed that the increase in cell concentration followed a consistent pattern, increasing with increasing D/L ratios until reaching a maximum concentration

at 4/1 D/L, then gradually declining with further increases inD/L ratios. Cell concentrations were found to be significantly different among the D/L ratios ($P<0.05$). The Continuous line in Figure 4.3 represents the maximum cell concentration reached at steady state of an algal culture under continuous illumination (87.3 mg/L). By providing dark periods during the cell growth, a significant 400% increase in cell concentration was obtained. This phenomenon of increase in photosynthetic biomass growth with longer dark period in relation to the light period was also reported by other researchers (Wood, 1979; Ogbonna and Tanaka, 2000).

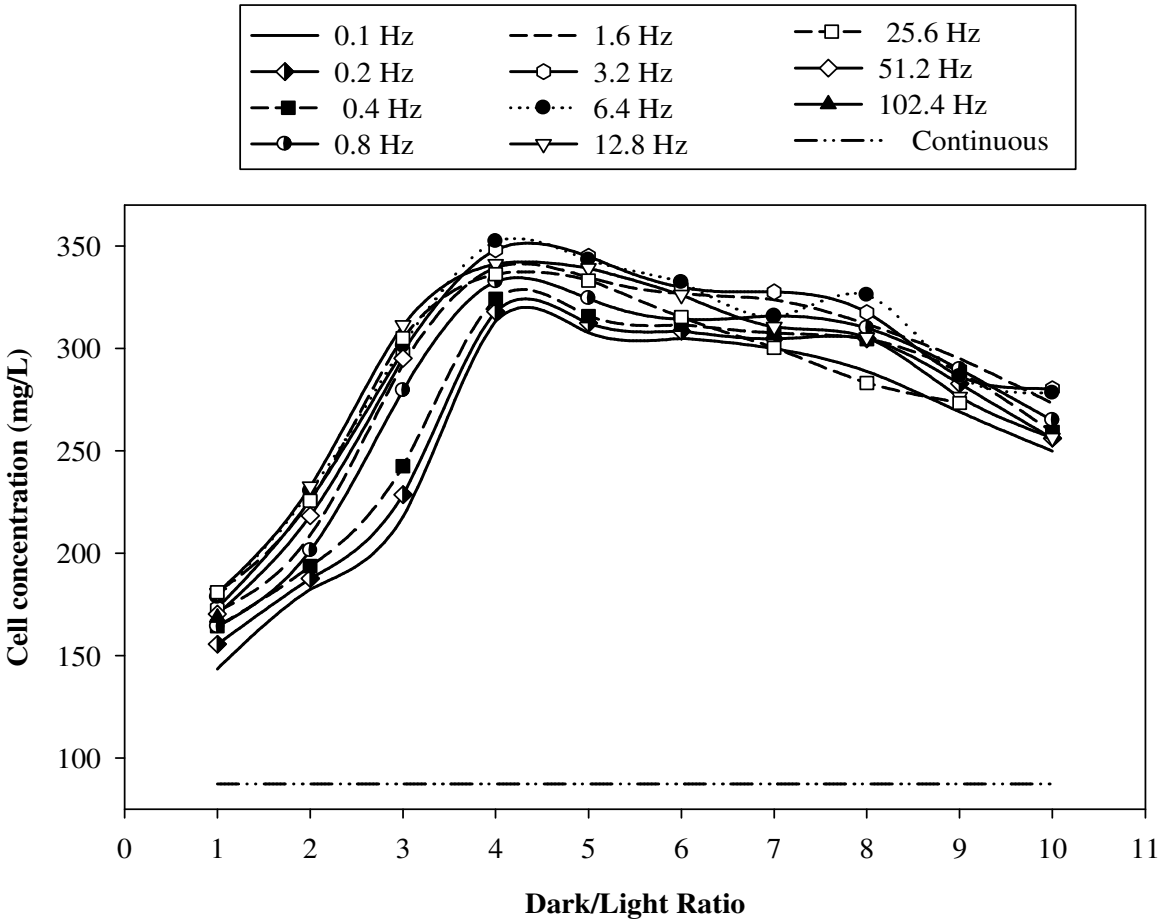

Figure 4.3. Maximum algal cell concentrations achieved at ratios ranging from 1/1 to 10/1 D/L and frequencies ranging from 0.1 to 102.4 Hz.

As observed in Figure 4.3, even at high D/L ratios there is a relatively high cell concentration (250 mg/L at 10/1 and 0.1 Hz). However, to track the concentrations at higher D/L ratios, the algal cells were subjected to longer periods of darkness (15/1 - 30/1) at 0.1 Hz frequency. Consecutively, a lower dark ratio (higher light ratio) was also investigated (1/2 and 1/3). Results are plotted in Figure 4.4. Further increase in dark periods did not increase the cell concentration in the bioreactor. In contrast, there was a significant decrease ($P<0.05$) comparing to 10/1 D/L ratio. Results imply that extended stay of algal cells in the dark region is detrimental to the algal culture, and because of the insufficient light input some of the biomass could be wasted for maintenance in dark (Yoon et al., 2008). However, these findings have a noteworthy importance from a large scale production point of view. It can be noticed that at higher D/L ratios (higher than 10/1 D/L) the biomass accumulation is still decently high. Between 10/1 and 20/1 D/L the cell concentrations are ranged from 250 to 158 mg/L respectively, which for an algal culture is still a high biomass concentration. If mixing of the algal cells can be controlled in such way that the cells would receive similar D/L ratios in an outdoor raceway or pond, the aerial biomass productivity can be significantly increased. At 10/1 D/L ratio the cell concentration is 57% higher compared to the cell concentration at 1/1 D/L. Theoretically this could be translated as increasing production by 50% while decreasing the areal land requirements by ten-folds. An increase in the light period (1/2 and 1/3 D/L) dramatically decreased the cell concentration, which were lower than the ones achieved with continuous lighting (Fig. 4.4). The decrease in cell concentration associated with the increase in the light periods is an indication of the photoinhibition phenomena.

In addition, cell concentrations showed to also be frequency dependent. In all cases the cell concentration increased with increasing D/L cycle frequency. However, the maximum cell

concentration was not reached at the highest frequencies studied. The concentrations increased to a maximum of 181 mg/L at 25.6 Hz for 1/1 D/L, and 232.5 and 311.5 mg/L at12.8 Hz for 2/1 and 3/1 D/L. At higher D/L ratios (from 3/1 to 10/1 D/L) the maximum concentrations reached were not found to be significantly different between 3.2 and 6.4 Hz ($P>0.05$), but significantly lower with decreasing or increasing frequencies beyond these two frequency range ($P<0.05$). Moreover, when dark periods beyond 7/1 D/L were increased, no significant difference ($P>0.05$) was noticed between the lowest and highest end frequencies (between 0.1 and 25.6 Hz) (Fig. 4.3).

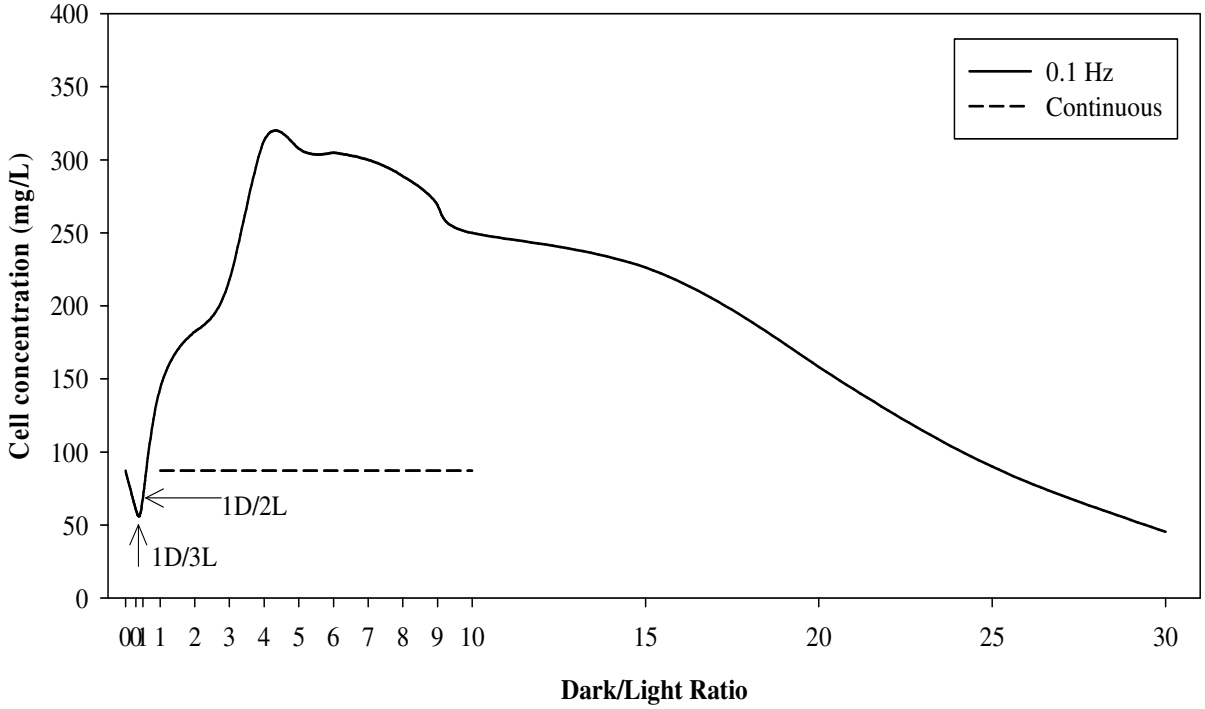

Figure 4.4. Maximum algal cell concentrations achieved at ratios ranging from 1/1 to 30/1 D/L at the frequency of 0.1 Hz.

D/L cycles of medium frequency (1-25 Hz) showed to enhance maximum algal cell concentrations compared to low and high frequencies. Similar findings were reported by other researchers at lower irradiance levels (Grobbelaar et al., 1992; Janssen et al., 2000; Xue et al.,

2011), confirming these results. However, the cell concentrations showed to be more dependent on the D/L ratio applied, rather than frequency. These findings are meaningful for microalgae production, for either outdoor pond or photobioreactor system used. A high D/L frequency requires a higher stirring or pumping energy input, while there is relatively little compensation in cell concentration by increasing the cell frequency compared to applying different D/L ratios. This is shown by the differences in biomass concentration loss between frequencies and D/L ratios. The loss in concentration was only about 40 mg/L (13%) with decreasing frequency (maximum loss was between 0.1 and 6.4 Hz at 4/1 D/L), while the loss in concentration with decreasing D/L ratio was more than 170 mg/L (60%) between 4/1 and 1/1 D/L (at 6.4 Hz) and 105 mg/L (35%) between 1/1 and 10/1 D/L.

4.3.2. Growth rates

Growth rates were calculated based on equation 4.1 in the material and methods section, and Figure 4.5 shows the changes in growth rates with time at the applied D/L ratios. Growth rates showed to be D/L ratio and cycle frequency dependent during the time of growth. The maximum growth rate of 0.1305 h^{-1} was detected at 4/1 D/L between 96 and 120 hours, which progressively decreased with further increases in dark periods. This justifies the maximum cell concentration reached at 4/1 D/L ratio. When compared to a culture grown under continuous lighting, the growth rates at all D/L ratios, with the exception of 1/1 D/L, were significantly higher ($P<0.05$) after approx. 55 hours (2 1/2 days). This is believed to happen due to a delay in response to the light cycle ratios, since the algae inoculum was grown under lower and continuous light irradiations (Yang et al., 1998). During the first 2 1/2 days after inoculation, the cultures grown under continuous light and 1/1 D/L ratios showed higher specific growth rates compare to 2/1-10/1 D/L ratios. Growth under 1/1 D/L exceeded the growth rate under

continuous lighting after 32 hours of growth.

An interesting phenomenon was observed when associating the amount of time needed to reach the maximum growth rate. As seen in Fig. 4.5, the time needed to reach the peak growth, shifted with D/L ratios. The peak growth for 1/1 D/L appears to happen at the 48 hour time. For 2/1 and 3/1 ratio the peak growth was observed at the 72 hours line, the growth rate for 4/1 D/L peaked after 108 hours, and at 5/1 after112 h of growth. The growth rate peaks, further shifted in time with increasing the dark period. At 9/1 and 10/1 ratios, the maximum growth rates were reached at around 168 hours of growth, which coincides with the minimal growth rate for cells subjected to continuous lighting.

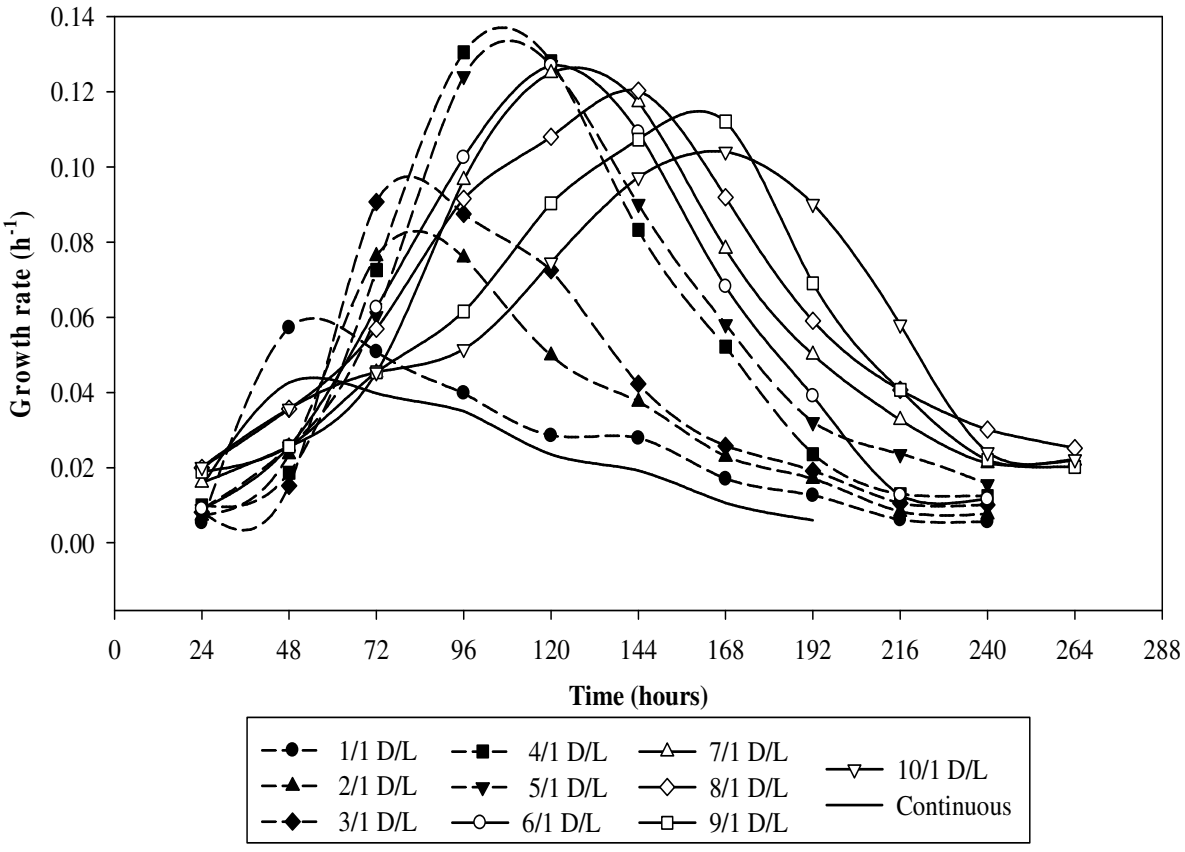

Figure 4.5. Growth rates at D/L ratios studied versus time.

The growth rates also showed to be directly dependent on frequency. Figure 4.6 has the plots of the growth rates versus time for 1/1 D/L ratios. The results for the other ratios (2/1-10/1 D/L) are being presented in Appendix II. It is shown that the growth rates increase with increasing cycle frequencies, although, the maximum growth rates were evidenced at or in between 1.6-25.6 Hz. Overall, the maximum growth rates (μ_{max}) observed were at low frequencies for high D/L ratios (>7/1 D/L), medium frequencies for medium D/L ratios (≥ 4/1 and 7/1≤ D/L), and at medium to high frequencies for low D/L ratios (1/1-3/1 D/L) as presented in Figure 4.7.

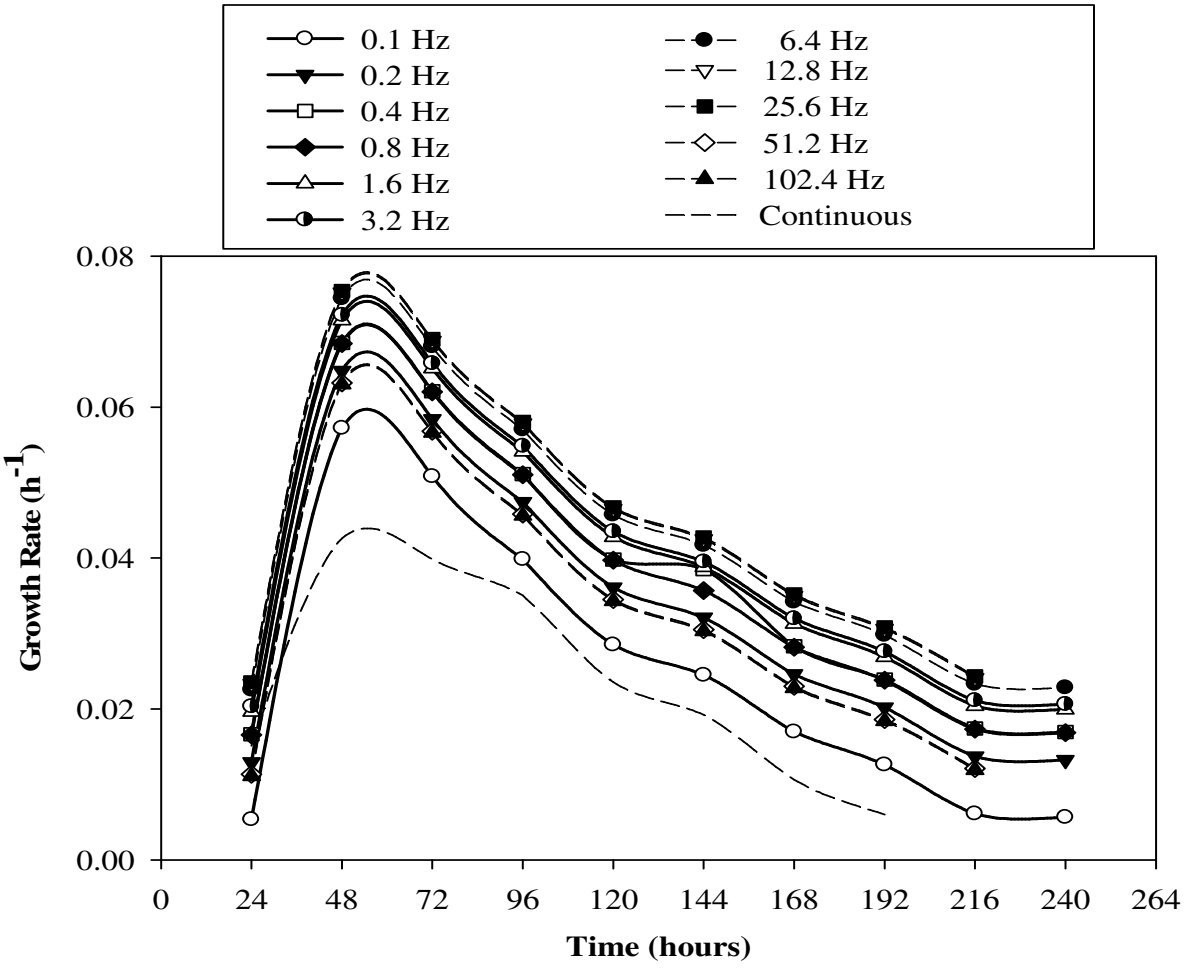

Figure 4.6. Growth rate for 1/1 D/L ratio at the frequencies studied versus time.

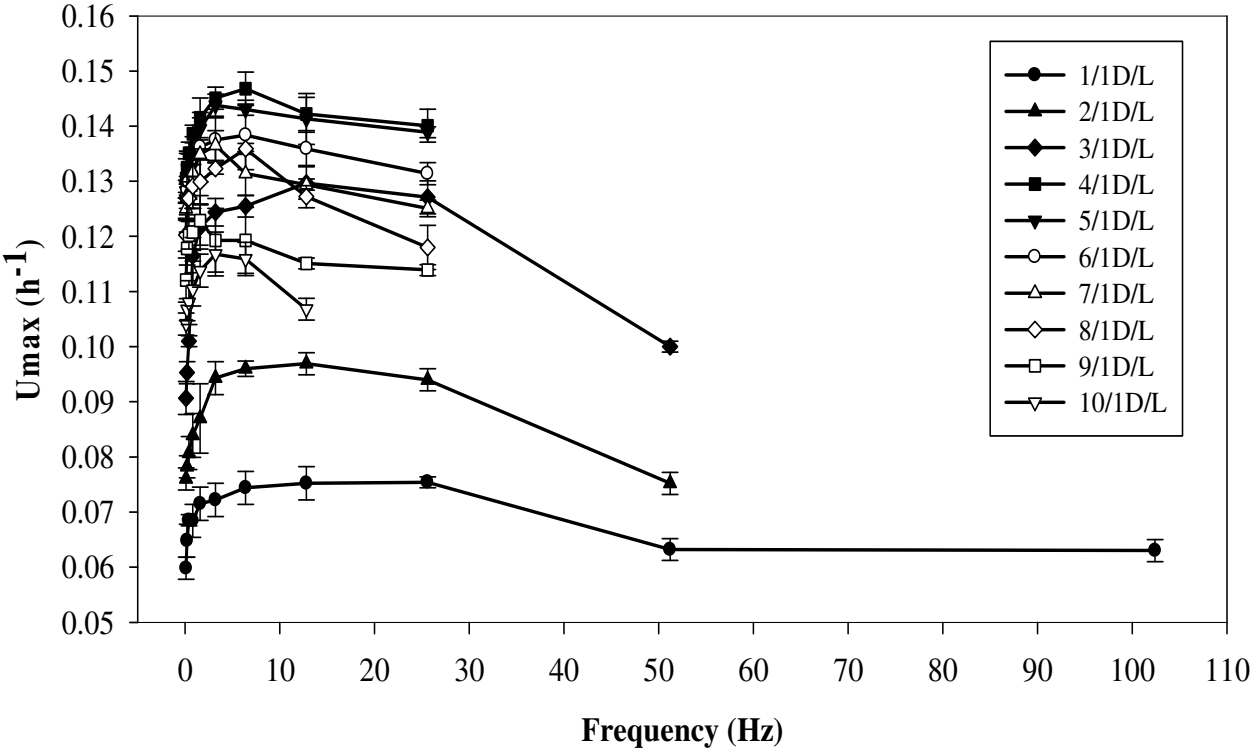

Figure 4.7. Maximum growth rates (μ_{max}) for 1/1-10/1 D/L ratios at the frequencies studied.

The effect of medium frequency D/L cycles on growth rates of microalgae have been previously investigated, however, conflicting results were found. It was suggested by some researchers that medium cycle frequencies enhance growth and productivity greatly (Merchuk et al., 1998; Janssen et al., 2000; Xue et al., 2011), while several other reported that medium frequency cycles exerted little influence on cell growth (Grobbelaar, 1991). These finding were indicated for cells grown under lower light irradiances (<1000 μmol/s/m^2) and single D/L ratio. In this study the results clearly showed that at a high light irradiance maximum growth can significantly be enhanced by applying medium frequencies if medium light periods are used. If lower light periods are applied (10/1 D/L), lower frequencies would be more appropriate for higher growth and higher frequencies for higher light periods (1/1 D/L).

4.3.3. Chlorophyll content

Total chlorophyll content (Chl a + Chl b; mg/g biomass dry weight) at the frequencies studied show to closely follow the biomass concentration trend with increasing the D/L ratios (Fig. 4.8). The total chlorophyll content varied with frequency, increasing with increasing the dark period of the D/L ratio. However, little change in total chlorophyll content was observed between 4/1 and 8/1 D/L ratios. Total chlorophyll decreased once the dark period was increased beyond 4/1 D/L ratio.

Total chlorophyll content also varied with frequency. Highest Chl content was observed at 3.2 and 6.4 Hz for all D/L ratios with no significant differences between the two ($P>0.05$). Chl content did not show major variations with frequency at higher dark periods (5/1-10/1 D/L) with the exception at 25.6 and 102.4 Hz, where Chl content was the lowest.

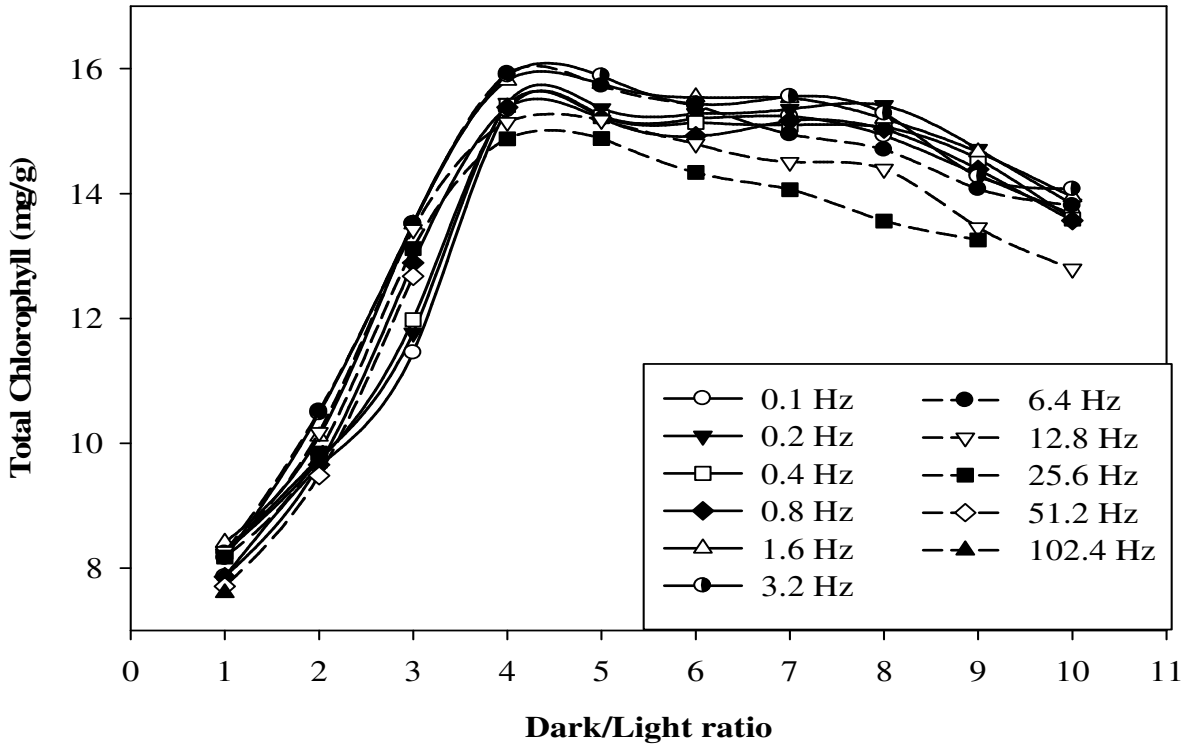

Figure 4.8. Total chlorophyll concentration in the biomass (Chl a + Chl b; mg/g dry weight biomass) at the D/L ratios and frequencies studied (Appendix II).

Chlorophyll composition in terms of Chl a and Chl b showed significant changes (Fig. 4.9). Chl a and b increased with increasing the D/L ratios. Chl a (Fig. 4.9 A) increased with increasing the dark periods from 1/1 to 4/1 D/L, a then decreased with further increasing the dark periods. This similar trend was observed in biomass concentration as well, Chl a being also used in literature for biomass concentration measurements. Chl b (Fig. 4.9 B) increased at similar rates, reason why the total Chl content did not showed major concentration fluctuations. Chl b concentrations increased with increasing the D/L ratios, achieving the highest concentration at 10/1 D/L ratio, however significant differences were not observed between 8/1, 9/1 and 10/1 D/L ratios ($P>0.05$) in Chl b. Concentrations of Chl a and Chl b showed to decrease with increasing frequency at all ratios studied. Chl c, although measured, was present in very low concentrations, $<10^{-3}$ mg/g or not present at all, therefore was not included in the result section.

Higher concentration of Chl b present in the biomass is believed to directly enhance the light gathering efficiencies, especially in cultures grown under low light irradiances (since it is a photochemically active pigment), and is attributed to higher corresponding specific growth rates (Wood, 1979). This can explain the higher growth rates achieved at 4/1 D/L ratios and Figure 4.7. Longer exposure time of algae to photoinhibitory irradiance brings structural and functional adjustments in the photosynthetic apparatus. These adjustments involve the thylakoid membrane which acclimates to adverse conditions. Algae cells, when exposed to long-term photoinhibition conditions, respond by decreasing the antenna size of PSI and PSII (which contain the D1 and D2 reaction center proteins) and by lowering the absolute amount of PSI in the chloroplast thylakoids (Baroli and Melis, 1996). At long-term and high irradiances, the higher weight protein complexes containing the D1 and D2 reaction-center proteins tend to accumulate in the thylakoid membrane, thereby, resulting in accelerated damage to PSII. As a consequence, the chloroplasts

are unable to rapidly process photodamaged D1 and efficiently restore the function of PSII, which ensues in loss of photosynthetic capacity. In decreasing the exposure time (increasing frequency) and amount of light (increasing the D/L ratio) the photosynthetic capacity increases. Chl b is a light gathering efficiency enhancer; therefore, by increasing the Chl b concentration (Fig. 4.9 B) optimum light requirement is accomplished. In this study the D/L ratio of 4/1 appears to be the ratio with the highest photosynthetic efficiency, which is also confirmed by the higher growth rates and higher cell concentration measured at this ratio (Figures 4.3, 4.5 and 4.7). In terms of frequency, the light efficiency increases with increasing frequency between 6.4-25.6 Hz (Fig. 4.9) and slowly decreases with further increases in frequency. This phenomenon is explained by the fact that at high frequencies the photosystems perceive the incoming light as continuous (Tanaka and Melis, 1997; Hortensteiner and Krautler, 2011) reducing the efficiency. Similarly, at very low frequencies there is abundance of light which damages the photosystem, lowering the photosynthetic efficiency.

In the photosystems, Chl b occurs at variable ratios to Chl a, and the results of this study are computed and plotted in Figure 4.10 (Chl a/Chl b ratio versus D/L ratio). As a direct consequence of increasing Chl a and in Chl b the Chl a/Chl b ratios displayed an initial increase with increasing the dark periods. After the 4/1 D/L ratio, the Chl a/Chl b ratio then decreased with further increases in dark periods. The chlorophyll ratio was also frequency dependent, ratios increasing with frequency at all D/L ratios.

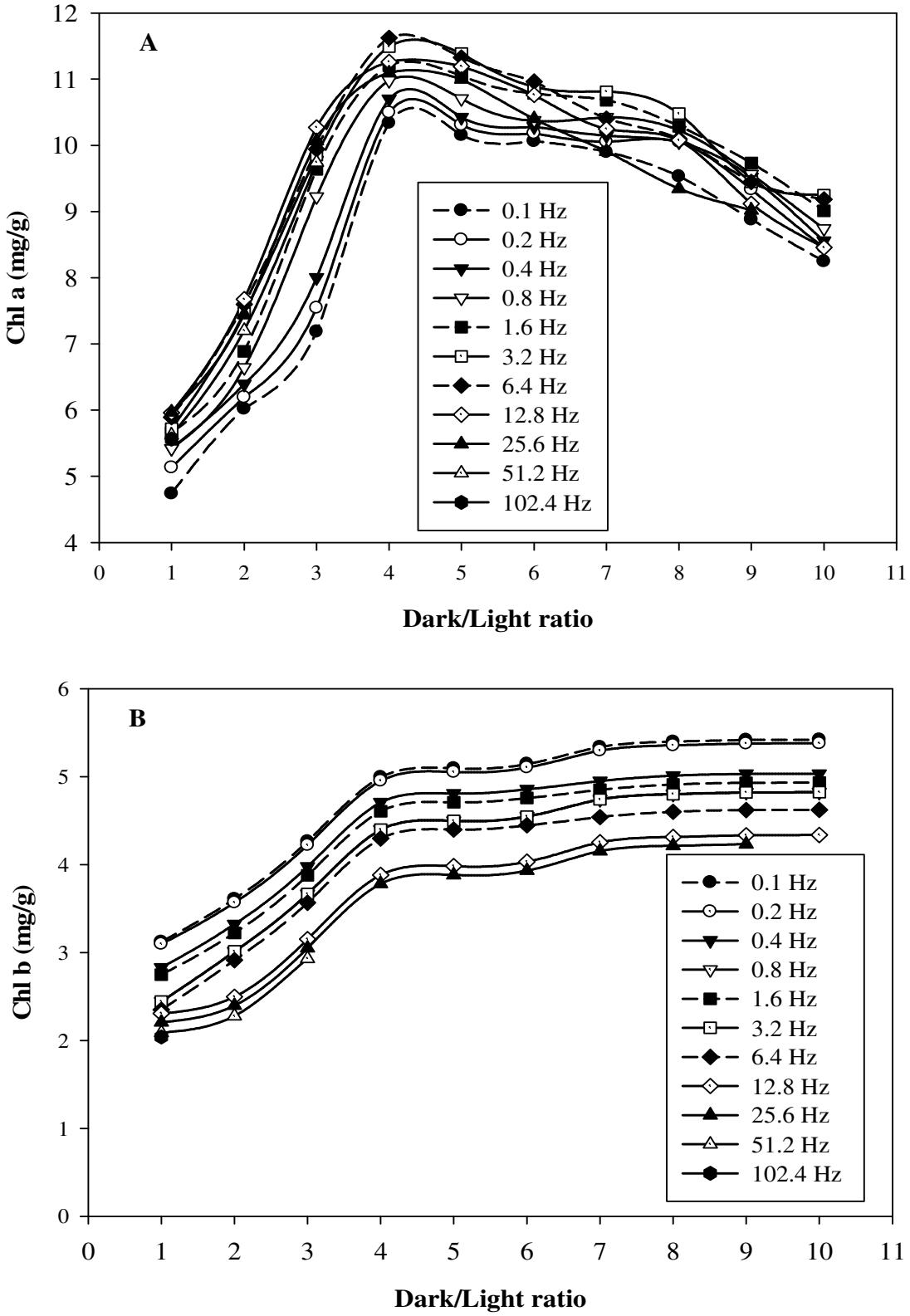

Figure 4.9. Chlorophyll a (A) and Chl b (B) concentrations for the frequencies studied versus D/L ratios.

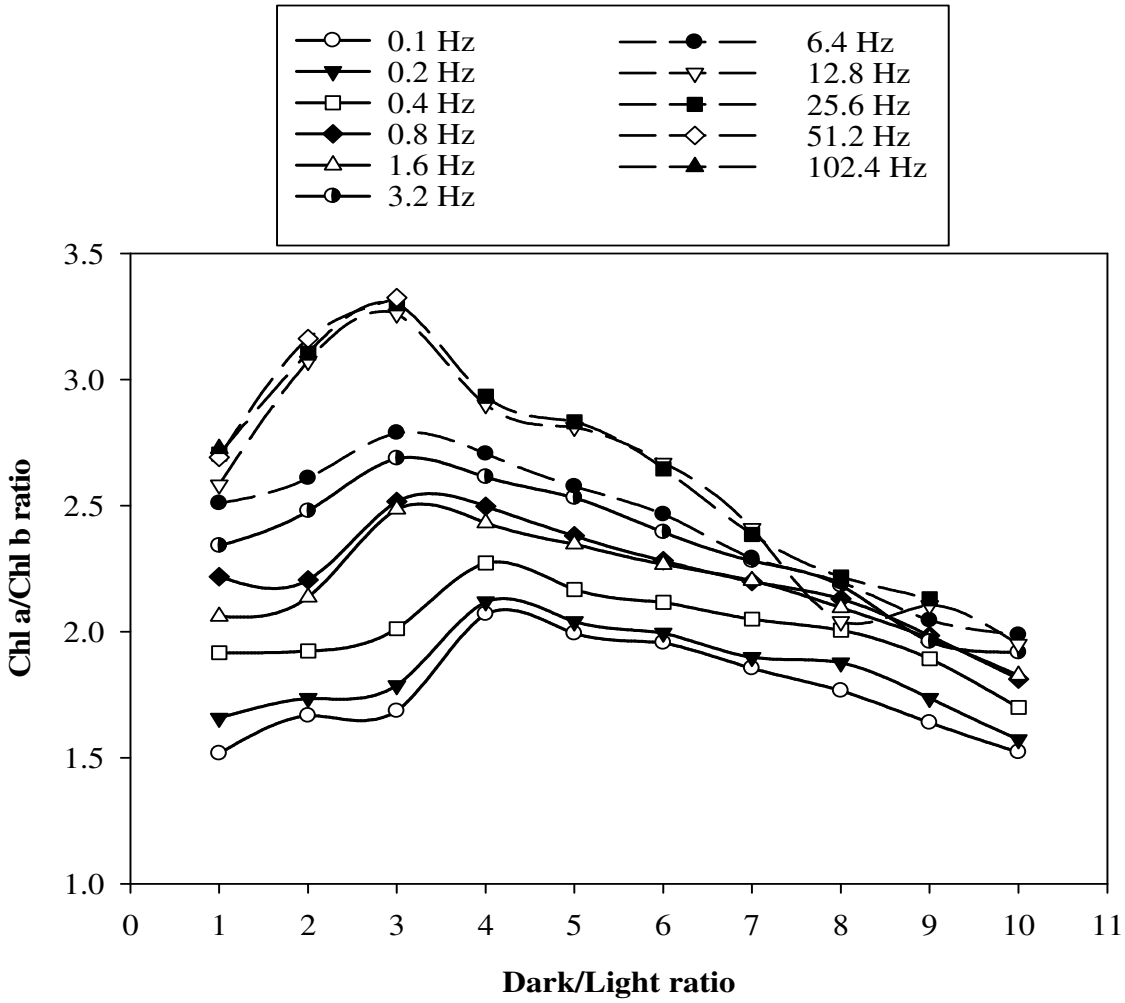

Figure 4.10. Changes in Chl a/Chl b ratios for the D/L ratios and frequencies considered.

Chlorophyll a to b ratios are known to be higher at high growth irradiances (2000 μmol/s/m^2), and similar values in ratios (> 2) were found in literature (Baroli and Melis, 1996). The high Chl a/Chl b ratio under increased light periods is accompanied by a significant decrease in the cellular content of Chl a and smaller light harvesting antenna size in the PSII. The lowering of the Chl a /Chl b ratios reflects accumulation of Chl b resulting in an increase in the light harvesting chlorophyll antenna size of the photosystem, increasing the light gathering efficiency.

4.4. Outdoor Intermittent light study

To substantiate the hypothesis from the indoor small-scale D/L experiments, a larger scale outdoor set-up was constructed. The set-up consisted of a closed, continuous loop bioreactor. The bioreactor was fabricated out of 40 sch, 4 in diameter standard PVC pipe and 40 sch, 4 in diameter clear rigid PVC pipe (item 34141, US Plastic Corporation®, Lima, OH). The D/L ratio was based on the length of the clear PVC/standard PVC. Light portions with different D/L ratios were provided by the clear PVC, while the dark portion was provided by the standard pipe PVC. The total length of each bioreactor was 305 cm, and total volume was 25 liters. Three identical bioreactors were constructed, each with a clear PVC section of 152.5, 61, and 27.7 cm, and standard PVC section of 152.5, 244 and 277.3 cm, representing 1/1, 4/1 and 10/1 D/L ratios (Fig. 4.11).

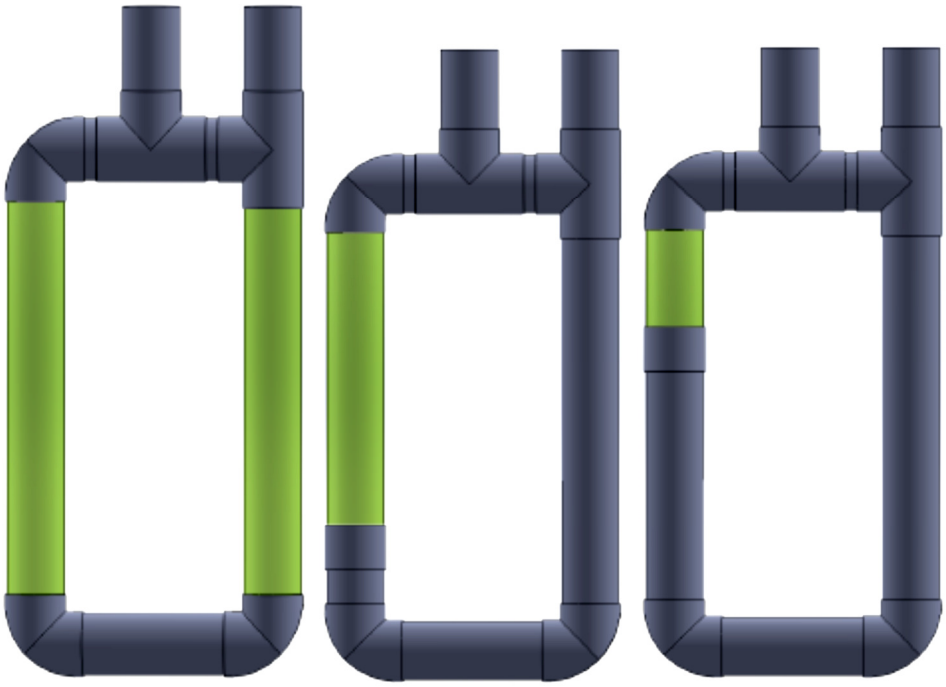

Figure 4.11. Illustration of the set-ups used in the outdoor intermittent light study. From left to right: 1/1, 4/1 and 10/1 D/L ratios.

The mixing in the bioreactors was provided by a 6"L x 1.5"W air diffuser (AS15L, Pentair Aquatic Eco-Systems Inc., Apopka, FL) connected to an air pump. Experiments were run during the month of November, and although the outdoor temperatures during the day were between 25-30°C, during the night aquarium heaters were used to maintain these constant temperatures.

Temperatures of the algal cultures and direct solar irradiation were continuously monitored with HOBO®Data Loggers (U12-008, Onset®, Bourne, MA) and a LI-COR Quantum Sensor (LI-190, Lincoln, NE) (for pictures showing the bioreactors at work, see Appendix II). Total biomass concentration (mg/L) and growth rate (h^{-1}) measurements were calculated as previously described in the Material and Methods section (section 4.2.). Optical densities were measured twice a day, at 9 am and 5 pm, respectively, daily for the entire duration of the experiment. The algal cultures were grown until reaching a steady state. Once the steady state was reached, 1/4 of the volume (6.25 L) was discarded daily, and replaced with F/2 media, for a semi-continuous bioreactor mode.

4.4.1. Biomass Cell Concentration and Net Productivity

The biomass cell concentrations of the three bioreactors versus time are plotted in Figure 4.11. The 1/1 and 4/1 D/L bioreactor concentrations were very similar to each other reaching at steady state 373.3 mg/L and 362.5 mg/L in TSS. At 10/1 D/L, the concentration in the bioreactor significantly ($P<0.05$) fell behind the other two, reaching only 233.3 mg/L at steady state. The concentrations at steady state for 4/1 and 10/1 D/L are comparable with the concentrations achieved during the indoor experiments at the same D/L ratios. However, the steady state biomass concentration for 1/1 D/L was significantly higher ($P<0.05$) than the concentration reached indoor at 1/1 D/L and was comparable with the concentration achieved at 4/1 D/L.

During the indoor experiments, however, the concentration at 1/1 D/L was found to be significantly lower than at 4/1 D/L. The main reason for this change could be attributed to the partial transparency of the clear PVC pipe. Although the outdoor experiments were performed under natural sun irradiance, the clear PVC pipe was not 100% transparent. It was calculated that the clear PVC pipe was blocking approximately 20% of the sun's intensity, and out of the 1700 μmol/s/m^2 (average maximum intensity at mid-day during the month of November) PAR intensity only 1400 μmol/s/m^2 would pass through the clear PVC pipe and reach the algal cells. Compared to the indoor trials, which were performed under 2000 μmol/s/m^2, photoinhibition was less likely to occur (or at a lower rate) outdoors at 1/1 D/L ratio and was probably avoided by the clear PVC's partial light blocking. The clear pipe had a slightly blue color, which would likely also block UVA/UVB radiation (not measured), impacting the cells growth. These results, however, are in agreement with the previous results, showing that biomass accumulation is in direct correlation with the light cycle ratio received by the culture.

The bioreactors were operated in a semi-continuous mode for four days after reaching steady state. At the beginning of each day, 1/4 of the total volume was discharged and replaced with fresh F/2 media. The final concentrations at the end of each day for all bioreactors, was lower than the final concentration achieved the previous day. The concentrations for 1/1 and 4/1 D/L bioreactors were very similar during the semi-continuous mode, reaching a TSS value after 4 days of 275 and 262.5 mg/L, approximately 25% decrease from the steady state biomass concentration (Fig. 4.12). The 10/1 D/L bioreactor cell concentration followed a similar trend, reaching a final TSS of 172.5 mg/L after four days of semi-continuous operation, a 25% decrease compared to the steady state TSS.

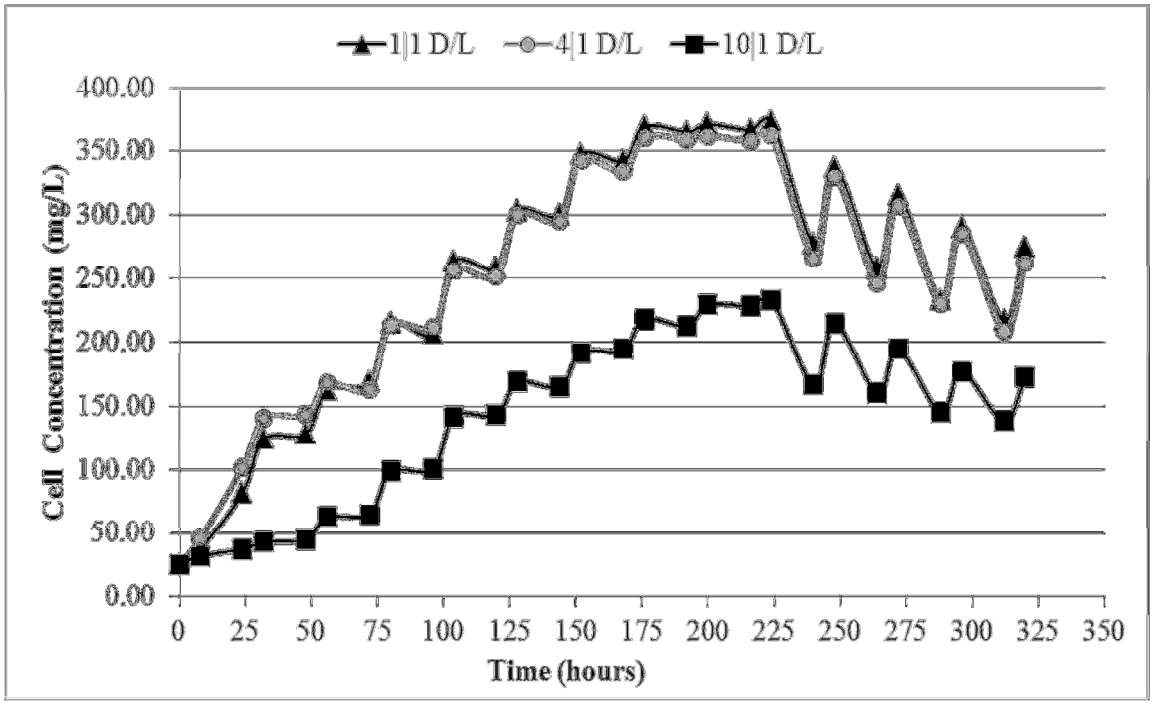

Figure 4.12. Cell concentrations for the bioreactors operated at 1/1, 4/1 and 10/1 D/L ratios with time. After achieving steady state the bioreactors were operated in a semi-continuous mode.

At steady state, the calculated aerial net productivity was the highest for the bioreactor operated at 1/1 D/L (47.5 g/m^2/day) followed closely by the 4/1 D/L bioreactor (46 g/m^2/day), as shown in Figure 4.13. The 10/1 D/L operated bioreactor reached a steady state productivity of 30 g/m^2/day. The lower productivity for the 10/1 D/L bioreactor is a consequence of insufficient light availability, given not only by the low light ratio but also by the clear PVC partial blockage. Aerial net productivities at steady state for 1/1 and 4/1 D/L are similar to the productivity values achieved in the continuous outdoor system for *Nannochloris* sp. in Chapter 3 (43.4 g/m^2/day at 6 HRT). The area receiving direct light from the sun was 2 1/2 times greater for the 1/1 D/L bioreactor compared to the 4/1 D/L bioreactor and the outdoor continuous system.

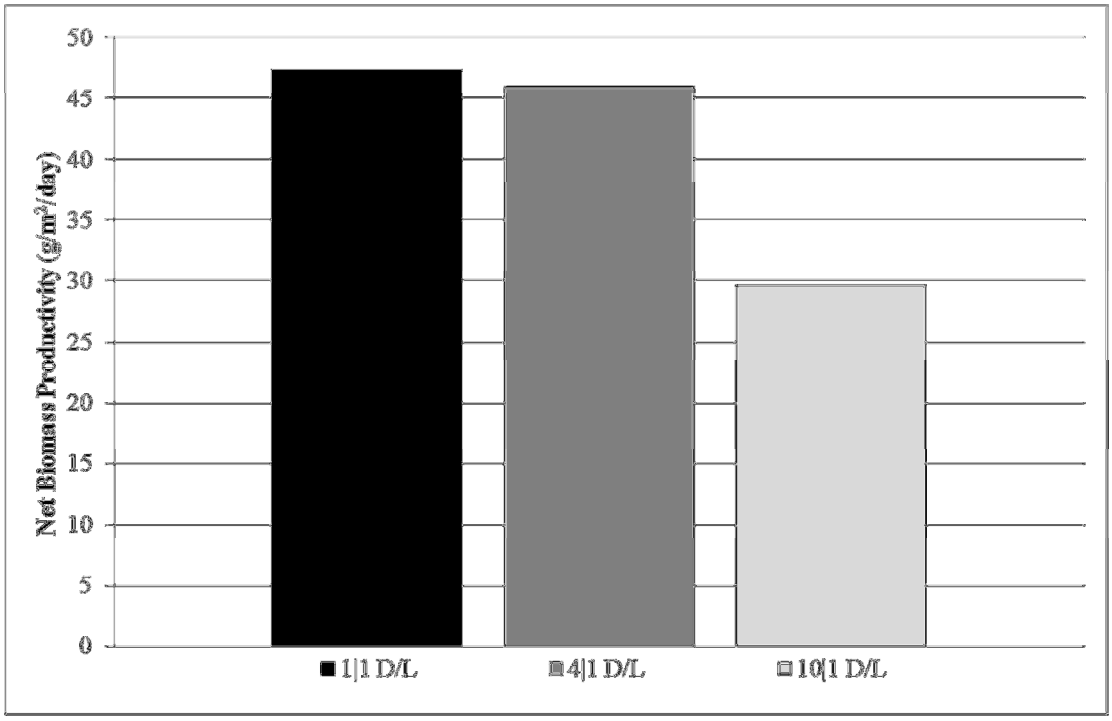

Figure 4.13. Net aerial productivities for the three bioreactors at steady state.

4.4.2. Growth Rate

Growth rates followed a similar trend for all three bioreactors (Figure 4.14). As found during the indoor experiments, the growth rates were D/L ratio dependent in the outdoor systems as well. On day one, the bioreactor operated at 4/1 D/L had the highest μ, followed by 1/1 and 10/1 D/L. While the 1/1 D/L bioreactor reached its max growth rate, μ_{max}, during day one of operation, the other two did not reached their maximum growth until after day one. The μ_{max} for 1/1 and 10/1 were observed on the 2nd and 4th day, respectively. After μ_{max} was achieved, growth rates progressively decreased with time and increase in cell concentration. Once the semi-continuous operation was initiated, the growth rates plateau for all bioreactors, maintaining values of approx. 0.03 h^{-1} (0.245 d^{-1}) and matching the dilution rate (0.25 d^{-1}). These findings are the result of one single run; therefore a triplicate run is necessary to conclude on a possible trend in growth rates.

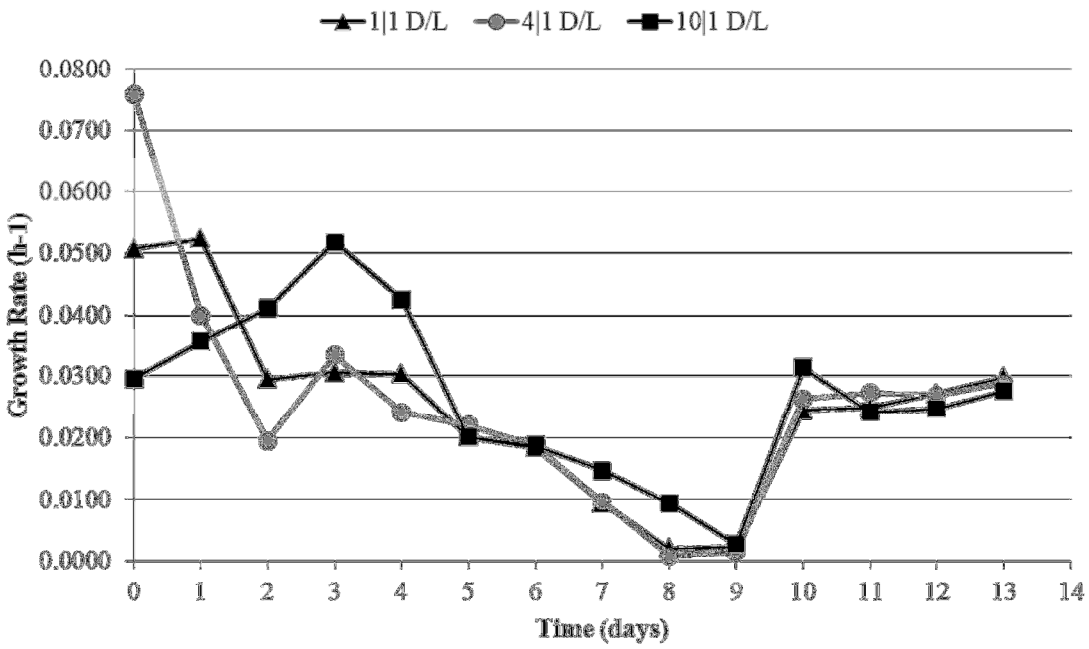

Figure 4.14. Growth rates changes versus time for 1/1, 4/1 and 10/1 D/L bioreactors.

4.5. Conclusion

An indoor photobioreactor system with an D/L alternation system was constructed in order to investigate *Nannochloris* sp. growth characteristics under intermittent illumination using high intensity lights (2000 μmols/s/m^2), mimicking the peak intensity of the sun during a clear summer day. The results obtained here indicate that enhancement of the photosynthetic utilization of high intensity light due to light modulation can be achieved. The algal cultures under flashing light with low frequencies (<3.2 Hz) and higher light periods reached lower growth rates and productivities than those performed under medium and higher frequencies (>3.2 Hz). However both growth rates and cell concentrations were at maximum under medium light cycle ratio (4/1 D/L) and medium frequencies (6.4-25.6 Hz), and progressively decreased with further increases in D/L ratio and frequency. Light efficiency measurements based on chlorophylls content showed that efficiency can be significantly improved by applying medium

durations of medium light fractions. Chlorophyll measurement results were interrelated with the cell concentrations and growth rates. The biomass cell concentration and growth rate found under intermittent light was higher than those obtained under continuous light, at every D/L ratio studied.

Outdoor studies suggested that productivities could be significantly maximized by increasing the culture volume for a given light exposed area if an optimum D/L ratio is maintained. These results could have significant impact on the outdoor productivities and bioreactor raceway designs. The practical outcome of the present work is to increase aerial yield and lower infrastructure cost by improved light utilization and culture circulation.

4.6. References

American Public Health Association (APHA), American Water Works Association (AWWA), (WEF), W.E.F., 2009. Standard Methods of the Examination of Water and Wastewater. Wachington D.C.

Baroli, I., Melis, A., 1996. Photoinhibition and repair in Dunaliella salina acclimated to different growth irradiances. Planta (Heidelberg) 198(4), 640-646.

EPA, E.P.A.U.S., 2011. ESS Method 340.2: Total SuspendedSolids, Mass Balance, Volatile Suspended Solids. EPA. http://www.epa.gov/greatlakes/lmmb/methods/methd340.pdf.

Fernandez, F.G.A., Sevilla, J.M.F., Perez, J.A.S., Grima, E.M., Chisti, Y., 2001. Airlift-driven external-loop tubular photobioreactors for outdoor production of microalgae: assessment of design and performance. Chemical Engineering Science 56(8), 2721-2732.

Grima, E.M., Fernandez, F.G.A., Camacho, F.G., Chisti, Y., 1999. Photobioreactors: light regime, mass transfer, and scaleup. Journal of Biotechnology 70(1-3), 231-247.

Grobbelaar, J.U., 1991. The influence of light dark cycles in mixed algal cultures on their productivity Bioresource Technology 38(2-3), 189-194.

Grobbelaar, J.U., Kroon, B.M.A., Burgerwiersma, T., Mur, L.R., 1992. Influence of medium frequency light dark cycles of equal duration on the photosynthesis and respiration of chlorella-pyrenoidosa. Hydrobiologia 238, 53-62.

Grobbelaar, J.U., Nedbal, L., Tichy, V., 1996. Influence of high frequency light/dark fluctuations on photosynthetic characteristics of microalgae photoacclimated to different light intensities and implications for mass algal cultivation. Journal of Applied Phycology 8(4-5), 335-343.

Hortensteiner, S., Krautler, B., 2011. Chlorophyll breakdown in higher plants. Biochimica et Biophysica Acta 1807(8), 977-988.

Janssen, M., de Bresser, L., Baijens, T., Tramper, J., Mur, L.R., Snel, J.F.H., Wijffels, R.H., 2000. Scale-up aspects of photobioreactors: effects of mixing-induced light/dark cycles. Journal of Applied Phycology 12(3-5), 225-237.

Janssen, M., de Winter, M., Tramper, J., Mur, L.R., Snel, J., Wijffels, R.H., 2000. Efficiency of light utilization of Chlamydomonas reinhardtii under medium-duration light/dark cycles. Journal of Biotechnology 78(2), 123-137.

Janssen, M., Kuijpers, T.C., Veldhoen, B., Ternbach, M.B., Tramper, J., Mur, L.R., Wijffels, R.H., 1999. Specific growth rate of Chlamydomonas reinhardtii and Chlorella sorokiniana under medium duration light dark cycles: 13-87 s. Journal of Biotechnology 70(1-3), 323-333.

Jeffrey, S.W., Humphrey, G.F., 1975. New spectrophotometric equations for determining chlorophylls a, b, c1 and c2 in higher plants, algae and natural phytoplankton.

Jiang, J.-G., Zhu, Y.-H., 2010. Preliminary and comparative studies on the cultivations of dunaliella salina between outdoors and in the photobioreactor. Journal of Food Process Engineering 33(1), 104-114.

Katsuda, T., Shimahara, K., Shiraishi, H., Yamagami, K., Ranjbar, R., Katoh, S., 2006. Effect of flashing light from blue light emitting diodes on cell growth and astaxanthin production of Haematococcus pluvialis. Journal of Bioscience and Bioengineering 102(5), 442-446.

Kim, Z.H., Kim, S.H., Lee, H.S., Lee, C.G., 2006. Enhanced production of astaxanthin by flashing light using Haematococcus pluvialis. Enzyme and Microbial Technology 39(3), 414-419.

Larkum, A.W.D., Douglas, S.E., Raven, J.A., 2003. Photosynthesis in algae. Kluwer Academic. Dordrecht, Boston.

Lee, C.G., Palsson, B.O., 1994. High-density algal photobioreactors using light-emitting-diodes. Biotechnology and Bioengineering 44(10), 1161-1167.

Marshall, J.S., Huang, Y., 2010. Simulation of light-limited algae growth in homogeneous turbulence. Chemical Engineering Science 65(12), 3865-3875.

Mata, T.M., Martins, A.A., Caetano, N.S., 2010. Microalgae for biodiesel production and other applications: A review. Renewable & Sustainable Energy Reviews 14(1), 217-232.

Melis, A., 1999. Review: Photosystem-II damage and repair cycle in chloroplasts: what modulates the rate of photodamage in vivo? Trends in Plant Science 4, 130-135.

Merchuk, J.C., Ronen, M., Giris, S., Arad, S., 1998. Light/dark cycles in the growth of the red microalga Porphyridium Sp. Biotechnology and Bioengineering 59(6), 705-713.

Miron, A.S., Camacho, F.G., Gomez, A.C., Grima, E.M., Chisti, Y., 2000. Bubble-column and airlift photobioreactors for algal culture. Aiche Journal 46(9), 1872-1887.

Nedbal, L., Tichy, V., Xiong, F.H., Grobbelaar, J.U., 1996. Microscopic green algae and cyanobacteria in high-frequency intermittent light. Journal of Applied Phycology 8(4-5), 325-333.

Ogbonna, J.C., Tanaka, H., 2000. Light requirement and photosynthetic cell cultivation - Development of processes for efficient light utilization in photobioreactors. Journal of Applied Phycology 12(3-5), 207-218.

Park, K.-H., Lee, C.-G., 2000. Optimization of algal photobioreactors using flashing lights. Biotechnology and Bioprocess Engineering 5(3), 186.

Park, S., Khamai, P., Garcia-Cerdan, J.G., Melis, A., 2007. REP27, a tetratricopeptide repeat nuclear-encoded and chloroplast- localized protein, functions in D1/32-kD reaction center protein turnover and photosystem II repair from photodamage. Plant Physiology 143(4), 1547-1560.

Rier, S.T., Stevenson, R.J., LaLiberte, G.D., 2006. Photo-acclimation response of benthic stream algae across experimentally manipulated light gradients: A comparison of growth rates and net primary productivity. Journal of Phycology 42(3), 560-567.

Seyedeh Fatemeh, M., Bryce, R., Nik, W., 2012. Spectral conversion of light for enhanced microalgae growth rates and photosynthetic pigment production. Bioresource Technology 125, 75-81.

Suh, I.S., Lee, C.G., 2003. Photobioreactor engineering: Design and performance. Biotechnology and Bioprocess Engineering 8(6), 313-321.

Tanaka, A., Melis, A., 1997. Irradiance-dependent changes in the size and composition of the chlorophyll a-b light-harvesting complex in the green alga Dunaliella salina. Plant and Cell Physiology 38(1), 17-24.

Theegala, C.S., Suleiman, A.A., Carriere, P.A., 2007. Toxicity and biouptake of lead and arsenic by Daphnia pulex. Journal of Environmental Science & Health, Part A: Toxic/Hazardous Substances & Environmental Engineering 42(1), 27-31.

Wahal, S., Viamajala, S., 2010. Maximizing Algal Growth in Batch Reactors Using Sequential Change in Light Intensity. Applied Biochemistry and Biotechnology 161(1-8), 511-522.

Weller, S., Franck, J., 1941. Photosynthesis in flashing light. Journal of Physical Chemistry 45(9), 1359-1373.

Wood, A.M., 1979. Chlorophyll a:b ratios in marine planktonic algae. Journal of Phycology 15(3), 330-332.

Xue, S., Su, Z., Cong, W., 2011. Growth of Spirulina platensis enhanced under intermittent illumination. Journal of Biotechnology 151(3), 271-277.

Yang, D.-H., Webster, J., Adam, Z., Lindahl, M., Andersson, B., 1998. Induction of acclimative proteolysis of the light-harvesting chlorophyll a/b protein of photosystem II in response to elevated light intensities. Plant Physiology (Rockville) 118(3), 827-834.

Yokthongwattana, K., Chrost, B., Behrman, S., Casper-Lindley, C., Melis, A., 2001. Photosystem II damage and repair cycle in the green alga Dunaliella salina: Involvement of a chloroplast-localized HSP70. Plant and Cell Physiology 42(12), 1389-1397.

Yoon, J.H., Shin, J.-H., Ahn, E.K., Park, T.H., 2008. High cell density culture of Anabaena variabilis with controlled light intensity and nutrient supply. Journal of Microbiology and Biotechnology 18(5), 918-925.

Yoshimoto, N., Sato, T., Kondo, Y., 2005. Dynamic discrete model of flashing light effect in photosynthesis of microalgae. Journal of Applied Phycology 17(3), 207-214.

Zijffers, J.W.F., Schippers, K.J., Zheng, K., Janssen, M., Tramper, J., Wijffels, R.H., 2010. Maximum Photosynthetic Yield of Green Microalgae in Photobioreactors. Marine Biotechnology 12(6), 708-718.

CHAPTER 5
MODELING THE LIGHT DYNAMICS AND THEIR IMPACT ON BIOMASS PRODUTIVITY AND GROWTH RATE IN AN OUTDOOR CONTINUOUS-FLOW SYSTEM

5.1. Introduction

Volatile oil prices observed from 2000 to the present have renewed interests in alternative fuels and mounting evidence of global climate change raised concern over the carbon footprint of using fossil fuels. The desire to reduce reliance on foreign oil imports and to improve energy security sparked interests in research and development of alternative fuels derived from microalgae, which has shown the potential to transform radiant energy into valuable fuel products and provide possible solutions to global warming and environmental problems.

Mass cultivation of microalgae has significant industrial potential, and therefore the growth of algal cultures is of great practical interest (Merchuk et al., 1998). Although several technologies for microalgae growth were optimized, the need to further upscale the commercial production has been recognized in recent literature (Chisti, 2007; Raja et al., 2008). Outdoor continuous systems is believed to make this technology more affordable (Miron et al., 2000; Chisti, 2007). Mathematical modeling is a very useful tool for design and optimization of bioprocesses. As the interest of microalgal mass culture increases, kinetic modeling of microalgal photosynthesis and/or growth is of significant importance because an accurate model is a prerequisite for designing an efficient photobioreactor, predicting process performance, and optimizing operating conditions.

A continuous culture bioreactor is an essential technique in generating steady-state productivities. Once steady-state is reached, the culture condition, biomass concentration,

biomass composition and growth are constant over time (Droop, 1975). Therefore, it is superior to batch culture for a number of purposes. The net specific growth rates and productivity in continuous outdoor cultures are directly dependent on the temperature, nutrient addition rate, incident light, and dilution rate in the system (Asenjo and Merchuk, 1994). When temperature and nutrients do not limit growth (i.e., when light is the only growth-limiting factor), productivity will depend on the irradiance on the culture surface and on how efficiently radiant energy is converted into chemical energy (Tredici and Zittelli, 1998). For example, light cannot be assumed to be distributed homogeneously in a reactor due to self-shading, which causes the incident light to progressively attenuate as it passes through the culture. Productivity is increased at higher solar irradiances because light penetration into the culture is greater and a greater portion (depth) of the culture is exposed to light, although light utilization efficiency is significantly reduced (Grima et al., 1999; Taulbee et al., 2005; Grobbelaar, 2009; Becerra-Dorame et al., 2010; Fanta et al., 2010). Light availability can be controlled by providing different dilution rates to the system, and optimize the system to a desired biomass concentration by varying the dilution rate so that light penetrates deeper in the culture (Grima et al., 1994; Grima et al., 1996). However, predicting the exact effect of light availbility in a continuous culture is not straightforward.

Many researchers have suggested various kinds of mathematical models on algal growth kinetics and/or photosynthesis over the years (Steele, 1965; Bannister, 1979; Aiba, 1982; Evers, 1991; Grima et al., 1994; Prokop et al., 1995; Fernandez et al., 1997; Rubio et al., 2003). These models differ in the way they express the light dependency of microalgal photosynthesis. In some models, the algal photosynthesis is assumed to be dependent on the average photon flux density obtained by volume-averaging the spatial distributed photon flux density inside the

photobioreactor (Grima et al., 1994; Prokop et al., 1995); other models use the volume-averaged photon absorption rate (Aiba, 1982), while others are based on more sophisticated theories that individual algal cells respond to the photon flux density upon their local position (Evers, 1991; Cornet et al., 1992; Cornet et al., 1992). An extended discussion on different models is presented in the Background and Literature review chapter (Chapter 2) of this thesis. Although these mathematical models can fit the observed data well by adjusting the parameters properly, they do not prove to be adequate to explain the dynamic variation in photosynthesis. One reason is because most of these models express the cells response to irradiance in a static way. In natural conditions the cells experience an extremely variable irradiance during the day. In order to estimate photosynthetic production accurately, it is essential to incorporate the dynamic aspects into the photosynthetic models.

This chapter describes a deterministic model developed to describe and investigate the light-limited growth and productivity on outdoor continuous-flow bioreactors operated at various dilution rates. Therefore, the following only applies to situations in which nutrients are present in excess or is not a limiting factor. The objectives of this work was to develop a light-limited-based model for algal growth, calibrate the model against bench scale continuous-flow outdoor bioreactors, and predict the effect of average light availability on algal growth and productivity.

5.2. Materials and Methods

5.2.1 Outdoor Culture System and Data Acquisition

Experiments aimed at maximizing the biomass production in an outdoor continuous system were completed during the months of June and July (2011), at Louisiana State University (Baton Rouge, LA). The experiments were conducted in twelve 75 L, 40 cm deep plastic round containers, which had an overflow port at 36 cm from the bottom. The total liquid volumes of the

cultures were 55 L. The system was operated in continuous mode at 6, 12, 18 and 24 hours hydraulic retention times until biomass reached steady state. The sterilized media (F/2 stock media, Pentair Aquatic Eco-Systems Inc., Apopka, FL) required for the daily flow was stored in a 2,100 L aerated fiberglass tank. To minimize contamination, the tank was covered with a tarp and a 1/5 HP (Item # JGP12000 Jebao, World Pump, Tucson, AZ) pump was used to continuously circulate the media through a series of 3 UV sterilizers (Gamma Model #1400-8W, Vista, CA).The flows were maintained from 8 am to 8 pm, the time representing approximate sunlight hours in the summer in Louisiana. The flows were stopped daily at 8 pm to avoid overnight flushout of the active algae cultures. A comprehensive description of the set-up was already presented in Chapter 3, Figure 3.1.

Selenastrum capricornutum (Cat. no. 1648, UTEX, TX) was used as inoculum for all 55 L cultures and was maintained as the dominant species under field conditions for this experiment. The biomass density (mg/L) was estimated from optical density readings and regressed against Total Suspended Solids culture samples (American Public Health Association (APHA) et al., 2012).

A Photosynthetic Light (PAR) Smart Sensor and HOBO Micro Station Data Logger (S-LIA-M003, H21-002, Onset®, Bourne, MA) was used to continuously (day and night) measure the Photosynthetic Photon Flux Density (PFFD) as PAR ($\mu mol/s/m^2$) at the top surface of the culture. Additionally, once the cultures reached steady state, PAR measurements were performed for each bioreactor in triplicate, at three different depths into the culture column (7.6, 17.8 and 28 cm from top surface). This information was further used in the light and growth studies described below.

Temperatures of the cultures were continuously monitored with a HOBO DataLogger (U12-008, Onset®, Bourne, MA). The average day time high and night time low temperatures during the tested period were 38°C and 23°C. All experiments were performed in triplicate for further statistical validity.

5.2.2. Governing Equation

The governing equation in the bioreactor was based on a mass balance on biomass concentration around the reactor:

$$\frac{\partial X}{\partial t}V = Q_{in}X_{in} - Q_{out}X + UXV \quad \text{(Eq. 5.1)}$$

where: X_{in} = algal concentration entering the system (g dry wt m^{-3})

X = algal concentration leaving the system (g dry wt m^{-3})

Q_{in} = flow rate entering the system (m^3/day)

Q_{out} = flow rate leaving the system (m^3/day)

V = volume of bioreactor (m^3)

U = net specific growth rate (day^{-1})

t = time (days)

Under the assumption that the concentration of biomass in the inflow was always 0 (X_{in}=0 g dry wt m^{-3}) the equation reduces to:

$$\frac{\partial X}{\partial t}V = -Q_{out}X + UXV \quad \text{(Eq. 5.2)}$$

5.2.2.1. Growth Kinetics

Dividing the last term of Equations 5.1 and 5.2 by volume (V) yields the net biomass growth occurring in each bioreactor, and can be rewritten as:

$$UX = \mu X - k_d X \quad \text{(Eq. 5.3)}$$

where: μ = growth rate (h^{-1})

k_d = decay rate (h^{-1})

Models for light dependent growth rates have been well documented over the years (Aiba, 1982; Fernandez et al., 1997; Grima et al., 1999; Fredrickson and Tsuchiya, 1977). Steele's equation (Steele, 1965), is an exponential peak shaped function which was and still is widely used in microbiological modeling projects, mainly because of its simplicity and photoinhibition related parameters (Packer et al., 2011; Fredrickson and Tsuchiya, 1977). Steeles's model was also used for this modeling chapter:

$$\mu = \mu_{max} \frac{I_a}{I_{opt}} e^{1 - \frac{I_a}{I_{opt}}} \quad \text{(Eq. 5.4)}$$

where: I_a = average PAR intensity ($\mu mol/sec/m^2$)

I_{opt} = PAR intensity at which μ achieves its maximum value (μ_{max}) ($\mu mol/s/m^2$)

The decay rate (k_d) is known and expected to increase with cells average age (Wouter and Kohki, 2009). The average cell age it is often estimated by calculating the average cell residence time in a reactor (τ) which is function of dilution rate (D):

$$\tau = D^{-1} \quad \text{(Eq. 5.5)}$$

The value of k_d for fresh water phytoplankton has been reported to range from 0.1-0.5 d^{-1}, depending on the environments the cells are exposed to (Barsanti and Gualtieri, 2005; Rier et al., 2006; Eriksen, 2008; Chen et al., 2011). The decay rate does not necessarily mean death of a cell. Decay rate is also used as a term to express photorespiration and dark respiration processes, which results in a net loss of carbon from the cell (Zhang et al., 1997). For consistency, in this chapter the decay rate term will be used to represent the death rate, photorespiration, and dark

respiration all together. It has been suggested that the decay rate can significantly impact the growth rate of a cell and that it is light intensity dependent (Burris et al., 1977; Eriksen, 2008). As photosynthesis does not occur at night, the decay rate is much higher compared to the decay rate during the day (Zhang et al., 1977). The term k_d is assumed to be proportional to the ratio of the light deficit and the optimum light in the reactor.

$$k_d = k_{max} \frac{I_{opt} - I_a}{I_{opt}} \quad \text{(Eq. 5.6)}$$

where k_{max} = maximum decay rate (h^{-1}). As average light intensity approaches minimum values the decay rate increases, reaching the maximum when light is unavailable.

5.2.2.2. Light Dynamics

In moderate density cultures (< 1000 mg/L biomass concentration), the irradiance at a given depth in a reactor can be calculated for a specified surface intensity using Lambert-Beer Law (Camacho et al., 1999; Evens et al., 2000). Irradiance at any depth is a function of the intensity at the surface, multiplied by the antilog of the negative extinction coefficient at that depth:

$$I_z = I_0 e^{-k_c z} \quad \text{(Eq. 5.7)}$$

where: I_z= PAR ($\mu mol/s/m^2$) at z depth

I_0 = the PAR surface intensity ($\mu mol/s/m^2$)

k_c = the culture attenuation coefficient (cm^{-1})

z = depth (cm)

In algal cultures, the light availability varies along the depth of the culture vessel because of the culture light attenuation (k_c). Additionally, since algae respond to the average light intensity to which they are exposed as a physiological adaptation, it is important that this

parameter (k_c) be calculated (Grima et al., 1994). The k_c was estimated through a nonlinear regression of measured I_z versus the known depth *z* for each HRT treatment. X was factored into k_c in the exponential equation since the overall attenuation coefficient is a function of culture (k_a) and biomass (X) (Benson et al., 2008):

$$k_c = k_a{*}X \qquad \text{(Eq. 5.8)}$$

where, k_a = the culture attenuation coefficient (L/mg/cm). The depth-integrated light I_a as a function of I_0 and biomass X, can be calculated by integrating the Lambert-Beer equation (Eq.5.6) over the depth of the reactor (d):

$$I_a = \frac{1}{d}\int_0^d I_z dz = \frac{I_0}{k_a X d}\left(1\text{-}e^{-k_a X d}\right) \qquad \text{(Eq. 5.9)}$$

The mathematical model determines the distance of an incident ray of light from the top surface to any point inside the culture and estimates the local irradiance taking into account the light attenuation due to biomass.

The complete governing equation (Eq. 5.2) around the bioreactor expands to:

$$\frac{\partial X}{\partial t}V = -QX + \left(\mu_{max}\,\frac{\frac{I_0}{k_a X d}\left(1\text{-}\,e^{-k_a X d}\right)}{I_{opt}}\,e^{\left(1-\frac{\frac{I_0}{k_a X d}\left(1-e^{-k_a X d}\right)}{I_{opt}}\right)} - k_{max}\left(\frac{I_{opt} - \frac{I_0}{k_a X d}\left(1-e^{-k_a X d}\right)}{I_{opt}}\right)\right)XV \qquad \text{(Eq. 5.10)}$$

5.3. Model Development

Using an approach similar to that used by Benson et al., (2008), a model was developed that integrated the mass balance analysis around the bioreactor with light dynamics and the effect of light on microalgal growth kinetics. The specific growth rate for each system is unique to each module. Since different flow rates are applied to the system, this will control the light availability in the bioreactor water column, which will directly impact the growth rate of biomass in the

bioreactor. Using this information, the model is capable of estimating the biomass generated within the bioreactor.

The model (Fig. 5.1) was integrated using STELLA®9.0.2 modeling platform (isee Systems Inc., Lebanon, NH). In a continuous culture, the biomass productivity is a function of the cell concentration X (mg/L) in the effluent and the dilution rate (Grima et al., 1999). The daily microalgal volumetric productivity (Pv, g/m^3/day) of the model is represented in the outflow, which takes the biomass concentration from the reactor and multiplies it by the specific dilution rate (Q/V). To acquire the areal productivity Pa, the volumetric productivity was multiplied by the cultures total depth (0.3556 m).

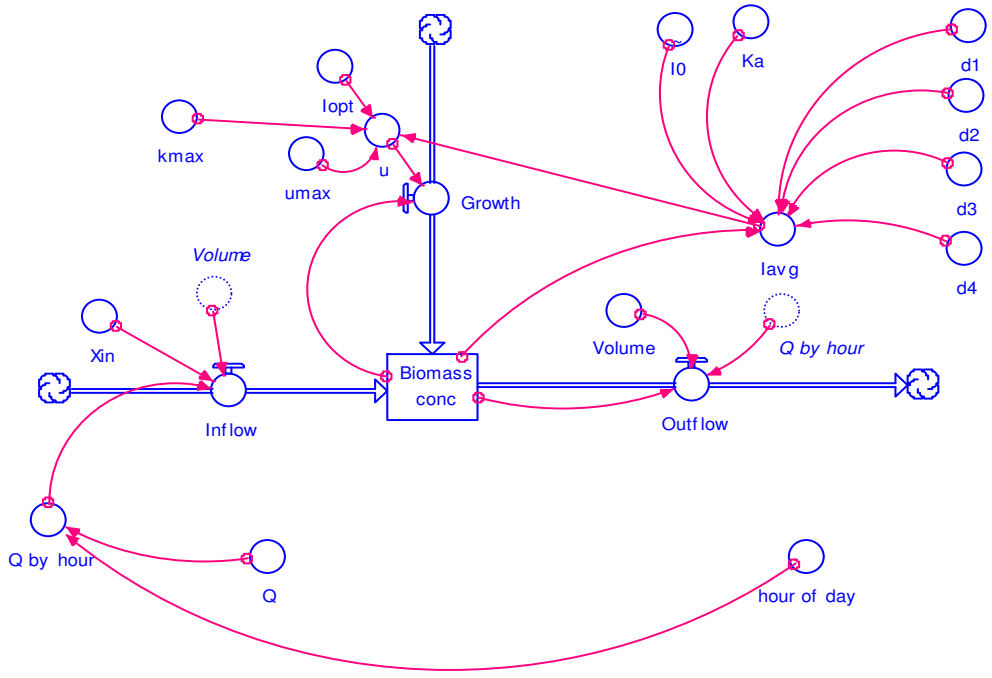

Figure 5.1. The Stella diagram productivity model of the light dynamics and growth kinetics in the bioreactor.

The model included the integrated Lambert-Beer equation over the reactors depth at the instant biomass concentration in the reactor at that time, to determine the instantaneous average intensity. Four depths points, 7.6, 17.8, 28 and 35.5 cm from top surface (represented by d1, d2,

d3 and d4 in the model), giving four depth intervals, were used to calculate I_a of the total average irradiance within the bioreactor columns. Three out of the four depths represent the depths at which manual irradiance measurements from actual experiments were acquired, namely 7.6, 17.8 and 28 cm from top surface. The irradiance at 35.5 cm from top surface was calculated using Eq. 5.7. The light at each of these depths was calculated using Eq. 5.7. The average light (I_a) within each interval was determined by implementing Eq. 5.9, and then all four intervals were averaged to calculate the total I_a within the bioreactor. Since surface intensity, I_0, varies during the day it was inputted as a hourly graphical function in the model. The graphical function measured for I_0 during the month of June in Baton Rouge, LA, is plotted in Figure 5.

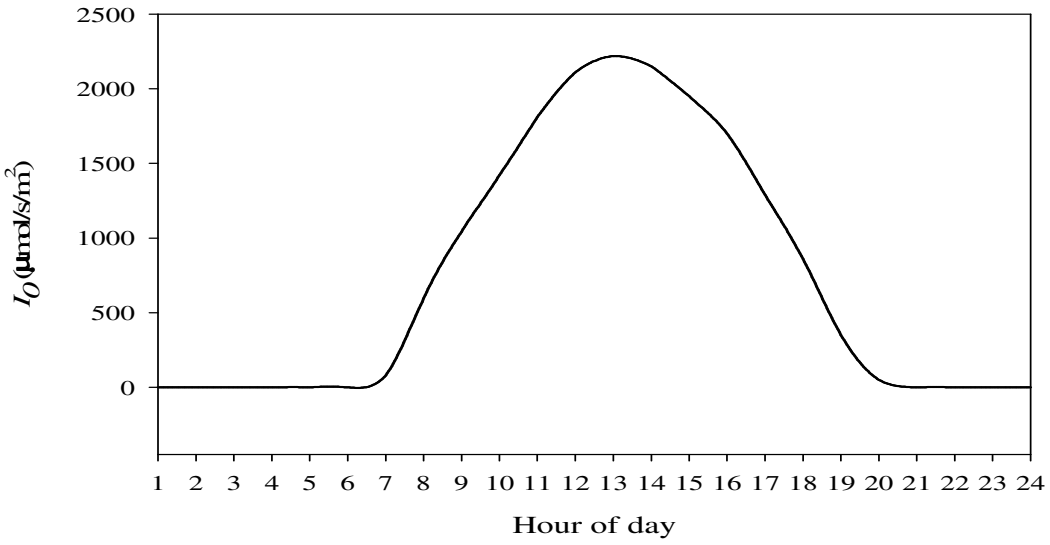

Figure 5.2. Direct surface irradiance measured during the day for the month of July (2011).

Beer-Lamberts law (Eq. 5.7) was used to describe light penetration in the microalgal culture. The results were compared to actual manual measurements performed for the outside continuous culture at steady state. The results are presented in Table 5.1. The value at 0 cm depth was the average outdoor irradiance measured at the time of data collection. This value (2110

μmol/s/m^2) was used as I_0 to calculate I_z and I_a. Table 5.1 shows a minimal difference between the values measured and calculated.

Table 5.1. Values of the measured and calculated I_z and I_a.

	Measured I_z (μmol/sec/m^2)				**Calculated I_z (μmol/sec/m^2)**			
HRT (h) / d (cm)	**6**	**12**	**18**	**24**	**6**	**12**	**18**	**24**
0	2110	2110	2110	2110	2110	2110	2110	2110
7.6	1231.4	858.7	591	325	1258.4	841.2	588.5	327.8
17.6	607.8	216.5	93.5	35.2	628.9	244.8	106.1	26.9
28	350.7	82.8	30.1	7.5	314.3	71.2	19.1	2.2
35.56	-	-	-	-	187.9	28.5	5.36	0.35
$I_{average}$	**1233.1**	**876.9**	**653.7**	**555.9**	**1255.2**	**904.4**	**662.8**	**494.1**

While growth kinetics at different PAR intensities are usually performed to investigate I_{opt}, in our study the maximum growth rate observed was at the beginning of the experiment, when the biomass concentration was low. To estimate the I_{opt}, a regression analysis was performed that included the average light available in the reactor and TSS measured during the outdoor experiments. Regression results showed that optimum growth (μ_{max}) conditions take place in the vicinity of 1800 μmol/s/m^2 PAR irradiance (R^2=0.99). Therefore this value was used as I_{opt} for modeling the growth rate in Eq. 5.4.

The maximum cell-specific growth rate, $\mu_{max,}$ represents the highest growth rate attainable during the exponential growth phase. The maximum cell growth rate for this modeling effort was used after computing the regression analysis of the observed growth rates from the biomass accumulation in the outdoor study. A simple exponential decay equation was generated which fit our data (R^2>0.97). The maxim value of μ is given by the μ_{max} term in the exponential equation (Fig. 5.3). Four maximum growth rates μ_{max} (day^{-1}) were generated, representing the maximum growth capacities achieved at each treatment. These values were further used in Eq. 5.4 to calculate the growth at each time interval used in the model.

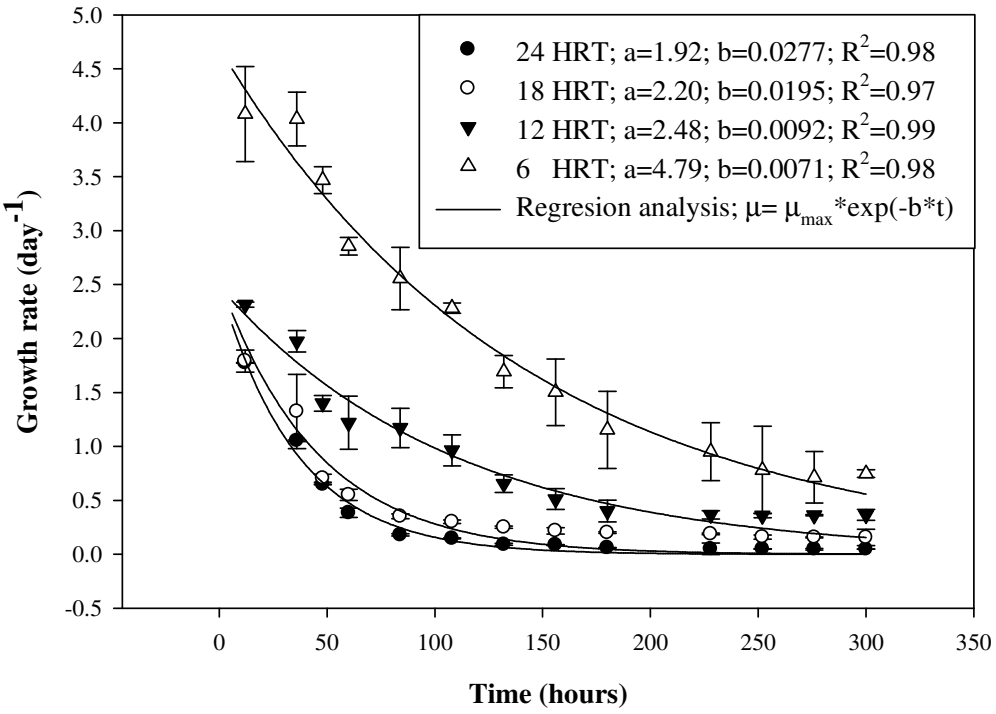

Figure 5.3. Growth rates calculated for the outdoor system versus time. The continuous lines represent regression analysis used to find μ_{max} for each of HRT's applied to the system.

The k_c was estimated through a nonlinear regression of measured I_z versus the known depth *z* for each HRT (Figure 5.4). To calculate k_a, the k_c term (b coefficient in Figure 5.3) was divided by X at steady-state in the culture for each HRT studied, and the mean average values from triplicate reading was used in the model. Values reported for k_a in literature for cultures grown under natural incident radiation were found to range from 0.0001-0.0025 L/mg·cm (Dubinsky and Berman, 1979; Jorgensen, 1979; Kirk, 1983). The k_a values in our study were in between 0.001113-0.002052 L/mg·cm, which is within the reported range. Decay rate was calculated from the outdoor continuous-flow experiments, by calculating the growth rate between the biomass measured at 8 p.m and 8 a.m. A table containing a summary of the estimated experimental parameters used for the productivity model is presented in Table 5.2.

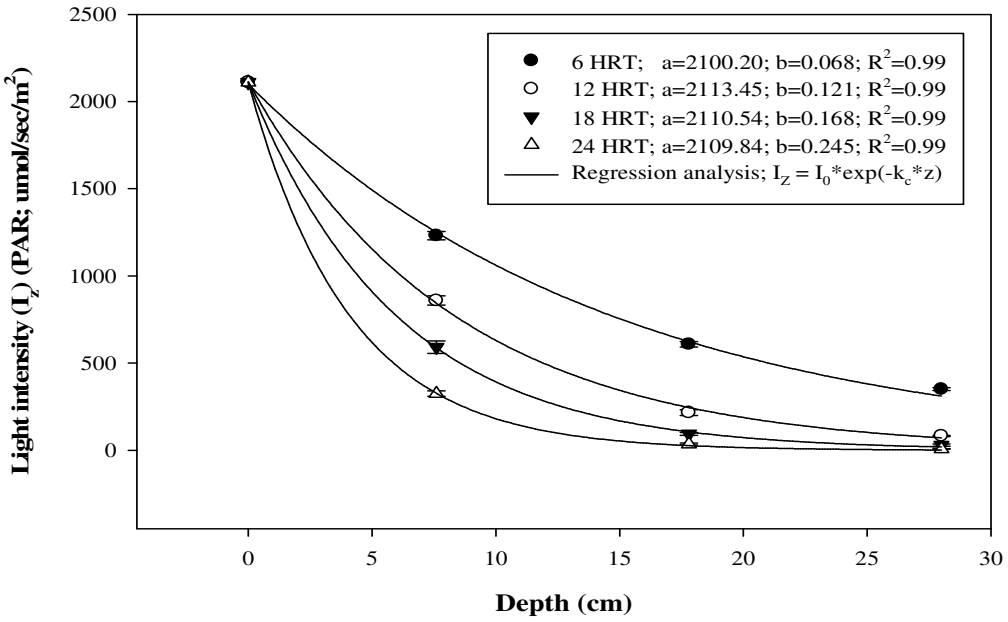

Figure 5.4. A plot of observed light irradiance (PAR) at given depth used to determine the light attenuation coefficent. Continuous line represents the regression analysis where "I_z" is the light intensity at depth "z", "I_0" the light intensity at surface and "k_c" the culture attenuation coefficient (Eq. 5.7)

Table 5.2. The summary of regression analysis for the estimated experimental parameters used for the productivity model.

Parameter	Theoretically calculated or Experimental estimation	R^2	P-value
I_0 (µmol/s/m^2)	0-2220		
I_{opt} (µmol/s/m^2)	1800	0.9968	<0.0001
k_a (L/mg·cm)			
If: HRT=6	0.001283	0.9956	<0.0001
HRT=12	0.001198	0.9936	<0.0001
HRT=18	0.001077	0.9926	<0.0001
HRT=24	0.001184	0.9945	<0.0001
μ_{max} (h^{-1})			
If: HRT=6	0.220	0.9878	<0.0001
HRT=12	0.104	0.9945	<0.0001
HRT=18	0.095	0.9712	<0.0001
HRT=24	0.080	0.9823	<0.0001
k_d (h^{-1})			
If: HRT=6	0.004		
HRT=12	0.011		
HRT=18	0.018		
HRT=24	0.025		

5.3.1. Model Calibration and Validation

The model simulations were compared against data collected from actual experiments (Fig 5.5). The data collected represent experiment performed in triplicate at four different treatments (6, 12, 18 and 24 h HRT).

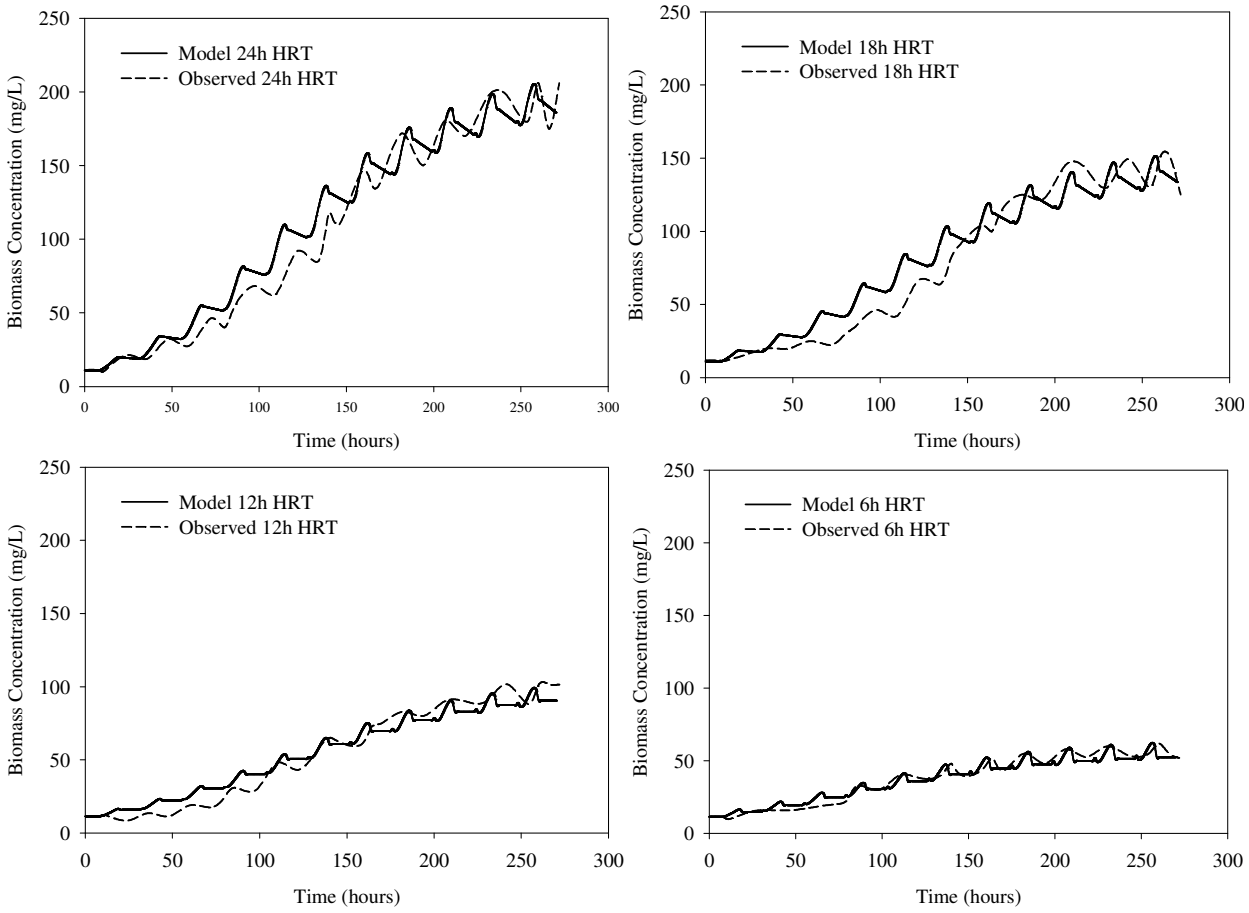

Figure 5.5. Comparison in change of biomass concentration for the four observed data sets and the productivity model simulations.

The four model simulations mimicked the outdoor experimental data. The simulated biomass concentrations over time are shown to correspond closely with the actual data. However there are a few noticeable alterations that need to be addressed. It can be noticed that at the beginning of the simulations, during the transition phase, there is a time period of 1-2 days

during which the model slightly overestimates the biomass concentrations. This phenomenon was previously observed in literature (Benson, 2003), and was accounted due to calibration of the models with data that had already reached steady-state. The overestimation reflects the cell adaptation period needed after inoculation. It has been reported that after inoculation, the algal cells experience a "lag" phase as they adapt to the new environmental conditions (Yang et al., 1998). This period of adaptation is dependent on the degree of change in conditions. In our experiments the inoculum cells were grown indoor in batch mode, under medium light intensity (200 μmol/s/m^2) and constant temperature (25°C). Hence, the algal cells required some time to adapt to the outdoor environment (~2000 μmol/s/m^2) and dilution rates (continuous cultures). Adaptation periods to high light irradiances were also noticed during the experiments described in Chapter 4.

In order to evaluate the validity of the models, the model projections were compared with the experimental results (Fig. 5.6). All models showed to successfully describe the experimental results and were able to predict biomass concentrations with high accuracy as confirmed by the R^2 values. Still, it was noticed that the prediction of the models showed some slightly deviations depending on the cell concentrations, i.e., marginally underestimating at low concentrations and overestimating at high concentrations. However, the under or over estimations were still within or very close to the 95% confidence interval.

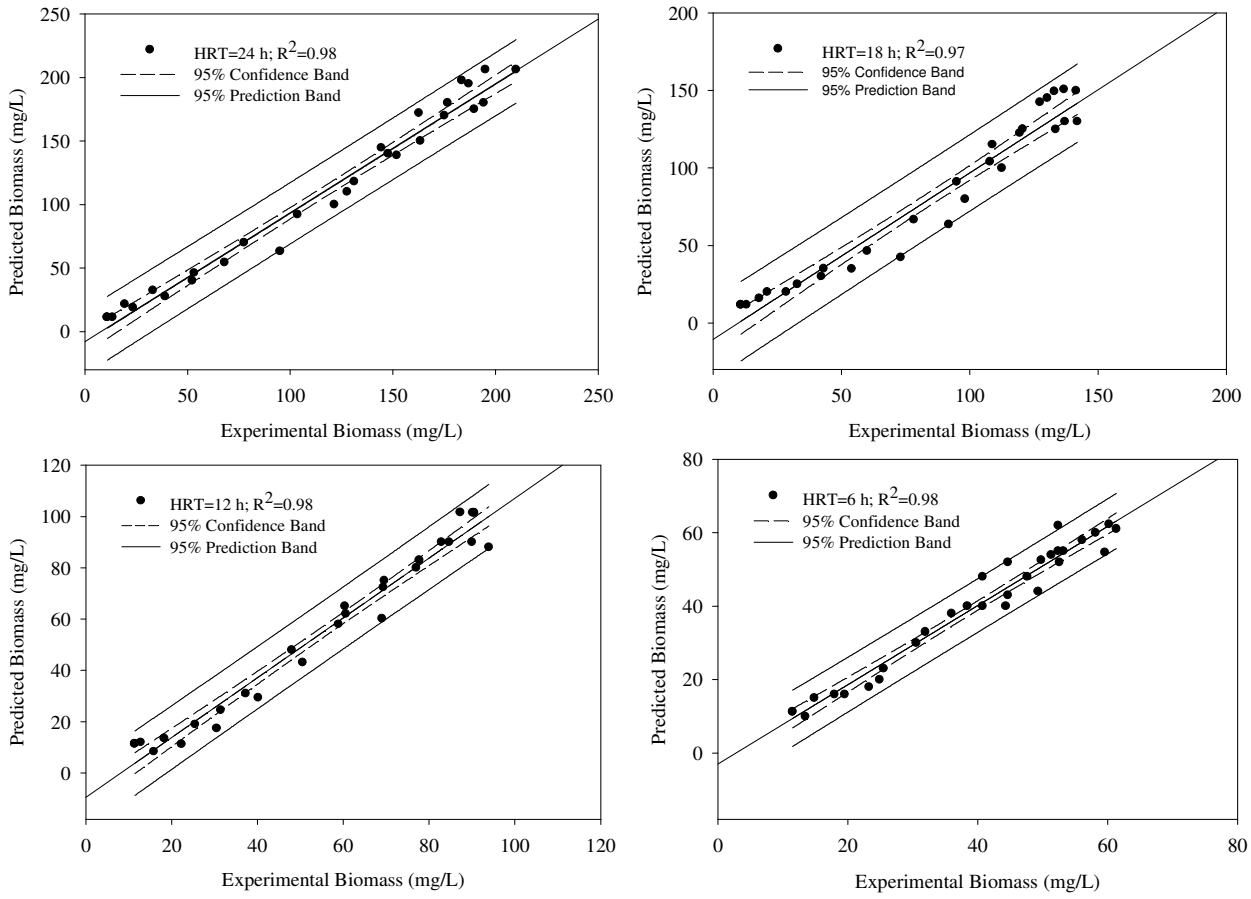

Figure 5.6. Comparison between experimental and results of the models at the four HRTs studied.

The Root Mean Square Error (RMSE) was also calculated for accuracy purposes. The RMSE was determined for the entire data set from the beginning until steady-state was achieved by using the RMSE formula:

$$\mathrm{RMSE} = \left(\frac{1}{n}\sum_{i=1}^{n}\left(\mathrm{model_i} - \mathrm{observed_i}\right)^2\right)^{\frac{1}{2}} \qquad \text{(Eq. 5.11)}$$

where: n=the number of samples included in the data set. The RMSE return values were 1.8, 3.6, 6.0, and 6.5 % for the data sets at 6, 12, 18 and 24 h HRT. A value below 20% RMSE is considered an acceptable value to validate a model (Acien Fernandez et al., 1998; Mendenhall and Sincich, 2007).

5.3.2. One set parameter model

Although the above model can fit the observed data well, it was developed by using the actual observed parameters during the outdoor continuous-flow experiments. The parameters showed to change with changing the light conditions in the outdoor experiments (Table 5.1). To fit the data well for each dilution rate, each parameter (μ_{max}, k_d, k_a) was different. A mathematical model that uses only one set of parameters is a more useful tool to predict the performance of a reactor and for optimizing the operating conditions.

A model that would fit the experimental data using the same parameters was created. The same light parameters values, I_0 and I_{opt}, as for the previous model was used. The light culture attenuation coefficients calculated for each dilution rate were averaged to result in one single k_a. The growth rate among the different dilution rates was calculated to peak at the lowest densities of the highest dilution rate (6 h HRT). Therefore, the maximum growth rate (μ_{max}) used was the maximum growth rate theoretically calculated by means of regression for the highest I_a(6 h HRT) data set. The maximum decay rate (k_{max}) value observed among the four dilution rates applied was used in the model. The maximum decay rate was observed at the lowest I_a (24 h HRT). A complete summary of the parameters used for the model are presented in Table 5.3.

Table 5.3. The summary of regression analysis for the estimated experimental parameters used for the productivity model.

Parameter	Theoretically calculated or Experimental estimation	R^2
I_0 (μmol/s/m^2)	0-2220	
I_{opt} (μmol/s/m^2)	1800	0.997
k_a (L/mg·cm)	0.001168	
μ_{max} (h^{-1})	0.23	0.986
k_{max} (h^{-1})	0.025	0.979

Efforts were made to validate the new model, called here the one parameter model. The result of the model using one set of parameters was compared with the observed data. The model showed to fit the data well with a RMSE of 15. However, a lower RMSE was desired for the model. To lower the error an adjustment to μ_{max} was made. Maximum growth was increased to a value of 0.23 h^{-1}, a 0.02 increase from the initial value of 0.21 h^{-1}. The new calibrated model was again compared to the experimental set of data (Fig. 5.7).

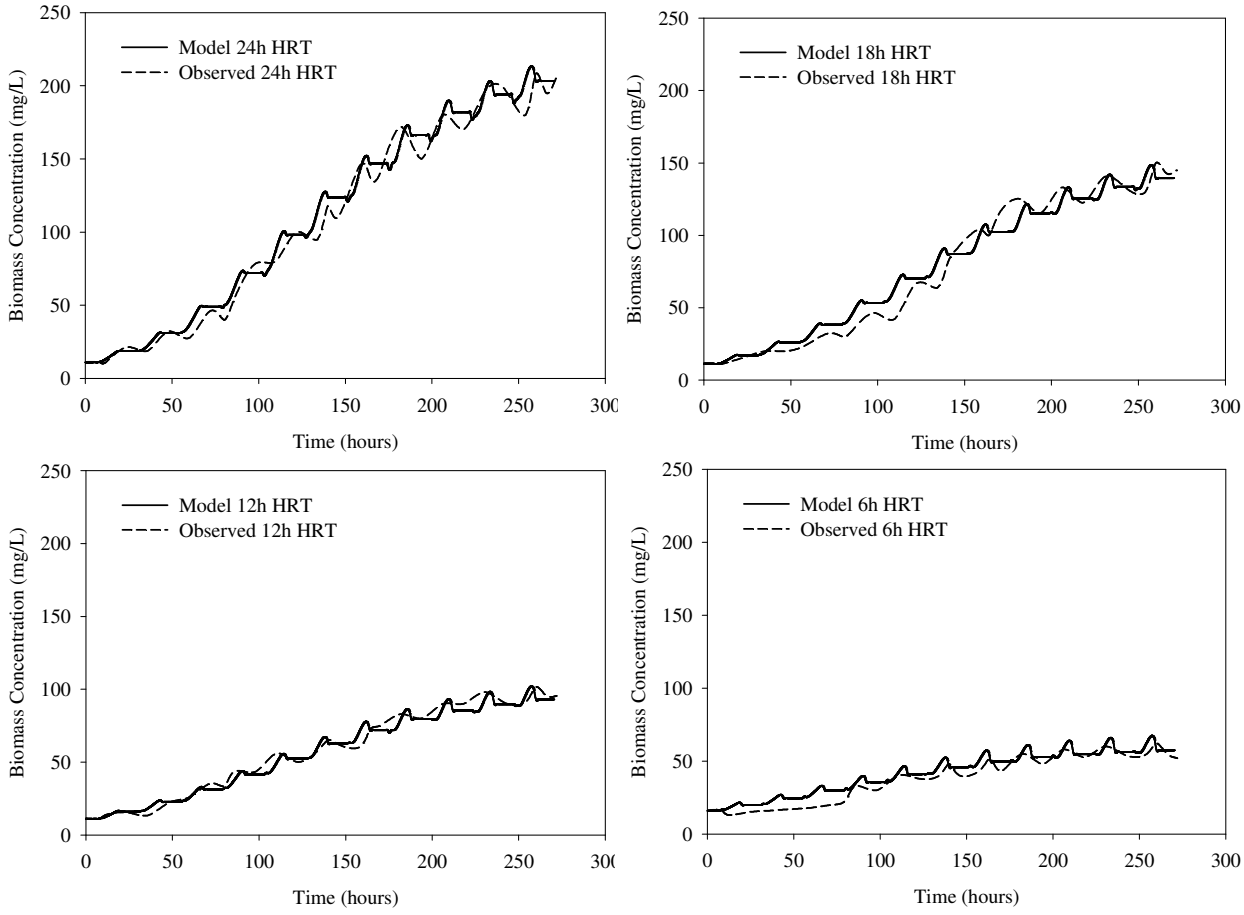

Figure 5.7. Comparison in change of biomass concentration for the four observed data sets and the productivity model simulations with the one parameter model.

The one parameter model showed to fit the observed data very well. Slight differences were observed when compared some of the data points between the model and observed data. These errors can be assumed to exist due to inconsistencies during the outdoor experiments e.g. weather conditions and variations in lighting intensities. The model has an integrated light dependency parameter based on which the I_a is hourly calculated. The direct light intensity in the model, although dependent on the hour of the day, is constant from day to day. For the experimental data, although the sun intensity for the duration of the outdoor experiments was similar from day to day, there were still inconsistencies due to periodical overcast skies. These inconsistencies could impact the growth in the algal reactor.

To validate the model, statistical comparisons between the model predictions and experimental observation for four HRT's were used. The predicted and observed results showed to be in good correlations for all four scenarios (Fig. 5.8). The R^{2}'s of the statistical analysis were high (R^2 >0.96) for all scenarios, with the lowest R^2 being found at 6 h HRT treatment.

The RMSE was also calculated for each scenario. The RMSE values were 8.1, 7.8, 3.8 and 3.2 for the scenarios at 6, 12, 18 and 24 h HRT. These values validate the model as a good model to predict the productivities using the one set of constants.

In Figure 5.7 a trend in biomass concentration was observed during the day and night hours. A biomass concentration depicting the day and night concentration changes is presented in Figure 5.9. The concentration shows to be at steady-state after 8 pm when the inflow was stopped. Once the flow was restarted at 8 am a decrease in concentration is observed. This phenomenon is likely due to insufficient light availability at early hours of the day. Insufficient light availability keeps the growth rate smaller than the dilution rate ($D > \mu$), which result in flush-out of the biomass.

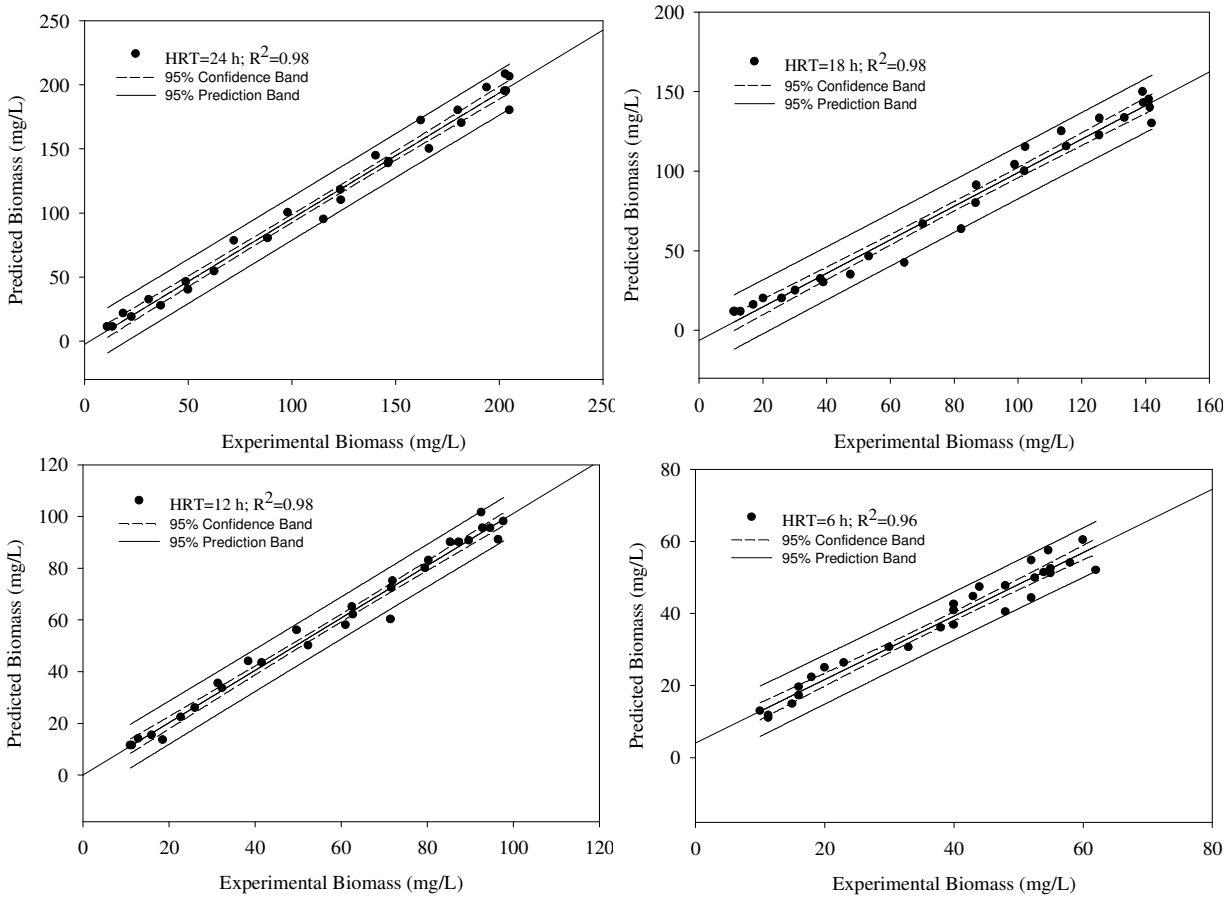

Figure 5.8. Comparison between experimental and results of the models at the four HRTs studied with fixed constants.

Once sufficient light is available, the growth rate exceeds the dilution rate ($D < \mu$) and an increase in biomass is observed. This flush-out phenomenon can be observed between 8 and 10 am and at the end of the day after 6 pm. The trend was noticed especially at higher HRT's (24 and 18 h HRT) after reaching higher biomass concentrations in the reactor. These minor flush outs may be avoided by starting the inflow only after sufficient light is available for growth. At lower HRT's (12 and 6 h HRT) this phenomenon was minimized due to lower biomass concentration and deeper light penetration.

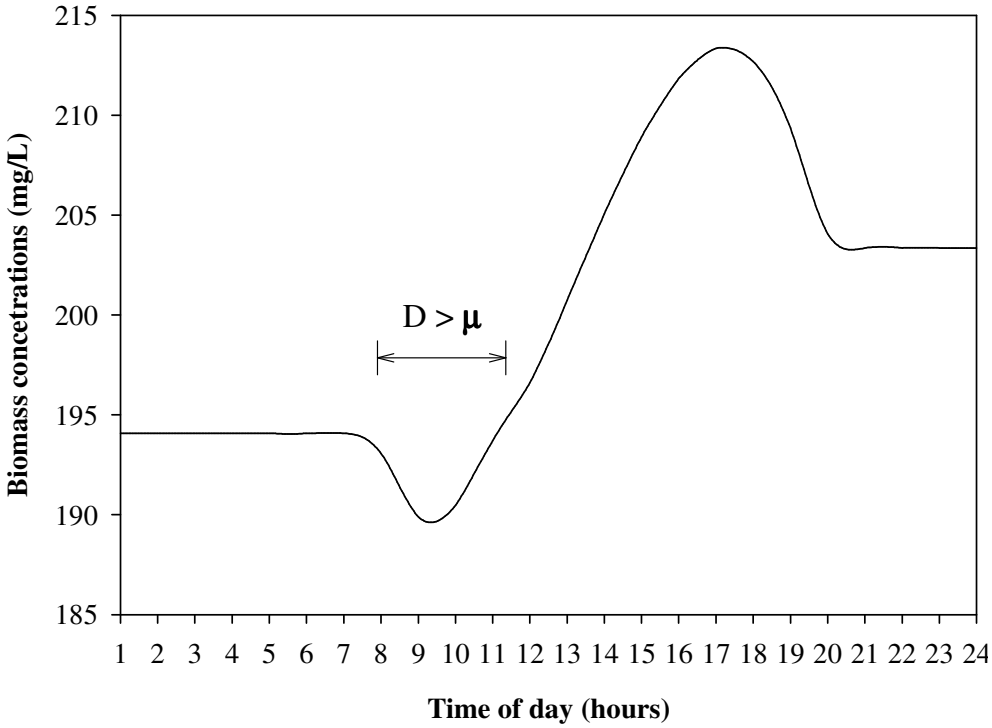

Figure 5.9. Biomass concentration fluctuations in the bioreactor during one day period. Dilution rate exceeds growth rate resulting in a flush out phenomenon due to insufficient light availability.

5.4. Model Projections

Simulations for scenarios for different HRT's were performed to exemplify the impact of the biomass accumulation over time on the average irradiance accessible in the bioreactor. The changes in light availabilities over time were inversely related to biomass concentration for all HRT's studied (Fig. 5.10). The average light available for photosynthesis inside the culture is reduced as biomass accumulates over time, and directly impacts the growth. While availability of light is plentiful at higher dilution rates, this is getting scarce at lower dilution rates, as the biomass concentration is higher and the self-shading effect occurs (Grima et al., 1996).

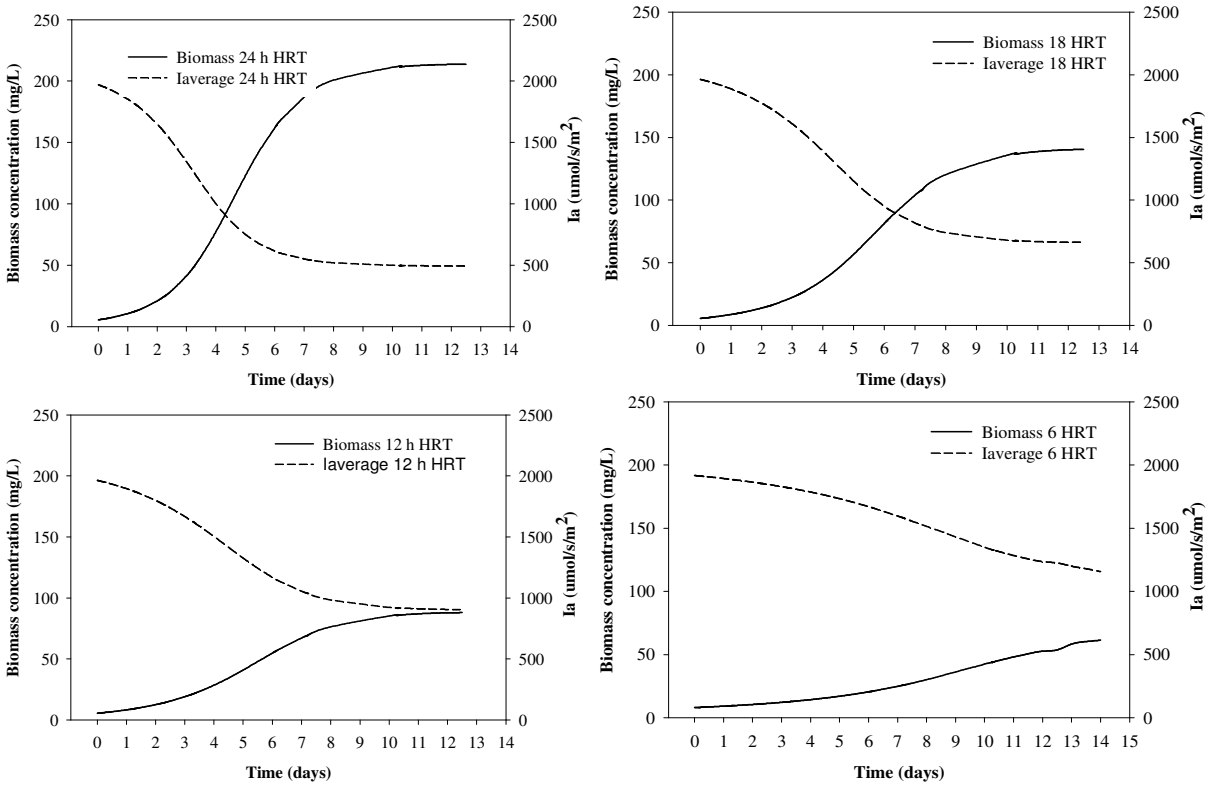

Figure 5.10. Results of the simulations showing the average light availability related to biomass concentration in the bioreactor.

These results were used to determine a relationship between the average light availability and the biomass concentrations in our experimental bioreactors (Fig. 5.11). All the correlations resulted in following an exponential decay equation, which fitted very well all our data (R^2 ≥0.99). This correlation is very useful in estimating the average irradiance available in a bioreactor during growth. While these results are in harmony with other results found in literature (Tredici and Zittelli, 1998; Rodolfi et al., 2009; Gutierrez-Wing et al., 2012), it is worth mentioning that these results and correlation parameters are established here are based on a very high initial direct solar irradiance, as it was measured during the peak hours on a clear sky summer day.

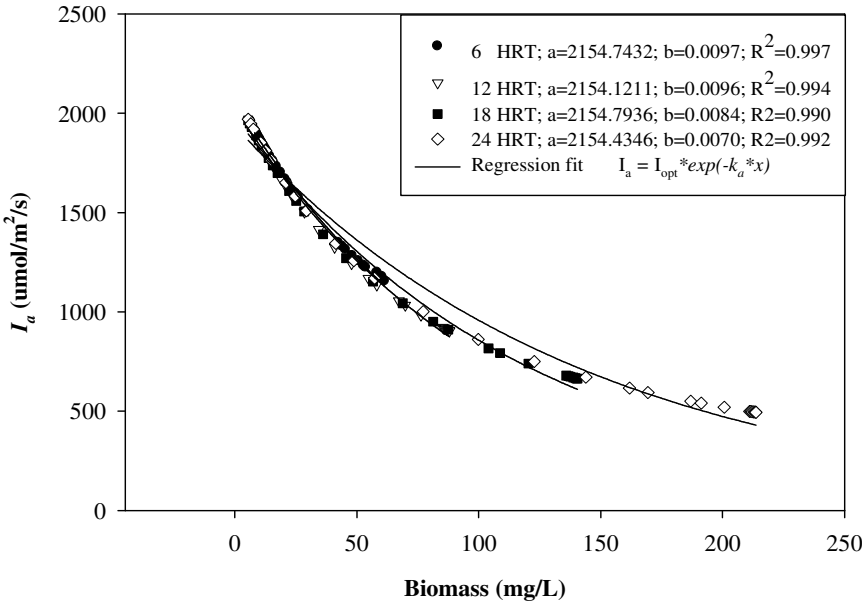

Figure 5.11. Correlation between average light availability through the bioreactor with respect to the concentration of biomass in the bioreactor.

The light availability directly affects growth rates of a system. At longer HRTs (>24 h HRT), due to high cellular densities, the self-shading effect occurs (Taulbee et al., 2005; Chisti, 2007; Yoon et al., 2008). During this phenomenon, the algal cells become shade-adapted and have displayed decreased light photosynthetic activity, which would lead to lower growth rates. On the contrary, higher growth rates are achieved at shorter HRTs (6 h HRT) due to lower cell densities. At lower cell densities the light penetration into the culture is greater. This occurrence is particularly noticeable at lower HRTs, meaning higher dilution rates and at early stages after inoculation, where the biomass density is low (Fig 5.12). Therefore, as light availability within the bioreactor declines due to increased concentration over time, so does the growth rate of the system.

Over time, as the system reaches steady state, these growth rates will eventually reach their steady state as well. The growth rates in a continuous flow system are highly dependent on the dilution rate applied to the system, among other parameters. At steady state, as expected, the

growth rates were slightly higher than their individual dilution rates. This is necessary in order to avoid algal flush-out. Similar results were obtained by direct measurements of the growth rates in the actual outdoor experiment, again showing the validity of the model.

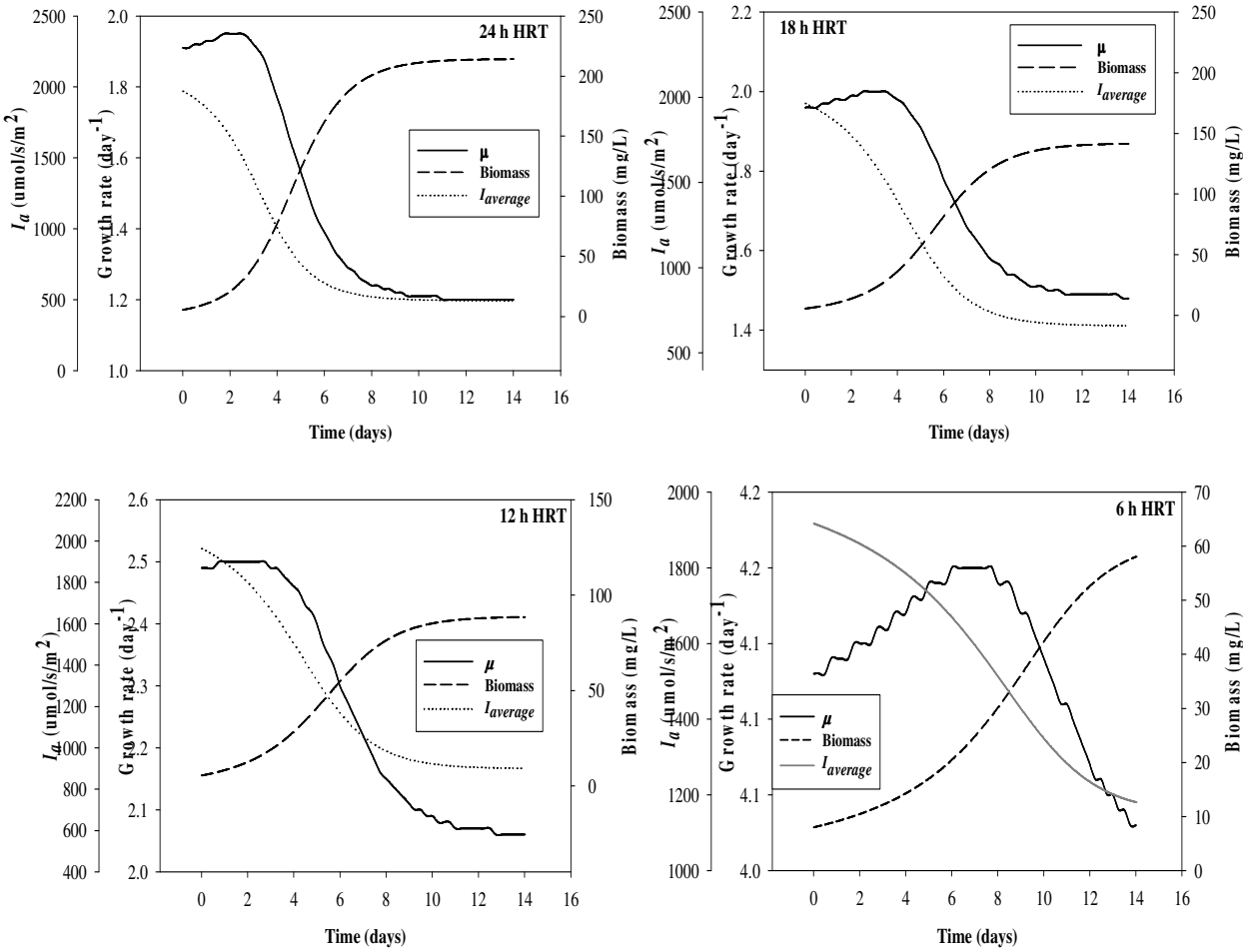

Figure 5.12. Growth rate dependency based on average light availability and biomass concentration within the system with identical constants.

The one parameter productivity model was also used to examine the effect of different dilutions on volumetric productivity (Pv) and aerial productivity (Pa). The model simulations were generated at several HRTs (V/Q) by holding the volume of the bioreactor constant and varying the inflow. Although higher cell concentrations were achieved at lower dilution rates (longer HRTs), it was observed that the productivities are higher at faster flow rates (shorter

HRTs). In terms of Pv, it increased as the HRT decreased. The highest volumetric productivity was reached with the 6 h HRT, achieving roughly 125 $g/m^3 \cdot day$ at steady state. It was followed by 12 h HRT, which was closely followed by 18 h HRT (106 and 105 $g/m^3 \cdot day$). The lowest Pv was achieved at 24 h HRT, 35 $g/m^3 \cdot day$ (Figure 5.13).

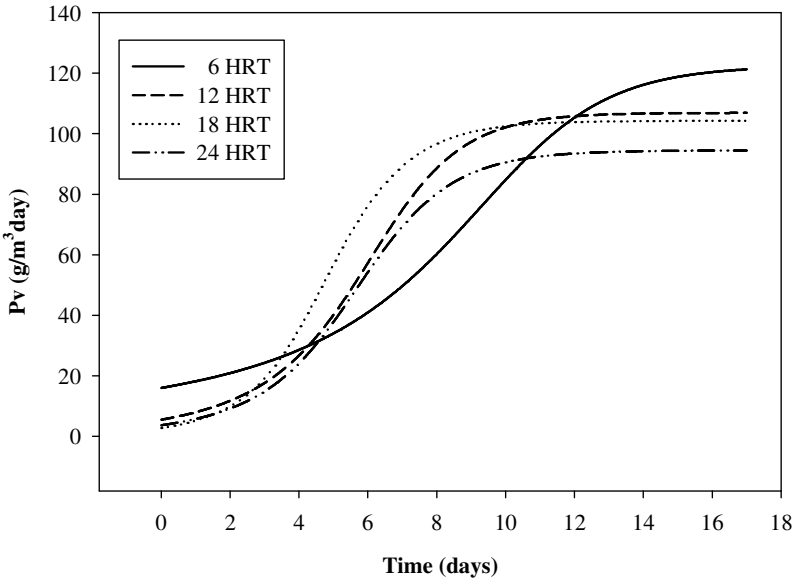

Figure 5.13. Volumetric productivity model simulation at four different HRTs.

In terms of areal productivity the results showed a similar trend as the Pv. The areal productivity was calculated based on surface area that receives solar irradiation. The highest Pa was achieved at 6 h HRT, followed by 12, 18 and 24 h HRT (Fig. 5.14).

These simulations coincide very closely with our direct measurements at steady-state from the outdoor system, where the Pv ($g/m^3 \cdot day$) and Pa ($g/m^2 \cdot day$) calculated were 110 and 39 for 6 h HRT, 99 and 35 for 12 h HRT, 84 and 30 at 18 h HRT and 93 and 33 for 24 h HRT. The lowest productivities calculated during the outdoor experimental set-up were at 18 HRT, due to weather inconsistencies and variations in lighting availabilities.

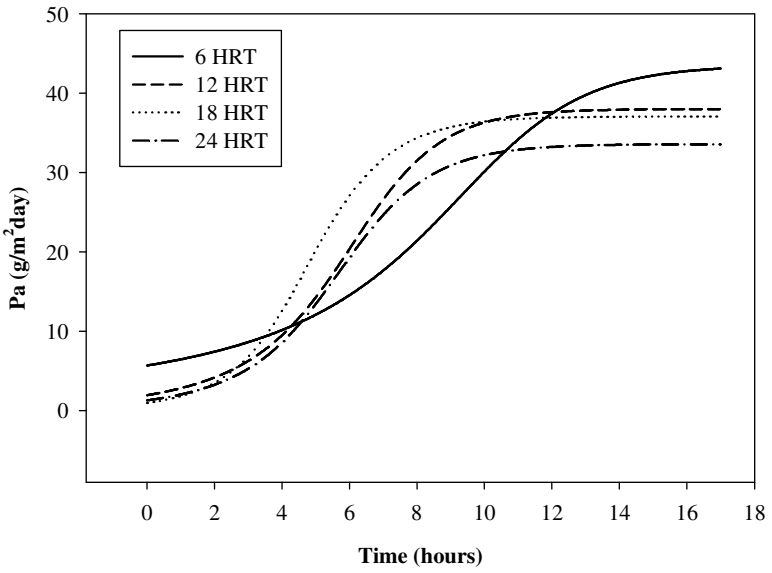

Figure 5.14. Areal productivity simulation at four different HRTs.

5.5. Conclusions

In conclusion, a deterministic mass balance model was developed to simulate microalgal productivities in outdoor continuous flow systems. The productivity models were comparable to the actual experimental data and statistically calibrated. Higher biomass cell concentrations was achieved at longer HRTs and declined with shortening the HRTs. In contrast, the highest volumetric and areal production was achieved at the shorter, 6 h HRT, producing 125 $g/m^3 \cdot day$ and 43 $g/m^2 \cdot day$, respectively. Growth variations due to fluctuations in available average light intensities and biomass concentrations were also simulated in this chapter, concluding that growth is directly dependent on light availability and biomass concentrations in algal bioreactors.

5.6. References

Aiba, S., 1982. Growth kinetics pf photosynthetic microorganisms. Advanced Biochemical Engineering 23, 85-156.

American Public Health Association (APHA), American Water Works Association (AWWA), (WEF), W.E.F., 2012. Standard Methods for the Examination of Water and Wastewater. Washington, DC.

Asenjo, J.A., Merchuk, J.C., 1994. Bioreactor system design (Biotechnology and Bioprocesing). CRC Press.

Bannister, T.T., 1979. Quantitative Description of Steady-State, Nutrient-Saturated Algal Growth, Including Adaptation. Limnology and Oceanography 24(1), 76-96.

Barsanti, L., Gualtieri, P., 2005. Algae. Anatomy, Biochemistry, and Biotechnology. Taylor and Francis Group. Boca Raton, Fl.

Becerra-Dorame, M., Antonio Lopez-Elias, J., Martinez-Cordova, L.R., 2010. An alternative outdoor production system for the microalgae Chaetoceros muelleri and Dunaliella sp during winter and spring in Northwest Mexico. Aquacultural Engineering 43(1), 24-28.

Benson, B., 2003. Optimization of the light dynamics in the hydraulically integrated serial turbidostat algal reactor (HISTAR). PhD Dissertation, Department of Civil and Environmental Engineering, Louisiana State University, Baton Rouge, LA.

Benson, B.C., Gutierrez-Wing M.T., Rusch K.A.,2008. Optimization of the lighting system for a Hydraulically Integrated Serial Turbidostat Algal Reactor (HISTAR): Economic implications. Aquacultural Engineering 40(1), 45-53.

Camacho, F.G., Gomez, A.C., Fernandez, F.G.A., Sevilla, J.F., Grima, E.M., 1999. Use of concentric-tube airlift photobioreactors for microalgal outdoor mass cultures. Enzyme and Microbial Technology 24(3-4), 164-172.

Chen, M., Tang, H., Ma, H., Holland, T.C., Ng, K.Y.S., Salley, S.O., 2011. Effect of nutrients on growth and lipid accumulation in the green algae *Dunaliella tertiolecta*. Bioresource Technology 102(2), 1649-1655.

Chisti, Y., 2007. Biodiesel from microalgae. Biotechnology Advances 25(3), 294-306.

Cornet, J.F., Dussap, C.G., Cluzel, P., Dubertret, G., 1992. A Structured Model for Simulation of Cultures of the Cyanobacterium Spirulina-Platensis in Photobioreactors .2. Identification of Kinetic-Parameters under Light and Mineral Limitations. Biotechnology and Bioengineering 40(7), 826-834.

Cornet, J.F., Dussap, C.G., Dubertret, G., 1992. A Structured Model for Simulation of Cultures of the Cyanobacterium Spirulina-Platensis in Photobioreactors .1. Coupling between Light Transfer and Growth-Kinetics. Biotechnology and Bioengineering 40(7), 817-825.

Droop, M.R., 1975. The chemostat in mariculture. 10th European Symposium on Marine Biology, Ostend, Belgium University Press.

Dubinsky, Z., Berman, T., 1979. Seasonal-Changes in the Spectral Composition of Downwelling Irradiance in Lake Kinneret (Israel). Limnology and Oceanography 24(4), 652-663.

Eriksen, N.T., 2008. The technology of microalgal culturing. Biotechnology Letters 30(9), 1525-1536.

Evens, T.J., Chapman, D.J., Robbins, R.A., D'Asaro, E.A., 2000. An analytical flat-plate photobioreactor with a spectrally attenuated light source for the incubation of phytoplankton under dynamic light regimes. Hydrobiologia 434(1-3), 55-62.

Evers, E.G., 1991. A model for light-limited continuous cultures - growth, shading, and maintenance. Biotechnology and Bioengineering 38(3), 254-259.

Fanta, S.E., Hill, W.R., Smith, T.B., Roberts, B.J., 2010. Applying the light: nutrient hypothesis to stream periphyton. Freshwater Biology 55(5), 931-940.

Fernandez, F.G.A., Camacho, F.G., Perez, J.A.S., Sevilla, J.M.F., Grima, E.M., 1997. A model for light distribution and average solar irradiance inside outdoor tubular photobioreactors for the microalgal mass culture. Biotechnology and Bioengineering 55(5), 701-714.

Fredrickson, A.G., Tsuchiya, H.M. 1977, Microbial kinetics and dynamics. Chemical Reactor Theory. Lapidus, L., Amundson, N. Englewood Cliffs, NJ, Prentice-Hall**:** 405-483.

Grima, E.M., Camacho, F.G., Perez, J.A.S., Sevilla, J.M.F., Fernandez, F.G.A., Gomez, A.C., 1994. A Mathematical-Model of Microalgal Growth in Light-Limited Chemostat Culture. Journal of Chemical Technology and Biotechnology 61(2), 167-173.

Grima, E.M., Fernandez, F.G.A., Camacho, F.G., Chisti, Y., 1999. Photobioreactors: light regime, mass transfer, and scaleup. Journal of Biotechnology 70(1-3), 231-247.

Grima, E.M., Perez, J.A.S., Camacho, F.G., Fernandez, F.G.A., Sevilla, J.M.F., Sanz, F.V., 1994. Effect of Dilution Rate on Eicosapentaenoic Acid Productivity of Phaeodactylum-Tricornutum Utex-640 in Outdoor Chemostat Culture. Biotechnology Letters 16(10), 1035-1040.

Grima, E.M., Sevilla, J.M.F., Perez, J.A.S., Camacho, F.G., 1996. A study on simultaneous photolimitation and photoinhibition in dense microalgal cultures taking into account incident and averaged irradiances. Journal of Biotechnology 45(1), 59-69.

Grobbelaar, J.U., 2009. Factors governing algal growth in photobioreactors: the "open" versus "closed" debate. Journal of Applied Phycology 21(5), 489-492.

Gutierrez-Wing, M.T., Benson, B.C., Rusch, K.A., 2012. Impact of light quality and quantity on growth rate kinetics of Selenastrum capricornutum. Engineering in Life Sciences 12(1), 79-88.

Jorgensen, E., 1979. Handbook of Environmental Data and Ecological Parameters. Pergamon Press. New York.

Kirk, J.T.O., 1983. Light and photosynthesis in aquatic ecosystems. Cambridge University Press. Cambridge, Great Britain

Miron, A.S., Camacho, F.G., Gomez, A.C., Grima, E.M., Chisti, Y., 2000. Bubble-column and airlift photobioreactors for algal culture. Aiche Journal 46(9), 1872-1887.

Molina, E., Fernandez, J., Acien, F.G., Chisti, Y., 2001. Tubular photobioreactor design for algal cultures. Journal of Biotechnology 92(2), 113-131.

Packer, A., Li, Y., Andersen, T., Hu, Q., Kuang, Y., Sommerfeld, M., 2011. Growth and neutral lipid synthesis in green microalgae: A mathematical model. Bioresource Technology 102(1), 111-117.

Prokop, R., Dostal, P., Bakosova, M., 1995. Control of continuous stirred tank reactors based on delta model representation. Hungarian Journal of Industrial Chemistry 23(4), 263-269.

Rier, S.T., Stevenson, R.J., LaLiberte, G.D., 2006. Photo-acclimation response of benthic stream algae across experimentally manipulated light gradients: A comparison of growth rates and net primary productivity. Journal of Phycology 42(3), 560-567.

Rodolfi, L., Zittelli, G.C., Bassi, N., Padovani, G., Biondi, N., Bonini, G., Tredici, M.R., 2009. Microalgae for Oil: Strain Selection, Induction of Lipid Synthesis and Outdoor Mass Cultivation in a Low-Cost Photobioreactor. Biotechnology and Bioengineering 102(1), 100-112.

Rubio, F.C., Camacho, F.G., Sevilla, J.M.F., Chisti, Y., Grima, E.M., 2003. A mechanistic model of photosynthesis in microalgae. Biotechnology and Bioengineering 81(4), 459-473.

Steele, J.H. 1965, Notes on some theoretical problems in production ecology. Primary production in Aquatic Environments. Goldman, C.R. Berkley, CA, University of Callifornia Press**:** 383-398.

Taulbee, W.K., Cooper, S.D., Melack, J.M., 2005. Effects of nutrient enrichment on algal biomass across a natural light gradient. Archiv Fur Hydrobiologie 164(4), 449-464.

Tredici, M.R., Zittelli, G.C., 1998. Efficiency of sunlight utilization: Tubular versus flat photobioreactors. Biotechnology and Bioengineering 57(2), 187-197.

Wouter, G.v.D., Kohki, Y., 2009. Review: Role of chloroplasts and other plastids in ageing and death of plants and animals: A tale of Vishnu and Shiva. Ageing Research Reviews 9, 117-130.

Yang, D.-H., Webster, J., Adam, Z., Lindahl, M., Andersson, B., 1998. Induction of acclimative proteolysis of the light-harvesting chlorophyll a/b protein of photosystem II in response to elevated light intensities. Plant Physiology (Rockville) 118(3), 827-834.

Yoon, J.H., Shin, J.-H., Ahn, E.K., Park, T.H., 2008. High cell density culture of Anabaena variabilis with controlled light intensity and nutrient supply. Journal of Microbiology and Biotechnology 18(5), 918-925.

CHAPTER 6
CONCLUSIONS AND RECOMMENDATIONS

6.1. Summary and conclusions

This dissertation is a comprehensive document describing in details the methods, results, and implications of the research which was completed for the purpose of optimizing light requirements and dilution rates for maximizing algal cell growth and lipid content for biofuel feedstock production. Beside the introductory, background and literature review and concluding chapters, this thesis is composed of three stand-alone manuscripts, which will be submitted for publication in refereed journals.

The first study (Chapter 3) determined the optimal dilution rates for maximizing the net biomass production and lipid yields in a continuous, outdoor system using three different microalgae species, *Nannochloris sp., Selenastrum capricornutum*, and *Scenedesmus dimorphus*. For biofuel applications, increasing net lipid productivity from continuous flow microalgal cultures is critically important. The parameters that affect net lipid productivity include: cell lipid content, culture flow rate or hydraulic retention time, and biomass concentration. However, these parameters are interlinked and cannot be independently altered. This work, designed at probing the interdependence between variables and maximizing net lipids from outdoor algal cultures. The representative algal species were grown in an outdoor continuous-flow system at four different HRTs of 6, 12, 18 and 24 hrs. The highest biomass cell concentration (250 mg/L) occurred at the longest HRT (24 hr) and decreased progressively with shorter HRTs. However, net aerial biomass productivity numbers did not follow a specific pattern. The highest net aerial productivity of 43.4 g/m^2/day was achieved with *Nannochloris sp.* species at 6 hr HRT, compared to 32.1 g/m^2/day at 24 hr HRT by *S. capricornutum* species. Net lipid productivity was

found to be significantly higher ($P<0.05$) at 24 hr HRT, achieving 7.9, 9.6 and 10.4 g/m^2/day for *Nannochloris sp., S. capricornutum*, and *S. dimorphus* respectively. When the media flow was curtailed, the lipid concentrations increased at the expense of protein and carbohydrate contents of the cell.

Results indicated that variation in light availability has a major bearing on biomass and lipid productivities. Although not valid for all tested species and HRTs, in general, higher net biomass productivity was achieved at shorter HRTs. However, the maximum net lipid productivity was achieved at longest retention time for all algal species studied. The study also indicated that cultures that are closer to the physiological cell density limit divert the incident energy more towards lipid production.

Modeling the light intensity inside bioreactors is complicated: algae are exposed to high-intensity sunlight in the so-called photic zone close to the reactor surface and can be exposed to complete darkness in the bottom of the reactor. As a result of mixing of the reactor liquid, algae are exposed to light-gradient/dark cycles. This light regime can have a considerable influence on the efficiency of light utilization for biomass growth, also referred to as the photosynthetic efficiency. Because light is the growth limiting substrate, light supply plays a key role in reactor design.

In this dissertation, the efficiency of light utilization of microalgae was studied under various dark/light cycles and frequencies (Chapter 4). A photobioreactor system with an D/L alternation system was constructed in order to investigate *Nannochloris sp.* growth characteristics under intermittent illumination at high intensity lights (2000 μmol/s/m^2), mimicking the peak intensity of the sun during a clear summer day. The results obtained indicated that enhancement of the photosynthetic utilization of high intensity light due to light

modulation can be achieved. The algal cultures under flashing light with a relative low frequency (<3.2 Hz) and higher light cycle ratio showed lower growth kinetics and productivity than those performed under higher frequencies (>3.2 Hz). However both growth rates and cell concentrations were at maximum under medium light cycle ratio (4/1 D/L) and medium frequencies (6.4-25.6 Hz), and progressively decreasing with further decreasing the light ratio and frequency. Light efficiency measurements based on chlorophylls content showed that efficiency can be significantly improved by applying medium durations of medium light fractions. Chlorophyll measurement results were interrelated with the cell concentration and growth rate results. The biomass cell concentration and growth rate found under intermittent light was higher than those observed under continuous light, at every D/L ratio studied.

Outdoor studies suggested that the same productivity could be achieved by increasing the volume per unit area if an optimum D/L ratio is maintained. These results could have significant impact on the outdoor productivities and bioreactors design. The practical expectation of the present work is the contribution of D/L ratios and frequencies under high light intensities to improve aerial productivity, growth rate and ultimately light efficiency in high-density outdoor algal systems.

Mathematical modeling is a very useful tool for design and optimization of bioprocesses. Developing a fundamental understanding of light dynamics within any reactor is critical to the proper establishment of design and operating criteria. Chapter 5 describes a deterministic model developed to describe and investigate the light dynamics and their impact on biomass productivity and growth rate in an outdoor continuous-flow system operated at various HRTs. Therefore, the following only applies to situations in which nutrients are present in excess or is not the limiting factor.

In this model, the primary input is light, which is represented as a volumetric average light intensity calculated based on light intensity at reactor surface. Lambert-Beer's law was sufficiently accurate in estimating the light distribution inside the culture, assuming constant light absorption proportional to the length of the light path and the biomass concentration. Steele's growth model was used to describe the growth rate inside the reactors. The model was calibrated and validated against data collected from actual experiments over one month period, at Louisiana State University (Baton Rouge, LA), presented in Chapter 3. Several mathematical relationships were developed in this chapter that helped with the model: the relationship between the average PAR and the biomass concentration; the relationship between the average PAR and growth rate; and the relationship between irradiance light and depth.

A successful deterministic model was developed to simulate microalgal productivities in outdoor continuous flow systems. The productivity models were comparable to the actual experimental data and statistical efforts validated these models. Higher biomass cell concentrations was achieved at longer HRTs and declined with shortening the HRTs. In contrast, the highest volumetric and areal production was achieved at the shorter, 6 h HRT, producing 125 $g/m^3 \cdot day$ and 46 $g/m^2 \cdot day$, respectively. Growth variations due to fluctuations in available average light intensities and biomass concentrations were also simulated in Chapter 5, concluding that growth is directly dependent on light availability and biomass concentrations in a microalgal system. This information is fundamental in assisting with an optimum design for maximizing light efficiency and ultimately growth rate and biomass productivities of a continuous-flow bioreactor.

6.2. Recommendations for future research

Although the results of this research can significantly improve biomass and lipid productivities, together with specific growth rates, there is always room for improvement and optimization. Some of the future work recommendations that should not be overlooked are:

- Efforts should be made in validating the D/L ratio results from the indoor study. Validation of these results is critical, and could have a major impact in outdoor mass cultivation systems. Although a set of experiment data was already validated in an outdoor environment (1/1, 4/1 and 10/1 D/L ratios), these need to be triplicated before any conclusion can be drawn.
- On the same topic, these results should be validated during summer days (June-September) since the outdoor cycling experiments were performed later in the year (November) when the direct solar irradiance was lower than during summer days. This could influence the outcome of the results.
- To go even further, a deep outdoor pond/raceway should be constructed and validate the D/L ratio results. However this would need some significant space, labor, and funds to materialize.
- It would be interesting to evaluate the lipid composition changes in the algal cell during growth under different D/L ratios. Studies reported in literature deal with photosynthetic efficiencies based on oxygen formation for different light fractions in the cycle but not with lipid productivities specifically.

APPENDIX I: OUTDOOR EXPERIMENTAL DATA

Table I.1. Experimental raw data from outdoor continuous-flow system for *Nannochloris* sp; 24 h HRT, Q=38.2 ml/min.

Hours at reading	OD (nm)			TSS (mg/L)			Average TSS (mg/L)	SD
	1	2	3	1	2	3		
6	0.01	0.011	0.01	1.27	0.85	1.27	1.13	0.24
12	0.009	0.013	0.012	1.69	0.02	0.43	0.71	0.87
24	0.009	0.013	0.012	1.69	0.02	0.43	0.71	0.87
30	0.019	0.025	0.024	2.49	4.99	4.58	4.02	1.34
36	0.035	0.044	0.045	9.17	12.92	13.34	11.81	2.30
48	0.031	0.037	0.039	7.50	10.00	10.84	9.45	1.74
54	0.063	0.068	0.069	20.86	22.94	23.36	22.39	1.34
60	0.096	0.103	0.096	34.63	37.55	34.63	35.61	1.69
72	0.1	0.107	0.098	36.30	39.22	35.47	37.00	1.97
78	0.161	0.172	0.156	61.77	66.36	59.68	62.60	3.42
84	0.205	0.207	0.17	80.13	80.97	65.52	75.54	8.69
96	0.169	0.197	0.161	65.11	76.79	61.77	67.89	7.89
108	0.27	0.307	0.262	107.27	122.71	103.93	111.30	10.02
120	0.246	0.298	0.237	97.25	118.96	93.49	103.23	13.75
132	0.325	0.328	0.354	130.23	131.48	142.33	134.68	6.66
144	0.301	0.31	0.322	120.21	123.97	128.98	124.38	4.40
150	0.375	0.379	0.348	151.10	152.77	139.83	147.90	7.04
168	0.401	0.405	0.34	161.95	163.62	136.49	154.02	15.21
174	0.399	0.408	0.385	161.12	164.88	155.27	160.42	4.84
192	0.396	0.385	0.366	159.87	155.27	147.34	154.16	6.34
240	0.435	0.465	0.423	176.15	188.67	171.14	178.65	9.03
246	0.476	0.488	0.472	193.26	198.27	191.59	194.38	3.48
252	0.508	0.519	0.498	206.62	211.21	202.45	206.76	4.38
264	0.465	0.49	0.434	188.67	199.11	175.73	187.84	11.71
276	0.523	0.531	0.505	212.88	216.22	205.37	211.49	5.56
288	0.495	0.508	0.483	201.19	206.62	196.18	201.33	5.22
300	0.525	0.534	0.508	213.74	217.47	206.62	212.60	5.51

Table I.2. Experimental raw data from outdoor continuous-flow system for *Nannochloris* sp; 18 h HRT, Q=50.9 ml/min.

Hours at reading	OD (nm)			TSS (mg/L)			Average TSS (mg/L)	SD
	1	2	3	1	2	3		
6	0.009	0.008	0.008	1.69	2.10	2.10	1.97	0.24
12	0.009	0.008	0.007	1.69	2.10	2.52	2.10	0.42
24	0.009	0.006	0.009	1.69	2.94	1.69	2.10	0.72
30	0.014	0.01	0.015	0.40	1.27	0.82	0.02	1.10
36	0.027	0.017	0.025	5.83	1.65	4.99	4.16	2.21
48	0.024	0.013	0.022	4.58	3.02	3.74	3.77	2.45
54	0.043	0.038	0.04	12.51	10.42	11.25	11.39	1.05
60	0.066	0.046	0.062	22.11	13.76	20.44	18.77	4.42
72	0.069	0.051	0.069	23.36	15.85	23.36	20.86	4.34
78	0.103	0.086	0.107	37.55	30.46	39.22	35.74	4.65
84	0.124	0.114	0.134	46.32	42.15	50.49	46.32	4.17
96	0.122	0.109	0.127	45.49	40.06	47.57	44.37	3.88
108	0.184	0.144	0.189	71.37	54.67	73.45	66.50	10.30
120	0.168	0.129	0.171	64.69	48.41	65.94	59.68	9.78
132	0.214	0.158	0.194	83.89	60.51	75.54	73.32	11.85
144	0.2	0.15	0.173	78.05	57.17	66.78	67.33	10.45
150	0.246	0.182	0.206	97.25	70.53	80.55	82.78	13.50
168	0.276	0.178	0.206	109.77	68.86	80.55	86.40	21.07
174	0.267	0.187	0.217	106.02	72.62	85.14	87.93	16.87
192	0.259	0.188	0.215	102.68	73.04	84.31	86.67	14.96
240	0.357	0.312	0.326	143.59	124.80	130.64	133.01	9.61
246	0.356	0.332	0.328	143.17	133.15	131.48	135.93	6.32
252	0.36	0.341	0.328	144.84	136.91	131.48	137.74	6.72
264	0.35	0.322	0.313	140.66	128.98	125.22	131.62	8.06
276	0.342	0.358	0.321	137.32	144.00	128.56	136.63	7.75
288	0.328	0.342	0.302	131.48	137.32	120.63	129.81	8.47
300	0.358	0.361	0.326	144.00	145.26	130.64	139.97	8.10

Table I.3. Experimental raw data from outdoor continuous-flow system for *Nannochloris* sp; 12 h HRT, Q=76.4 ml/min.

Hours at reading	OD (nm)			TSS (mg/L)			Average TSS (mg/L)	SD
	1	2	3	1	2	3		
6	0.008	0.008	0.007	2.10	2.10	2.52	2.24	0.24
12	0.008	0.007	0.009	2.10	2.52	1.69	2.10	0.42
24	0.007	0.006	0.008	2.52	2.94	2.10	2.52	0.42
30	0.008	0.013	0.013	2.10	0.02	0.02	0.71	1.21
36	0.013	0.016	0.024	0.02	1.24	4.58	1.93	2.37
48	0.008	0.014	0.02	2.10	0.40	2.91	0.40	2.50
54	0.017	0.026	0.047	1.65	5.41	14.18	7.08	6.43
60	0.026	0.041	0.043	5.41	11.67	12.51	9.86	3.88
72	0.027	0.044	0.073	5.83	12.92	25.03	14.59	9.71
78	0.045	0.063	0.117	13.34	20.86	43.40	25.86	15.64
84	0.059	0.074	0.152	19.19	25.45	58.01	34.21	20.84
96	0.062	0.073	0.139	20.44	25.03	52.58	32.68	17.38
108	0.101	0.100	0.144	36.72	36.30	54.67	42.56	10.49
120	0.093	0.095	0.138	33.38	34.21	52.16	39.92	10.61
132	0.158	0.111	0.181	60.51	40.89	70.11	57.17	14.89
144	0.132	0.108	0.134	49.66	39.64	50.49	46.60	6.04
150	0.151	0.117	0.137	57.59	43.40	51.75	50.91	7.13
168	0.136	0.117	0.141	51.33	43.40	53.42	49.38	5.29
174	0.14	0.136	0.148	53.00	51.33	56.34	53.56	2.55
192	0.138	0.137	0.136	52.16	51.75	51.33	51.75	0.42
240	0.258	0.249	0.234	102.26	98.50	92.24	97.67	5.06
246	0.243	0.264	0.251	96.00	104.76	99.34	100.03	4.42
252	0.255	0.265	0.251	101.01	105.18	99.34	101.84	3.01
264	0.255	0.254	0.248	101.01	100.59	98.08	99.89	1.58
276	0.251	0.265	0.255	99.34	105.18	101.01	101.84	3.01
288	0.254	0.265	0.254	100.59	105.18	100.59	102.12	2.65
300	0.256	0.254	0.251	101.42	100.59	99.34	100.45	1.05

Table I.3. Experimental raw data from outdoor continuous-flow system for *Nannochloris* sp; 6 h HRT, Q=152.8 ml/min.

Hours at reading	OD (nm)			TSS (mg/L)			Average TSS (mg/L)	SD
	1	2	3	1	2	3		
6	0.008	0.008	0.009	2.10	2.10	1.69	1.97	0.24
12	0.003	0.002	0.003	4.19	4.61	4.19	4.33	0.24
24	0.002	0.002	0.002	4.61	4.61	4.61	4.61	0.00
30	0.002	0.003	0.003	4.61	4.19	4.19	4.33	0.24
36	0.003	0.002	0.003	4.19	4.61	4.19	4.33	0.24
48	0.001	0.001	0.001	5.03	5.03	5.03	5.03	0.00
54	0.002	0.002	0.011	4.61	4.61	0.85	3.36	2.17
60	0.006	0.006	0.014	2.94	2.94	0.40	1.83	1.93
72	0.006	0.007	0.019	2.94	2.52	2.49	0.99	3.02
78	0.009	0.009	0.009	1.69	1.69	1.69	1.69	0.00
84	0.011	0.01	0.006	0.85	1.27	2.94	1.69	1.10
96	0.014	0.017	0.005	0.40	1.65	3.36	0.43	2.61
108	0.023	0.021	0.014	4.16	3.32	0.40	2.63	1.97
120	0.018	0.023	0.017	2.07	4.16	1.65	2.63	1.34
132	0.022	0.03	0.019	3.74	7.08	2.49	4.44	2.37
144	0.031	0.05	0.023	7.50	15.43	4.16	9.03	5.79
150	0.031	0.049	0.023	7.50	15.01	4.16	8.89	5.56
168	0.048	0.078	0.041	14.59	27.12	11.67	17.79	8.21
174	0.044	0.061	0.037	12.92	20.02	10.00	14.32	5.15
192	0.06	0.067	0.05	19.60	22.53	15.43	19.19	3.57
240	0.158	0.156	0.152	60.51	59.68	58.01	59.40	1.28
246	0.129	0.148	0.141	48.41	56.34	53.42	52.72	4.01
252	0.168	0.188	0.179	64.69	73.04	69.28	69.00	4.18
264	0.144	0.151	0.174	54.67	57.59	67.19	59.82	6.55
276	0.157	0.163	0.169	60.10	62.60	65.11	62.60	2.50
288	0.159	0.161	0.167	60.93	61.77	64.27	62.32	1.74
300	0.155	0.154	0.169	59.26	58.84	65.11	61.07	3.50

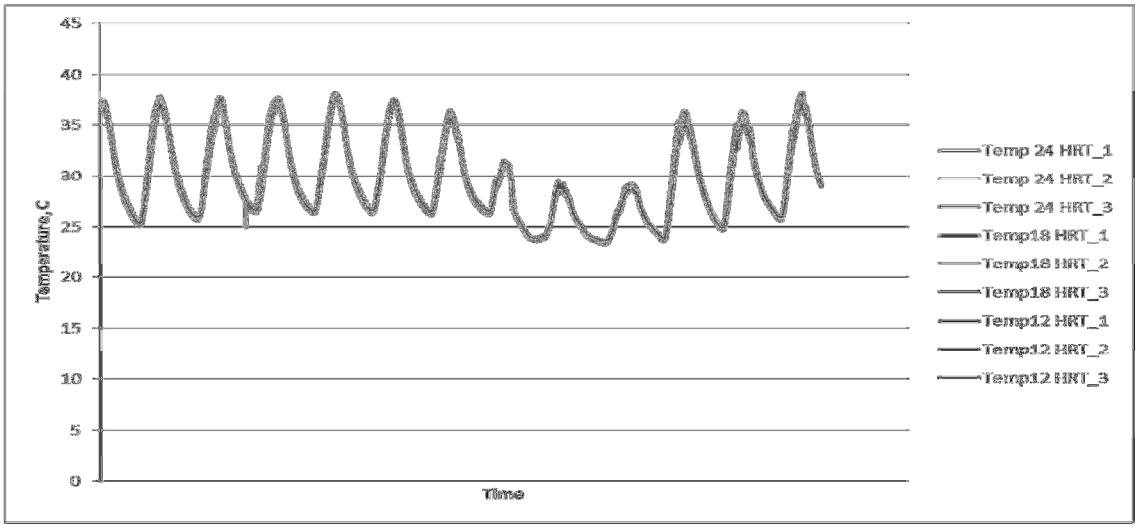

Figure I.1. Temperature results for outdoor continuous flow system for *Nannochloris* sp. Lower values represent night time temperatures.

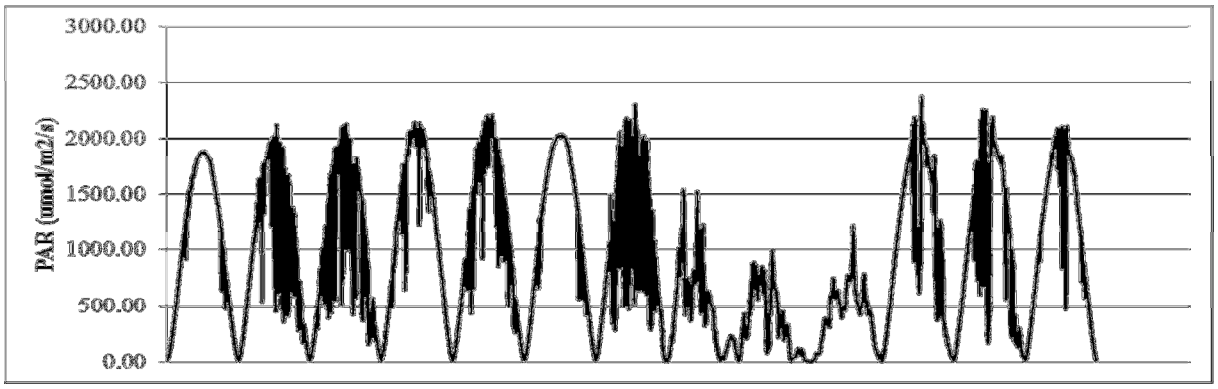

Figure I.2. PAR results for outdoor continuous flow system for *Nannochloris* sp.

Table I.5. Oil content of *Nannochloris* sp at the four HRT's studied.

Container	C weight	C+mix	C+oil	OIL (g)	OIL (mg/g dw)	%	AV	sd
24 HRT_1	27.9309	33.6806	27.9543	0.1170	234	23.4	23.62	0.696
24 HRT_2	27.93	33.6876	27.9544	0.1220	244	24.4		
24 HRT_3	27.9265	33.6756	27.9426	0.1153	230.6	23.06		
18 HRT_1	27.9572	35.5445	27.973	0.0790	158	15.8	16.20	0.368
18 HRT_2	27.9526	33.2999	27.9711	0.0815	163	16.3		
18 HRT_3	27.9358	33.4691	27.8952	0.0826	165.2	16.52		
12 HRT_1	27.7606	34.6585	27.7858	0.0620	124	12.4	12.49	0.276
12 HRT_2	27.7716	35.0863	27.8343	0.0614	122.7	12.27		
12 HRT_3	27.9563	35.1293	27.7859	0.0640	128	12.8		
6 HRT_1	27.9289	34.8097	27.9553	0.0423	84.6	8.46	8.45	0.270
6 HRT_2	27.8715	30.9574	27.8775	0.0409	81.8	8.18		
6 HRT_3	27.9259	32.2481	27.9456	0.0436	87.2	8.72		

Table I.6. Experimental raw data from outdoor continuous-flow system for *Selenastrum capricornutum*; 24 h HRT, Q=38.2 ml/min.

Hours at reading	OD (nm)			TSS (mg/L)			Average TSS (mg/L)	SD
	1	2	3	1	2	3		
0	0.024	0.028	0.028	10.04	11.71	11.71	11.15	0.97
12	0.048	0.058	0.048	20.07	24.26	20.07	21.47	2.41
24	0.045	0.05	0.04	18.82	20.91	16.73	18.82	2.09
36	0.078	0.082	0.072	32.62	34.29	30.11	32.34	2.10
48	0.065	0.073	0.06	27.18	30.53	25.09	27.60	2.74
60	0.113	0.118	0.1	47.26	49.35	41.82	46.14	3.89
72	0.098	0.103	0.086	40.98	43.08	35.97	40.01	3.65
80	0.13	0.132	0.128	54.37	55.20	53.53	54.37	0.84
86	0.161	0.17	0.159	67.33	71.10	66.50	68.31	2.45
98	0.15	0.158	0.145	62.73	66.08	60.64	63.15	2.74
110	0.215	0.228	0.218	89.92	95.35	91.17	92.15	2.85
122	0.21	0.22	0.206	87.82	92.01	86.15	88.66	3.02
134	0.28	0.292	0.274	117.10	122.12	114.59	117.94	3.83
140	0.315	0.301	0.31	131.74	125.88	129.65	129.09	2.97
146	0.34	0.355	0.342	142.19	148.46	143.03	144.56	3.41
158	0.325	0.338	0.331	135.92	141.35	138.43	138.57	2.72
164	0.4	0.41	0.396	167.28	171.47	165.61	168.12	3.02
170	0.432	0.446	0.425	180.67	186.52	177.74	181.64	4.47
182	0.42	0.428	0.396	175.65	178.99	165.61	173.42	6.96
194	0.475	0.489	0.466	198.65	204.50	194.89	199.35	4.85
206	0.463	0.478	0.45	193.63	199.90	188.19	193.91	5.86
218	0.483	0.495	0.473	202.00	207.01	197.81	202.27	4.61
230	0.472	0.485	0.461	197.40	202.83	192.79	197.67	5.02
242	0.497	0.511	0.492	207.85	213.71	205.76	209.11	4.12
254	0.493	0.505	0.481	206.18	211.20	201.16	206.18	5.02
260	0.495	0.508	0.483	207.01	212.45	202.00	207.15	5.23

Table I.7. Experimental raw data from outdoor continuous-flow system for *Selenastrum capricornutum*; 18h HRT, Q=50.9 ml/min.

Hours at reading	OD (nm)			TSS (mg/L)			Average TSS (mg/L)	SD
	1	2	3	1	2	3		
0	0.031	0.028	0.025	12.96	11.71	10.46	11.71	1.25
12	0.032	0.032	0.04	13.38	13.38	16.73	14.50	1.93
24	0.028	0.026	0.028	11.71	10.87	11.71	11.43	0.48
36	0.049	0.035	0.036	20.49	14.64	15.06	16.73	3.27
48	0.046	0.022	0.034	19.24	9.20	14.22	14.22	5.02
60	0.062	0.04	0.058	25.93	16.73	24.26	22.30	4.90
72	0.053	0.031	0.062	22.17	12.96	25.93	20.35	6.67
80	0.076	0.082	0.093	31.78	34.29	38.89	34.99	3.61
86	0.103	0.112	0.118	43.08	46.84	49.35	46.42	3.16
98	0.096	0.101	0.107	40.15	42.24	44.75	42.38	2.30
110	0.154	0.16	0.164	64.40	66.91	68.59	66.63	2.10
122	0.149	0.15	0.157	62.31	62.73	65.66	63.57	1.82
134	0.184	0.191	0.198	76.95	79.88	82.81	79.88	2.93
140	0.213	0.222	0.219	89.08	92.84	91.59	91.17	1.92
146	0.248	0.248	0.25	103.72	103.72	104.55	103.99	0.48
158	0.233	0.24	0.244	97.44	100.37	102.04	99.95	2.33
164	0.266	0.275	0.285	111.24	115.01	119.19	115.15	3.97
170	0.306	0.293	0.298	127.97	122.54	124.63	125.04	2.74
182	0.297	0.288	0.294	124.21	120.44	122.95	122.54	1.92
194	0.34	0.346	0.355	142.19	144.70	148.46	145.12	3.16
206	0.332	0.336	0.354	138.85	140.52	148.05	142.47	4.90
218	0.364	0.368	0.361	152.23	153.90	150.97	152.37	1.47
230	0.355	0.364	0.353	148.46	152.23	147.63	149.44	2.45
242	0.36	0.372	0.356	150.56	155.57	148.88	151.67	3.48
254	0.355	0.37	0.35	148.46	154.74	146.37	149.86	4.35
260	0.358	0.372	0.352	149.72	155.57	147.21	150.83	4.29

Table I.8. Experimental raw data from outdoor continuous-flow system for *Selenastrum capricornutum*; 12h HRT, Q=76.4 ml/min.

Hours at reading	OD (nm)			TSS (mg/L)			Average TSS (mg/L)	SD
	1	2	3	1	2	3		
0	0.03	0.028	0.024	12.55	11.71	10.04	11.43	1.28
12	0.03	0.036	0.02	12.55	15.06	8.36	11.99	3.38
24	0.02	0.018	0.022	8.36	7.53	9.20	8.36	0.84
36	0.032	0.029	0.036	13.38	12.13	15.06	13.52	1.47
48	0.026	0.022	0.033	10.87	9.20	13.80	11.29	2.33
60	0.046	0.04	0.05	19.24	16.73	20.91	18.96	2.10
72	0.043	0.038	0.044	17.98	15.89	18.40	17.43	1.34
80	0.062	0.05	0.064	25.93	20.91	26.77	24.53	3.17
86	0.08	0.069	0.073	33.46	28.86	30.53	30.95	2.33
98	0.073	0.062	0.076	30.53	25.93	31.78	29.41	3.08
110	0.106	0.128	0.11	44.33	53.53	46.00	47.95	4.90
122	0.103	0.1	0.106	43.08	41.82	44.33	43.08	1.25
134	0.1	0.109	0.093	41.82	45.58	38.89	42.10	3.35
140	0.091	0.103	0.112	38.06	43.08	46.84	42.66	4.41
146	0.141	0.146	0.158	58.97	61.06	66.08	62.03	3.65
158	0.135	0.142	0.155	56.46	59.39	64.82	60.22	4.24
164	0.16	0.177	0.182	66.91	74.02	76.11	72.35	4.82
170	0.203	0.195	0.206	84.90	81.55	86.15	84.20	2.38
182	0.201	0.192	0.202	84.06	80.30	84.48	82.94	2.30
194	0.24	0.233	0.243	100.37	97.44	101.63	99.81	2.15
206	0.238	0.228	0.239	99.53	95.35	99.95	98.28	2.54
218	0.248	0.235	0.251	103.72	98.28	104.97	102.32	3.56
230	0.242	0.23	0.246	101.21	96.19	102.88	100.09	3.48
242	0.244	0.236	0.249	102.04	98.70	104.13	101.63	2.74
254	0.242	0.233	0.247	101.21	97.44	103.30	100.65	2.97
260	0.243	0.235	0.25	101.63	98.28	104.55	101.493	3.14

Table I.9. Experimental raw data from outdoor continuous-flow system for *Selenastrum capricornutum*; 6h HRT, Q=152.8 ml/min.

Hours at reading	OD (nm)			TSS (mg/L)			Average TSS (mg/L)	SD
	1	2	3	1	2	3		
0	0.029	0.026	0.023	12.13	10.87	9.62	10.87	1.25
12	0.013	0.017	0.012	5.44	7.11	5.02	5.85	1.11
24	0.022	0.025	0.023	9.20	10.46	9.62	9.76	0.64
36	0.008	0.007	0.005	3.35	2.93	2.09	2.79	0.64
48	0.035	0.03	0.032	14.64	12.55	13.38	13.52	1.05
60	0.041	0.039	0.044	17.15	16.31	18.40	17.29	1.05
72	0.002	0.002	0.011	0.84	0.84	4.60	2.09	2.17
80	0.006	0.006	0.014	2.51	2.51	5.85	3.62	1.93
86	0.006	0.007	0.019	2.51	2.93	7.95	4.46	3.03
98	0.009	0.009	0.009	3.76	3.76	3.76	3.76	0.00
110	0.011	0.01	0.006	4.60	4.18	2.51	3.76	1.11
122	0.014	0.017	0.005	5.85	7.11	2.09	5.02	2.61
134	0.023	0.021	0.014	9.62	8.78	5.85	8.09	1.98
140	0.018	0.023	0.017	7.53	9.62	7.11	8.09	1.34
146	0.022	0.03	0.019	9.20	12.55	7.95	9.90	2.38
158	0.031	0.05	0.023	12.96	20.91	9.62	14.50	5.80
164	0.031	0.049	0.023	12.96	20.49	9.62	14.36	5.57
170	0.048	0.078	0.041	20.07	32.62	17.15	23.28	8.22
182	0.044	0.061	0.037	18.40	25.51	15.47	19.80	5.16
194	0.06	0.067	0.05	25.09	28.02	20.91	24.67	3.57
206	0.086	0.094	0.1	35.97	39.31	41.82	39.03	2.94
218	0.112	0.123	0.135	46.84	51.44	56.46	51.58	4.81
230	0.1	0.113	0.122	41.82	47.26	51.02	46.70	4.63
242	0.12	0.123	0.14	50.19	51.44	58.55	53.39	4.51
254	0.116	0.12	0.136	48.51	50.19	56.88	51.86	4.43
260	0.119	0.121	0.137	49.77	50.60	57.29	52.56	4.13

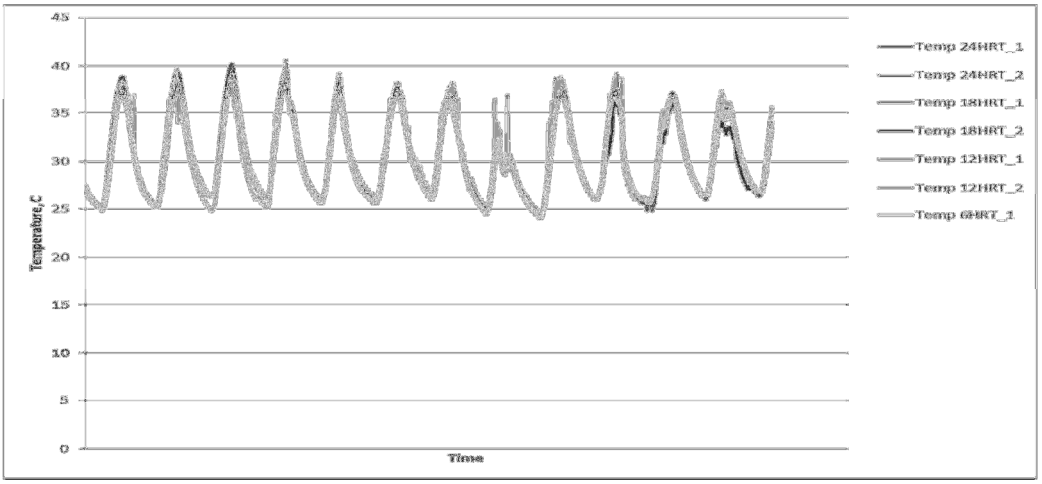

Figure I.3. Temperature results for outdoor continuous flow system for *Selenastrum capricornutum*. Lower values represent night time temperatures.

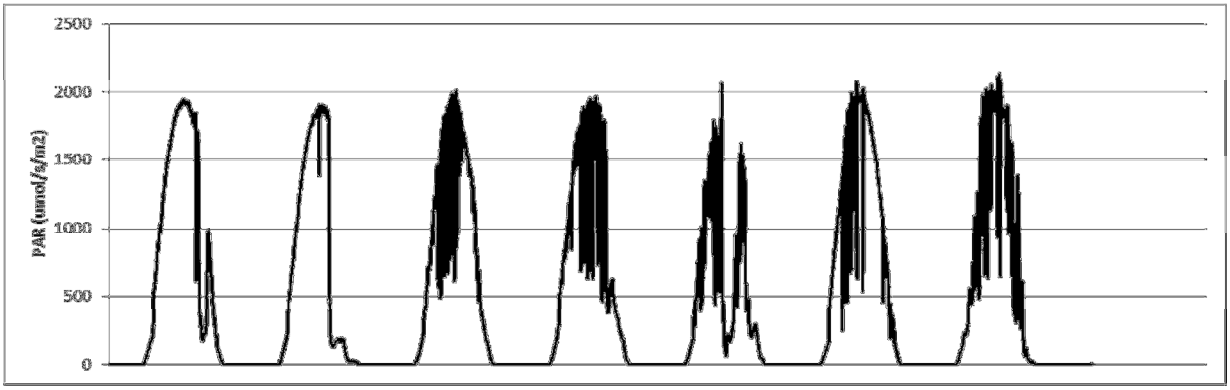

Figure I.4. PAR results for outdoor continuous flow system for *Selenastrum capricornutum*.

Table I.10. Oil content of *Selenastrum capricornutum* at the four HRT's studied.

Container	C weight	C+mix	C+oil	OIL (g)	OIL (mg/g dw)	%	AV	sd
1	27.9991	33.6806	28.3212	0.3221	322.1	32.21	32.59	0.34
2	27.8906	33.6876	28.2176	0.3270	327	32.7		
3	27.7439	33.6756	28.0726	0.3287	328.7	32.87		
4	27.7439	35.5445	27.9806	0.2367	236.7	23.67	23.39	0.25
5	27.9076	33.2999	28.1408	0.2332	233.2	23.32		
6	27.9434	33.4691	28.1752	0.2318	231.8	23.18		
7	27.8741	34.6585	28.0829	0.2088	208.8	20.88	20.74	1.20
8	27.9434	35.0863	28.1382	0.1948	194.8	19.48		
9	27.9563	35.1293	28.1749	0.2186	218.6	21.86		
10	27.7877	34.8097	27.9012	0.1135	113.5	11.35	11.37	0.59
11	27.9213	30.9574	28.0292	0.1079	107.9	10.79		
12	27.9259	32.2481	28.0456	0.1197	119.7	11.97		

Table I.11. Experimental raw data from outdoor continuous-flow system for *Scenedesmus dimorphus*; 24 h HRT, Q=38.2 ml/min.

Hours at reading	OD (nm)			TSS (mg/L)			Average TSS (mg/L)	SD
	1	2	3	1	2	3		
0	0.03	0.029	0.03	19.22	18.58	19.22	19.00	0.37
6	0.041	0.04	0.046	26.27	25.62	29.47	27.12	2.06
12	0.058	0.064	0.068	37.16	41.00	43.56	40.57	3.22
24	0.055	0.061	0.064	35.23	39.08	41.00	38.44	2.94
30	0.078	0.086	0.083	49.97	55.09	53.17	52.74	2.59
36	0.116	0.123	0.121	74.31	78.80	77.51	76.87	2.31
48	0.112	0.119	0.114	71.75	76.23	73.03	73.67	2.31
54	0.122	0.135	0.133	78.15	86.48	85.20	83.28	4.48
60	0.149	0.154	0.145	95.45	98.65	92.89	95.66	2.89
72	0.132	0.14	0.136	84.56	89.69	87.12	87.12	2.56
78	0.155	0.166	0.161	99.29	106.34	103.14	102.92	3.53
84	0.178	0.186	0.18	114.03	119.15	115.31	116.16	2.67
96	0.165	0.181	0.17	105.70	115.95	108.90	110.18	5.24
102	0.182	0.201	0.212	116.59	128.76	135.81	127.05	9.72
108	0.21	0.235	0.231	134.53	150.54	147.98	144.35	8.60
120	0.201	0.229	0.224	128.76	146.70	143.50	139.65	9.57
126	0.264	0.289	0.275	169.12	185.14	176.17	176.81	8.03
132	0.301	0.322	0.317	192.82	206.28	203.07	200.72	7.03
144	0.302	0.318	0.32	193.46	203.71	205.00	200.72	6.32
150	0.358	0.362	0.368	229.34	231.90	235.74	232.33	3.22
156	0.389	0.392	0.396	249.20	251.12	253.68	251.33	2.25
168	0.375	0.382	0.39	240.23	244.71	249.84	244.93	4.81
180	0.388	0.395	0.407	248.56	253.04	260.73	254.11	6.16
192	0.372	0.386	0.39	238.31	247.28	249.84	245.14	6.05
204	0.386	0.39	0.398	247.28	249.84	254.96	250.69	3.91

Table I.12. Experimental raw data from outdoor continuous-flow system for *Scenedesmus dimorphus*; 18 h HRT, Q=50.9 ml/min.

Hours at reading	OD (nm)			TSS (mg/L)			Average TSS (mg/L)	SD
	1	2	3	1	2	3		
0	0.031	0.028	0.028	19.86	17.94	20.50	19.43	1.33
6	0.045	0.046	0.046	28.83	29.47	29.47	29.25	0.37
12	0.058	0.053	0.053	37.16	33.95	32.03	34.38	2.59
24	0.055	0.051	0.051	35.23	32.67	30.75	32.88	2.25
30	0.062	0.063	0.063	39.72	40.36	37.80	39.29	1.33
36	0.089	0.083	0.083	57.01	53.17	52.53	54.24	2.43
48	0.081	0.078	0.078	51.89	49.97	48.69	50.18	1.61
54	0.091	0.09	0.09	58.30	57.65	55.73	57.23	1.33
60	0.101	0.099	0.099	64.70	63.42	60.22	62.78	2.31
72	0.098	0.096	0.096	62.78	61.50	55.09	59.79	4.12
78	0.112	0.109	0.109	71.75	69.83	66.62	69.40	2.59
84	0.12	0.11	0.11	76.87	70.47	73.67	73.67	3.20
96	0.115	0.098	0.098	73.67	62.78	65.34	67.26	5.69
102	0.125	0.11	0.11	80.08	70.47	73.67	74.74	4.89
108	0.14	0.135	0.135	89.69	86.48	87.12	87.76	1.69
120	0.128	0.126	0.126	82.00	80.72	78.15	80.29	1.96
126	0.157	0.158	0.158	100.58	101.22	105.06	102.28	2.43
132	0.187	0.179	0.179	119.79	114.67	108.90	114.46	5.45
144	0.177	0.172	0.172	113.39	110.18	106.98	110.18	3.20
150	0.211	0.223	0.223	135.17	142.86	154.39	144.14	9.67
156	0.243	0.254	0.254	155.67	162.71	174.89	164.42	9.72
168	0.246	0.255	0.255	157.59	163.36	179.37	166.77	11.29
180	0.271	0.259	0.259	173.61	165.92	182.57	174.03	8.34
192	0.26	0.251	0.251	166.56	160.79	180.01	169.12	9.86
204	0.27	0.255	0.255	172.96	163.36	185.78	174.03	11.25

Table I.13. Experimental raw data from outdoor continuous-flow system for *Scenedesmus dimorphus*; 12 h HRT, Q=74.6 ml/min.

Hours at reading	OD (nm)			TSS (mg/L)			Average TSS (mg/L)	SD
	1	2	3	1	2	3		
0	0.028	0.031	0.03	17.94	19.86	19.22	19.00	0.98
6	0.041	0.04	0.039	26.27	25.62	24.98	25.62	0.64
12	0.048	0.046	0.052	30.75	29.47	33.31	31.18	1.96
24	0.046	0.042	0.05	29.47	26.91	32.03	29.47	2.56
30	0.056	0.055	0.072	35.87	35.23	46.12	39.08	6.11
36	0.079	0.078	0.08	50.61	49.97	51.25	50.61	0.64
48	0.075	0.072	0.077	48.05	46.12	49.33	47.83	1.61
54	0.081	0.08	0.081	51.89	51.25	51.89	51.68	0.37
60	0.086	0.087	0.089	55.09	55.73	57.01	55.95	0.98
72	0.072	0.084	0.085	46.12	53.81	54.45	51.46	4.63
78	0.09	0.094	0.092	57.65	60.22	58.94	58.94	1.28
84	0.095	0.099	0.095	60.86	63.42	60.86	61.71	1.48
96	0.085	0.095	0.08	54.45	60.86	51.25	55.52	4.89
102	0.09	0.102	0.083	57.65	65.34	53.17	58.72	6.16
108	0.095	0.115	0.09	60.86	73.67	57.65	64.06	8.47
120	0.085	0.111	0.083	54.45	71.11	53.17	59.58	10.01
126	0.113	0.139	0.115	72.39	89.04	73.67	78.37	9.27
132	0.132	0.172	0.143	84.56	110.18	91.61	95.45	13.24
144	0.123	0.163	0.119	78.80	104.42	76.23	86.48	15.59
150	0.142	0.134	0.128	90.97	85.84	82.00	86.27	4.50
156	0.13	0.163	0.152	83.28	104.42	97.37	95.02	10.76
168	0.125	0.15	0.14	80.08	96.09	89.69	88.62	8.06
180	0.129	0.154	0.133	82.64	98.65	85.20	88.83	8.60
192	0.115	0.144	0.125	73.67	92.25	80.08	82.00	9.44
204	0.12	0.16	0.13	76.87	102.50	83.28	87.55	13.34

Table I.14. Experimental raw data from outdoor continuous-flow system for *Scenedesmus dimorphus*; 6 h HRT, Q=152.8 ml/min.

Hours at reading	OD (nm)			TSS (mg/L)			Average TSS (mg/L)	SD
	1	2	3	1	2	3		
0	0.0277	0.03	0.031	17.74	19.22	19.86	18.94	1.08
6	0.04	0.039	0.038	25.62	24.98	24.34	24.98	0.64
12	0.044	0.046	0.0474	28.19	29.47	30.36	29.34	1.09
24	0.042	0.044	0.046	26.91	28.19	29.47	28.19	1.28
30	0.051	0.054	0.052	32.67	34.59	33.31	33.53	0.98
36	0.057	0.06	0.061	36.51	38.44	39.08	38.01	1.33
48	0.055	0.056	0.058	35.23	35.87	37.16	36.09	0.98
54	0.0558	0.06	0.061	35.75	38.44	39.08	37.75	1.77
60	0.062	0.064	0.067	39.72	41.00	42.92	41.21	1.61
72	0.059	0.06	0.064	37.80	38.44	41.00	39.08	1.69
78	0.065	0.068	0.072	41.64	43.56	46.12	43.78	2.25
84	0.068	0.074	0.077	43.56	47.41	49.33	46.76	2.94
96	0.063	0.068	0.062	40.36	43.56	39.72	41.21	2.06
102	0.066	0.071	0.065	42.28	45.48	41.64	43.13	2.06
108	0.068	0.075	0.066	43.56	48.05	42.28	44.63	3.03
120	0.062	0.077	0.064	39.72	49.33	41.00	43.35	5.22
126	0.062	0.073	0.061	39.72	46.76	39.08	41.85	4.27
132	0.072	0.078	0.074	46.12	49.97	47.41	47.83	1.96
144	0.07	0.063	0.065	44.84	40.36	41.64	42.28	2.31
150	0.082	0.073	0.074	52.53	46.76	47.41	48.90	3.16
156	0.093	0.094	0.087	59.58	60.22	55.73	58.51	2.43
168	0.08	0.082	0.08	51.25	52.53	51.25	51.68	0.74
180	0.081	0.079	0.073	51.89	50.61	46.76	49.75	2.67
192	0.075	0.074	0.069	48.05	47.41	44.20	46.55	2.06
204	0.078	0.08	0.07	49.97	51.25	44.84	48.69	3.39

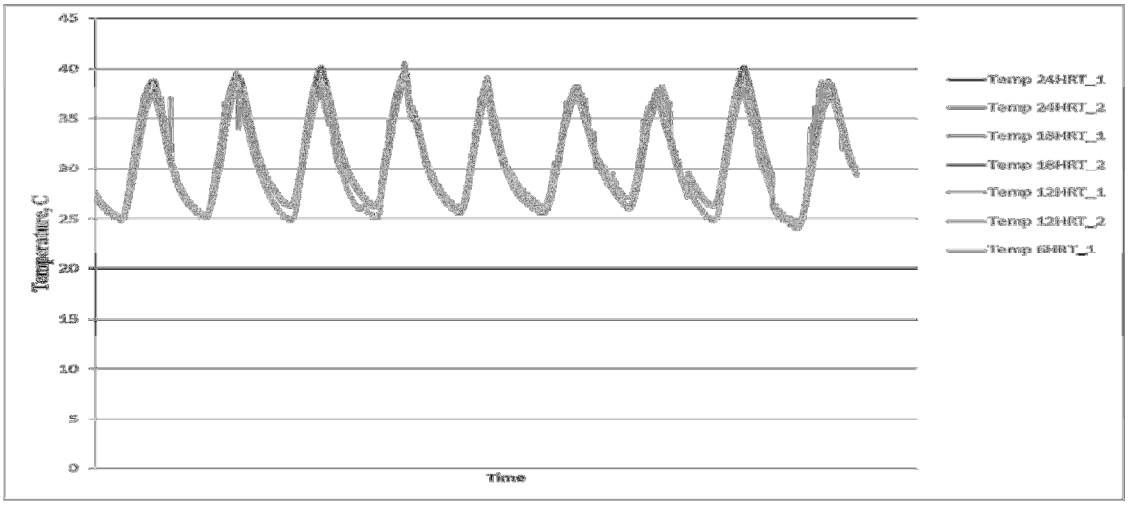

Figure I.5. Temperature results for outdoor continuous flow system for *Scenedesmus dimorphus*. Lower values represent night time temperatures.

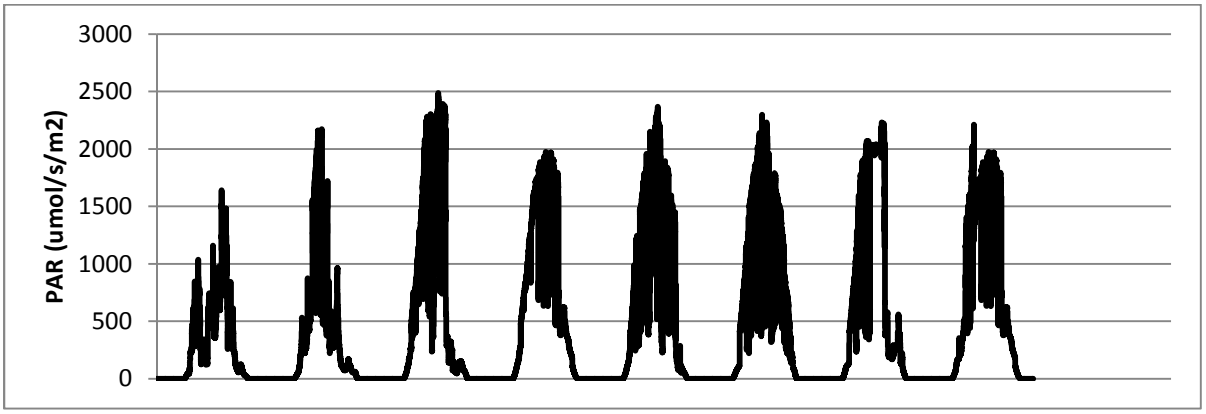

Figure I.6. PAR results for outdoor continuous flow system for *Scenedesmus dimorphus*.

Table I.15. Oil content of *Scenedesmus dimorphus* at the four HRT's studied.

Container	C weight	C+mix	C+oil	OIL (g)	OIL (mg/g dw)	%	AV	sd
1	27.9987	33.6806	28.2498	0.2511	251.1	25.11	25.91	0.78
2	27.8901	33.6876	28.1568	0.2667	266.7	26.67		
3	27.7432	33.6756	28.0026	0.2594	259.4	25.94		
4	27.7449	35.5445	27.9326	0.1877	187.7	18.77	18.05	0.67
5	27.9072	33.2999	28.0865	0.1793	179.3	17.93		
6	27.9442	33.4691	28.1186	0.1744	174.4	17.44		
7	27.8731	34.6585	27.996	0.1229	122.9	12.29	11.94	0.31
8	27.9444	35.0863	28.063	0.1186	118.6	11.86		
9	27.9553	35.1293	28.0721	0.1168	116.8	11.68		
10	27.7863	34.8097	27.8504	0.0641	64.1	6.41	7.37	0.84
11	27.9222	30.9574	28.0016	0.0794	79.4	7.94		
12	27.9247	32.2481	28.0023	0.0776	77.6	7.76		

Table I.16. Experimental raw data from outdoor continuous-flow system for *Selenastrum capricornutum* extended study; 24 h HRT, Q=38.2 ml/min.

Hours at reading	OD (nm)			TSS (mg/L)			Average TSS (mg/L)	SD
	1	2	3	1	2	3		
0	0.043	0.042	0.039	17.98	17.56	16.31	17.29	0.87
6	0.047	0.044	0.041	19.66	18.40	17.15	18.40	1.25
30	0.092	0.1	0.09	38.48	41.82	37.64	39.31	2.21
54	0.143	0.146	0.15	59.80	61.06	62.73	61.20	1.47
78	0.186	0.205	0.211	77.79	85.73	88.24	83.92	5.46
96	0.216	0.228	0.248	90.33	95.35	103.72	96.47	6.76
104	0.257	0.275	0.277	107.48	115.01	115.84	112.78	4.61
126	0.336	0.353	0.358	140.52	147.63	149.72	145.96	4.82
150	0.371	0.396	0.396	155.16	165.61	165.61	162.13	6.04
166	0.418	0.432	0.432	174.81	180.67	180.67	178.72	3.38
190	0.456	0.475	0.469	190.70	198.65	196.14	195.16	4.06
214	0.492	0.496	0.486	205.76	207.43	203.25	205.48	2.10
238	0.49	0.501	0.49	204.92	209.52	204.92	206.46	2.66
286	0.51	0.513		213.29	214.54		213.91	0.89
382	0.526			219.98			219.98	

Table I.17. Experimental raw data from outdoor continuous-flow system for *Selenastrum capricornutum* extended study; 18 h HRT, Q=50.9 ml/min.

Hours at reading	OD (nm)			TSS (mg/L)			Average TSS (mg/L)	SD
	1	2	3	1	2	3		
0	0.036	0.031	0.032	15.06	12.96	13.38	13.80	1.11
6	0.039	0.033	0.034	16.31	13.80	14.22	14.78	1.34
30	0.069	0.065	0.058	28.86	27.18	24.26	26.77	2.33
54	0.144	0.113	0.114	60.22	47.26	47.68	51.72	7.37
78	0.167	0.135	0.167	69.84	56.46	69.84	65.38	7.73
96	0.191	0.162	0.19	79.88	67.75	79.46	75.70	6.88
104	0.218	0.206	0.235	91.17	86.15	98.28	91.87	6.09
126	0.291	0.282	0.298	121.70	117.94	124.63	121.42	3.35
150	0.299	0.304	0.31	125.04	127.14	129.65	127.28	2.30
166	0.32	0.325	0.32	133.83	135.92	133.83	134.52	1.21
190	0.349	0.341	0.348	145.96	142.61	145.54	144.70	1.82
214	0.352	0.349	0.35	147.21	145.96	146.37	146.51	0.64
238	0.353	0.35	0.351	147.63	146.37	146.79	146.93	0.64
286	0.389	0.392		162.68	163.94		163.31	0.89
382	0.48			200.74			200.74	

Table I.18. Experimental raw data from outdoor continuous-flow system for *Selenastrum capricornutum* extended study; 12 h HRT, Q=74.6 ml/min.

Hours at reading	OD (nm)			TSS (mg/L)			Average TSS (mg/L)	SD
	1	2	3	1	2	3		
0	0.05	0.032	0.026	20.91	13.38	10.87	15.06	5.22
6	0.055	0.035	0.028	23.00	14.64	11.71	16.45	5.86
30	0.068	0.057	0.051	28.44	23.84	21.33	24.53	3.61
54	0.099	0.09	0.082	41.40	37.64	34.29	37.78	3.56
78	0.145	0.135	0.117	60.64	56.46	48.93	55.34	5.93
96	0.175	0.16	0.148	73.19	66.91	61.90	67.33	5.66
104	0.203	0.193	0.184	84.90	80.71	76.95	80.85	3.97
126	0.235	0.218	0.206	98.28	91.17	86.15	91.87	6.09
150	0.252	0.23	0.226	105.39	96.19	94.52	98.70	5.85
166	0.254	0.244	0.212	106.23	102.04	88.66	98.98	9.18
190	0.25	0.256	0.245	104.55	107.06	102.46	104.69	2.30
214	0.251	0.25	0.251	104.97	104.55	104.97	104.83	0.24
238	0.25	0.254	0.253	104.55	106.23	105.81	105.53	0.87
286	0.328	0.333		137.17	139.26		138.22	1.48
382	0.445			186.10			186.10	

Table I.19. Experimental raw data from outdoor continuous-flow system for *Selenastrum capricornutum* extended study; 6 h HRT, Q=152.8 ml/min.

Hours at reading	OD (nm)			TSS (mg/L)			Average TSS (mg/L)	SD
	1	2	3	1	2	3		
0	0.021	0.017	0.016	8.78	7.11	6.69	7.53	1.11
6	0.022	0.018	0.016	9.20	7.53	6.69	7.81	1.28
30	0.03	0.028	0.021	12.55	11.71	8.78	11.01	1.98
54	0.03	0.022	0.033	12.55	9.20	13.80	11.85	2.38
78	0.062	0.035	0.037	25.93	14.64	15.47	18.68	6.29
96	0.092	0.063	0.071	38.48	26.35	29.69	31.51	6.26
104	0.101	0.068	0.082	42.24	28.44	34.29	34.99	6.93
126	0.122	0.092	0.098	51.02	38.48	40.98	43.49	6.64
150	0.131	0.102	0.116	54.79	42.66	48.51	48.65	6.07
166	0.136	0.125	0.126	56.88	52.28	52.69	53.95	2.54
190	0.149	0.132	0.14	62.31	55.20	58.55	58.69	3.56
214	0.148	0.137	0.145	61.90	57.29	60.64	59.94	2.38
238	0.145	0.138	0.143	60.64	57.71	59.80	59.39	1.51
286	0.286	0.283		119.61	118.35		118.98	0.89
382	0.397			166.03			166.03	

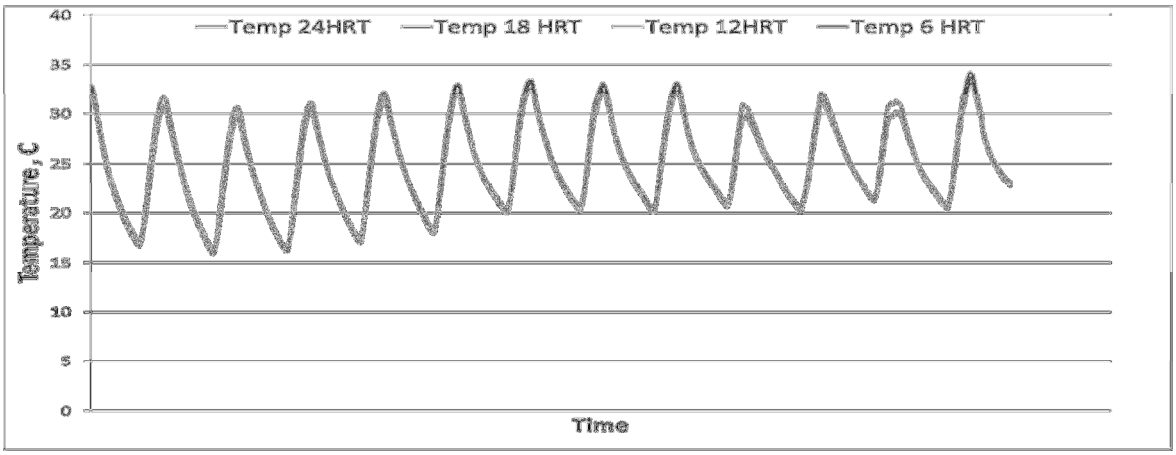

Figure I.7. Temperature results for outdoor continuous flow system for *Selenastrum capricornutum*. Lower values represent night time temperatures.

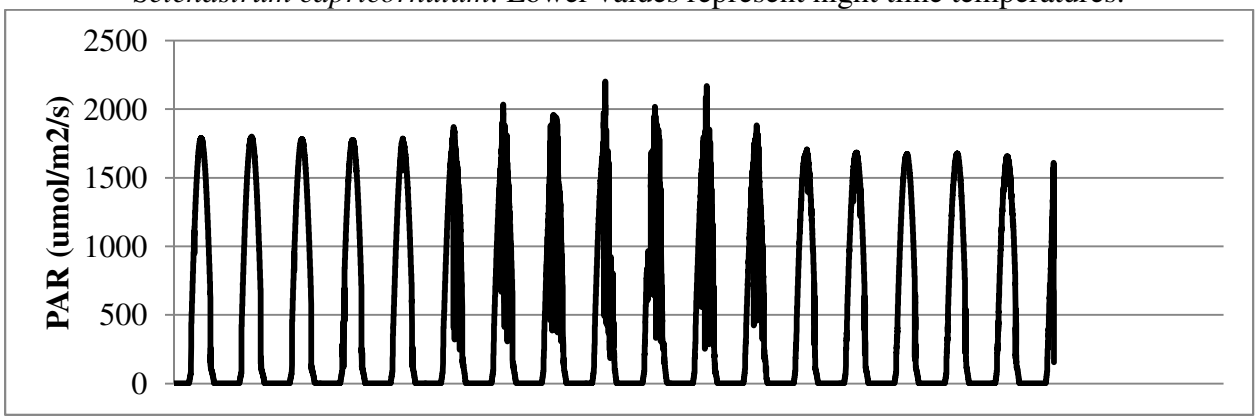

Figure I.8. PAR results for outdoor continuous flow system for *Selenastrum capricornutum*.

Table I.20. Oil content of *Selenastrum capricornutum* at the four HRT's studied.

		Container	C weight	Sample mass,g	C+oil	OIL (g)	OIL (mg/g dw)	%
24HRT	ss	3	27.8911	0.5106	28.0421	0.151	151	29.573
	2day	2	27.881	0.5095	28.0356	0.1546	154.6	30.343
	6day	1	27.8548	0.5261	28.0368	0.182	182	34.594
18HRT	ss	6	27.8455	0.5032	27.9601	0.1146	114.6	22.774
	2day	5	27.7413	0.523	27.8753	0.134	134	25.621
	6day	4	27.8576	0.5223	28.0114	0.1538	153.8	29.446
12HRT	ss	9	28.0325	0.515	28.1263	0.0938	93.8	18.213
	2day	8	27.8837	0.5124	28.0057	0.122	122	23.809
	6day	7	27.7526	0.5045	27.8906	0.138	138	27.353
6HRT	ss	12	27.839	0.5096	27.899	0.06	60	11.773
	2day	11	27.9037	0.5069	27.9759	0.0722	72.2	14.243
	6day	10	27.8422	0.5208	27.9448	0.1026	102.6	19.700

Table I.21. Biomass composition of *Selenastrum capricornutum* at the four HRT's studied.

		Sample	N %	C %	H %	Protein %	Lipid %	Carbohydrate %
24HRT	SS	3	8.34	52.46	7.49	37.04	29.57	33.39
	2DAy SS	2	7.76	51.25	7.44	34.45	30.34	35.20
	6DAY SS	1	7.30	51.22	7.31	32.40	34.59	33.00
18HRT	SS	6	8.51	50.40	7.41	37.77	22.77	39.46
	2DAy SS	5	8.09	52.33	7.46	35.93	25.62	38.45
	6DAY SS	4	7.41	51.30	7.50	32.91	29.45	37.65
12HRT	SS	9	8.54	51.67	7.43	37.93	18.21	43.86
	2DAy SS	8	8.12	51.14	7.47	36.04	23.81	40.15
	6DAY SS	7	7.52	51.78	7.50	33.38	27.35	39.27
6HRT	SS	12	8.66	51.70	7.44	38.44	11.77	49.79
	2DAy SS	11	8.20	49.65	7.28	36.42	14.24	49.34
	6DAY SS	10	7.72	51.29	7.43	34.26	19.70	46.04

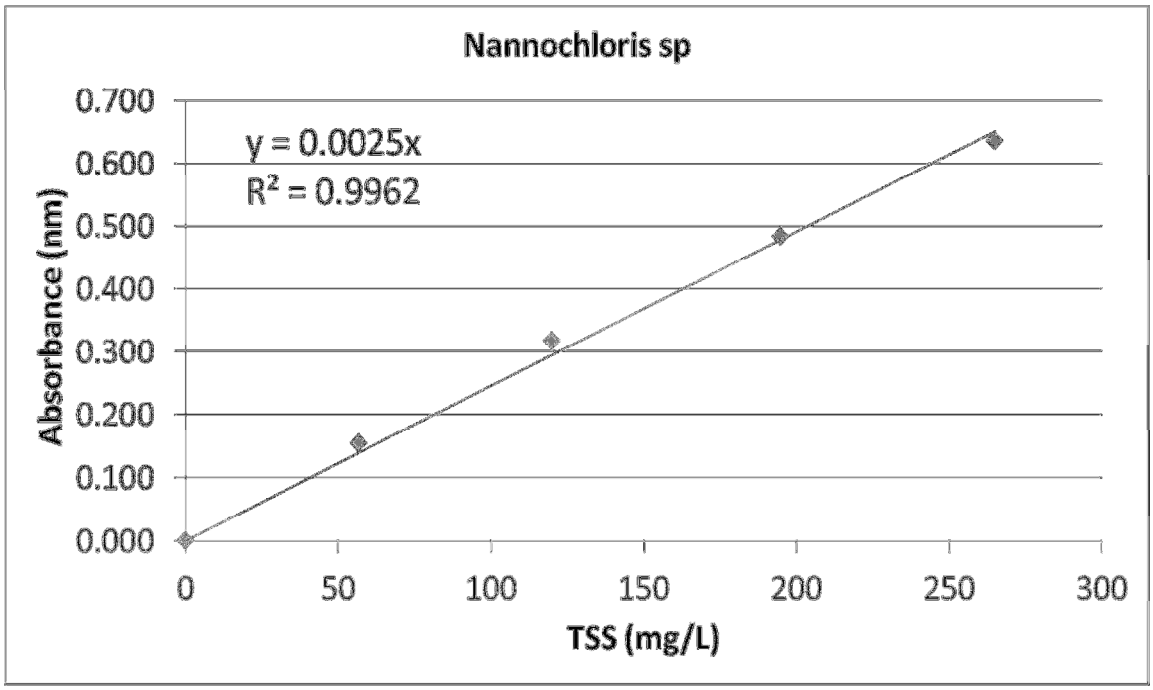

Figure I.9. Calibration curve for *Nannochloris* sp.

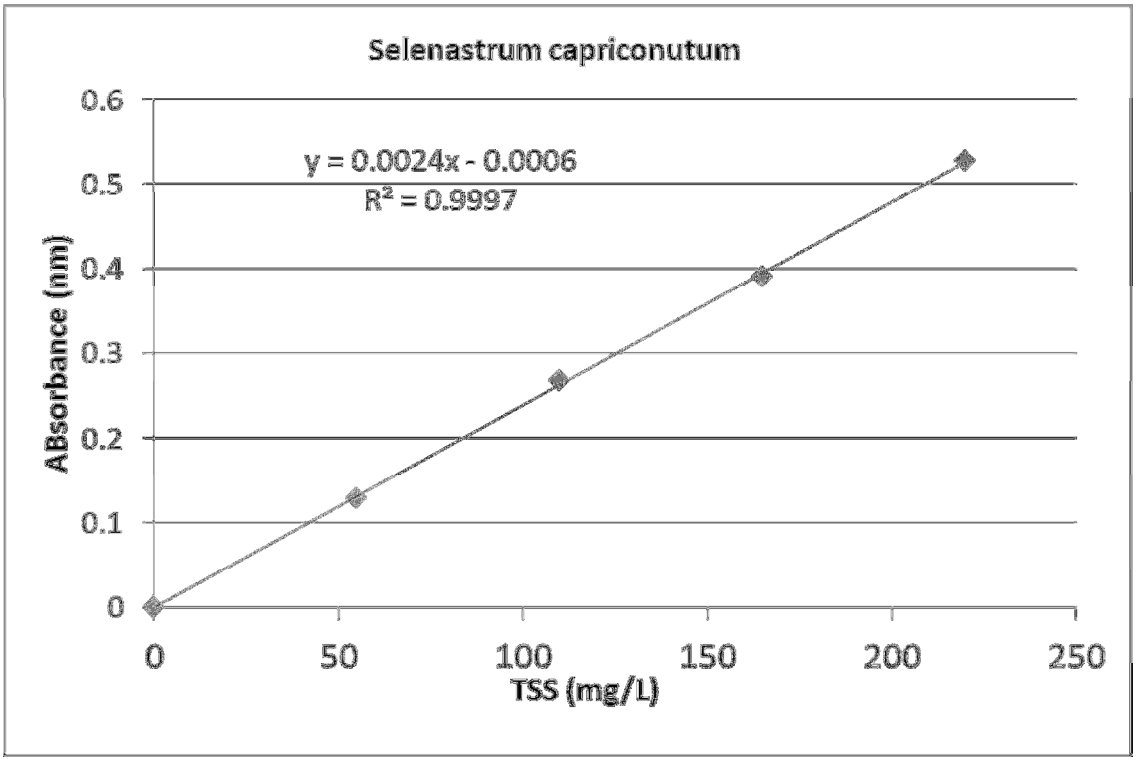

Figure I.10. Calibration curve for *Selenastrum capricornutum*

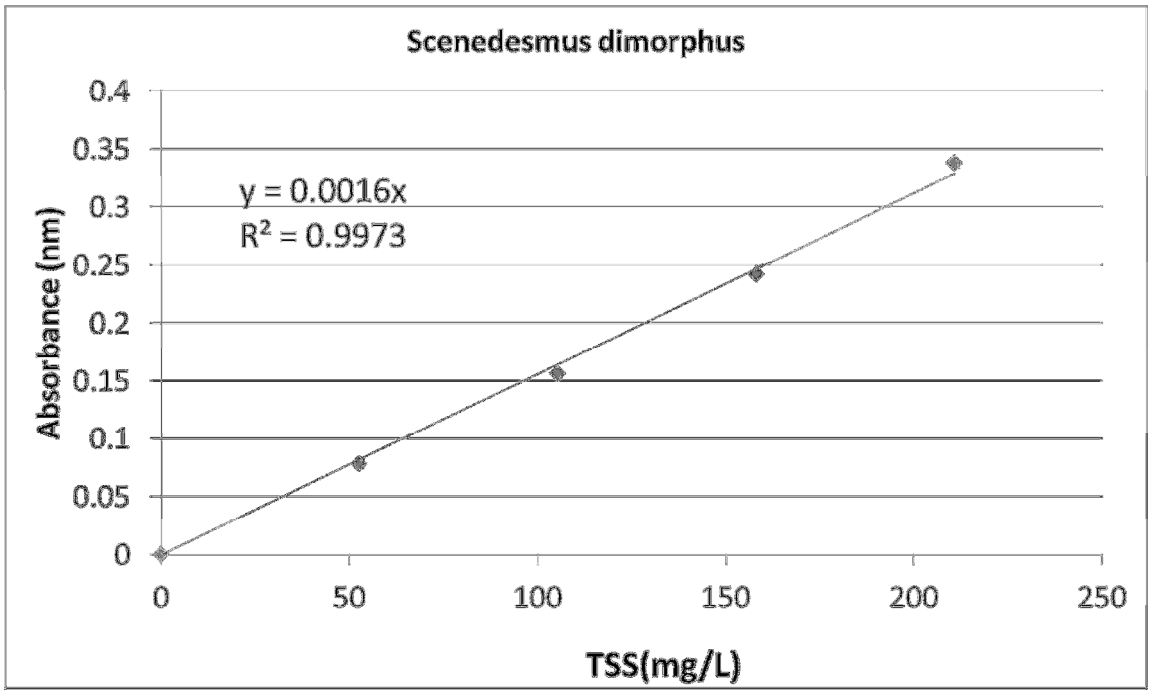

Figure I.11. Calibration curve for *Scenedesmus dimorphus*.

Table I.22. Analytical results of the media samples from the microalgal cultures collected at steady state (SS), two days after steady state (2D) and 6 days after steady state (6 D), for the HRTS studies (6, 12, 18, 24 hrs).

W.A Callegari Environmental Center
Water Quality Laboratory
Baton Rouge, LA 70820
Ph: (225) 765-5155
Fax: (225)765-5158

Analytical Results and QC Summary

Client Name:	Beatrice Terigar	**No. of Samples:**	12	**Containers:**	12	**Matrix:**	water
Address:	LSU	**Date Sampled:**	NA	**Date received**	12/1/11 12:00 PM	**Date Compl**	12/9/11 4:30 PM

Anions (Method: EPA 300.0)	0	1	2	5								
Sample Field ID:		**24 SS**	**24 2D**	**24 6D**	**18 SS**	**18 2D**	**18 6D**	**12 SS**	**12 2D**	**12 6D**	**6 SS**	**6 2D**	**6 6D**
	Media	*mg/L*	*mg/L*	*mg/L*	*mg/L*	*mg/L*	*mg/L*	*mg/L*	*mg/L*	*mg/L*	*mg/L*	*mg/L*	*mg/L*
Nitrate NO3	28.857	6.72	0.83	0.23	7.35	2.62	0.35	11.38	6.40	0.78	20.53	10.81	1.09
Nitrite NO2	38.245	20.62	11.68	2.55	24.84	12.01	6.52	29.41	14.41	9.00	33.45	20.60	11.01
Chloride	36.584	42.89	35.38	36.46	43.06	34.00	36.96	43.29	36.94	35.23	42.31	34.15	33.16
Fluoride	0.226	1.43	0.62	0.57	0.31	0.21	4.87	0.68	0.16	0.00	0.47	0.41	0.27
Sulfate	7.572	9.58	9.40	9.24	7.67	5.28	5.99	6.25	5.95	2.88	6.12	6.51	6.59
Phosphate	11.342	8.13	5.94	4.82	8.54	5.69	3.64	9.20	7.42	4.41	9.49	7.49	4.63

Metals (Method: EPA 200.7)												
Sample Field ID:	**24 SS**	**24 2D**	**24 6D**	**18 SS**	**18 2D**	**18 6D**	**12 SS**	**12 2D**	**12 6D**	**6 SS**	**6 2D**	**6 6D**
Unit:	*mg/L*	*mg/L*	*mg/L*	*mg/L*	*mg/L*	*mg/L*	*mg/L*	*mg/L*	*mg/L*	*mg/L*	*mg/L*	*mg/L*
Aluminum (Al)	0.0161	0.0221	0.0288	0.0103	0.0169	0.0245	0.0100	0.0149	0.0134	0.0174	0.0123	0.0091
Boron (B)	0.1435	0.1415	0.1230	0.1427	0.1226	0.1185	0.1168	0.1219	0.1146	0.1268	0.1027	0.1005
Barium (Ba)	0.0131	0.0278	0.0417	0.0111	0.0112	0.0301	0.0114	ND	0.0293	ND	ND	0.0210
Calcium (Ca)	0.3168	0.4897	0.6339	0.3058	0.3076	0.4944	0.3074	0.3547	0.4479	0.3179	0.3161	0.4202
Copper (Cu)	0.0219	0.0280	0.0285	0.0201	0.0246	0.0273	0.0228	0.0204	0.0233	0.0225	0.0212	0.0206
Iron (Fe)	0.8844	0.8177	0.7752	0.8454	0.8684	0.6882	0.8699	0.5062	0.6249	0.8212	0.7626	0.6115
Potassium (K)	0.9446	0.7946	0.4316	0.6983	0.4336	0.3154	0.6038	0.7145	0.3851	0.4972	0.4746	0.2636
Magnesium (Mg)	0.1053	0.2953	0.0364	0.0592	0.0525	0.0241	0.0295	0.0146	0.0314	0.0410	0.0083	0.0121
Manganese (Mn)	0.0231	0.0251	0.0224	0.0321	0.0625	0.0183	0.1887	0.1728	0.0146	0.2192	0.1708	0.0350
Sodium (Na)	15.5408	15.8202	16.3931	14.6721	14.5291	15.3976	14.9583	14.7457	14.9034	14.6666	14.6900	14.6748
Nickel (Ni)	0.0430	0.0426	0.0473	0.0414	0.0391	0.0438	0.0367	0.0413	0.0421	0.0348	0.0349	0.0390
Phosphorus (P)	3.4339	3.0330	2.9681	3.5341	3.3351	3.1286	3.6419	3.4428	2.9257	3.7475	3.3946	3.1393
Sulfur (S)	3.8060	3.6513	3.7268	4.1260	3.8480	3.9303	4.7559	4.3413	4.4750	5.1870	5.0750	5.0829
Silicon (Si)	20.5333	20.0398	22.1993	19.1529	18.1651	20.4371	17.0582	18.4507	19.1881	16.2476	16.2595	17.9119
Zinc (Zn)	0.1580	0.3187	0.1439	0.1788	0.2160	0.1286	0.0921	0.1092	0.1010	0.0824	0.0752	0.1089

Figure I.12. Actual set-up used for the different HRT's in the continuous-flow system.

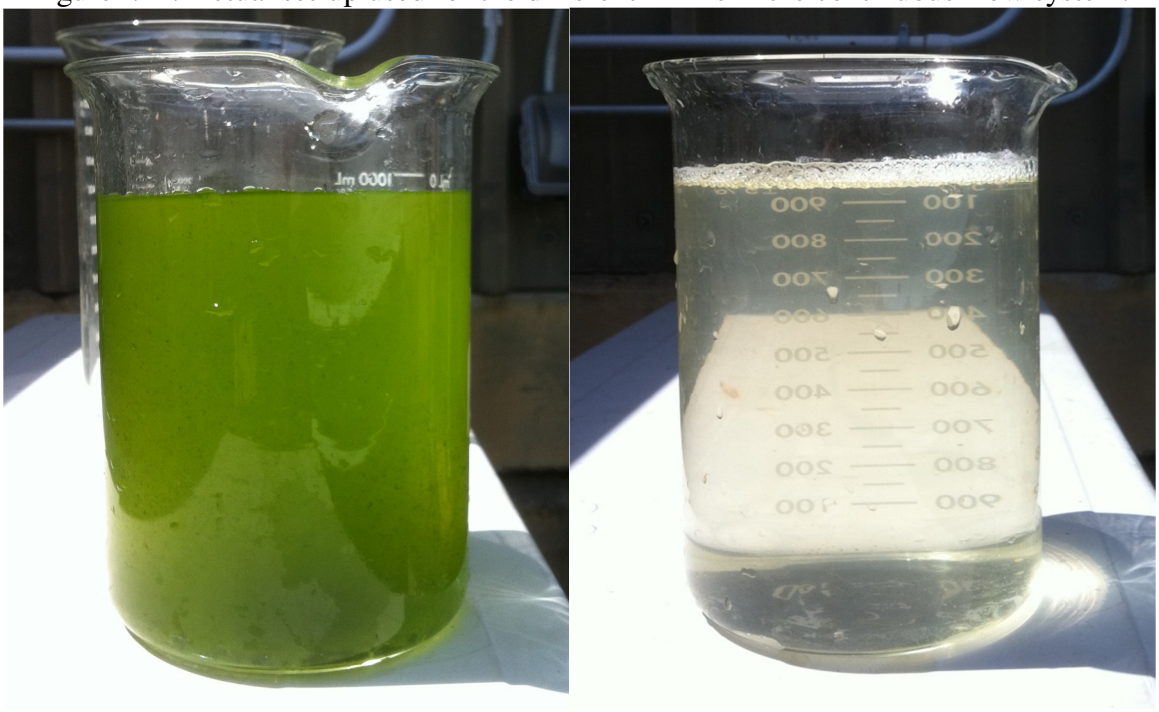

Figure I.22. Algae mixture before centrifugation, left; algae mixture after extraction. Centrifugation efficiency was calculated to be 92%.

APPENDIX II: INTERMITTENT LIGHT EXPERIMENTAL DATA

Table II.1.Table containing information about all the D/L ratios, periods of light and dark cycles, frequencies and physical information of the rotating disk.

L	D	t_{Light} (s)	t_{Dark} (s)	Frequency (Hz)	Disc speed (rpm)	Cycle Time (s)	Open Sector size (cm)	Openings
1	1	5.000	5.000	0.1	6	10.000	64	1
1	1	2.500	2.500	0.2	12	5.000	64	1
1	1	1.250	1.250	0.4	24	2.500	64	1
1	1	0.625	0.625	0.8	24	1.250	32	2
1	1	0.313	0.313	1.6	48	0.625	32	2
1	1	0.156	0.156	3.2	96	0.313	32	2
1	1	0.078	0.078	6.4	96	0.156	16	4
1	1	0.039	0.039	12.8	48	0.078	4	16
1	1	0.020	0.020	25.6	96	0.039	4	16
1	1	0.010	0.010	51.2	192	0.020	4	16
1	1	0.005	0.005	102.4	384	0.010	4	16
1	2	3.328	6.672	0.1	6	10.000	42.6	1
1	2	1.664	3.336	0.2	12	5.000	42.6	1
1	2	0.832	1.668	0.4	24	2.500	42.6	1
1	2	0.416	0.834	0.8	48	1.250	42.6	1
1	2	0.208	0.417	1.6	96	0.625	42.6	1
1	2	0.104	0.209	3.2	48	0.313	10.62	4
1	2	0.052	0.104	6.4	96	0.156	10.62	4
1	2	0.026	0.052	12.8	192	0.078	10.62	4
1	2	0.013	0.026	25.6	192	0.039	5.31	8
1	2	0.005	0.013	51.2	384	0.018	5.31	8
1	3	2.500	7.500	0.1	6	10.000	32	1
1	3	1.250	3.750	0.2	12	5.000	32	1
1	3	0.625	1.875	0.4	24	2.500	32	1
1	3	0.313	0.938	0.8	48	1.250	32	1
1	3	0.156	0.469	1.6	96	0.625	32	1
1	3	0.078	0.234	3.2	24	0.313	4	8
1	3	0.039	0.117	6.4	48	0.156	4	8
1	3	0.020	0.059	12.8	96	0.078	4	8
1	3	0.010	0.029	25.6	192	0.039	4	8
1	3	0.005	0.015	51.2	384	0.020	4	8
1	4	2.000	8.000	0.1	6	10.000	25.6	1

1	4	1.000	4.000	0.2	12	5.000	25.6	1
1	4	0.500	2.000	0.4	24	2.500	25.6	1
1	4	0.250	1.000	0.8	48	1.250	25.6	1
1	4	0.125	0.500	1.6	96	0.625	25.6	1
1	4	0.063	0.250	3.2	24	0.313	3.2	8
1	4	0.031	0.125	6.4	48	0.156	3.2	8
1	4	0.016	0.063	12.8	96	0.078	3.2	8
1	4	0.005	0.020	40.0	300	0.025	3.2	8
1	5	1.666	8.334	0.1	6	10.000	21.33	1
1	5	0.833	4.167	0.2	12	5.000	21.33	1
1	5	0.417	2.083	0.4	24	2.500	21.33	1
1	5	0.208	1.042	0.8	48	1.250	21.33	1
1	5	0.104	0.521	1.6	96	0.625	21.33	1
1	5	0.052	0.260	3.2	48	0.313	5.33	4
1	5	0.026	0.130	6.4	96	0.156	5.33	4
1	5	0.013	0.065	12.8	192	0.078	5.33	4
1	5	0.005	0.025	33.3	500	0.030	5.33	4
1	6	1.428	8.572	0.1	6	10.000	18.28	1
1	6	0.714	4.286	0.2	12	5.000	18.28	1
1	6	0.357	2.143	0.4	24	2.500	18.28	1
1	6	0.179	1.071	0.8	48	1.250	18.28	1
1	6	0.089	0.536	1.6	96	0.625	18.28	1
1	6	0.045	0.268	3.2	48	0.313	4.57	4
1	6	0.022	0.134	6.4	96	0.156	4.57	4
1	6	0.011	0.067	12.8	192	0.078	4.57	4
1	6	0.005	0.031	28.0	420	0.036	4.57	4
1	7	1.250	8.750	0.1	6	10.000	16.00	1
1	7	0.625	4.375	0.2	12	5.000	16.00	1
1	7	0.313	2.188	0.4	24	2.500	16.00	1
1	7	0.156	1.094	0.8	48	1.250	16.00	1
1	7	0.078	0.547	1.6	96	0.625	16.00	1
1	7	0.039	0.273	3.2	48	0.313	4.00	4
1	7	0.020	0.137	6.4	96	0.156	4.00	4
1	7	0.010	0.068	12.8	192	0.078	4.00	4
1	7	0.005	0.035	24.7	370	0.041	4.00	4
1	8	1.111	8.889	0.1	6	10.000	14.22	1
1	8	0.555	4.445	0.2	12	5.000	14.22	1
1	8	0.278	2.222	0.4	24	2.500	14.22	1
1	8	0.139	1.111	0.8	48	1.250	14.22	1
1	8	0.069	0.556	1.6	96	0.625	14.22	1
1	8	0.035	0.278	3.2	192	0.313	14.22	1

1	8	0.017	0.139	6.4	384	0.156	14.22	1
1	8	0.009	0.069	12.8	192	0.078	3.56	4
1	8	0.005	0.040	22.0	330	0.045	3.56	4
1	9	1.000	9.000	0.1	6	10.000	12.80	1
1	9	0.500	4.500	0.2	12	5.000	12.80	1
1	9	0.250	2.250	0.4	24	2.500	12.80	1
1	9	0.125	1.125	0.8	48	1.250	12.80	1
1	9	0.063	0.563	1.6	96	0.625	12.80	1
1	9	0.031	0.281	3.2	192	0.313	12.80	1
1	9	0.016	0.141	6.4	96	0.156	3.20	4
1	9	0.008	0.070	12.8	192	0.078	3.20	4
1	9	0.005	0.045	20.0	300	0.050	3.20	4
1	10	0.909	9.091	0.1	6	10.000	11.63	1
1	10	0.454	4.546	0.2	12	5.000	11.63	1
1	10	0.227	2.273	0.4	24	2.500	11.63	1
1	10	0.114	1.136	0.8	48	1.250	11.63	1
1	10	0.057	0.568	1.6	96	0.625	11.63	1
1	10	0.028	0.284	3.2	48	0.313	2.91	4
1	10	0.014	0.142	6.4	96	0.156	2.91	4
1	10	0.005	0.050	18.3	275	0.055	2.91	4
1	15	0.625	9.375	0.1	6	10.000	8.00	1
1	20	0.476	9.524	0.1	6	10.000	6.10	1
1	25	0.385	9.615	0.1	6	10.000	4.92	1
1	30	0.323	9.677	0.1	6	10.000	4.13	1
2	1	6.667	3.333	0.1	6	10.000	85.33	1
2	1	3.333	1.667	0.2	12	5.000	85.33	1
2	1	1.667	0.833	0.4	24	2.500	85.33	1
2	1	0.833	0.417	0.8	48	1.250	85.33	1
2	1	0.417	0.208	1.6	96	0.625	85.33	1
2	1	0.208	0.104	3.2	192	0.313	85.33	1
3	1	7.500	2.500	0.1	6	10.000	96.00	1
3	1	3.750	1.250	0.2	12	5.000	96.00	1
3	1	1.875	0.625	0.4	24	2.500	96.00	1
3	1	0.938	0.313	0.8	48	1.250	96.00	1
3	1	0.469	0.156	1.6	96	0.625	96.00	1
3	1	0.234	0.078	3.2	192	0.313	96.00	1

Table II.2. Data 1/1 D/L;

Time (h)	Optical reading (mV)			TSS (mg/L)			Average (mg/L)	SD
	1	2	3	1	2	3		
3	0.218	0.248	0.24	-13.0513	-9.72486	-22.1341	-14.9701	6.423272
6	0.216	0.258	0.24	-10.6592	-20.6578	-22.1341	-17.817	6.242655
9	0.213	0.25	0.238	-7.08105	-11.9019	-18.7759	-12.5863	5.8774
12	0.215	0.255	0.238	-9.46514	-17.3654	-18.7759	-15.2021	5.018197
15	0.214	0.258	0.238	-8.27242	-20.6578	-18.7759	-15.902	6.67411
18	0.215	0.255	0.237	-9.46514	-17.3654	-17.1059	-14.6455	4.48818
21	0.215	0.25	0.238	-9.46514	-11.9019	-18.7759	-13.381	4.828404
24	0.216	0.251	0.236	-10.6592	-12.9922	-15.442	-13.0311	2.391651
27	0.215	0.249	0.239	-9.46514	-10.8128	-20.452	-13.5766	5.992227
30	0.214	0.247	0.239	-8.27242	-8.63814	-20.452	-12.4542	6.928703
33	0.212	0.246	0.239	-5.89101	-7.55263	-20.452	-11.2985	7.970523
36	0.21	0.246	0.239	-3.51497	-7.55263	-20.452	-10.5065	8.846447
39	0.209	0.242	0.24	-2.32896	-3.22252	-22.1341	-9.22852	11.18547
42	0.206	0.239	0.241	1.221031	0.012504	-23.8223	-7.52957	14.12281
45	0.209	0.234	0.24	-2.32896	5.380279	-22.1341	-6.36092	14.1934
48	0.207	0.232	0.239	0.039042	7.519014	-20.452	-4.29797	14.48106
51	0.205	0.234	0.24	2.401678	5.380279	-22.1341	-4.78404	15.0992
54	0.204	0.225	0.234	3.580984	14.96691	-12.1324	2.138504	13.60711
57	0.202	0.228	0.235	5.935574	11.78213	-13.7842	1.311179	13.39581
60	0.2	0.22	0.233	8.2848	20.25094	-10.4867	6.016362	15.49385
63	0.198	0.214	0.233	10.62866	26.5523	-10.4867	8.898103	18.58002
66	0.195	0.221	0.236	14.1344	19.19653	-15.442	5.962968	18.70926
69	0.191	0.2	0.235	18.78994	41.088	-13.7842	15.36459	27.59599
72	0.19	0.198	0.234	19.95047	43.14539	-12.1324	16.98783	27.75772
75	0.189	0.193	0.232	21.10966	48.26792	-8.847	20.17686	28.56888
78	0.182	0.188	0.228	29.18646	53.36055	-2.349	26.73267	27.93572
81	0.18	0.188	0.225	31.48205	53.36055	2.460812	29.10114	25.53326
84	0.179	0.166	0.223	32.62783	75.4128	5.637033	37.89255	35.18455
87	0.177	0.186	0.22	34.91537	55.38922	10.35588	33.55349	22.54754
90	0.172	0.157	0.22	40.61076	84.26729	10.35588	45.07798	37.15765
93	0.17	0.154	0.218	42.87953	87.19725	13.47145	47.84941	37.11332
96	0.168	0.148	0.217	45.14293	93.02488	15.02015	51.06265	39.33786
99	0.168	0.148	0.213	45.14293	93.02488	21.15426	53.10736	36.59126
102	0.164	0.139	0.214	49.65365	101.6856	19.62983	56.98968	41.51686
105	0.158	0.135	0.21	56.3795	105.5037	25.69117	62.52478	40.25956
108	0.156	0.143	0.205	58.61072	97.84834	33.13139	63.19682	32.6013
111	0.153	0.131	0.204	61.94749	109.3026	34.60124	68.61712	37.79467
114	0.151	0.128	0.2	64.16531	112.1393	40.42	72.24153	36.53536
117	0.148	0.13	0.196	67.48197	110.2494	46.14172	74.62435	32.64518

120	0.143	0.123	0.191	72.98291	116.8431	53.15742	80.99448	32.58996
123	0.141	0.125	0.19	75.17391	114.9652	54.54237	81.56048	30.71351
126	0.139	0.124	0.185	77.35954	115.9047	61.37613	84.88013	28.03144
129	0.135	0.122	0.181	81.7147	117.7803	66.73398	88.74299	26.23888
132	0.133	0.12	0.176	83.88424	119.651	73.29484	92.2767	24.29094
135	0.129	0.11	0.171	88.20722	128.9331	79.70408	98.94813	26.31348
138	0.126	0.125	0.166	91.43538	114.9652	85.9617	97.45408	15.41002
141	0.125	0.109	0.165	92.50875	129.8547	87.19503	103.1862	23.24795
144	0.12	0.109	0.159	97.85549	129.8547	94.46766	107.3926	19.52635
147	0.12	0.11	0.157	97.85549	128.9331	96.84336	107.8773	18.24186
150	0.113	0.108	0.149	105.2846	130.7751	106.1035	114.0544	14.48635
153	0.113	0.102	0.149	105.2846	136.2726	106.1035	115.8869	17.65926
156	0.108	0.099	0.138	110.5509	139.0052	118.2026	122.5862	14.72494
159	0.104	0.095	0.138	114.7398	142.6318	118.2026	125.1914	15.20279
162	0.102	0.094	0.132	116.8262	143.5355	124.4927	128.2848	13.75254
165	0.094	0.092	0.127	125.1181	145.3393	129.5678	133.3417	10.62573
168	0.093	0.094	0.125	126.1486	143.5355	131.5553	133.7465	8.898167
171	0.09	0.092	0.122	129.2319	145.3393	134.4912	136.3541	8.213704
174	0.089	0.095	0.121	130.257	142.6318	135.4577	136.1155	6.213592
177	0.088	0.094	0.119	131.2808	143.5355	137.3724	137.3962	6.127417
180	0.088	0.095	0.118	131.2808	142.6318	138.3207	137.4111	5.72995
183	0.086	0.093	0.119	133.3242	144.438	137.3724	138.3782	5.624734
186	0.084	0.098	0.117	135.3624	139.9136	139.263	138.1797	2.461432
189	0.084	0.093	0.116	135.3624	144.438	140.1991	139.9998	4.5411
192	0.084	0.095	0.114	135.3624	142.6318	142.0533	140.0158	4.040381
195	0.084	0.094	0.114	135.3624	143.5355	142.0533	140.3171	4.354416
198	0.08	0.095	0.114	139.4225	142.6318	142.0533	141.3692	1.71052
201	0.082	0.095	0.113	137.3951	142.6318	142.9712	140.9994	3.126002
204	0.079	0.097	0.112	140.4342	140.8209	143.8831	141.7128	1.889535
207	0.081	0.088	0.112	138.4095	148.9325	143.8831	143.7417	5.262918
210	0.079	0.092	0.111	140.4342	145.3393	144.789	143.5208	2.687216
213	0.078	0.094	0.111	141.4446	143.5355	144.789	143.2564	1.689603
216	0.078	0.099	0.109	141.4446	139.0052	146.5825	142.3441	3.867918

Data 1/1 D/L; 0.2 Hz

Time (h)	Optical reading (mV)			TSS (mg/L)			Average (mg/L)	SD
	1	2	3	1	2	3		
3	0.267	0.228	0.254	-31.824	-12.1658	-62.1747	-35.3881	25.19426
6	0.268	0.228	0.248	-34.0448	-12.1658	-53.7229	-33.3112	20.78831
9	0.266	0.227	0.245	-29.6145	-10.9982	-49.5209	-30.0445	19.26499
12	0.266	0.255	0.244	-29.6145	-43.8369	-48.1238	-40.525	9.688904
15	0.266	0.258	0.245	-29.6145	-47.3733	-49.5209	-42.1696	10.92592
18	0.266	0.255	0.245	-29.6145	-43.8369	-49.5209	-40.9908	10.25388
21	0.267	0.25	0.243	-31.824	-37.9506	-46.7284	-38.8343	7.491418
24	0.267	0.251	0.244	-31.824	-39.1271	-48.1238	-39.6916	8.164559
27	0.267	0.249	0.242	-31.824	-36.7745	-45.3348	-37.9778	6.835317
30	0.265	0.247	0.239	-27.4163	-34.4235	-41.1646	-34.3348	6.874593
33	0.266	0.246	0.239	-29.6145	-33.2486	-41.1646	-34.6759	5.90587
36	0.264	0.246	0.238	-25.2294	-33.2486	-39.7781	-32.752	7.287041
39	0.262	0.242	0.237	-20.8895	-28.5527	-38.3933	-29.2785	8.774431
42	0.263	0.239	0.232	-23.0538	-25.0348	-31.4959	-26.5282	4.414752
45	0.264	0.234	0.233	-25.2294	-19.1795	-32.8719	-25.7602	6.861628
48	0.264	0.232	0.231	-25.2294	-16.84	-30.1218	-24.0637	6.717169
51	0.26	0.234	0.232	-16.5949	-19.1795	-31.4959	-22.4234	7.962596
54	0.261	0.225	0.228	-18.7365	-8.66411	-26.0099	-17.8035	8.71044
57	0.258	0.228	0.228	-12.3455	-12.1658	-26.0099	-16.8404	7.941534
60	0.259	0.22	0.225	-14.4645	-2.83575	-21.9139	-13.0714	9.61505
63	0.256	0.214	0.221	-8.14126	4.145546	-16.4772	-6.82432	10.37428
66	0.256	0.221	0.223	-8.14126	-4.00065	-19.192	-10.4446	7.853254
69	0.253	0.2	0.217	-1.91976	20.3812	-11.0689	2.464182	16.17688
72	0.253	0.198	0.215	-1.91976	22.6944	-8.37533	4.133107	16.39542
75	0.25	0.193	0.21	4.2	28.47066	-1.67232	10.33278	15.97993
78	0.25	0.188	0.208	4.2	34.23727	0.99652	13.1446	18.33688
81	0.246	0.188	0.204	12.2014	34.23727	6.312994	17.58389	14.7197
84	0.245	0.166	0.194	14.17348	59.49572	19.48051	31.0499	24.7773
87	0.244	0.186	0.195	16.13426	36.54121	18.17171	23.61572	11.24006
90	0.241	0.157	0.189	21.94876	69.77488	25.99801	39.24055	26.5209
93	0.236	0.154	0.186	31.41349	73.19432	29.88731	44.83171	24.5746
96	0.237	0.148	0.182	29.54316	80.02279	35.04831	48.20475	27.69237
99	0.235	0.148	0.178	33.27252	80.02279	40.18104	51.15878	25.2345
102	0.231	0.139	0.171	40.59558	90.23943	49.09531	59.97677	26.55057
105	0.227	0.135	0.167	47.73775	94.77012	54.1503	65.55272	25.50534
108	0.226	0.143	0.165	49.49503	85.70256	56.6672	63.95493	19.17236
111	0.22	0.131	0.156	59.80128	99.29464	67.90579	75.66724	20.85933
114	0.218	0.128	0.15	63.14625	102.684	75.31868	80.38297	20.24953
117	0.213	0.13	0.15	71.31084	100.4248	75.31868	82.35144	15.77975

120	0.206	0.123	0.142	82.26642	108.3252	85.10359	91.89839	14.29655
123	0.204	0.125	0.138	85.29484	106.0698	89.95364	93.77277	10.90136
126	0.202	0.124	0.129	88.27803	107.1977	100.7629	98.74621	9.619705
129	0.191	0.122	0.127	103.8772	109.4522	103.1455	105.4917	3.449405
132	0.184	0.12	0.123	113.0918	111.7052	107.8896	110.8955	2.693953
135	0.189	0.11	0.111	106.5665	122.9471	121.9521	117.1552	9.183598
138	0.185	0.125	0.117	111.8093	106.0698	114.9527	110.9439	4.504193
141	0.17	0.109	0.107	129.8589	124.0691	126.5831	126.837	2.903219
144	0.168	0.109	0.108	132.0733	124.0691	125.428	127.1901	4.283166
147	0.163	0.11	0.102	137.4115	122.9471	132.3321	130.8969	7.338234
150	0.163	0.108	0.105	137.4115	125.1908	128.888	130.4968	6.267163
153	0.159	0.102	0.099	141.4785	131.9127	135.7603	136.3838	4.813283
156	0.151	0.099	0.102	149.0699	135.2685	132.3321	138.8902	8.937363
159	0.147	0.095	0.095	152.5943	139.7374	140.3064	144.2127	7.264242
162	0.147	0.094	0.099	152.5943	140.8537	135.7603	143.0694	8.632988
165	0.144	0.092	0.09	155.1189	143.0851	145.9494	148.0511	6.286177
168	0.142	0.094	0.092	156.7454	140.8537	143.6975	147.0989	8.474287
171	0.139	0.092	0.089	159.1004	143.0851	147.0727	149.7527	8.337235
174	0.14	0.095	0.09	158.3267	139.7374	145.9494	148.0045	9.463505
177	0.14	0.094	0.089	158.3267	140.8537	147.0727	148.751	8.856585
180	0.139	0.095	0.089	159.1004	139.7374	147.0727	148.6369	9.775789
183	0.139	0.093	0.088	159.1004	141.9696	148.1942	149.7547	8.671365
186	0.138	0.098	0.087	159.8628	136.3863	149.314	148.521	11.75831
189	0.137	0.093	0.087	160.6139	141.9696	149.314	150.6325	9.391809
192	0.138	0.095	0.089	159.8628	139.7374	147.0727	148.891	10.18514
195	0.138	0.094	0.088	159.8628	140.8537	148.1942	149.6369	9.586308
198	0.138	0.095	0.087	159.8628	139.7374	149.314	149.6381	10.06659
201	0.137	0.095	0.087	160.6139	139.7374	149.314	149.8884	10.45006
204	0.137	0.093	0.086	160.6139	141.9696	150.432	151.0052	9.335344
207	0.136	0.088	0.086	161.3537	147.5432	150.432	153.1096	7.284175
210	0.135	0.089	0.085	162.0821	146.4293	151.5482	153.3532	7.980998
213	0.134	0.089	0.082	162.7993	146.4293	154.8863	154.7049	8.186506
216	0.132	0.088	0.082	164.1997	147.5432	154.8863	155.5431	8.347627
	Data 1/1 D/L; 0.4 Hz							
3	0.266	0.251	0.283	-35.5911	-12.9922	-23.4867	-18.2394	7.420757
6	0.289	0.242	0.262	-82.2304	-3.22252	5.815133	1.296308	6.390583
9	0.255	0.234	0.254	-14.8211	5.380279	16.48618	10.93323	7.853058
12	0.295	0.239	0.259	-95.1117	0.012504	9.848557	4.930531	6.95514
15	0.246	0.242	0.262	1.433306	-3.22252	5.815133	1.296308	6.390583
18	0.245	0.239	0.259	3.198288	0.012504	9.848557	4.930531	6.95514
21	-0.085	0.234	0.254	137.0892	5.380279	16.48618	10.93323	7.853058

24	-0.189	0.235	0.255	-6.06588	4.309116	15.16713	9.738123	7.677775
27	-0.392	0.233	0.253	-541.415	6.450245	17.80099	12.12562	8.02619
30	-1.784	0.231	0.251	-13329.8	8.586588	20.4179	14.50224	8.366002
33	-0.124	0.23	0.25	93.81602	9.652965	21.72	15.68648	8.532682
36	0.308	0.23	0.25	-124.036	9.652965	21.72	15.68648	8.532682
39	0.305	0.226	0.246	-117.238	13.90651	26.88602	20.39626	9.177899
42	-0.479	0.223	0.243	-874.457	17.08411	30.71604	23.90007	9.63923
45	0.256	0.218	0.238	-16.6682	22.35618	37.01465	29.68542	10.36511
48	0.241	0.216	0.236	10.17608	24.45663	39.50444	31.98053	10.6404
51	0.272	0.218	0.238	-47.339	22.35618	37.01465	29.68542	10.36511
54	0.245	0.209	0.229	3.198288	31.77054	48.08519	39.92786	11.5362
57	0.266	0.212	0.232	-35.5911	28.64319	44.43315	36.53817	11.16519
60	0.245	0.204	0.224	3.198288	36.95887	54.08717	45.52302	12.11154
63	0.258	0.198	0.218	-20.3871	43.14539	61.14971	52.14755	12.73098
66	0.254	0.205	0.225	-12.9822	35.9236	52.89525	44.40942	12.00077
69	0.25	0.184	0.204	-5.70875	57.41311	77.0357	67.22441	13.87526
72	0.241	0.182	0.202	10.17608	59.43222	79.23732	69.33477	14.00432
75	0.244	0.177	0.197	4.955056	64.45905	84.66723	74.56314	14.28934
78	0.254	0.172	0.192	-12.9822	69.45597	89.9912	79.72358	14.5206
81	0.234	0.172	0.192	22.07103	69.45597	89.9912	79.72358	14.5206
84	0.228	0.15	0.17	31.94638	91.08713	112.1581	101.6226	14.89942
87	0.231	0.17	0.19	27.04566	71.44637	92.09112	81.76874	14.59805
90	0.228	0.141	0.161	31.94638	99.76935	120.6352	110.2023	14.75439
93	0.232	0.138	0.158	25.39566	102.6419	123.3846	113.0133	14.66734
96	0.225	0.132	0.152	36.77319	108.3547	128.7691	118.5619	14.43517
99	0.211	0.132	0.152	58.32092	108.3547	128.7691	118.5619	14.43517
102	0.226	0.123	0.143	35.17247	116.8431	136.5597	126.7014	13.94176
105	0.262	0.119	0.139	-27.9234	120.5846	139.912	130.2483	13.66655
108	0.157	0.127	0.147	126.3546	113.0824	133.1396	123.111	14.18256
111	0.246	0.115	0.135	1.433306	124.307	143.1966	133.7518	13.35693
114	0.235	0.112	0.132	20.39639	127.0862	145.6155	136.3509	13.10214
117	0.163	0.114	0.134	119.9779	125.2346	144.0071	134.6209	13.27415
120	0.259	0.107	0.127	-22.2588	131.6944	149.5622	140.6283	12.63447
123	0.139	0.109	0.129	143.7104	129.8547	147.9962	138.9255	12.82799
126	-0.202	0.108	0.128	-30.2062	130.7751	148.7813	139.7782	12.73231
129	0.055	0.106	0.126	189.5199	132.6124	150.3389	141.4756	12.53449
132	0.216	0.104	0.124	50.8101	134.4449	151.8794	143.1622	12.32807
135	0.074	0.094	0.114	184.2297	143.5355	159.328	151.4317	11.16693
138	0.079	0.109	0.129	182.3448	129.8547	147.9962	138.9255	12.82799
141	0.054	0.093	0.113	189.7162	144.438	160.0495	152.2438	11.03899
144	0.247	0.093	0.113	-0.33989	144.438	160.0495	152.2438	11.03899

147	-0.011	0.094	0.114	184.8587	143.5355	159.328	151.4317	11.16693
150	0.141	0.092	0.112	141.9134	145.3393	160.7668	153.0531	10.9089
153	0.12	0.086	0.106	159.1436	150.7219	164.9817	157.8518	10.08319
156	0.144	0.083	0.107	139.1563	153.3971	164.2898	158.8434	7.702333
159	0.151	0.079	0.106	132.4355	156.9472	164.9817	160.9644	5.681255
162	0.152	0.078	0.105	131.4425	157.8317	165.6693	161.7505	5.54203
165	0.087	0.076	0.105	178.9019	159.5972	165.6693	162.6333	4.29364
168	0.04	0.078	0.103	191.602	157.8317	167.0319	162.4318	6.505521
171	-0.195	0.076	0.105	-17.0351	159.5972	165.6693	162.6333	4.29364
174	-0.035	0.079	0.104	174.2937	156.9472	166.3527	161.65	6.650738
177	0.047	0.078	0.104	190.8603	157.8317	166.3527	162.0922	6.025274
180	-0.013	0.079	0.103	184.159	156.9472	167.0319	161.9895	7.130984
183	0.219	0.077	0.104	46.20504	158.7151	166.3527	162.5339	5.400656
186	-0.056	0.082	0.102	161.1687	154.2864	167.7068	160.9966	9.489702
189	-0.187	0.077	0.102	-2.47517	158.7151	167.7068	163.211	6.358153
192	0.075	0.079	0.103	183.8692	156.9472	167.0319	161.9895	7.130984
195	-0.28	0.078	0.103	-204.196	157.8317	167.0319	162.4318	6.505521
198	-0.038	0.079	0.102	172.6404	156.9472	167.7068	162.327	7.608235
201	0.019	0.079	0.102	191.4124	156.9472	167.7068	162.327	7.608235
204	0.005	0.081	0.101	189.2739	155.1745	168.3775	161.776	9.335954
207	0.131	0.08	0.102	150.57	156.0614	167.7068	161.8841	8.234545
210	0.024	0.076	0.101	191.7861	159.5972	168.3775	163.9874	6.208635
213	0.101	0.078	0.1	171.6119	157.8317	169.044	163.4379	7.928282
216	0.151	0.076	0.1	132.4355	159.5972	169.044	164.3206	6.679892
	Data 1/1 D/L; 0.4 Hz							
3	0.177	0.208	0.2	34.91537	-1.14429	8.2848	14.01863	18.70113
6	0.175	0.218	0.2	37.19755	-13.0513	8.2848	10.81034	25.21946
9	0.172	0.21	0.198	40.61076	-3.51497	10.62866	15.90815	22.53164
12	0.174	0.215	0.198	38.33663	-9.46514	10.62866	13.16672	24.00174
15	0.173	0.218	0.198	39.47436	-13.0513	10.62866	12.35056	26.30515
18	0.174	0.215	0.197	38.33663	-9.46514	11.79858	13.55669	23.94933
21	0.174	0.21	0.198	38.33663	-3.51497	10.62866	15.15011	21.289
24	0.175	0.211	0.196	37.19755	-4.70232	12.96716	15.15413	21.03537
27	0.174	0.209	0.199	38.33663	-2.32896	9.457402	15.15502	20.92294
30	0.173	0.207	0.199	39.47436	0.039042	9.457402	16.3236	20.59477
33	0.171	0.206	0.199	41.74581	1.221031	9.457402	17.47475	21.41898
36	0.169	0.206	0.199	44.0119	1.221031	9.457402	18.23011	22.70429
39	0.168	0.202	0.2	45.14293	5.935574	8.2848	19.78777	21.98961
42	0.165	0.199	0.201	48.52798	9.457402	7.110858	21.69875	23.2644
45	0.168	0.194	0.2	45.14293	15.30029	8.2848	22.90934	19.57176
48	0.166	0.192	0.199	47.40097	17.62807	9.457402	24.82881	19.9704

51	0.164	0.194	0.2	49.65365	15.30029	8.2848	24.41291	22.13877
54	0.163	0.185	0.194	50.77798	25.73302	15.30029	30.60376	18.23347
57	0.161	0.188	0.195	53.02261	22.26751	14.1344	29.80817	20.51144
60	0.159	0.18	0.193	55.26188	31.48205	16.46485	34.40292	19.56274
63	0.157	0.174	0.193	57.49578	38.33663	16.46485	37.43242	20.5304
66	0.154	0.181	0.196	60.83658	30.33492	12.96716	34.71289	24.23314
69	0.15	0.16	0.195	65.2722	54.14291	14.1344	44.5165	26.89367
72	0.149	0.158	0.194	66.37775	56.3795	15.30029	46.01918	27.06896
75	0.148	0.153	0.192	67.48197	61.94749	17.62807	49.01918	27.32598
78	0.141	0.148	0.188	75.17391	67.48197	22.26751	54.97446	28.58496
81	0.139	0.148	0.185	77.35954	67.48197	25.73302	56.85817	27.40389
84	0.138	0.126	0.183	78.45034	91.43538	28.03666	65.97412	33.49017
87	0.136	0.146	0.18	80.62792	69.68637	31.48205	60.59878	25.80247
90	0.131	0.117	0.18	86.04841	101.0474	31.48205	72.8593	36.61011
93	0.129	0.114	0.178	88.20722	104.2273	33.77227	75.40227	36.93174
96	0.127	0.108	0.177	90.36067	110.5509	34.91537	78.60897	39.16324
99	0.127	0.108	0.173	90.36067	110.5509	39.47436	80.12864	36.62634
102	0.123	0.099	0.174	94.65147	119.9457	38.33663	84.31127	41.77559
105	0.117	0.095	0.17	101.0474	124.0863	42.87953	89.33776	41.8506
108	0.115	0.103	0.165	103.1687	115.7836	48.52798	89.16011	35.74928
111	0.112	0.091	0.164	106.3405	128.2055	49.65365	94.73322	40.54189
114	0.11	0.088	0.16	108.4484	131.2808	54.14291	97.95736	39.62459
117	0.107	0.09	0.156	111.6001	129.2319	58.61072	99.81425	36.7562
120	0.102	0.083	0.151	116.8262	136.3794	64.16531	105.7903	37.35054
123	0.1	0.085	0.15	118.9072	134.344	65.2722	106.1745	36.25355
126	0.098	0.084	0.145	120.9829	135.3624	70.78656	109.0439	33.90299
129	0.094	0.082	0.141	125.1181	137.3951	75.17391	112.5624	32.95611
132	0.092	0.08	0.136	127.1777	139.4225	80.62792	115.7427	31.02049
135	0.088	0.07	0.131	131.2808	149.479	86.04841	122.2694	32.66136
138	0.085	0.085	0.126	134.344	134.344	91.43538	120.0411	24.77329
141	0.084	0.069	0.125	135.3624	150.4773	92.50875	126.1161	30.07006
144	0.079	0.069	0.119	140.4342	150.4773	98.92081	129.9441	27.33222
147	0.079	0.07	0.117	140.4342	149.479	101.0474	130.3202	25.75121
150	0.072	0.068	0.109	147.4785	151.4743	109.5003	136.151	23.1665
153	0.072	0.062	0.109	147.4785	157.4277	109.5003	138.1355	25.29283
156	0.067	0.059	0.098	152.4699	160.3863	120.9829	144.613	20.8436
159	0.063	0.055	0.098	156.4388	164.3124	120.9829	147.2447	23.08162
162	0.061	0.054	0.092	158.4153	165.2906	127.1777	150.2945	20.31274
165	0.053	0.052	0.087	166.2674	167.2429	132.3032	155.2711	19.89682
168	0.052	0.054	0.085	167.2429	165.2906	134.344	155.6258	18.45643
171	0.049	0.052	0.082	170.1613	167.2429	137.3951	158.2664	18.13387

174	0.048	0.055	0.081	171.1314	164.3124	138.4095	157.9511	17.26354
177	0.047	0.054	0.079	172.1001	165.2906	140.4342	159.275	16.66803
180	0.047	0.055	0.078	172.1001	164.3124	141.4446	159.2857	15.93399
183	0.045	0.053	0.079	174.0337	166.2674	140.4342	160.2451	17.59068
186	0.043	0.058	0.077	175.9618	161.3699	142.4536	159.9284	16.80058
189	0.043	0.053	0.076	175.9618	166.2674	143.4612	161.8968	16.68529
192	0.043	0.055	0.074	175.9618	164.3124	145.4725	161.9156	15.38532
195	0.043	0.054	0.074	175.9618	165.2906	145.4725	162.2416	15.47163
198	0.039	0.055	0.074	179.8021	164.3124	145.4725	163.1957	17.192
201	0.041	0.055	0.073	177.8846	164.3124	146.4762	162.8911	15.7524
204	0.038	0.057	0.072	180.7588	162.3521	147.4785	163.5298	16.67139
207	0.04	0.048	0.072	178.844	171.1314	147.4785	165.818	16.34392
210	0.038	0.052	0.071	180.7588	167.2429	148.4794	165.4937	16.21061
213	0.037	0.054	0.071	181.7142	165.2906	148.4794	165.1614	16.61774
216	0.037	0.059	0.069	181.7142	160.3863	150.4773	164.1926	15.96247
	Data 1/1 D/L; 0.8 Hz							
3	0.281	0.242	0.269	-63.9441	20.0219	-36.2769	-26.733	42.78886
6	0.282	0.242	0.263	-66.3232	20.0219	-23.0538	-23.1184	43.17258
9	0.28	0.241	0.26	-61.5763	21.94876	-16.5949	-18.7408	41.80387
12	0.28	0.269	0.259	-61.5763	-36.2769	-14.4645	-37.4392	23.5774
15	0.28	0.272	0.26	-61.5763	-43.0411	-16.5949	-40.4041	22.60637
18	0.28	0.269	0.26	-61.5763	-36.2769	-16.5949	-38.1494	22.5491
21	0.281	0.264	0.258	-63.9441	-25.2294	-12.3455	-33.8396	26.8553
24	0.281	0.265	0.259	-63.9441	-27.4163	-14.4645	-35.275	25.65885
27	0.281	0.263	0.257	-63.9441	-23.0538	-10.2377	-32.4119	28.0495
30	0.279	0.261	0.254	-59.2198	-18.7365	-3.98228	-27.3129	28.60004
33	0.28	0.26	0.254	-61.5763	-16.5949	-3.98228	-27.3845	30.27507
36	0.278	0.26	0.253	-56.8747	-16.5949	-1.91976	-25.1298	28.45425
39	0.276	0.256	0.252	-52.2183	-8.14126	0.131469	-20.076	28.14164
42	0.277	0.253	0.247	-54.5408	-1.91976	10.218	-15.4142	34.42384
45	0.278	0.248	0.248	-56.8747	8.223309	8.223309	-13.476	37.58434
48	0.278	0.246	0.246	-56.8747	12.2014	12.2014	-10.824	39.88109
51	0.274	0.248	0.247	-47.6071	8.223309	10.218	-9.72191	32.82465
54	0.275	0.239	0.243	-49.907	25.76857	18.08373	-2.01823	41.65051
57	0.272	0.242	0.243	-43.0411	20.0219	18.08373	-1.64515	35.86302
60	0.273	0.234	0.24	-45.3184	35.12024	23.86432	4.555384	43.5571
63	0.27	0.228	0.236	-38.5203	45.96916	31.41349	12.95411	45.16835
66	0.27	0.235	0.238	-38.5203	33.27252	27.66152	7.471239	39.92854
69	0.267	0.214	0.232	-31.824	69.70053	38.78177	25.55277	52.03904
72	0.267	0.212	0.23	-31.824	72.90984	42.39808	27.82798	53.86566
75	0.264	0.207	0.225				35.58229	54.69024

78	0.264	0.202	0.223	-25.2294	80.73525	51.241	39.24922	58.30957
81	0.26	0.202	0.219	-25.2294	88.27803	54.69903	44.38752	54.48561
84	0.259	0.18	0.209	-16.5949	88.27803	61.47942	60.42766	67.94169
87	0.258	0.2	0.21	-14.4645	118.1085	77.639	51.64815	55.93485
90	0.255	0.171	0.204	-12.3455	91.216	76.07392	69.32448	68.79994
93	0.25	0.168	0.201	-6.05612	128.7347	85.29484	75.34199	65.14327
96	0.251	0.162	0.197	4.2	132.0733	89.75267	78.71825	69.67654
99	0.249	0.162	0.193	2.171387	138.4452	95.53816	81.93509	68.17444
102	0.245	0.153	0.186	6.217307	138.4452	101.1428	90.64299	68.72306
105	0.241	0.149	0.182	14.17348	147.2399	110.5156	96.14208	66.6244
108	0.24	0.157	0.18	21.94876	150.8547	115.6227	95.139	63.01218
111	0.234	0.145	0.171	23.86432	143.4442	118.1085	106.0479	62.73993
114	0.232	0.142	0.165	35.12024	154.2887	128.7347	110.2791	62.83923
117	0.227	0.144	0.165	38.78177	156.7454	135.3101	112.7223	57.14312
120	0.22	0.137	0.157	47.73775	155.1189	135.3101	121.2865	53.93533
123	0.218	0.139	0.153	59.80128	160.6139	143.4442	123.1622	52.31255
126	0.216	0.138	0.144	63.14625	159.1004	147.2399	127.1426	52.61825
129	0.205	0.136	0.142	66.446	159.8628	155.1189	133.9618	43.51431
132	0.198	0.134	0.138	83.78628	161.3537	156.7454	138.9236	38.83857
135	0.203	0.124	0.126	94.10875	162.7993	159.8628	141.4236	47.3162
138	0.199	0.139	0.132	86.79208	169.3491	168.1296	138.656	39.90832
141	0.184	0.123	0.122	92.66803	159.1004	164.1997	151.1857	32.99159
144	0.182	0.123	0.123	113.0918	169.9419	170.5234	151.8355	31.36119
147	0.177	0.124	0.117	115.6227	169.9419	169.9419	154.7876	28.67617
150	0.177	0.122	0.12	121.7523	169.3491	173.2613	154.6427	28.48954
153	0.173	0.116	0.114	121.7523	170.5234	171.6525	158.3319	27.61289
156	0.165	0.113	0.117	126.4525	173.775	174.7684	161.2732	22.5066
159	0.161	0.109	0.11	135.3101	175.2481	173.2613	164.3804	21.57619
162	0.161	0.108	0.114	139.4676	177.054	176.6195	163.9044	21.20619
165	0.158	0.106	0.105	139.4676	177.4773	174.7684	166.4786	20.79557
168	0.156	0.108	0.107	142.467	178.2898	178.6791	166.5922	19.21135
171	0.153	0.106	0.104	144.4101	177.4773	177.8892	168.1956	18.1522
174	0.154	0.109	0.105	147.2399	178.2898	179.0571	167.347	18.23848
177	0.154	0.108	0.104	146.308	177.054	178.6791	167.6141	18.46856
180	0.153	0.109	0.104	146.308	177.4773	179.0571	167.7837	17.81958
183	0.153	0.107	0.103	147.2399	177.054	179.0571	168.1843	18.15457
186	0.152	0.112	0.102	147.2399	177.8892	179.4238	167.8854	17.20256
189	0.151	0.107	0.102	148.1606	175.7166	179.7791	168.9128	17.21034
192	0.152	0.109	0.104	149.0699	177.8892	179.7791	168.0906	17.2889
195	0.152	0.108	0.103	148.1606	177.054	179.0571	168.3539	17.51496
198	0.152	0.109	0.102	148.1606	177.4773	179.4238	168.3313	17.52137

201	0.151	0.109	0.102	148.1606	177.054	179.7791	168.6344	16.99799
204	0.151	0.107	0.101	149.0699	177.054	179.7791	169.0274	17.31976
207	0.15	0.102	0.101	149.0699	177.8892	180.1232	169.9568	17.31166
210	0.149	0.103	0.1	149.968	179.7791	180.1232	170.2448	16.80024
213	0.148	0.103	0.097	150.8547	179.4238	180.456	170.8468	16.58454
216	0.146	0.102	0.097	151.7302	179.4238	181.3865	171.5376	15.68738
	Data 1/1 D/L; 6.4 Hz							
3	0.274	0.26	0.292	-51.3207	-24.1388	-88.6341	-56.3864	45.60506
6	0.297	0.251	0.271	-99.4712	-7.5148	-45.3605	-26.4376	26.76092
9	0.263	0.243	0.263	-29.828	6.703611	-29.828	-11.5622	25.83173
12	0.303	0.248	0.268	-112.747	-2.1213	-39.4742	-20.7977	26.41247
15	0.254	0.251	0.271	-12.9822	-7.5148	-45.3605	-26.4376	26.76092
18	0.253	0.248	0.268	-11.1515	-2.1213	-39.4742	-20.7977	26.41247
21	-0.077	0.243	0.263	144.4217	6.703611	-29.828	-11.5622	25.83173
24	-0.181	0.244	0.264	8.099844	4.955056	-31.7408	-13.3929	25.94788
27	-0.384	0.242	0.262	-513.911	8.443954	-27.9234	-9.73971	25.71558
30	-1.776	0.24	0.26	-13210.8	11.9	-24.1388	-6.1194	25.48328
33	-0.116	0.239	0.259	103.711	13.6157	-22.2588	-4.32157	25.36713
36	0.316	0.239	0.259	-142.525	13.6157	-22.2588	-4.32157	25.36713
39	0.313	0.235	0.255	-135.53	20.39639	-14.8211	2.787637	24.90253
42	-0.471	0.232	0.252	-841.237	25.39566	-9.32906	8.033304	24.55408
45	0.264	0.227	0.247	-31.7408	33.56353	-0.33989	16.61182	23.97334
48	0.249	0.225	0.245	-3.91092	36.77319	3.198288	19.98574	23.74104
51	0.28	0.227	0.247	-63.4628	33.56353	-0.33989	16.61182	23.97334
54	0.253	0.218	0.238	-11.1515	47.74827	15.32319	31.53573	22.92799
57	0.274	0.221	0.241	-51.3207	43.09394	10.17608	26.63501	23.27644
60	0.253	0.213	0.233	-11.1515	55.34123	23.73745	39.53934	22.34725
63	0.266	0.207	0.227	-35.5911	64.18175	33.56353	48.87264	21.65035
66	0.262	0.214	0.234	-27.9234	53.83907	22.07103	37.95505	22.4634
69	0.258	0.193	0.213	-20.3871	83.65981	55.34123	69.50052	20.02426
72	0.249	0.191	0.211	-3.91092	86.31098	58.32092	72.31595	19.79196
75	0.252	0.186	0.206	-9.32906	92.79519	65.62643	79.21081	19.21121
78	0.262	0.181	0.201	-27.9234	99.07406	72.7266	85.90033	18.63047
81	0.242	0.181	0.201	8.443954	99.07406	72.7266	85.90033	18.63047
84	0.236	0.159	0.179	18.71354	124.2619	101.5281	112.895	16.07518
87	0.239	0.179	0.199	13.6157	101.5281	75.50918	88.51865	18.39817
90	0.236	0.15	0.17	18.71354	133.4203	112.1649	122.7926	15.02984
93	0.24	0.147	0.167	11.9	136.3252	115.5626	125.9439	14.68139
96	0.233	0.141	0.161	23.73745	141.9134	122.1363	132.0249	13.98449
99	0.219	0.141	0.161	46.20504	141.9134	122.1363	132.0249	13.98449
102	0.234	0.132	0.152				140.5919	12.93915

105	0.27	0.128	0.148	22.07103	149.7413	131.4425	144.1859	12.47455
108	0.165	0.136	0.156	-43.3901	153.0068	135.3651	136.8665	13.40375
111	0.254	0.124	0.144	117.7867	146.3443	127.3886	147.6486	12.00995
114	0.243	0.121	0.141	-12.9822	156.1409	139.1563	150.1593	11.66151
117	0.171	0.123	0.143	6.703612	158.4052	141.9134	148.4937	11.8938
120	0.267	0.116	0.136	111.0158	156.9039	140.0835	154.1796	11.08076
123	0.147	0.118	0.138	-37.5285	162.0149	146.3443	152.5961	11.31306
126	-0.194	0.117	0.137	136.3252	160.5957	144.5966	153.392	11.19691
129	0.063	0.115	0.135	-15.1864	161.3094	145.4746	154.959	10.96461
132	0.224	0.113	0.133	187.6538	162.7122	147.2059	156.4932	10.73231
135	0.082	0.103	0.123	38.3657	164.0821	148.9044	163.6715	9.570818
138	0.087	0.118	0.138	181.1153	170.4391	156.9039	152.5961	11.31306
141	0.062	0.102	0.122	178.9019	160.5957	144.5966	164.3441	9.454668
144	0.255	0.102	0.122	187.9158	171.0296	157.6587	164.3441	9.454668
147	-0.003	0.103	0.123	-14.8211	171.0296	157.6587	163.6715	9.570818
150	0.149	0.101	0.121	187.3291	170.4391	156.9039	165.0086	9.338519
153	0.128	0.095	0.115	134.3968	171.6119	158.4052	168.8227	8.641623
156	0.152	0.092	0.116	153.0068	174.9333	162.7122	169.249	10.23057
159	0.159	0.088	0.115	131.4425	176.4831	162.0149	170.5734	11.11738
162	0.16	0.087	0.114	124.2619	178.4345	162.7122	171.1516	10.96058
165	0.095	0.085	0.114	123.2032	178.9019	163.4013	171.6066	11.60406
168	0.048	0.087	0.112	174.9333	179.8119	163.4013	171.8283	10.0035
171	-0.187	0.085	0.114	190.7215	178.9019	164.7548	171.6066	11.60406
174	-0.027	0.088	0.113	-2.47517	179.8119	163.4013	171.2583	10.14869
177	0.055	0.087	0.113	178.341	178.4345	164.0821	171.492	10.47914
180	-0.005	0.088	0.112	189.5199	178.9019	164.0821	171.5947	9.673051
183	0.227	0.086	0.113	186.7608	178.4345	164.7548	171.7216	10.80378
186	-0.048	0.091	0.111	33.56353	179.361	164.0821	171.2013	8.177025
189	-0.179	0.086	0.111	166.5957	176.9833	165.4192	172.3901	9.858315
192	0.083	0.088	0.112	11.55914	179.361	165.4192	171.5947	9.673051
195	-0.272	0.087	0.112	180.6891	178.4345	164.7548	171.8283	10.0035
198	-0.03	0.088	0.111	-184.052	178.9019	164.7548	171.9269	9.203221
201	0.027	0.088	0.111	176.8849	178.4345	165.4192	171.9269	9.203221
204	0.013	0.09	0.11	191.9117	178.4345	165.4192	171.7754	8.060876
207	0.139	0.089	0.111	190.693	177.4753	166.0755	171.6891	8.866963
210	0.032	0.085	0.11	143.7104	177.959	165.4192	172.9437	9.713128
213	0.109	0.087	0.109	191.9569	179.8119	166.0755	172.8127	8.611435
216	0.159	0.085	0.109	166.7235	178.9019	166.7235	173.2677	9.254913
				124.2619	179.8119	166.7235		

Table II.3. Data 2/1 D/L;

Time (h)	Optical reading (mV)			TSS (mg/L)			Average (mg/L)	SD
	1	2	3	1	2	3		
	Data 2/1 D/L; 0.1 Hz							
3	0.203	0.208	0.18	4.75895	-1.14429	31.48205	11.6989	17.3851
6	0.204	0.218	0.18	3.580984	-13.0513	31.48205	7.337234	22.50306
9	0.202	0.21	0.178	5.935574	-3.51497	33.77227	12.06429	19.38441
12	0.202	0.215	0.178	5.935574	-9.46514	33.77227	10.0809	21.91475
15	0.202	0.218	0.178	5.935574	-13.0513	33.77227	8.885505	23.55078
18	0.204	0.215	0.177	3.580984	-9.46514	34.91537	9.677073	22.80963
21	0.203	0.21	0.178	4.75895	-3.51497	33.77227	11.67208	19.58132
24	0.205	0.211	0.176	2.401678	-4.70232	36.05713	11.25216	21.77341
27	0.204	0.209	0.179	3.580984	-2.32896	32.62783	11.29329	18.71106
30	0.204	0.207	0.179	3.580984	0.039042	32.62783	12.08262	17.88059
33	0.204	0.206	0.179	3.580984	1.221031	32.62783	12.47662	17.49131
36	0.203	0.206	0.179	4.75895	1.221031	32.62783	12.86927	17.20261
39	0.204	0.202	0.18	3.580984	5.935574	31.48205	13.6662	15.47383
42	0.205	0.199	0.181	2.401678	9.457402	30.33492	14.06467	14.52538
45	0.205	0.194	0.18	2.401678	15.30029	31.48205	16.39467	14.57104
48	0.204	0.192	0.179	3.580984	17.62807	32.62783	17.94563	14.52603
51	0.203	0.194	0.18	4.75895	15.30029	31.48205	17.18043	13.46039
54	0.202	0.214	0.174	5.935574	-8.27242	38.33663	11.99993	23.88898
57	0.202	0.214	0.175	5.935574	-8.27242	37.19755	11.62023	23.2619
60	0.203	0.215	0.205	4.75895	-9.46514	2.401678	-0.76817	7.623459
63	0.202	0.214	0.204	5.935574	-8.27242	3.580984	0.414712	7.614837
66	0.201	0.213	0.203	7.110858	-7.08105	4.75895	1.596253	7.606216
69	0.2	0.212	0.203	8.2848	-5.89101	4.75895	2.384246	7.380233
72	0.2	0.212	0.203	8.2848	-5.89101	4.75895	2.384246	7.380233
75	0.201	0.213	0.203	7.110858	-7.08105	4.75895	1.596253	7.606216
78	0.199	0.208	0.202	9.457402	-1.14429	5.935574	4.749563	5.399437
81	0.199	0.208	0.201	9.457402	-1.14429	7.110858	5.141324	5.568505
84	0.198	0.204	0.2	10.62866	3.580984	8.2848	7.498149	3.589088
87	0.198	0.204	0.2	10.62866	3.580984	8.2848	7.498149	3.589088
90	0.196	0.204	0.2	12.96716	3.580984	8.2848	8.277648	4.693092
93	0.195	0.204	0.199	14.1344	3.580984	9.457402	9.057595	5.288054
96	0.196	0.204	0.197	12.96716	3.580984	11.79858	9.448909	5.115251
99	0.192	0.204	0.191	17.62807	3.580984	18.78994	13.333	8.465447
102	0.193	0.205	0.192	16.46485	2.401678	17.62807	12.16486	8.475148
105	0.189	0.201	0.189	21.10966	7.110858	21.10966	16.4434	8.082215
108	0.188	0.2	0.187	22.26751	8.2848	23.42402	17.99211	8.426644
111	0.185	0.197	0.187	25.73302	11.79858	23.42402	20.31854	7.468278

114	0.187	0.199	0.186	23.42402	9.457402	24.57919	19.15354	8.416943
117	0.185	0.197	0.184	25.73302	11.79858	26.88551	21.47237	8.397542
120	0.184	0.196	0.184	26.88551	12.96716	26.88551	22.24606	8.035762
123	0.185	0.197	0.183	25.73302	11.79858	28.03666	21.85609	8.785882
126	0.182	0.194	0.182	29.18646	15.30029	29.18646	24.55774	8.017182
129	0.178	0.19	0.182	33.77227	19.95047	29.18646	27.6364	7.040067
132	0.179	0.191	0.18	32.62783	18.78994	31.48205	27.63327	7.679949
135	0.178	0.19	0.178	33.77227	19.95047	33.77227	29.16501	7.98002
138	0.176	0.188	0.176	36.05713	22.26751	36.05713	31.46059	7.961439
141	0.174	0.186	0.175	38.33663	24.57919	37.19755	33.37112	7.635306
144	0.171	0.183	0.174	41.74581	28.03666	38.33663	36.0397	7.137378
147	0.17	0.182	0.173	42.87953	29.18646	39.47436	37.18012	7.129004
150	0.168	0.18	0.167	45.14293	31.48205	46.27262	40.96587	8.232629
153	0.166	0.178	0.167	47.40097	33.77227	46.27262	42.48196	7.563878
156	0.165	0.177	0.167	48.52798	34.91537	46.27262	43.23866	7.295854
159	0.161	0.173	0.166	53.02261	39.47436	47.40097	46.63265	6.806722
162	0.16	0.172	0.166	54.14291	40.61076	47.40097	47.38488	6.766091
165	0.16	0.172	0.165	54.14291	40.61076	48.52798	47.76055	6.79864
168	0.158	0.17	0.165	56.3795	42.87953	48.52798	49.26234	6.779878
171	0.156	0.168	0.165	58.61072	45.14293	48.52798	50.76054	7.005967
174	0.154	0.166	0.164	60.83658	47.40097	49.65365	52.6304	7.19546
177	0.154	0.166	0.161	60.83658	47.40097	53.02261	53.75339	6.747547
180	0.148	0.16	0.158	67.48197	54.14291	56.3795	59.33479	7.143733
183	0.15	0.162	0.159	65.2722	51.90096	55.26188	57.47835	6.955721
186	0.145	0.157	0.157	70.78656	57.49578	57.49578	61.92604	7.673435
189	0.148	0.16	0.156	67.48197	54.14291	58.61072	60.07853	6.789584
192	0.144	0.156	0.156	71.88541	58.61072	58.61072	63.03561	7.664145
195	0.135	0.147	0.157	81.7147	68.58484	57.49578	69.26511	12.12378
198	0.136	0.148	0.156	80.62792	67.48197	58.61072	68.90687	11.07755
201	0.133	0.145	0.15	83.88424	70.78656	65.2722	73.31433	9.560033
204	0.133	0.145	0.15	83.88424	70.78656	65.2722	73.31433	9.560033
207	0.124	0.136	0.151	93.58078	80.62792	64.16531	79.458	14.74259
210	0.123	0.135	0.151	94.65147	81.7147	64.16531	80.17716	15.30113
213	0.123	0.135	0.145	94.65147	81.7147	70.78656	82.38424	11.94653
216	0.121	0.133	0.144	96.78882	83.88424	71.88541	84.18616	12.45445
219	0.119	0.131	0.144	98.92081	86.04841	71.88541	85.61821	13.52284
222	0.116	0.128	0.14	102.1087	89.28462	76.26739	89.22025	12.92079
225	0.114	0.126	0.138	104.2273	91.43538	78.45034	91.37101	12.88861
228	0.112	0.124	0.134	106.3405	93.58078	82.80014	94.24049	11.78406
231	0.108	0.12	0.133	110.5509	97.85549	83.88424	97.4302	13.33841
234	0.107	0.119	0.127	111.6001	98.92081	90.36067	100.2939	10.68609

237	0.103	0.115	0.133	115.7836	103.1687	83.88424	100.9455	16.06548
240	0.101	0.113	0.127	117.8674	105.2846	90.36067	104.5042	13.76994
243	0.098	0.11	0.128	120.9829	108.4484	89.28462	106.2386	15.96425
246	0.096	0.108	0.124	123.0532	110.5509	93.58078	109.0616	14.79253
249	0.093	0.105	0.123	126.1486	113.6946	94.65147	111.4982	15.86301
252	0.091	0.104	0.12	128.2055	114.7398	97.85549	113.6002	15.20705
255	0.089	0.099	0.118	130.257	119.9457	99.9848	116.7292	15.3903
258	0.086	0.085	0.115	133.3242	134.344	103.1687	123.6123	17.71203
261	0.08	0.084	0.099	139.4225	135.3624	119.9457	131.5769	10.27542
264	0.075	0.084	0.096	144.4676	135.3624	123.0532	134.2944	10.74706
267	0.075	0.085	0.094	144.4676	134.344	125.1181	134.6432	9.678186
270	0.073	0.085	0.093	146.4762	134.344	126.1486	135.6562	10.22713
273	0.069	0.085	0.092	150.4773	134.344	127.1777	137.333	11.93394
276	0.067	0.086	0.091	152.4699	133.3242	128.2055	137.9999	12.79008
279	0.067	0.085	0.09	152.4699	134.344	129.2319	138.6819	12.21121
282	0.065	0.086	0.086	154.457	133.3242	133.3242	140.3685	12.20101
285	0.062	0.086	0.083	157.4277	133.3242	136.3794	142.3771	13.1234
288	0.062	0.086	0.083	157.4277	133.3242	136.3794	142.3771	13.1234
291	0.062	0.086	0.083	157.4277	133.3242	136.3794	142.3771	13.1234
	Data 2/1 D/L; 0.2 Hz							
3	0.251	0.257	0.254	2.171387	-10.2377	-3.98228	-4.0162	6.204617
6	0.251	0.257	0.254	2.171387	-10.2377	-3.98228	-4.0162	6.204617
9	0.251	0.257	0.254	2.171387	-10.2377	-3.98228	-4.0162	6.204617
12	0.25	0.256	0.253	4.2	-8.14126	-1.91976	-1.95367	6.1707
15	0.25	0.256	0.253	4.2	-8.14126	-1.91976	-1.95367	6.1707
18	0.25	0.256	0.253	4.2	-8.14126	-1.91976	-1.95367	6.1707
21	0.25	0.256	0.253	4.2	-8.14126	-1.91976	-1.95367	6.1707
24	0.25	0.256	0.253	4.2	-8.14126	-1.91976	-1.95367	6.1707
27	0.25	0.256	0.253	4.2	-8.14126	-1.91976	-1.95367	6.1707
30	0.249	0.255	0.252	6.217307	-6.05612	0.131469	0.097552	6.136784
33	0.249	0.255	0.252	6.217307	-6.05612	0.131469	0.097552	6.136784
36	0.249	0.255	0.252	6.217307	-6.05612	0.131469	0.097552	6.136784
39	0.247	0.253	0.25	10.218	-1.91976	4.2	4.166083	6.068951
42	0.247	0.253	0.25	10.218	-1.91976	4.2	4.166083	6.068951
45	0.247	0.253	0.25	10.218	-1.91976	4.2	4.166083	6.068951
48	0.247	0.253	0.25	10.218	-1.91976	4.2	4.166083	6.068951
51	0.247	0.253	0.25	10.218	-1.91976	4.2	4.166083	6.068951
54	0.247	0.253	0.25	10.218	-1.91976	4.2	4.166083	6.068951
57	0.246	0.252	0.249	12.2014	0.131469	6.217307	6.18339	6.035035
60	0.24	0.246	0.243	23.86432	12.2014	18.08373	18.04982	5.831536
63	0.241	0.247	0.244	21.94876	10.218	16.13426	16.10034	5.865453

66	0.241	0.247	0.244	21.94876	10.218	16.13426	16.10034	5.865453
69	0.241	0.247	0.244	21.94876	10.218	16.13426	16.10034	5.865453
72	0.244	0.25	0.247	16.13426	4.2	10.218	10.18409	5.967202
75	0.246	0.252	0.249	12.2014	0.131469	6.217307	6.18339	6.035035
78	0.247	0.253	0.25	10.218	-1.91976	4.2	4.166083	6.068951
81	0.247	0.253	0.25	10.218	-1.91976	4.2	4.166083	6.068951
84	0.246	0.252	0.249	12.2014	0.131469	6.217307	6.18339	6.035035
87	0.248	0.254	0.251	8.223309	-3.98228	2.171387	2.13747	6.102867
90	0.247	0.253	0.25	10.218	-1.91976	4.2	4.166083	6.068951
93	0.247	0.253	0.25	10.218	-1.91976	4.2	4.166083	6.068951
96	0.247	0.253	0.25	10.218	-1.91976	4.2	4.166083	6.068951
99	0.246	0.252	0.249	12.2014	0.131469	6.217307	6.18339	6.035035
102	0.25	0.256	0.253	4.2	-8.14126	-1.91976	-1.95367	6.1707
105	0.25	0.256	0.253	4.2	-8.14126	-1.91976	-1.95367	6.1707
108	0.25	0.256	0.253	4.2	-8.14126	-1.91976	-1.95367	6.1707
111	0.25	0.256	0.253	4.2	-8.14126	-1.91976	-1.95367	6.1707
114	0.25	0.256	0.253	4.2	-8.14126	-1.91976	-1.95367	6.1707
117	0.25	0.256	0.253	4.2	-8.14126	-1.91976	-1.95367	6.1707
120	0.249	0.255	0.252	6.217307	-6.05612	0.131469	0.097552	6.136784
123	0.249	0.255	0.252	6.217307	-6.05612	0.131469	0.097552	6.136784
126	0.249	0.255	0.252	6.217307	-6.05612	0.131469	0.097552	6.136784
129	0.247	0.253	0.25	10.218	-1.91976	4.2	4.166083	6.068951
132	0.247	0.253	0.25	10.218	-1.91976	4.2	4.166083	6.068951
135	0.247	0.253	0.25	10.218	-1.91976	4.2	4.166083	6.068951
138	0.247	0.253	0.25	10.218	-1.91976	4.2	4.166083	6.068951
141	0.247	0.253	0.25	10.218	-1.91976	4.2	4.166083	6.068951
144	0.247	0.253	0.25	10.218	-1.91976	4.2	4.166083	6.068951
147	0.246	0.252	0.249	12.2014	0.131469	6.217307	6.18339	6.035035
150	0.244	0.25	0.247	16.13426	4.2	10.218	10.18409	5.967202
153	0.243	0.249	0.246	18.08373	6.217307	12.2014	12.16748	5.933286
156	0.24	0.246	0.243	23.86432	12.2014	18.08373	18.04982	5.831536
159	0.239	0.245	0.242	25.76857	14.17348	20.0219	19.98798	5.79762
162	0.239	0.245	0.242	25.76857	14.17348	20.0219	19.98798	5.79762
165	0.237	0.243	0.24	29.54316	18.08373	23.86432	23.8304	5.729787
168	0.239	0.245	0.242	25.76857	14.17348	20.0219	19.98798	5.79762
171	0.238	0.244	0.241	27.66152	16.13426	21.94876	21.91485	5.763704
174	0.238	0.244	0.241	27.66152	16.13426	21.94876	21.91485	5.763704
177	0.237	0.243	0.24	29.54316	18.08373	23.86432	23.8304	5.729787
180	0.237	0.243	0.24	29.54316	18.08373	23.86432	23.8304	5.729787
183	0.236	0.242	0.239	31.41349	20.0219	25.76857	25.73465	5.695871
186	0.235	0.241	0.238	33.27252	21.94876	27.66152	27.6276	5.661955

189	0.234	0.24	0.237	35.12024	23.86432	29.54316	29.50924	5.628038
192	0.237	0.243	0.24	29.54316	18.08373	23.86432	23.8304	5.729787
195	0.237	0.243	0.24	29.54316	18.08373	23.86432	23.8304	5.729787
198	0.236	0.242	0.239	31.41349	20.0219	25.76857	25.73465	5.695871
201	0.233	0.239	0.236	36.95666	25.76857	31.41349	31.37957	5.594122
204	0.233	0.239	0.236	36.95666	25.76857	31.41349	31.37957	5.594122
207	0.232	0.238	0.235	38.78177	27.66152	33.27252	33.2386	5.560206
210	0.232	0.238	0.235	38.78177	27.66152	33.27252	33.2386	5.560206
213	0.231	0.237	0.234	40.59558	29.54316	35.12024	35.08633	5.526289
216	0.23	0.236	0.233	42.39808	31.41349	36.95666	36.92274	5.492373
219	0.23	0.236	0.233	42.39808	31.41349	36.95666	36.92274	5.492373
222	0.229	0.235	0.232	44.18928	33.27252	38.78177	38.74786	5.458457
225	0.229	0.235	0.232	44.18928	33.27252	38.78177	38.74786	5.458457
228	0.229	0.235	0.232	44.18928	33.27252	38.78177	38.74786	5.458457
231	0.228	0.234	0.231	45.96916	35.12024	40.59558	40.56166	5.42454
234	0.228	0.234	0.231	45.96916	35.12024	40.59558	40.56166	5.42454
237	0.227	0.233	0.23	47.73775	36.95666	42.39808	42.36416	5.390624
240	0.228	0.234	0.231	45.96916	35.12024	40.59558	40.56166	5.42454
243	0.228	0.234	0.231	45.96916	35.12024	40.59558	40.56166	5.42454
246	0.225	0.231	0.228	51.241	40.59558	45.96916	45.93525	5.322791
249	0.226	0.232	0.229	49.49503	38.78177	44.18928	44.15536	5.356708
252	0.227	0.233	0.23	47.73775	36.95666	42.39808	42.36416	5.390624
255	0.228	0.234	0.231	45.96916	35.12024	40.59558	40.56166	5.42454
258	0.225	0.231	0.228	51.241	40.59558	45.96916	45.93525	5.322791
261	0.219	0.225	0.222	61.47942	51.241	56.41108	56.37717	5.119294
264	0.219	0.225	0.222	61.47942	51.241	56.41108	56.37717	5.119294
267	0.219	0.225	0.222	61.47942	51.241	56.41108	56.37717	5.119294
270	0.222	0.227	0.226	56.41108	47.73775	49.49503	51.21462	4.585241
273	0.222	0.227	0.226	56.41108	47.73775	49.49503	51.21462	4.585241
276	0.225	0.23	0.229	51.241	42.39808	44.18928	45.94279	4.674977
279	0.227	0.232	0.231	47.73775	38.78177	40.59558	42.3717	4.7348
282	0.227	0.232	0.231	47.73775	38.78177	40.59558	42.3717	4.7348
	Data 2/1 D/L; 0.4Hz							
3	-0.19	0.271	0.267	-7.87355	-45.3605	-37.5285	-41.4445	5.538024
6	0.258	0.249	0.245	-20.3871	-3.91092	3.198288	-0.35631	5.026966
9	0.294	0.254	0.25	-92.9443	-12.9822	-5.70875	-9.34548	5.143116
12	0.291	0.252	0.248	-86.4913	-9.32906	-2.1213	-5.72518	5.096656
15	0.285	0.251	0.247	-73.8071	-7.5148	-0.33989	-3.92734	5.073426
18	0.284	0.251	0.247	-71.7218	-7.5148	-0.33989	-3.92734	5.073426
	0.291	0.251	0.247	-86.4913	-7.5148	-0.33989	-3.92734	5.073426

21	0.237	0.253	0.249	17.02247	-11.1515	-3.91092	-7.53122	5.119886
24	-1.364	0.254	0.25	-7794.79	-12.9822	-5.70875	-9.34548	5.143116
27	-2.932	0.252	0.248	-35850.8	-9.32906	-2.1213	-5.72518	5.096656
30	0.156	0.253	0.249	127.3886	-11.1515	-3.91092	-7.53122	5.119886
33	-0.41	0.254	0.25	-605.22	-12.9822	-5.70875	-9.34548	5.143116
36	0.298	0.253	0.249	-101.663	-11.1515	-3.91092	-7.53122	5.119886
39	0.282	0.254	0.25	-67.5759	-12.9822	-5.70875	-9.34548	5.143116
42	-3.803	0.253	0.249	-60159.1	-11.1515	-3.91092	-7.53122	5.119886
45	-0.956	0.254	0.25	-3805.21	-12.9822	-5.70875	-9.34548	5.143116
48	0.3	0.254	0.25	-106.072	-12.9822	-5.70875	-9.34548	5.143116
51	-0.156	0.254	0.25	48.97986	-12.9822	-5.70875	-9.34548	5.143116
54	-0.076	0.252	0.248	145.3013	-9.32906	-2.1213	-5.72518	5.096656
57	0.275	0.252	0.248	-53.3238	-9.32906	-2.1213	-5.72518	5.096656
60	-0.264	0.252	0.248	-164.432	-9.32906	-2.1213	-5.72518	5.096656
63	-3.668	0.252	0.248	-55983.5	-9.32906	-2.1213	-5.72518	5.096656
66	0.295	0.251	0.247	-95.1117	-7.5148	-0.33989	-3.92734	5.073426
69	-2.802	0.251	0.247	-32757	-7.5148	-0.33989	-3.92734	5.073426
72	0.332	0.251	0.247	-181.08	-7.5148	-0.33989	-3.92734	5.073426
75	-0.605	0.25	0.246	-1467	-5.70875	1.433306	-2.13772	5.050196
78	0.319	0.25	0.246	-149.594	-5.70875	1.433306	-2.13772	5.050196
81	0.267	0.249	0.245	-37.5285	-3.91092	3.198288	-0.35631	5.026966
84	-0.069	0.249	0.245	151.2286	-3.91092	3.198288	-0.35631	5.026966
87	-0.416	0.248	0.244	-627.079	-2.1213	4.955056	1.41688	5.003736
90	-0.498	0.246	0.242	-955.461	1.433306	8.443954	4.93863	4.957277
93	-0.352	0.245	0.241	-409.153	3.198288	10.17608	6.687186	4.934047
96	-1.023	0.242	0.238	-4366.54	8.443954	15.32319	11.88357	4.864357
99	-0.005	0.241	0.237	186.7608	10.17608	17.02247	13.59928	4.841127
102	0.064	0.24	0.236	187.3836	11.9	18.71354	15.30677	4.817898
105	-0.153	0.238	0.234	53.54051	15.32319	22.07103	18.69711	4.771438
108	0.072	0.237	0.233	184.9262	17.02247	23.73745	20.37996	4.748208
111	0.18	0.235	0.231	100.3052	20.39639	27.04566	23.72103	4.701748
114	0.08	0.233	0.229	181.9432	23.73745	30.32102	27.02924	4.655288
117	-0.735	0.235	0.231	-2215.03	20.39639	27.04566	23.72103	4.701748
120	-0.213	0.233	0.229	-51.7168	23.73745	30.32102	27.02924	4.655288
123	-0.147	0.232	0.228	62.44007	25.39566	31.94638	28.67102	4.632059
126	-0.657	0.231	0.227	-1749.56	27.04566	33.56353	30.3046	4.608829
129	-1.555	0.229	0.225	-10132.3	30.32102	36.77319	33.54711	4.562369
132	-0.091	0.229	0.225	131.2449	30.32102	36.77319	33.54711	4.562369
135	0.296	0.227	0.223	-97.2873	33.56353	39.94999	36.75676	4.515909
138	-3.446	0.225	0.221	-49442.2	36.77319	43.09394	39.93357	4.469449
141	0.024	0.222	0.218	191.7861	41.52607	47.74827	44.63717	4.39976

144	0.254	0.222	0.218	-12.9822	41.52607	47.74827	44.63717	4.39976
147	-0.578	0.218	0.214	-1329.05	47.74827	53.83907	50.79367	4.30684
150	-1.191	0.214	0.21	-5936.18	53.83907	59.79845	56.81876	4.213921
153	-0.102	0.212	0.208	119.7624	56.83518	62.72886	59.78202	4.167461
156	-0.631	0.21	0.206	-1605.5	59.79845	65.62643	62.71244	4.121001
159	-0.782	0.209	0.205	-2519.63	61.26776	67.06289	64.16533	4.097771
162	0.145	0.209	0.205	138.2208	61.26776	67.06289	64.16533	4.097771
165	-0.341	0.206	0.202	-375.085	65.62643	71.32299	68.47471	4.028082
168	0.02	0.207	0.203	191.5036	64.18175	69.91117	67.04646	4.051312
171	-0.459	0.207	0.203	-792.393	64.18175	69.91117	67.04646	4.051312
174	0.172	0.205	0.201	109.8586	67.06289	72.7266	69.89475	4.004852
177	-0.119	0.206	0.202	100.062	65.62643	71.32299	68.47471	4.028082
180	-0.364	0.202	0.198	-447.452	71.32299	76.88815	74.10557	3.935162
183	0.215	0.202	0.198	52.32869	71.32299	76.88815	74.10557	3.935162
186	-0.008	0.198	0.194	185.8467	76.88815	82.32191	79.60503	3.842243
189	0.093	0.202	0.198	175.9747	71.32299	76.88815	74.10557	3.935162
192	0.088	0.2	0.196	178.4345	74.122	79.62146	76.87173	3.888703
195	0.135	0.201	0.197	147.2059	72.7266	78.25891	75.49276	3.911933
198	0.117	0.2	0.196	161.3094	74.122	79.62146	76.87173	3.888703
201	0.032	0.196	0.192	191.9569	79.62146	84.9895	82.30548	3.795783
204	0.233	0.193	0.189	23.73745	83.65981	88.9293	86.29456	3.726094
207	-0.2	0.192	0.188	-26.402	84.9895	90.22614	87.60782	3.702864
210	0.085	0.193	0.189	179.8119	83.65981	88.9293	86.29456	3.726094
213	0.159	0.188	0.184	124.2619	90.22614	95.33138	92.77876	3.609944
216	0.241	0.186	0.182	10.17608	92.79519	97.83471	95.31495	3.563484
219	0.144	0.187	0.183	139.1563	91.51477	96.58715	94.05096	3.586714
222	-0.038	0.183	0.179	172.6404	96.58715	101.5281	99.05764	3.493795
225	-0.07	0.178	0.174	150.4065	102.7428	107.5195	105.1312	3.377645
228	-0.07	0.177	0.173	150.4065	103.9493	108.6932	106.3213	3.354416
231	0.223	0.176	0.172	39.94999	105.1476	109.8586	107.5031	3.331186
234	0.189	0.171	0.167	88.9293	111.0158	115.5626	113.2892	3.215036
237	0.094	0.174	0.17	175.4581	107.5195	112.1649	109.8422	3.284726
240	-0.052	0.166	0.162	163.9479	116.6787	121.0612	118.87	3.098887
243	0.144	0.164	0.16	139.1563	118.8864	123.2032	121.0448	3.052427
246	0.236	0.163	0.159	18.71354	119.9779	124.2619	122.1199	3.029197
249	0.196	0.162	0.158	79.62146	121.0612	125.3123	123.1868	3.005967
252	0.214	0.16	0.156	53.83907	123.2032	127.3886	125.2959	2.959508
255	0.161	0.156	0.152	122.1363	127.3886	131.4425	129.4156	2.866588
258	0.092	0.144	0.14	176.4831	139.1563	142.816	140.9861	2.58783
261	0.195	0.143	0.139	80.97579	140.0835	143.7104	141.897	2.5646
264	0.115	0.14	0.136	162.7122	142.816	146.3443	144.5802	2.49491

267	-0.082	0.133	0.129	139.9005	148.9044	152.2027	150.5535	2.332301
270	0	0.129	0.125	188.12	152.2027	155.3697	153.7862	2.239382
273	0.183	0.127	0.123	96.58715	153.8026	156.9039	155.3533	2.192922
276	0.129	0.126	0.122	152.2027	154.5903	157.6587	156.1245	2.169692
279	-0.002	0.122	0.118	187.601	157.6587	160.5957	159.1272	2.076773
282	0.131	0.123	0.119	150.57	156.9039	159.8737	158.3888	2.100002
285	0.131	0.123	0.119	150.57	156.9039	159.8737	158.3888	2.100002
288	0.131	0.123	0.119				158.3888	2.100002
291								
	Data 2/1 D/L; 0.8 Hz							
3	0.203	0.208	0.18	4.75895	-1.14429	31.48205	11.6989	17.3851
6	0.204	0.218	0.18	3.580984	-13.0513	31.48205	7.337234	22.50306
9	0.202	0.21	0.178	5.935574	-3.51497	33.77227	12.06429	19.38441
12	0.202	0.215	0.178	5.935574	-9.46514	33.77227	10.0809	21.91475
15	0.202	0.218	0.178	5.935574	-13.0513	33.77227	8.885505	23.55078
18	0.204	0.215	0.177	3.580984	-9.46514	34.91537	9.677073	22.80963
21	0.203	0.21	0.178	4.75895	-3.51497	33.77227	11.67208	19.58132
24	0.205	0.211	0.176	2.401678	-4.70232	36.05713	11.25216	21.77341
27	0.204	0.209	0.179	3.580984	-2.32896	32.62783	11.29329	18.71106
30	0.204	0.207	0.179	3.580984	0.039042	32.62783	12.08262	17.88059
33	0.204	0.206	0.179	3.580984	1.221031	32.62783	12.47662	17.49131
36	0.203	0.206	0.179	4.75895	1.221031	32.62783	12.86927	17.20261
39	0.204	0.202	0.18	3.580984	5.935574	31.48205	13.6662	15.47383
42	0.205	0.199	0.181	2.401678	9.457402	30.33492	14.06467	14.52538
45	0.205	0.194	0.18	2.401678	15.30029	31.48205	16.39467	14.57104
48	0.204	0.192	0.179	3.580984	17.62807	32.62783	17.94563	14.52603
51	0.203	0.194	0.18	4.75895	15.30029	31.48205	17.18043	13.46039
54	0.202	0.214	0.174	5.935574	-8.27242	38.33663	11.99993	23.88898
57	0.202	0.214	0.175	5.935574	-8.27242	37.19755	11.62023	23.2619
60	0.203	0.215	0.205	4.75895	-9.46514	2.401678	-0.76817	7.623459
63	0.202	0.214	0.204	5.935574	-8.27242	3.580984	0.414712	7.614837
66	0.201	0.213	0.203	7.110858	-7.08105	4.75895	1.596253	7.606216
69	0.2	0.212	0.203	8.2848	-5.89101	4.75895	2.384246	7.380233
72	0.2	0.212	0.203	8.2848	-5.89101	4.75895	2.384246	7.380233
75	0.201	0.213	0.203	7.110858	-7.08105	4.75895	1.596253	7.606216
78	0.199	0.208	0.202	9.457402	-1.14429	5.935574	4.749563	5.399437
81	0.199	0.208	0.201	9.457402	-1.14429	7.110858	5.141324	5.568505
84	0.198	0.204	0.2	10.62866	3.580984	8.2848	7.498149	3.589088
87	0.198	0.204	0.2	10.62866	3.580984	8.2848	7.498149	3.589088
90	0.196	0.204	0.2	12.96716	3.580984	8.2848	8.277648	4.693092
93	0.195	0.204	0.199	14.1344	3.580984	9.457402	9.057595	5.288054

96	0.196	0.204	0.197	12.96716	3.580984	11.79858	9.448909	5.115251
99	0.192	0.204	0.191	17.62807	3.580984	18.78994	13.333	8.465447
102	0.193	0.205	0.192	16.46485	2.401678	17.62807	12.16486	8.475148
105	0.189	0.201	0.189	21.10966	7.110858	21.10966	16.4434	8.082215
108	0.188	0.2	0.187	22.26751	8.2848	23.42402	17.99211	8.426644
111	0.185	0.197	0.187	25.73302	11.79858	23.42402	20.31854	7.468278
114	0.187	0.199	0.186	23.42402	9.457402	24.57919	19.15354	8.416943
117	0.185	0.197	0.184	25.73302	11.79858	26.88551	21.47237	8.397542
120	0.184	0.196	0.184	26.88551	12.96716	26.88551	22.24606	8.035762
123	0.185	0.197	0.183	25.73302	11.79858	28.03666	21.85609	8.785882
126	0.182	0.192	0.176	29.18646	17.62807	36.05713	27.62389	9.313369
129	0.178	0.186	0.169	33.77227	24.57919	44.0119	34.12112	9.721049
132	0.172	0.178	0.161	40.61076	33.77227	53.02261	42.46855	9.758708
135	0.166	0.17	0.15	47.40097	42.87953	65.2722	51.8509	11.841
138	0.16	0.156	0.142	54.14291	58.61072	74.07908	62.27757	10.4617
141	0.152	0.146	0.136	63.05707	69.68637	80.62792	71.12379	8.873181
144	0.149	0.143	0.135	66.37775	72.98291	81.7147	73.69179	7.693008
147	0.148	0.142	0.134	67.48197	74.07908	82.80014	74.78706	7.68359
150	0.146	0.14	0.128	69.68637	76.26739	89.28462	78.41279	9.973709
153	0.144	0.138	0.128	71.88541	78.45034	89.28462	79.87345	8.78647
156	0.143	0.137	0.128	72.98291	79.5398	89.28462	80.60244	8.202638
159	0.139	0.133	0.127	77.35954	83.88424	90.36067	83.86815	6.500581
162	0.138	0.132	0.127	78.45034	84.967	90.36067	84.59267	5.963982
165	0.138	0.132	0.126	78.45034	84.967	91.43538	84.9509	6.492535
168	0.136	0.13	0.126	80.62792	87.12849	91.43538	86.39726	5.440708
171	0.134	0.128	0.126	82.80014	89.28462	91.43538	87.84005	4.495211
174	0.132	0.126	0.125	84.967	91.43538	92.50875	89.63704	4.079831
177	0.132	0.126	0.122	84.967	91.43538	95.72082	90.70773	5.413711
180	0.126	0.12	0.119	91.43538	97.85549	98.92081	96.07056	4.049371
183	0.128	0.122	0.119	89.28462	95.72082	98.92081	94.64208	4.907833
186	0.123	0.117	0.118	94.65147	101.0474	99.9848	98.56123	3.427391
189	0.126	0.12	0.117	91.43538	97.85549	101.0474	96.77944	4.895543
192	0.122	0.116	0.117	95.72082	102.1087	101.0474	99.62567	3.42308
195	0.113	0.107	0.116	105.2846	111.6001	102.1087	106.3312	4.831459
198	0.114	0.108	0.114	104.2273	110.5509	104.2273	106.3352	3.650909
201	0.111	0.105	0.108	107.3951	113.6946	110.5509	110.5469	3.149713
204	0.111	0.105	0.105	107.3951	113.6946	113.6946	111.5948	3.636973
207	0.102	0.096	0.1	116.8262	123.0532	118.9072	119.5955	3.170055
210	0.101	0.095	0.093	117.8674	124.0863	126.1486	122.7008	4.310977
213	0.101	0.095	0.089	117.8674	124.0863	130.257	124.0702	6.194843
216	0.099	0.093	0.086	119.9457	126.1486	133.3242	126.4728	6.695164

219	0.097	0.091	0.084	122.0187	128.2055	135.3624	128.5288	6.677715
222	0.094	0.088	0.081	125.1181	131.2808	138.4095	131.6028	6.65154
225	0.092	0.086	0.079	127.1777	133.3242	140.4342	133.6454	6.634091
228	0.09	0.084	0.076	129.2319	135.3624	143.4612	136.0185	7.137313
231	0.086	0.08	0.072	133.3242	139.4225	147.4785	140.0751	7.099639
234	0.085	0.079	0.068	134.344	140.4342	151.4743	142.0842	8.683509
237	0.081	0.075	0.064	138.4095	144.4676	155.4486	146.1085	8.637264
240	0.079	0.073	0.062	140.4342	146.4762	157.4277	148.1127	8.614142
243	0.076	0.07	0.059	143.4612	149.479	160.3863	151.1089	8.579458
246	0.074	0.068	0.055	145.4725	151.4743	164.3124	153.7531	9.62444
249	0.071	0.065	0.055	148.4794	154.457	164.3124	155.7496	7.995237
252	0.069	0.064	0.054	150.4773	155.4486	165.2906	157.0722	7.538897
255	0.067	0.059	0.054	152.4699	160.3863	165.2906	159.3823	6.469062
	Data 2/1 D/L; 1.6 Hz							
3	0.249	0.214		9.472274	8.245714	8.514905	8.744	0.645
6	0.248	0.216		12.5635	5.35129	8.514905	8.810	3.615
9	0.249	0.217		9.472274	3.917702	8.514905	7.302	2.969
12	0.25	0.219		6.37	1.077778	6.739407	4.729	3.167
15	0.251	0.217		3.256674	3.917702	6.739407	4.638	1.850
18	0.25	0.216		6.37	5.35129	6.739407	6.154	0.719
21	0.251	0.215		3.256674	6.79396	6.739407	5.597	2.027
24	0.25	0.215		6.37	6.79396	10.29744	7.820	2.156
27	0.249	0.216		9.472274	5.35129	10.29744	8.374	2.650
30	0.248	0.214		12.5635	8.245714	10.29744	10.369	2.160
33	0.249	0.215		9.472274	6.79396	8.514905	8.260	1.357
36	0.247	0.216		15.64367	5.35129	8.514905	9.837	5.272
39	0.245	0.216		21.77086	5.35129	8.514905	11.879	8.711
42	0.247	0.216		15.64367	5.35129	4.97095	8.655	6.055
45	0.248	0.216		12.5635	5.35129	4.97095	7.629	4.278
48	0.248	0.216		12.5635	5.35129	4.97095	7.629	4.278
51	0.248	0.214		12.5635	8.245714	4.97095	8.593	3.808
54	0.247	0.214		15.64367	8.245714	3.209533	9.033	6.254
57	0.247	0.214		15.64367	8.245714	3.209533	9.033	6.254
60	0.246	0.215		18.71279	6.79396	3.209533	9.572	8.116
63	0.246	0.213		18.71279	9.70655	8.514905	12.311	5.576
66	0.245	0.213		21.77086	9.70655	6.739407	12.739	7.961
69	0.246	0.213		18.71279	9.70655	1.455156	9.958	8.632
72	0.245	0.213		21.77086	9.70655	3.209533	11.562	9.419
75	0.245	0.213		21.77086	9.70655	4.97095	12.149	8.662
78	0.244	0.213		24.81788	9.70655	4.97095	13.165	10.366
81	0.246	0.212		18.71279	11.17647	4.97095	11.620	6.882

84	0.245	0.210	21.77086	14.14356	4.97095	13.628	8.412
87	0.244	0.210	24.81788	14.14356	8.514905	15.825	8.281
90		0.210		14.14356	8.514905	11.329	3.980
93		0.210		14.14356	8.514905	11.329	3.980
96		0.211		12.65547	6.739407	9.697	4.183
99		0.211		12.65547	6.739407	9.697	4.183
102		0.211		12.65547	6.739407	9.697	4.183
105		0.211		12.65547	6.739407	9.697	4.183
108		0.211		12.65547	4.97095	8.813	5.434
111		0.211		12.65547	4.97095	8.813	5.434
114		0.209		15.64073	4.97095	10.306	7.545
117		0.209		15.64073	4.97095	10.306	7.545
120	0.31	0.209		15.64073	8.514905	12.078	5.039
123	0.309	0.209		15.64073	8.514905	12.078	5.039
126	0.308	0.209		15.64073	8.514905	12.078	5.039
129	0.306	0.212		11.17647	8.514905	9.846	1.882
132	0.304	0.212		11.17647	17.498	14.337	4.470
135	0.305	0.212		11.17647	17.498	14.337	4.470
138	0.304	0.212		11.17647	17.498	14.337	4.470
141	0.302	0.212		11.17647	17.498	14.337	4.470
144	0.3	0.212		11.17647	30.37003	20.773	13.572
147	0.299	0.212		11.17647	30.37003	20.773	13.572
150	0.297	0.210		14.14356	30.37003	22.257	11.474
153	0.294	0.210		14.14356	37.88036	26.012	16.784
156	0.25	0.210		14.14356	43.58704	28.865	20.820
159	0.249	0.209		15.64073	55.19048	35.416	27.966
162	0.249	0.208	9.472274	17.14698	71.056	32.558	33.560
165	0.247	0.208	15.64367	17.14698	75.09278	35.961	33.897
168	0.245	0.207	21.77086	18.66232	77.12173	39.185	32.891
171	0.242	0.207	30.87876	18.66232	83.25083	44.264	34.312
174	0.24	0.206	36.89544	20.18674	79.15772	45.413	30.394
177	0.239	0.202	39.8872	26.37525	83.25083	49.838	29.715
180	0.238	0.201	42.86791	27.94508	85.30794	52.040	29.761
183	0.236	0.199	48.79618	31.112	87.3721	55.760	28.769
186	0.235	0.198	51.74374	32.70909	87.3721	57.275	27.748
189	0.234	0.198	54.68025	32.70909	91.52153	59.637	29.718
192	0.232	0.197	60.52011	34.31525	93.6068	62.814	29.712
195	0.23	0.192	66.31576	42.48234	95.69912	68.166	26.657
198	0.23	0.192	66.31576	42.48234	97.79848	68.866	27.746
201	0.229	0.185	69.19701	54.29776	104.1388	75.878	25.583
204	0.228	0.185	72.06721	54.29776	108.4009	78.255	27.577

207	0.226	0.180		77.77445	63.00984	108.4009	83.062	23.153
210	0.225	0.166		80.6115	88.61173	110.5425	93.255	15.496
213	0.223	0.167		86.25244	86.72398	114.8468	95.941	16.375
216	0.221	0.166		91.84917	88.61173	117.0095	99.157	15.545
219	0.22	0.152		94.63096	115.9939	121.3561	110.660	14.138
222	0.218	0.143		100.1614	134.5369	127.9287	120.876	18.241
225	0.214	0.142		111.0896	136.6426	136.7908	128.174	14.796
228	0.211	0.138		119.1698	145.1564	141.2641	135.197	14.016
231	0.208	0.137		127.1504	147.3076	143.5113	139.323	10.711
234	0.207	0.136		129.7886	149.4678	148.0268	142.428	10.970
237	0.202	0.134		142.8134	153.8156	150.2951	148.975	5.619
240	0.2	0.132		147.946	158.1996	150.2951	152.147	5.372
243	0.199	0.132		150.4957	158.1996	152.5705	153.755	3.986
246	0.197	0.133		155.562	156.0031	157.1424	156.236	0.815
249	0.195	0.131		160.5841	160.4053	159.4389	160.143	0.616
252	0.195	0.130		160.5841	162.62	161.7424	161.649	1.021
255	0.195	0.130		160.5841	162.62	161.7424	161.649	1.021
	Data 2/1 D/L; 1.6 Hz							
3	-0.155	0.24	0.244	11.9	4.955056		8.428	4.910817
6	0.293	0.239	0.243	13.6157	6.703612		10.160	4.887587
9	0.329	0.239	0.243	13.6157	6.703612		10.160	4.887587
12	0.326	0.239	0.243	13.6157	6.703612		10.160	4.887587
15	0.32	0.239	0.241	13.6157	10.17608		11.896	2.432179
18	0.319	0.237	0.242	17.02247	8.443954		12.733	6.065928
21	0.326	0.237	0.241	17.02247	10.17608		13.599	4.841127
24	0.272	0.237	0.241	17.02247	10.17608		13.599	4.841127
27	-1.329	0.237	0.241	17.02247	10.17608		13.599	4.841127
30	-2.897	0.235	0.241	20.39639	10.17608		15.286	7.226846
33	0.191	0.236	0.235	18.71354	20.39639		19.555	1.189956
36	-0.375	0.238	0.233	15.32319	23.73745		19.530	5.949779
39	0.333	0.239	0.23	13.6157	28.68745		21.152	10.65733
42	0.317	0.239	0.226	13.6157	35.17247		24.394	15.24293
45	-3.768	0.237	0.224	17.02247	38.3657		27.694	15.09194
48	-0.921	0.237	0.221	17.02247	43.09394		30.058	18.43531
51	0.335	0.237	0.218	17.02247	47.74827		32.385	21.72642
54	-0.121	0.234	0.216	22.07103	50.8101		36.441	20.32159
57	-0.041	0.231	0.214	27.04566	53.83907		40.442	18.9458
60	0.31	0.225	0.214	36.77319	53.83907		45.306	12.0674
63	-0.229	0.217	0.216	49.28329	50.8101		50.047	1.079614
66	-3.633	0.21	0.215	59.79845	52.32869		56.064	5.28192
69	0.33	0.209	0.213	61.26776	55.34123		58.304	4.190691

72	-2.767	0.205	0.21	67.06289	59.79845	63.431	5.136733
75	0.367	0.201	0.208	72.7266	62.72886	67.728	7.069469
78	-0.57	0.2	0.206	74.122	65.62643	69.874	6.007278
81	0.354	0.2	0.205	74.122	67.06289	70.592	4.991546
84	0.302	0.199	0.205	75.50918	67.06289	71.286	5.972433
87	-0.034	0.199	0.203	75.50918	69.91117	72.710	3.958392
90	-0.381	0.198	0.2	76.88815	74.122	75.505	1.955966
93	-0.463	0.196	0.198	79.62146	76.88815	78.255	1.932736
96	-0.317	0.195	0.198	80.97579	76.88815	78.932	2.890393
99	-0.988	0.192	0.196	84.9895	79.62146	82.305	3.795783
102	0.03	0.191	0.193	86.31098	83.65981	84.985	1.874662
105	0.099	0.19	0.19	87.62425	87.62425	87.624	0
108	-0.118	0.188	0.188	90.22614	90.22614	90.226	0
111	0.107	0.187	0.186	91.51477	92.79519	92.155	0.90539
114	0.215	0.185	0.184	94.06739	95.33138	94.699	0.893775
117	0.115	0.183	0.181	96.58715	99.07406	97.831	1.758512
120	-0.7	0.185	0.183	94.06739	96.58715	95.327	1.781742
123	-0.178	0.183	0.181	96.58715	99.07406	97.831	1.758512
126	-0.112	0.182	0.18	97.83471	100.3052	99.070	1.746897
129	-0.622	0.181	0.179	99.07406	101.5281	100.301	1.735282
132	-1.52	0.179	0.177	101.5281	103.9493	102.739	1.712053
135	-0.056	0.179	0.177	101.5281	103.9493	102.739	1.712053
138	0.331	0.177	0.175	103.9493	106.3377	105.144	1.688823
141	-3.411	0.175	0.173	106.3377	108.6932	107.515	1.665593
144	0.059	0.172	0.17	109.8586	112.1649	111.012	1.630748
147	0.289	0.172	0.17	109.8586	112.1649	111.012	1.630748
150	-0.543	0.168	0.166	114.4382	116.6787	115.558	1.584288
153	-1.156	0.164	0.162	118.8864	121.0612	119.974	1.537829
156	-0.067	0.162	0.16	121.0612	123.2032	122.132	1.514599
159	-0.596	0.16	0.158	123.2032	125.3123	124.258	1.491369
162	-0.747	0.159	0.157	124.2619	126.3546	125.308	1.479754
165	0.18	0.159	0.157	124.2619	126.3546	125.308	1.479754
168	-0.306	0.156	0.154	127.3886	129.432	128.410	1.444909
171	0.055	0.157	0.155	126.3546	128.4144	127.384	1.456524
174	-0.424	0.157	0.155	126.3546	128.4144	127.384	1.456524
177	0.207	0.155	0.153	128.4144	130.4414	129.428	1.433294
180	-0.084	0.156	0.154	127.3886	129.432	128.410	1.444909
183	-0.329	0.152	0.15	131.4425	133.4203	132.431	1.398449
186	0.25	0.152	0.15	131.4425	133.4203	132.431	1.398449
189	0.027	0.148	0.146	135.3651	137.2771	136.321	1.35199
192	0.128	0.152	0.15	131.4425	133.4203	132.431	1.398449

195	0.123	0.15	0.148	133.4203	135.3651		134.393	1.375219
198	0.17	0.151	0.149	132.4355	134.3968		133.416	1.386834
201	0.152	0.15	0.148	133.4203	135.3651		134.393	1.375219
204	0.067	0.146	0.144	137.2771	139.1563		138.217	1.32876
207	0.268	0.143	0.141	140.0835	141.9134		140.998	1.293915
210	-0.165	0.142	0.14	141.0026	142.816		141.909	1.2823
213	0.12	0.143	0.141	140.0835	141.9134		140.998	1.293915
216	0.194	0.138	0.136	144.5966	146.3443		145.470	1.23584
	0.276	0.136	0.134	146.3443	148.0592		147.202	1.21261
	0.179	0.137	0.135	145.4746	147.2059		146.340	1.224225
	-0.003	0.133	0.131	148.9044	150.57		149.737	1.177766
	-0.035	0.128	0.126	153.0068	154.5903		153.799	1.119691
	-0.035	0.127	0.125	153.8026	155.3697		154.586	1.108076
	0.258	0.126	0.124	154.5903	156.1409		155.366	1.096461
	0.224	0.121	0.119	158.4052	159.8737		159.139	1.038386
	0.129	0.124	0.122	156.1409	157.6587		156.900	1.073231
	-0.017	0.116	0.114	162.0149	163.4013		162.708	0.980312
	0.179	0.114	0.112	163.4013	164.7548		164.078	0.957082
	0.271	0.113	0.111	164.0821	165.4192		164.751	0.945467
	0.231	0.112	0.11	164.7548	166.0755		165.415	0.933852
	0.249	0.11	0.108	166.0755	167.3633		166.719	0.910622

Table II.3. Data 3/1 D/L;

Time (h)	Optical reading (mV)			TSS (mg/L)			Average	SD
	1	2	3	1	2	3	(mg/L)	
3	0.204	0.269	0.268	8.139792	8.668912	-92.8579	-25.9039	56.04209
6	0.204	0.268	0.269	8.139792	8.668912	-90.5859	-25.3497	58.46438
9	0.204	0.268	0.268	9.634908	8.668912	-88.315	-24.5924	57.15267
12	0.203	0.268	0.267	9.634908	8.668912	-90.5859	-23.3371	56.27462
15	0.203	0.268	0.268	8.139792	4.734268	-88.315	-24.094	57.58568
18	0.204	0.269	0.267	6.6513	-3.19629	-92.8579	-25.147	54.7316
21	0.205	0.271	0.269	5.169432	0.7792	-88.315	-29.801	54.83043
24	0.206	0.270	0.267	5.169432	12.58313	-90.5859	-27.4555	52.7516
27	0.206	0.267	0.268	6.6513	20.3503	3.864648	-24.2778	57.54404
30	0.205	0.265	0.226	8.139792	20.3503	6.090306	10.28875	8.824254
33	0.204	0.265	0.225	5.169432	20.3503	10.53839	11.5268	7.709781
36	0.206	0.265	0.223	6.6513	24.20325	12.76082	12.01937	7.69803
39	0.205	0.264	0.222	5.169432	16.47693	14.98216	14.53845	8.909979
42	0.206	0.266	0.221	5.169432	8.668912	17.20244	12.20951	6.142523

45	0.206	0.268	0.220	5.169432	8.668912	21.63975	10.34693	6.189515
48	0.206	0.268	0.218	5.169432	8.668912	21.63975	11.82603	8.677174
51	0.206	0.268	0.218	5.169432	8.668912	23.85678	11.82603	8.677174
54	0.206	0.268	0.217	5.169432	4.734268	23.85678	12.56504	9.934242
57	0.206	0.269	0.217	8.139792	8.668912	21.63975	11.25349	10.91694
60	0.204	0.268	0.218	6.6513	0.7792	21.63975	12.81615	7.646037
63	0.205	0.270	0.218	8.139792	4.734268	21.63975	9.690082	10.75715
66	0.204	0.269	0.218	11.13665	4.734268	21.63975	11.5046	8.940931
69	0.202	0.269	0.218	11.13665	4.734268	17.20244	12.50355	8.535228
72	0.202	0.269	0.220	11.13665	4.734268	17.20244	11.02445	6.234841
75	0.202	0.269	0.220	11.13665	8.668912	17.20244	11.02445	6.234841
78	0.202	0.268	0.220	12.64501	12.58313	17.20244	12.336	4.391365
81	0.201	0.267	0.220	14.16	24.20325	21.63975	14.14353	2.649274
84	0.200	0.264	0.218	14.16	20.3503	21.63975	20.001	5.218317
87	0.200	0.265	0.218	15.68161	39.4108	21.63975	18.71668	3.998522
90	0.199	0.260	0.218	14.16	39.4108	19.42163	25.57739	12.34493
93	0.200	0.260	0.219	14.16	39.4108	19.42163	24.33081	13.322
96	0.200	0.260	0.219	20.28619	39.4108	21.63975	24.33081	13.322
99	0.196	0.260	0.218	20.28619	39.4108	26.07275	27.11225	10.67234
102	0.196	0.260	0.216	23.38903	46.89203	28.28763	28.58991	9.807637
105	0.194	0.258	0.215	24.95039	46.89203	32.71417	32.85623	12.39967
108	0.193	0.258	0.213	24.95039	54.29157	34.92582	34.8522	11.12597
111	0.193	0.256	0.212	28.09297	50.60201	30.50144	38.05592	14.91893
114	0.191	0.257	0.214	32.85653	50.60201	32.71417	36.39881	12.35914
117	0.188	0.257	0.213	40.92827	57.9607	39.34589	38.72424	10.2867
120	0.183	0.255	0.210	44.20333	61.60941	50.37721	46.07829	10.32084
123	0.181	0.254	0.205	47.50489	68.84555	54.7822	52.06332	8.824686
126	0.179	0.252	0.203	54.1875	72.43299	59.18288	57.04421	10.84866
129	0.175	0.251	0.201	57.56855	68.84555	61.3816	61.93446	9.42883
132	0.173	0.252	0.200	64.41013	72.43299	74.55131	62.59857	5.736154
135	0.169	0.251	0.194	69.61087	79.54659	74.55131	70.46481	5.349408
138	0.166	0.249	0.194	71.3577	79.54659	76.74249	74.56959	4.967883
141	0.165	0.249	0.193	80.1912	79.54659	76.74249	75.88226	4.161667
144	0.160	0.249	0.193	80.1912	83.07275	78.93259	78.82676	1.833579
147	0.160	0.248	0.192	92.83631	83.07275	83.30957	80.73218	2.122433
150	0.153	0.248	0.190	92.83631	90.06381	89.86695	86.40621	5.569887
153	0.153	0.246	0.187	102.0672	86.57849	89.86695	90.92236	1.660452
156	0.148	0.247	0.187	109.5712	86.57849	100.7744	92.83756	8.160502
159	0.144	0.247	0.182	113.363	93.5287	107.3059	98.9747	11.60154
162	0.142	0.245	0.179	128.7949	90.06381	124.6759	104.7325	10.16446
165	0.134	0.246	0.171	130.7537	90.06381	133.335	114.5115	21.27227

168	0.133	0.246	0.167	136.6698	90.06381	159.209	118.0508	24.27181
171	0.130	0.246	0.155	138.6551	93.5287	146.2914	128.6475	35.26374
174	0.129	0.245	0.161	146.6625	107.184	167.7992	126.1584	28.51493
177	0.125	0.241	0.151	152.7376	110.5468	165.6532	140.5486	30.76661
180	0.122	0.240	0.152	156.8208	117.2111	184.9278	142.9792	28.82013
183	0.120	0.238	0.143	177.6342	120.5126	210.4915	152.9866	34.02081
186	0.110	0.237	0.131	188.2893	120.5126	210.4915	169.5461	45.53147
189	0.105	0.237	0.131	199.11	123.7936	206.2417	173.0978	46.87364
192	0.100	0.236	0.133	203.4846	139.8927	208.3671	176.3818	45.68203
195	0.098	0.231	0.132	205.6819	139.8927	210.4915	183.9148	38.20237
198	0.097	0.231	0.131	210.0963	161.5735	210.4915	185.3554	39.44522
201	0.095	0.224	0.131	210.0963	161.5735	212.6148	194.0538	28.12944
204	0.095	0.224	0.130	214.5372	176.4471	212.6148	194.7615	28.76926
207	0.093	0.219	0.130	214.5372	215.3767	214.737	201.1997	21.45793
210	0.093	0.205	0.129	216.7676	212.7288	221.0972	214.8836	0.438539
213	0.092	0.206	0.126	216.7676	215.3767	221.0972	216.8645	4.185078
216	0.092	0.205	0.126				217.7472	2.983431
	Data 3/1 D/L; 0.8 Hz							
3	0.244	0.275	0.262	8.511555		9.578239	9.578239	#DIV/0!
6	0.244	0.274	0.263	8.511555		7.62292	7.62292	#DIV/0!
9	0.246	0.276	0.262	3.306991		9.578239	9.578239	#DIV/0!
12	0.245	0.275	0.259	5.912205		15.43855	15.43855	#DIV/0!
15	0.246	0.276	0.258	3.306991		17.39011	17.39011	#DIV/0!
18	0.244	0.275	0.258	8.511555		17.39011	17.39011	#DIV/0!
21	0.244	0.242	0.261	8.511555	0.566363	11.53262	6.04949	7.754313
24	0.245	0.242	0.261	5.912205	0.566363	11.53262	6.04949	7.754313
27	0.245	0.242	0.260	5.912205	0.566363	13.48606	7.026209	9.135603
30	0.244	0.242	0.260	8.511555	0.566363	13.48606	7.026209	9.135603
33	0.243	0.246	0.259	11.10504	-4.58165	15.43855	5.428454	14.15642
36	0.243	0.242	0.259	11.10504	0.566363	15.43855	8.002459	10.51623
39	0.244	0.239	0.260	8.511555	4.485387	13.48606	8.985721	6.364434
42	0.245	0.238	0.258	5.912205	5.802779	17.39011	11.59645	8.193483
45	0.245	0.236	0.258	5.912205	8.454139	17.39011	12.92213	6.318688
48	0.245	0.234	0.257	5.912205	11.1276	19.34073	15.23417	5.807561
51	0.245	0.229	0.255	5.912205	17.90795	23.23915	20.57355	3.769728
54	0.246	0.225	0.256	3.306991	23.43169	21.29041	22.36105	1.51411
57	0.245	0.228	0.254	5.912205	19.2806	25.18695	22.23377	4.176423
60	0.241	0.225	0.252	16.27442	23.43169	29.07973	26.25571	3.993769
63	0.239	0.219	0.252	21.42035	31.88305	29.07973	30.48139	1.98225
66	0.239	0.217	0.250	21.42035	34.74438	32.96875	33.85657	1.25556
69	0.238	0.219	0.246	23.98452	31.88305	40.73551	36.30928	6.259632

72	0.236	0.218	0.246	29.09527	33.31095	40.73551	37.02323	5.249954
75	0.235	0.216	0.240	31.64185	36.18333	52.35746	44.27039	11.43683
78	0.234	0.212	0.242	34.18256	41.99439	48.48723	45.24081	4.591135
81	0.233	0.210	0.240	36.71741	44.93307	52.35746	48.64526	5.249834
84	0.230	0.207	0.240	44.28678	49.38253	52.35746	50.86999	2.103589
87	0.229	0.207	0.239	46.79818	49.38253	54.29116	51.83684	3.470922
90	0.227	0.205	0.237	51.80338	52.37647	58.15574	55.2661	4.086563
93	0.225	0.204	0.235	56.78513	53.88172	62.01656	57.94914	5.752201
96	0.223	0.204	0.232	62.97933	53.88172	67.80075	60.84124	9.842238
99	0.227	0.204	0.228	51.80338	53.88172	75.49984	64.69078	15.28632
102	0.228	0.203	0.220	49.30371	55.3925	90.8529	73.1227	25.07429
105	0.227	0.202	0.209	51.80338	56.90881	111.8652	84.38698	38.86
108	0.228	0.200	0.208	49.30371	59.958	113.7697	86.86386	38.05063
111	0.226	0.191	0.206	54.29718	73.95286	117.576	95.76444	30.84624
114	0.228	0.185	0.204	49.30371	83.53141	121.3786	102.455	26.76199
117	0.223	0.185	0.204	61.74342	83.53141	121.3786	102.455	26.76199
120	0.220	0.177	0.204	69.13688	96.61223	121.3786	108.9954	17.51245
123	0.218	0.175	0.201	74.03654	99.93769	127.0754	113.5065	19.18923
126	0.219	0.174	0.202	71.58964	101.6087	125.1774	113.393	16.66556
129	0.218	0.172	0.200	74.03654	104.9673	128.9724	116.9699	16.97416
132	0.209	0.171	0.198	95.79474	106.6549	132.7637	119.7093	18.46168
135	0.203	0.170	0.195	110.0364	108.348	138.4435	123.3958	21.28073
138	0.203	0.168	0.194	110.0364	111.7508	140.3349	126.0429	20.21201
141	0.202	0.167	0.181	112.3894	113.4605	164.8377	139.1491	36.32913
144	0.202	0.165	0.171	112.3894	116.8965	183.5779	150.2372	47.15085
147	0.209	0.162	0.165	95.79474	122.0919	194.7769	158.4344	51.39605
150	0.208	0.162	0.162	98.183	122.0919	200.3637	161.2278	55.34652
153	0.208	0.160	0.161	98.183	125.5831	202.2241	163.9036	54.19335
156	0.195	0.155	0.160	128.6968	134.4079	204.0835	169.2457	49.26814
159	0.192	0.153	0.161	135.5977	137.9764	202.2241	170.1003	45.42994
162	0.188	0.150	0.156	144.7169	143.3708	211.5119	177.4413	48.1831
165	0.180	0.135	0.154	162.6737	171.0882	215.2205	193.1544	31.20625
168	0.176	0.130	0.151	171.5114	180.6036	220.7763	200.69	28.40637
171	0.164	0.125	0.148	197.4615	190.2572	226.3236	208.2904	25.50283
174	0.170	0.123	0.145	184.592	194.1573	231.8625	213.0099	26.66162
177	0.160	0.123	0.142	205.9239	194.1573	237.3929	215.7751	30.57222
180	0.161	0.120	0.139	203.8171	200.0489	242.9149	221.4819	30.31085
183	0.152	0.117	0.140	222.5673	205.9902	241.0752	223.5327	24.80882
186	0.140	0.113	0.138	246.8287	213.9893	244.7537	229.3715	21.75368
189	0.140	0.111	0.138	246.8287	218.022	244.7537	231.3878	18.90212
192	0.142	0.110	0.139	242.8438	220.0467	242.9149	231.4808	16.17027

195	0.141	0.108	0.139	244.8392	224.1125	242.9149	233.5137	13.29527
198	0.140	0.107	0.138	246.8287	226.1538	244.7537	235.4537	13.15212
201	0.140	0.107	0.138	246.8287	226.1538	244.7537	235.4537	13.15212
204	0.139	0.106	0.137	248.8124	228.2005	246.5915	237.396	13.0044
207	0.139	0.104	0.138	248.8124	232.3106	244.7537	238.5321	8.7986
210	0.138	0.103	0.137	250.7902	234.3739	246.5915	240.4827	8.639156
213	0.135	0.102	0.136	256.6884	236.4427	248.4284	242.4356	8.475141
216	0.135	0.102	0.136	256.6884	236.4427	248.4284	242.4356	8.475141

Table II.4. Data 4/1 D/L; 0.1 Hz

Time (h)	Optical reading (mV)			TSS (mg/L)			Average (mg/L)	SD
	1	2	3	1	2	3		
3	0.203	0.268	0.224	9.634908	8.668912	8.314887	8.872902	0.683244
6	0.204	0.269	0.225	8.139792	4.734268	6.090306	6.321455	1.714489
9	0.205	0.270	0.224	6.6513	0.7792	8.314887	5.248462	3.958865
12	0.205	0.268	0.223	6.6513	8.668912	10.53839	8.619534	1.944016
15	0.206	0.268	0.224	5.169432	8.668912	8.314887	7.38441	1.926377
18	0.206	0.269	0.223	5.169432	4.734268	10.53839	6.81403	3.232721
21	0.206	0.267	0.225	5.169432	12.58313	6.090306	7.947623	4.040787
24	0.205	0.266	0.223	6.6513	16.47693	10.53839	11.22221	4.948378
27	0.205	0.265	0.224	6.6513	20.3503	8.314887	11.77216	7.475307
30	0.205	0.266	0.226	6.6513	16.47693	3.864648	8.997625	6.625431
33	0.204	0.265	0.225	8.139792	20.3503	6.090306	11.5268	7.709781
36	0.205	0.266	0.224	6.6513	16.47693	8.314887	10.48104	5.258793
39	0.204	0.266	0.223	8.139792	16.47693	10.53839	11.71837	4.291995
42	0.206	0.265	0.224	5.169432	20.3503	8.314887	11.27821	8.01253
45	0.204	0.266	0.224	8.139792	16.47693	8.314887	10.9772	4.763707
48	0.207	0.264	0.225	3.694188	24.20325	6.090306	11.32925	11.2134
51	0.205	0.265	0.225	6.6513	20.3503	6.090306	11.03064	8.075939
54	0.204	0.265	0.224	8.139792	20.3503	8.314887	12.26833	6.999742
57	0.202	0.264	0.225	11.13665	24.20325	6.090306	13.81007	9.347729
60	0.200	0.265	0.225	14.16	20.3503	6.090306	13.53354	7.150608
63	0.198	0.263	0.221	17.20985	28.03577	14.98216	20.07593	6.982834
66	0.195	0.262	0.223	21.8343	31.84787	10.53839	21.40685	10.66117
69	0.191	0.262	0.217	28.09297	31.84787	23.85678	27.93254	3.997958
72	0.190	0.261	0.215	29.6742	35.63955	28.28763	31.20046	3.906376
75	0.189	0.261	0.210	31.26205	35.63955	39.34589	35.41583	4.046559
78	0.182	0.260	0.208	42.56249	39.4108	43.76165	41.91165	2.247259
81	0.180	0.259	0.204	45.8508	43.16163	52.58024	47.19756	4.851588
84	0.179	0.257	0.194	47.50489	50.60201	74.55131	57.55274	14.80242

87	0.177	0.257	0.195	50.83295	50.60201	72.35905	57.93134	12.4953
90	0.172	0.256	0.189	59.26901	54.29157	85.49644	66.35234	16.76503
93	0.170	0.254	0.186	62.6898	61.60941	92.05059	72.1166	17.27179
96	0.168	0.252	0.182	66.13709	68.84555	100.7744	78.58567	19.26364
99	0.168	0.252	0.178	66.13709	68.84555	109.4809	81.48785	24.2805
102	0.164	0.251	0.177	73.11115	72.43299	111.6549	85.733	22.45155
105	0.158	0.250	0.176	83.77097	76	113.8277	91.19956	19.97804
108	0.156	0.248	0.175	87.37723	83.07275	115.9995	95.48316	17.89755
111	0.153	0.247	0.173	92.83631	86.57849	120.3398	99.91822	17.9603
114	0.151	0.245	0.172	96.50881	93.5287	122.5084	104.182	15.94095
117	0.148	0.242	0.170	102.0672	103.8008	126.8423	110.9035	13.83062
120	0.143	0.240	0.167	111.4638	110.5468	133.335	118.4485	12.90022
123	0.141	0.238	0.165	115.2688	117.2111	137.6581	123.3793	12.40388
126	0.139	0.237	0.166	119.1003	120.5126	135.4971	125.0366	9.086508
129	0.135	0.235	0.165	126.8427	127.0543	137.6581	130.5184	6.184107
132	0.133	0.233	0.156	130.7537	133.5143	157.0588	140.4423	14.45636
135	0.129	0.230	0.150	138.6551	143.0512	169.944	150.5501	16.93885
138	0.126	0.229	0.150	144.6507	146.1893	169.944	153.5947	14.17983
141	0.125	0.229	0.149	146.6625	146.1893	172.0878	154.9799	14.81779
144	0.120	0.224	0.149	156.8208	161.5735	172.0878	163.494	7.812597
147	0.120	0.226	0.156	156.8208	155.4811	157.0588	156.4535	0.850537
150	0.113	0.220	0.155	171.3206	173.5132	159.209	168.0143	7.703997
153	0.113	0.218	0.155	171.3206	179.3605	159.209	169.9634	10.14409
156	0.108	0.218	0.142	181.8764	179.3605	187.0641	182.767	3.928234
159	0.104	0.215	0.139	190.4402	187.9783	193.4663	190.6283	2.748821
162	0.102	0.213	0.135	194.7618	193.6214	201.9875	196.7902	4.536944
165	0.094	0.208	0.127	212.3134	207.3716	218.9782	212.8878	5.824583
168	0.093	0.213	0.123	214.5372	193.6214	227.4478	211.8688	17.07034
171	0.090	0.200	0.111	221.2482	228.31	252.7529	234.1037	16.53212
174	0.089	0.199	0.117	223.4985	230.8354	240.1197	231.4845	8.329615
177	0.085	0.195	0.107	232.5657	240.7327	261.1534	244.8173	14.72505
180	0.082	0.194	0.108	239.4357	243.156	259.0549	247.2155	10.42056
183	0.080	0.192	0.099	244.0488	247.9412	277.9028	256.6309	18.52449
186	0.070	0.191	0.087	267.5118	250.3032	302.8976	273.5709	26.8156
189	0.065	0.191	0.087	279.4917	250.3032	302.8976	277.5642	26.35012
192	0.060	0.190	0.089	291.6372	252.6448	298.7426	281.0082	24.81901
195	0.058	0.185	0.088	296.5418	264.0463	300.8206	287.1362	20.11059
198	0.057	0.185	0.087	299.004	264.0463	302.8976	288.6493	21.39558
201	0.055	0.178	0.087	303.9483	279.1506	302.8976	295.3322	14.0235
204	0.055	0.178	0.086	303.9483	279.1506	304.9735	296.0241	14.6219
207	0.053	0.173	0.086	308.9191	289.3267	304.9735	301.0731	10.36224

210	0.053	0.159	0.085	308.9191	315.1032	307.0483	310.3569	4.215541
213	0.052	0.160	0.082	311.4144	313.3948	313.2663	312.6919	1.10813
216	0.052	0.159	0.082	311.4144	315.1032	313.2663	313.2613	1.844395

Table II.5. Data 5/1 D/L; 0.1 Hz.

Time (h)	Optical reading (mV)			TSS (mg/L)			Average (mg/L)	SD
	1	2	3	1	2	3		
3	0.203	0.268	0.224	9.634908	8.668912	8.314887	8.872902	0.683244
6	0.204	0.269	0.225	8.139792	4.734268	6.090306	6.321455	1.714489
9	0.205	0.270	0.224	6.6513	0.7792	8.314887	5.248462	3.958865
12	0.205	0.268	0.223	6.6513	8.668912	10.53839	8.619534	1.944016
15	0.206	0.268	0.224	5.169432	8.668912	8.314887	7.38441	1.926377
18	0.206	0.269	0.223	5.169432	4.734268	10.53839	6.81403	3.232721
21	0.206	0.267	0.225	5.169432	12.58313	6.090306	7.947623	4.040787
24	0.205	0.266	0.223	6.6513	16.47693	10.53839	11.22221	4.948378
27	0.205	0.265	0.224	6.6513	20.3503	8.314887	11.77216	7.475307
30	0.205	0.266	0.226	6.6513	16.47693	3.864648	8.997625	6.625431
33	0.204	0.265	0.225	8.139792	20.3503	6.090306	11.5268	7.709781
36	0.205	0.266	0.224	6.6513	16.47693	8.314887	10.48104	5.258793
39	0.204	0.266	0.223	8.139792	16.47693	10.53839	11.71837	4.291995
42	0.206	0.265	0.224	5.169432	20.3503	8.314887	11.27821	8.01253
45	0.204	0.266	0.224	8.139792	16.47693	8.314887	10.9772	4.763707
48	0.207	0.264	0.225	3.694188	24.20325	6.090306	11.32925	11.2134
51	0.205	0.265	0.225	6.6513	20.3503	6.090306	11.03064	8.075939
54	0.204	0.265	0.224	8.139792	20.3503	8.314887	12.26833	6.999742
57	0.202	0.264	0.225	11.13665	24.20325	6.090306	13.81007	9.347729
60	0.205	0.269	0.224	6.6513	4.734268	8.314887	6.566818	1.791804
63	0.203	0.267	0.224	9.634908	12.58313	8.314887	10.17764	2.185269
66	0.200	0.266	0.226	14.16	16.47693	3.864648	11.50053	6.713569
69	0.196	0.266	0.220	20.28619	16.47693	17.20244	17.98852	2.022639
72	0.195	0.265	0.218	21.8343	20.3503	21.63975	21.27478	0.806513
75	0.194	0.265	0.213	23.38903	20.3503	32.71417	25.4845	6.442789
78	0.186	0.264	0.220	36.06535	24.20325	17.20244	25.82368	9.53529
81	0.184	0.264	0.204	39.30067	24.20325	52.58024	38.69472	14.1982
84	0.183	0.262	0.194	40.92827	31.84787	74.55131	49.10915	22.49647
87	0.181	0.268	0.195	44.20333	8.668912	72.35905	41.74377	31.91623
90	0.176	0.267	0.189	52.50691	12.58313	85.49644	50.19549	36.51157

93	0.174	0.258	0.186	55.87471	46.89203	92.05059	64.93911	23.90494
96	0.172	0.256	0.182	59.26901	54.29157	100.7744	71.44498	25.52163
99	0.172	0.256	0.178	59.26901	54.29157	109.4809	74.34716	30.52833
102	0.168	0.255	0.177	66.13709	57.9607	111.6549	78.58421	28.93033
105	0.162	0.254	0.176	76.63793	61.60941	113.8277	84.02502	26.8815
108	0.160	0.252	0.175	80.1912	68.84555	115.9995	88.34542	24.61183
111	0.157	0.251	0.173	85.57079	72.43299	120.3398	92.78121	24.75398
114	0.155	0.249	0.172	89.1903	79.54659	122.5084	97.08176	22.54187
117	0.152	0.246	0.170	94.66925	90.06381	126.8423	103.8584	20.03734
120	0.147	0.244	0.167	103.9333	96.97317	133.335	111.4138	19.30064
123	0.145	0.242	0.165	107.6853	103.8008	137.6581	116.3814	18.52824
126	0.143	0.241	0.166	111.4638	107.184	135.4971	118.0483	15.26187
129	0.139	0.239	0.165	119.1003	113.8891	137.6581	123.5492	12.49343
132	0.137	0.237	0.156	122.9582	120.5126	157.0588	133.5099	20.43058
135	0.133	0.234	0.150	130.7537	130.2945	169.944	143.6641	22.76026
138	0.130	0.233	0.150	136.6698	133.5143	169.944	146.7094	20.18355
141	0.129	0.233	0.149	138.6551	133.5143	172.0878	148.0857	20.94471
144	0.124	0.228	0.149	148.6809	149.307	172.0878	156.6919	13.33691
147	0.124	0.230	0.156	148.6809	143.0512	157.0588	149.597	7.048563
150	0.117	0.224	0.155	162.9953	161.5735	159.209	161.2592	1.912598
153	0.117	0.222	0.155	162.9953	167.5842	159.209	163.2628	4.194005
156	0.112	0.222	0.142	173.4185	167.5842	187.0641	176.0223	9.997539
159	0.108	0.219	0.139	181.8764	176.4471	193.4663	183.9299	8.693457
162	0.106	0.217	0.135	186.145	182.2535	201.9875	190.1287	10.45273
165	0.098	0.212	0.127	203.4846	196.4123	218.9782	206.2917	11.5419
168	0.097	0.217	0.123	205.6819	182.2535	227.4478	205.1277	22.60221
171	0.094	0.204	0.111	212.3134	218.0042	252.7529	227.6902	21.89064
174	0.093	0.203	0.117	214.5372	220.6113	240.1197	225.0894	13.36624
177	0.089	0.199	0.107	223.4985	230.8354	261.1534	238.4957	19.96208
180	0.086	0.198	0.108	230.289	233.3404	259.0549	240.8947	15.80099
183	0.084	0.196	0.099	234.8491	238.289	277.9028	250.347	23.92596
186	0.074	0.195	0.087	258.0471	240.7327	302.8976	267.2258	32.08279
189	0.069	0.195	0.087	269.8945	240.7327	302.8976	271.1749	31.10223
192	0.064	0.194	0.089	281.9076	243.156	298.7426	274.602	28.50431
195	0.062	0.189	0.088	286.7591	254.9659	300.8206	280.8486	23.49179
198	0.061	0.189	0.087	289.1949	254.9659	302.8976	282.3528	24.68747
201	0.059	0.182	0.087	294.0862	270.6421	302.8976	289.2086	16.67174
204	0.059	0.182	0.086	294.0862	270.6421	304.9735	289.9006	17.54424
207	0.057	0.177	0.086	299.004	281.2267	304.9735	295.068	12.35301
210	0.057	0.163	0.085	299.004	308.147	307.0483	304.7331	4.991868
213	0.056	0.164	0.082	301.4728	306.3568	313.2663	307.032	5.925658

216	0.056	0.163	0.082	301.4728	308.147	313.2663	307.6287	5.913798

Table II.6. Data 6/1 D/L; 0.1 Hz

Time (h)	Optical reading (mV)			TSS (mg/L)			Average (mg/L)	SD
	1	2	3	1	2	3		
3	0.203	0.268	0.224	9.635	8.669	8.315	8.873	0.683
6	0.204	0.269	0.225	8.140	4.734	6.090	6.321	1.714
9	0.205	0.270	0.224	6.651	0.779	8.315	5.248	3.959
12	0.205	0.268	0.223	6.651	8.669	10.538	8.620	1.944
15	0.206	0.268	0.224	5.169	8.669	8.315	7.384	1.926
18	0.206	0.269	0.223	5.169	4.734	10.538	6.814	3.233
21	0.206	0.267	0.225	5.169	12.583	6.090	7.948	4.041
24	0.205	0.266	0.223	6.651	16.477	10.538	11.222	4.948
27	0.205	0.265	0.224	6.651	20.350	8.315	11.772	7.475
30	0.205	0.266	0.226	6.651	16.477	3.865	8.998	6.625
33	0.204	0.265	0.225	8.140	20.350	6.090	11.527	7.710
36	0.205	0.266	0.224	6.651	16.477	8.315	10.481	5.259
39	0.204	0.266	0.223	8.140	16.477	10.538	11.718	4.292
42	0.206	0.265	0.224	5.169	20.350	8.315	11.278	8.013
45	0.204	0.266	0.224	8.140	16.477	8.315	10.977	4.764
48	0.207	0.264	0.225	3.694	24.203	6.090	11.329	11.213
51	0.205	0.265	0.225	6.651	20.350	6.090	11.031	8.076
54	0.204	0.265	0.224	8.140	20.350	8.315	12.268	7.000
57	0.202	0.264	0.225	11.137	24.203	6.090	13.810	9.348
60	0.205	0.269	0.224	6.651	4.734	8.315	6.567	1.792
63	0.203	0.267	0.224	9.635	12.583	8.315	10.178	2.185
66	0.200	0.266	0.226	14.160	16.477	3.865	11.501	6.714
69	0.197	0.268	0.221	18.745	8.669	14.982	14.132	5.091
72	0.196	0.267	0.219	20.286	12.583	19.422	17.430	4.220
75	0.195	0.267	0.214	21.834	12.583	30.501	21.640	8.961
78	0.187	0.266	0.221	34.458	16.477	14.982	21.972	10.838
81	0.185	0.266	0.205	37.680	16.477	50.377	34.845	17.127
84	0.184	0.264	0.195	39.301	24.203	72.359	45.288	24.630
87	0.182	0.270	0.196	42.562	0.779	70.166	37.836	34.934
90	0.177	0.269	0.190	50.833	4.734	83.310	46.292	39.484
93	0.175	0.260	0.187	54.188	39.411	89.867	61.155	25.940
96	0.173	0.258	0.183	57.569	46.892	98.595	67.685	27.296
99	0.173	0.258	0.179	57.569	46.892	107.306	70.589	32.243

102	0.169	0.257	0.178	64.410	50.602	109.481	74.831	30.792
105	0.163	0.256	0.177	74.871	54.292	111.655	80.273	29.061
108	0.161	0.254	0.176	78.411	61.609	113.828	84.616	26.656
111	0.158	0.253	0.174	83.771	65.238	118.170	89.060	26.860
114	0.156	0.251	0.173	87.377	72.433	120.340	93.383	24.512
117	0.153	0.248	0.171	92.836	83.073	124.676	100.195	21.756
120	0.148	0.246	0.168	102.067	90.064	131.172	107.768	21.139
123	0.146	0.244	0.166	105.806	96.973	135.497	112.759	20.181
126	0.144	0.243	0.167	109.571	100.397	133.335	114.434	16.999
129	0.140	0.241	0.166	117.181	107.184	135.497	119.954	14.359
132	0.138	0.239	0.157	121.026	113.889	154.907	129.941	21.914
135	0.134	0.236	0.151	128.795	123.794	167.799	140.129	24.093
138	0.131	0.235	0.151	134.691	127.054	167.799	143.182	21.659
141	0.130	0.235	0.150	136.670	127.054	169.944	144.556	22.506
144	0.125	0.230	0.150	146.663	143.051	169.944	153.219	14.596
147	0.125	0.232	0.157	146.663	136.714	154.907	146.095	9.110
150	0.118	0.226	0.156	160.930	155.481	157.059	157.823	2.804
153	0.118	0.224	0.156	160.930	161.573	157.059	159.854	2.442
156	0.113	0.224	0.143	171.321	161.573	184.928	172.607	11.730
159	0.109	0.221	0.140	179.752	170.559	191.333	180.548	10.410
162	0.107	0.219	0.136	184.007	176.447	199.859	186.771	11.948
165	0.099	0.214	0.128	201.294	190.810	216.858	202.987	13.106
168	0.098	0.219	0.124	203.485	176.447	225.332	201.755	24.488
171	0.095	0.206	0.112	210.096	212.729	250.650	224.492	22.692
174	0.094	0.205	0.118	212.313	215.377	238.010	221.900	14.036
177	0.090	0.201	0.108	221.248	225.764	259.055	235.356	20.648
180	0.087	0.200	0.109	228.019	228.310	256.955	237.761	16.623
183	0.085	0.198	0.100	232.566	233.340	275.813	247.240	24.748
186	0.075	0.197	0.088	255.698	235.825	300.821	264.114	33.305
189	0.070	0.197	0.088	267.512	235.825	300.821	268.052	32.501
192	0.065	0.196	0.090	279.492	238.289	296.663	271.481	30.000
195	0.063	0.191	0.089	284.330	250.303	298.743	277.792	24.873
198	0.062	0.191	0.088	286.759	250.303	300.821	279.294	26.073
201	0.060	0.184	0.088	291.637	266.265	300.821	286.241	17.898
204	0.060	0.184	0.087	291.637	266.265	302.898	286.933	18.764
207	0.058	0.179	0.087	296.542	277.054	302.898	292.164	13.466
210	0.058	0.165	0.086	296.542	304.546	304.974	302.021	4.750
213	0.057	0.166	0.083	299.004	302.715	311.195	304.305	6.249
216	0.057	0.165	0.083	299.004	304.546	311.195	304.915	6.104

Table II.7. Data 7/1 D/L; 0.1 Hz

Time (h)	Optical reading (mV)			TSS (mg/L)			Average (mg/L)	SD
	1	2	3	1	2	3		
3	0.218	0.248	0.24	9.634908	8.668912	8.314887	8.87	0.683
6	0.216	0.258	0.24	8.139792	4.734268	6.090306	6.32	1.714
9	0.213	0.25	0.238	6.6513	0.7792	8.314887	5.25	3.959
12	0.215	0.255	0.238	6.6513	8.668912	10.53839	8.62	1.944
15	0.214	0.258	0.238	5.169432	8.668912	8.314887	7.38	1.926
18	0.215	0.255	0.237	5.169432	4.734268	10.53839	6.81	3.233
21	0.215	0.25	0.238	5.169432	12.58313	6.090306	7.95	4.041
24	0.216	0.251	0.236	6.6513	16.47693	10.53839	11.22	4.948
27	0.215	0.249	0.239	6.6513	20.3503	8.314887	11.77	7.475
30	0.214	0.247	0.239	6.6513	16.47693	3.864648	9.00	6.625
33	0.212	0.246	0.239	8.139792	20.3503	6.090306	11.53	7.710
36	0.21	0.246	0.239	6.6513	16.47693	8.314887	10.48	5.259
39	0.209	0.242	0.24	8.139792	16.47693	10.53839	11.72	4.292
42	0.206	0.239	0.241	5.169432	12.58313	8.314887	8.69	3.721
45	0.209	0.234	0.24	3.694188	8.668912	8.314887	6.89	2.776
48	0.207	0.232	0.239	0.763572	16.47693	6.090306	7.78	7.991
51	0.205	0.234	0.24	3.694188	12.58313	6.090306	7.46	4.599
54	0.204	0.225	0.234	5.169432	12.58313	8.314887	8.69	3.721
57	0.202	0.228	0.235	8.139792	16.47693	-0.5899	8.01	8.534
60	0.2	0.22	0.233	3.694188	-3.19629	1.637912	0.71	3.537
63	0.198	0.214	0.233	6.6513	4.734268	1.637912	4.34	2.530
66	0.195	0.221	0.236	11.13665	8.668912	-2.81879	5.66	7.448
69	0.191	0.2	0.235	15.68161	0.7792	8.314887	8.26	7.451
72	0.19	0.198	0.234	17.20985	4.734268	12.76082	11.57	6.323
75	0.189	0.193	0.232	18.74471	4.734268	23.85678	15.78	9.900
78	0.182	0.188	0.228	31.26205	8.668912	8.314887	16.08	13.148
81	0.18	0.188	0.225	34.45763	8.668912	43.76165	28.96	18.180
84	0.179	0.166	0.223	36.06535	16.47693	65.77581	39.44	24.822
87	0.177	0.186	0.22	39.30067	-7.19221	63.57925	31.90	35.962
90	0.172	0.157	0.22	47.50489	-3.19629	76.74249	40.35	40.447
93	0.17	0.154	0.218	50.83295	31.84787	83.30957	55.33	26.024
96	0.168	0.148	0.217	54.1875	39.4108	92.05059	61.88	27.151
99	0.168	0.148	0.213	54.1875	39.4108	100.7744	64.79	32.026
102	0.164	0.139	0.214	60.97609	43.16163	102.9526	69.03	30.698
105	0.158	0.135	0.21	71.3577	46.89203	105.1298	74.46	29.243
108	0.156	0.143	0.205	74.87123	54.29157	107.3059	78.82	26.727
111	0.153	0.131	0.204	80.1912	57.9607	111.6549	83.27	26.979
114	0.151	0.128	0.2	83.77097	65.23769	113.8277	87.61	24.522

117	0.148	0.13	0.196	89.1903	76	118.1702	94.45	21.572
120	0.143	0.123	0.191	98.355	83.07275	124.6759	102.03	21.044
123	0.141	0.125	0.19	102.0672	90.06381	129.0076	107.05	19.944
126	0.139	0.124	0.185	105.806	93.5287	126.8423	108.73	16.848
129	0.135	0.122	0.181	113.363	100.3972	129.0076	114.26	14.326
132	0.133	0.12	0.176	117.1812	107.184	148.447	124.27	21.526
135	0.129	0.11	0.171	124.8972	117.2111	161.3582	134.49	23.585
138	0.126	0.125	0.166	130.7537	120.5126	161.3582	137.54	21.252
141	0.125	0.109	0.165	132.7191	120.5126	163.5062	138.91	22.156
144	0.12	0.109	0.159	142.6455	136.7137	163.5062	147.62	14.072
147	0.12	0.11	0.157	142.6455	130.2945	148.447	140.46	9.271
150	0.113	0.108	0.149	156.8208	149.307	150.6016	152.24	4.017
153	0.113	0.102	0.149	156.8208	155.4811	150.6016	154.30	3.273
156	0.108	0.099	0.138	167.1447	155.4811	178.5127	167.05	11.516
159	0.104	0.095	0.138	175.5231	164.5891	184.9278	175.01	10.179
162	0.102	0.094	0.132	179.752	170.5589	193.4663	181.26	11.528
165	0.094	0.092	0.127	196.9326	185.1261	210.4915	197.52	12.693
168	0.093	0.094	0.125	199.11	170.5589	218.9782	196.22	24.339
171	0.09	0.092	0.122	205.6819	207.3716	244.3351	219.13	21.845
174	0.089	0.095	0.121	207.8858	210.0604	231.676	216.54	13.153
177	0.088	0.094	0.119	216.7676	220.6113	252.7529	230.04	19.760
180	0.088	0.095	0.118	223.4985	223.198	250.65	232.45	15.763
183	0.086	0.093	0.119	228.0188	228.31	269.5367	241.96	23.887
186	0.084	0.098	0.117	251.0181	230.8354	294.5832	258.81	32.581
189	0.084	0.093	0.116	262.7662	230.8354	294.5832	262.73	31.874
192	0.084	0.095	0.114	274.6799	233.3404	290.4196	266.15	29.481
195	0.084	0.094	0.114	279.4917	245.5588	292.502	272.52	24.236
198	0.08	0.095	0.114	281.9076	245.5588	294.5832	274.02	25.447
201	0.082	0.095	0.113	286.7591	261.8068	294.5832	281.05	17.118
204	0.079	0.097	0.112	286.7591	261.8068	296.6634	281.74	17.962
207	0.081	0.088	0.112	291.6372	272.7999	296.6634	287.03	12.580
210	0.079	0.092	0.111	291.6372	300.8639	298.7426	297.08	4.833
213	0.078	0.094	0.111	294.0862	298.9921	304.9735	299.35	5.453
216	0.078	0.099	0.109	294.0862	300.8639	304.9735	299.97	5.498

Table II.8. Data 8/1 D/L; 0.1 Hz.

Time (h)	Optical reading (mV)			TSS (mg/L)			Average (mg/L)	SD
	1	2	3	1	2	3		
3	0.203	0.268	0.224	9.635	8.669	8.315	8.873	0.683
6	0.204	0.269	0.225	8.140	4.734	6.090	6.321	1.714
9	0.205	0.270	0.224	6.651	0.779	8.315	5.248	3.959
12	0.205	0.268	0.223	6.651	8.669	10.538	8.620	1.944
15	0.206	0.268	0.224	5.169	8.669	8.315	7.384	1.926
18	0.206	0.269	0.223	5.169	4.734	10.538	6.814	3.233
21	0.206	0.267	0.225	5.169	12.583	6.090	7.948	4.041
24	0.205	0.266	0.223	6.651	16.477	10.538	11.222	4.948
27	0.205	0.265	0.224	6.651	20.350	8.315	11.772	7.475
30	0.205	0.266	0.226	6.651	16.477	3.865	8.998	6.625
33	0.204	0.265	0.225	8.140	20.350	6.090	11.527	7.710
36	0.205	0.266	0.224	6.651	16.477	8.315	10.481	5.259
39	0.204	0.266	0.223	8.140	16.477	10.538	11.718	4.292
42	0.206	0.267	0.224	5.169	12.583	8.315	8.689	3.721
45	0.207	0.268	0.224	3.694	8.669	8.315	6.893	2.776
48	0.209	0.266	0.225	0.764	16.477	6.090	7.777	7.991
51	0.207	0.267	0.225	3.694	12.583	6.090	7.456	4.599
54	0.206	0.267	0.224	5.169	12.583	8.315	8.689	3.721
57	0.204	0.266	0.228	8.140	16.477	-0.590	8.009	8.534
60	0.207	0.271	0.227	3.694	-3.196	1.638	0.712	3.537
63	0.205	0.269	0.227	6.651	4.734	1.638	4.341	2.530
66	0.202	0.268	0.229	11.137	8.669	-2.819	5.662	7.448
69	0.199	0.270	0.224	15.682	0.779	8.315	8.259	7.451
72	0.198	0.269	0.222	17.210	4.734	12.761	11.568	6.323
75	0.197	0.269	0.217	18.745	4.734	23.857	15.779	9.900
78	0.192	0.268	0.224	26.518	8.669	8.315	14.501	10.409
81	0.190	0.268	0.216	29.674	8.669	26.073	21.472	11.233
84	0.189	0.266	0.206	31.262	16.477	48.173	31.971	15.860
87	0.187	0.272	0.207	34.458	-7.192	45.968	24.411	27.968
90	0.182	0.271	0.201	42.562	-3.196	59.183	32.850	32.304
93	0.180	0.267	0.198	45.851	12.583	65.776	41.403	26.874
96	0.178	0.265	0.194	49.166	20.350	74.551	48.022	27.119
99	0.178	0.265	0.190	49.166	20.350	83.310	50.942	31.517
102	0.174	0.264	0.189	55.875	24.203	85.496	55.191	30.652
105	0.168	0.263	0.188	66.137	28.036	87.682	60.618	30.204
108	0.166	0.261	0.187	69.611	35.640	89.867	65.039	27.401
111	0.163	0.260	0.185	74.871	39.411	94.233	69.505	27.802
114	0.161	0.258	0.184	78.411	46.892	96.415	73.906	25.067
117	0.158	0.255	0.182	83.771	57.961	100.774	80.835	21.557

120	0.153	0.253	0.179	92.836	65.238	107.306	88.460	21.373
123	0.151	0.251	0.177	96.509	72.433	111.655	93.532	19.780
126	0.149	0.250	0.178	100.208	76.000	109.481	95.230	17.287
129	0.145	0.248	0.177	107.685	83.073	111.655	100.804	15.484
132	0.143	0.246	0.168	111.464	90.064	131.172	110.900	20.560
135	0.139	0.243	0.162	119.100	100.397	144.135	121.211	21.945
138	0.136	0.242	0.162	124.897	103.801	144.135	124.278	20.174
141	0.135	0.242	0.161	126.843	103.801	146.291	125.645	21.271
144	0.130	0.237	0.161	136.670	120.513	146.291	134.491	13.027
147	0.130	0.239	0.168	136.670	113.889	131.172	127.244	11.888
150	0.123	0.233	0.167	150.706	133.514	133.335	139.185	9.978
153	0.123	0.231	0.167	150.706	139.893	133.335	141.311	8.772
156	0.118	0.231	0.154	160.930	139.893	161.358	154.060	12.272
159	0.114	0.228	0.151	169.229	149.307	167.799	162.112	11.112
162	0.112	0.226	0.147	173.419	155.481	176.372	168.424	11.306
165	0.104	0.221	0.139	190.440	170.559	193.466	184.822	12.444
168	0.103	0.226	0.135	192.598	155.481	201.988	183.355	24.592
171	0.100	0.213	0.123	199.110	193.621	227.448	206.726	18.154
174	0.099	0.212	0.129	201.294	196.412	214.737	204.148	9.490
177	0.095	0.208	0.119	210.096	207.372	235.900	217.789	15.743
180	0.092	0.207	0.120	216.768	210.060	233.789	220.206	12.232
183	0.090	0.205	0.111	221.248	215.377	252.753	229.793	20.100
186	0.080	0.204	0.099	244.049	218.004	277.903	246.652	30.034
189	0.075	0.204	0.099	255.698	218.004	277.903	250.535	30.281
192	0.070	0.203	0.101	267.512	220.611	273.722	253.948	29.037
195	0.068	0.198	0.100	272.284	233.340	275.813	260.479	23.569
198	0.067	0.198	0.099	274.680	233.340	277.903	261.974	24.850
201	0.065	0.191	0.099	279.492	250.303	277.903	269.233	16.413
204	0.065	0.191	0.098	279.492	250.303	279.992	269.929	16.998
207	0.063	0.186	0.098	284.330	261.807	279.992	275.376	11.950
210	0.063	0.172	0.097	284.330	291.301	282.079	285.903	4.808
213	0.062	0.173	0.094	286.759	289.327	288.336	288.141	1.295
216	0.062	0.172	0.094	286.759	291.301	288.336	288.799	2.306

Table II.9. Data 9/1 D/L; 0.1 Hz.

Time (h)	Optical reading (mV)			TSS (mg/L)			Average (mg/L)	SD
	1	2	3	1	2	3		
3	0.203	0.268	0.224	9.635	8.669	8.315	8.873	0.683
6	0.204	0.269	0.225	8.140	4.734	6.090	6.321	1.714
9	0.205	0.270	0.224	6.651	0.779	8.315	5.248	3.959
12	0.205	0.268	0.223	6.651	8.669	10.538	8.620	1.944
15	0.206	0.268	0.224	5.169	8.669	8.315	7.384	1.926
18	0.206	0.269	0.223	5.169	4.734	10.538	6.814	3.233
21	0.206	0.267	0.225	5.169	12.583	6.090	7.948	4.041
24	0.205	0.266	0.223	6.651	16.477	10.538	11.222	4.948
27	0.205	0.265	0.224	6.651	20.350	8.315	11.772	7.475
30	0.205	0.266	0.226	6.651	16.477	3.865	8.998	6.625
33	0.204	0.265	0.225	8.140	20.350	6.090	11.527	7.710
36	0.205	0.266	0.224	6.651	16.477	8.315	10.481	5.259
39	0.204	0.274	0.223	8.140	-15.245	10.538	1.144	14.244
42	0.206	0.275	0.224	5.169	-19.303	8.315	-1.939	15.119
45	0.207	0.276	0.224	3.694	-23.380	8.315	-3.790	17.122
48	0.209	0.274	0.225	0.764	-15.245	6.090	-2.797	11.105
51	0.207	0.275	0.225	3.694	-19.303	6.090	-3.173	14.020
54	0.206	0.275	0.224	5.169	-19.303	8.315	-1.939	15.119
57	0.204	0.274	0.228	8.140	-15.245	-0.590	-2.565	11.817
60	0.207	0.279	0.227	3.694	-35.735	1.638	-10.134	22.195
63	0.205	0.277	0.227	6.651	-27.478	1.638	-6.396	18.429
66	0.212	0.276	0.229	-3.583	-23.380	-2.819	-9.927	11.657
69	0.209	0.278	0.224	0.764	-31.597	8.315	-7.506	21.202
72	0.208	0.277	0.222	2.226	-27.478	12.761	-4.164	20.867
75	0.207	0.277	0.217	3.694	-27.478	23.857	0.024	25.863
78	0.202	0.276	0.224	11.137	-23.380	8.315	-1.310	19.166
81	0.200	0.276	0.216	14.160	-23.380	26.073	5.618	25.809
84	0.199	0.274	0.215	15.682	-15.245	28.288	9.575	22.400
87	0.197	0.280	0.216	18.745	-39.895	26.073	1.641	36.157
90	0.192	0.279	0.210	26.518	-35.735	39.346	10.043	40.161
93	0.190	0.275	0.207	29.674	-19.303	45.968	18.780	33.972
96	0.188	0.273	0.203	32.857	-11.209	54.782	25.477	33.609
99	0.188	0.273	0.199	32.857	-11.209	63.579	28.409	37.592
102	0.184	0.272	0.198	39.301	-7.192	65.776	32.628	36.939
105	0.178	0.271	0.197	49.166	-3.196	67.971	37.980	36.879
108	0.176	0.269	0.196	52.507	4.734	70.166	42.469	33.851
111	0.173	0.268	0.194	57.569	8.669	74.551	46.930	34.205
114	0.171	0.266	0.193	60.976	16.477	76.742	51.399	31.254
117	0.168	0.263	0.191	66.137	28.036	81.122	58.431	27.369

120	0.163	0.261	0.188	74.871	35.640	87.682	66.064	27.116
123	0.161	0.259	0.186	78.411	43.162	92.051	71.208	25.228
126	0.159	0.258	0.187	81.978	46.892	89.867	72.912	22.877
129	0.155	0.256	0.186	89.190	54.292	92.051	78.511	21.023
132	0.153	0.254	0.177	92.836	61.609	111.655	88.700	25.278
135	0.149	0.251	0.171	100.208	72.433	124.676	99.106	26.139
138	0.146	0.250	0.171	105.806	76.000	124.676	102.161	24.542
141	0.145	0.250	0.170	107.685	76.000	126.842	103.509	25.677
144	0.140	0.245	0.170	117.181	93.529	126.842	112.517	17.139
147	0.140	0.247	0.177	117.181	86.578	111.655	105.138	16.309
150	0.133	0.241	0.176	130.754	107.184	113.828	117.255	12.153
153	0.133	0.239	0.176	130.754	113.889	113.828	119.490	9.755
156	0.128	0.239	0.163	140.647	113.889	141.977	132.171	15.847
159	0.124	0.236	0.160	148.681	123.794	148.447	140.307	14.302
162	0.122	0.234	0.156	152.738	130.295	157.059	146.697	14.368
165	0.114	0.229	0.148	169.229	146.189	174.230	163.216	14.956
168	0.113	0.234	0.144	171.321	130.295	182.791	161.469	27.600
171	0.110	0.221	0.132	177.634	170.559	208.367	185.520	20.100
174	0.109	0.220	0.138	179.752	173.513	195.598	182.954	11.385
177	0.105	0.216	0.128	188.289	185.126	216.858	196.758	17.479
180	0.102	0.215	0.129	194.762	187.978	214.737	199.159	13.911
183	0.100	0.213	0.120	199.110	193.621	233.789	208.840	21.780
186	0.090	0.212	0.108	221.248	196.412	259.055	225.572	31.544
189	0.085	0.212	0.108	232.566	196.412	259.055	229.344	31.445
192	0.080	0.211	0.110	244.049	199.183	254.855	232.695	29.521
195	0.078	0.206	0.109	248.688	212.729	256.955	239.457	23.514
198	0.077	0.206	0.108	251.018	212.729	259.055	240.934	24.755
201	0.075	0.199	0.108	255.698	230.835	259.055	248.529	15.415
204	0.075	0.199	0.107	255.698	230.835	261.153	249.229	16.161
207	0.073	0.194	0.107	260.403	243.156	261.153	254.904	10.181
210	0.073	0.180	0.106	260.403	274.937	263.251	266.197	7.702
213	0.072	0.181	0.103	262.766	272.800	269.537	268.368	5.118
216	0.072	0.180	0.103	262.766	274.937	269.537	269.080	6.098

Table II.10. Data 10/1 D/L; 0.1 Hz.

Time (h)	Optical reading (mV)			TSS (mg/L)			Average (mg/L)	SD
	1	2	3	1	2	3		
3	0.203	0.268	0.224	9.635	8.669	8.315	8.873	0.683
6	0.204	0.269	0.225	8.140	4.734	6.090	6.321	1.714
9	0.205	0.270	0.224	6.651	0.779	8.315	5.248	3.959
12	0.205	0.268	0.223	6.651	8.669	10.538	8.620	1.944
15	0.206	0.268	0.224	5.169	8.669	8.315	7.384	1.926
18	0.206	0.269	0.223	5.169	4.734	10.538	6.814	3.233
21	0.206	0.267	0.225	5.169	12.583	6.090	7.948	4.041
24	0.205	0.266	0.223	6.651	16.477	10.538	11.222	4.948
27	0.205	0.265	0.224	6.651	20.350	8.315	11.772	7.475
30	0.205	0.266	0.226	6.651	16.477	3.865	8.998	6.625
33	0.204	0.265	0.225	8.140	20.350	6.090	11.527	7.710
36	0.205	0.266	0.224	6.651	16.477	8.315	10.481	5.259
39	0.204	0.267	0.223	8.140	12.583	10.538	10.420	2.224
42	0.206	0.267	0.224	5.169	12.583	8.315	8.689	3.721
45	0.207	0.267	0.224	3.694	12.583	8.315	8.197	4.446
48	0.209	0.266	0.225	0.764	16.477	6.090	7.777	7.991
51	0.207	0.266	0.225	3.694	16.477	6.090	8.754	6.795
54	0.206	0.267	0.224	5.169	12.583	8.315	8.689	3.721
57	0.204	0.268	0.228	8.140	8.669	-0.590	5.406	5.200
60	0.207	0.267	0.227	3.694	12.583	1.638	5.972	5.817
63	0.205	0.267	0.227	6.651	12.583	1.638	6.957	5.479
66	0.206	0.268	0.229	5.169	8.669	-2.819	3.673	5.888
69	0.205	0.268	0.224	6.651	8.669	8.315	7.878	1.077
72	0.204	0.269	0.222	8.140	4.734	12.761	8.545	4.029
75	0.203	0.268	0.225	9.635	8.669	6.090	8.131	1.832
78	0.202	0.269	0.232	11.137	4.734	-9.512	2.120	10.570
81	0.200	0.270	0.224	14.160	0.779	8.315	7.751	6.708
84	0.199	0.269	0.223	15.682	4.734	10.538	10.318	5.477
87	0.198	0.268	0.224	17.210	8.669	8.315	11.398	5.036
90	0.198	0.266	0.218	17.210	16.477	21.640	18.442	2.793
93	0.196	0.265	0.215	20.286	20.350	28.288	22.975	4.601
96	0.195	0.264	0.211	21.834	24.203	37.136	27.725	8.236
99	0.195	0.263	0.208	21.834	28.036	43.762	31.211	11.303
102	0.191	0.263	0.207	28.093	28.036	45.968	34.032	10.337
105	0.185	0.261	0.206	37.680	35.640	48.173	40.497	6.725
108	0.183	0.260	0.205	40.928	39.411	50.377	43.572	5.942
111	0.180	0.259	0.203	45.851	43.162	54.782	47.932	6.083
114	0.178	0.257	0.202	49.166	50.602	56.983	52.250	4.161
117	0.175	0.256	0.200	54.188	54.292	61.382	56.620	4.124

120	0.170	0.254	0.197	62.690	61.609	67.971	64.090	3.404
123	0.168	0.253	0.195	66.137	65.238	72.359	67.911	3.878
126	0.166	0.252	0.196	69.611	68.846	70.166	69.541	0.663
129	0.162	0.250	0.195	76.638	76.000	72.359	74.999	2.308
132	0.160	0.247	0.186	80.191	86.578	92.051	86.273	5.936
135	0.156	0.245	0.180	87.377	93.529	105.130	95.345	9.015
138	0.153	0.245	0.180	92.836	92.145	105.130	96.704	7.305
141	0.152	0.243	0.179	94.669	100.397	107.306	100.791	6.328
144	0.147	0.242	0.179	103.933	103.801	107.306	105.013	1.987
147	0.147	0.240	0.186	103.933	110.547	92.051	102.177	9.372
150	0.140	0.238	0.185	117.181	117.211	94.233	109.542	13.258
153	0.140	0.237	0.185	117.181	120.513	94.233	110.642	14.308
156	0.135	0.237	0.172	126.843	120.513	122.508	123.288	3.236
159	0.131	0.235	0.169	134.691	127.054	129.008	130.251	3.967
162	0.129	0.235	0.165	138.655	127.054	137.658	134.456	6.429
165	0.121	0.234	0.157	154.776	130.295	154.907	146.659	14.172
168	0.120	0.233	0.153	156.821	133.514	163.506	151.280	15.745
171	0.117	0.231	0.141	162.995	139.893	189.199	164.029	24.670
174	0.116	0.230	0.147	165.067	143.051	176.372	161.497	16.945
177	0.112	0.226	0.137	173.419	155.481	197.729	175.543	21.204
180	0.109	0.225	0.138	179.752	158.538	195.598	177.963	18.595
183	0.107	0.223	0.129	184.007	164.589	214.737	187.778	25.286
186	0.097	0.222	0.117	205.682	167.584	240.120	204.462	36.283
189	0.092	0.222	0.117	216.768	167.584	240.120	208.157	37.026
192	0.087	0.221	0.119	228.019	170.559	235.900	211.493	35.668
195	0.085	0.216	0.118	232.566	185.126	238.010	218.567	29.089
198	0.084	0.216	0.117	234.849	185.126	240.120	220.032	30.344
201	0.082	0.209	0.117	239.436	204.662	240.120	228.073	20.277
204	0.082	0.209	0.116	239.436	204.662	242.228	228.775	20.929
207	0.080	0.204	0.116	244.049	218.004	242.228	234.760	14.540
210	0.080	0.190	0.115	244.049	252.645	244.335	247.010	4.882
213	0.079	0.191	0.112	246.365	250.303	250.650	249.106	2.380
216	0.079	0.190	0.112	246.365	252.645	250.650	249.887	3.209

Table II.11. Data 15/1 D/L 0.1 Hz;

Time (h)	Optical reading (mV)			TSS (mg/L)			Average (mg/L)	SD
	1	2	3	1	2	3		
3	0.203	0.268	0.224	9.635	8.669	8.315	8.873	0.683
6	0.204	0.269	0.225	8.140	4.734	6.090	6.321	1.714
9	0.205	0.268	0.224	6.651	8.669	8.315	7.878	1.077
12	0.205	0.268	0.223	6.651	8.669	10.538	8.620	1.944
15	0.206	0.268	0.224	5.169	8.669	8.315	7.384	1.926
18	0.206	0.269	0.223	5.169	4.734	10.538	6.814	3.233
21	0.206	0.267	0.225	5.169	12.583	6.090	7.948	4.041
24	0.205	0.266	0.223	6.651	16.477	10.538	11.222	4.948
27	0.205	0.265	0.224	6.651	20.350	8.315	11.772	7.475
30	0.203	0.266	0.226	9.635	16.477	3.865	9.992	6.314
33	0.202	0.265	0.225	11.137	20.350	6.090	12.526	7.231
36	0.201	0.266	0.224	12.645	16.477	8.315	12.479	4.084
39	0.201	0.267	0.223	12.645	12.583	10.538	11.922	1.199
42	0.200	0.267	0.224	14.160	12.583	8.315	11.686	3.024
45	0.199	0.267	0.224	15.682	12.583	8.315	12.193	3.699
48	0.198	0.266	0.225	17.210	16.477	6.090	13.259	6.219
51	0.196	0.267	0.225	20.286	12.583	6.090	12.987	7.107
54	0.194	0.268	0.224	23.389	8.669	8.315	13.458	8.603
57	0.194	0.267	0.228	23.389	12.583	-0.590	11.794	12.009
60	0.193	0.267	0.227	24.950	12.583	1.638	13.057	11.663
63	0.191	0.269	0.227	28.093	4.734	1.638	11.488	14.463
66	0.190	0.268	0.229	29.674	8.669	-2.819	11.841	16.477
69	0.188	0.268	0.224	32.857	8.669	8.315	16.613	14.068
72	0.185	0.269	0.222	37.680	4.734	12.761	18.392	17.179
75	0.182	0.269	0.225	42.562	4.734	6.090	17.796	21.459
78	0.181	0.267	0.232	44.203	12.583	-9.512	15.758	26.998
81	0.178	0.266	0.224	49.166	16.477	8.315	24.652	21.618
84	0.176	0.265	0.223	52.507	20.350	10.538	27.799	21.953
87	0.174	0.264	0.224	55.875	24.203	8.315	29.464	24.212
90	0.172	0.263	0.218	59.269	28.036	21.640	36.315	20.134
93	0.170	0.260	0.215	62.690	39.411	28.288	43.463	17.555
96	0.169	0.259	0.218	64.410	43.162	21.640	43.071	21.385
99	0.168	0.258	0.215	66.137	46.892	28.288	47.106	18.926
102	0.162	0.256	0.214	76.638	54.292	30.501	53.810	23.072
105	0.158	0.254	0.213	83.771	61.609	32.714	59.365	25.602
108	0.156	0.253	0.212	87.377	65.238	34.926	62.514	26.332
111	0.153	0.252	0.210	92.836	68.846	39.346	67.009	26.792
114	0.152	0.250	0.209	94.669	76.000	41.554	70.741	26.945
117	0.150	0.249	0.207	98.355	79.547	45.968	74.623	26.538

120	0.149	0.247	0.204	100.208	86.578	52.580	79.789	24.529
123	0.145	0.246	0.202	107.685	90.064	56.983	84.911	25.741
126	0.141	0.245	0.203	115.269	93.529	54.782	87.860	30.639
129	0.139	0.244	0.202	119.100	96.973	56.983	91.019	31.484
132	0.137	0.242	0.193	122.958	103.801	76.742	101.167	23.220
135	0.136	0.240	0.187	124.897	110.547	89.867	108.437	17.610
138	0.132	0.239	0.187	132.719	113.889	89.867	112.158	21.478
141	0.130	0.239	0.186	136.670	113.889	92.051	114.203	22.311
144	0.129	0.238	0.186	138.655	117.211	92.051	115.972	23.327
147	0.128	0.235	0.193	140.647	127.054	76.742	114.815	33.665
150	0.125	0.232	0.192	146.663	136.714	78.933	120.770	36.572
153	0.122	0.232	0.192	152.738	136.714	78.933	122.795	38.821
156	0.119	0.230	0.179	158.872	143.051	107.306	136.410	26.417
159	0.118	0.229	0.176	160.930	146.189	113.828	140.316	24.094
162	0.116	0.226	0.172	165.067	155.481	122.508	147.685	22.324
165	0.115	0.224	0.164	167.145	161.573	139.818	156.179	14.440
168	0.115	0.220	0.160	167.145	173.513	148.447	163.035	13.029
171	0.112	0.217	0.148	173.419	182.254	174.230	176.634	4.883
174	0.110	0.215	0.154	177.634	187.978	161.358	175.657	13.420
177	0.108	0.214	0.144	181.876	190.810	182.791	185.159	4.915
180	0.106	0.213	0.145	186.145	193.621	180.652	186.806	6.510
183	0.104	0.210	0.136	190.440	201.933	199.859	197.411	6.125
186	0.102	0.208	0.124	194.762	207.372	225.332	209.155	15.363
189	0.097	0.207	0.124	205.682	210.060	225.332	213.691	10.316
192	0.092	0.206	0.126	216.768	212.729	221.097	216.865	4.185
195	0.090	0.205	0.125	221.248	215.377	223.215	219.947	4.078
198	0.089	0.203	0.124	223.498	220.611	225.332	223.147	2.380
201	0.087	0.201	0.124	228.019	225.764	225.332	226.372	1.443
204	0.087	0.199	0.123	228.019	230.835	227.448	228.767	1.814
207	0.085	0.197	0.123	232.566	235.825	227.448	231.946	4.223
210	0.085	0.196	0.122	232.566	238.289	229.562	233.472	4.433
213	0.084	0.197	0.119	234.849	235.825	235.900	235.525	0.586
216	0.084	0.196	0.119	234.849	238.289	235.900	236.346	1.763

Table II.12. Data 20/1 D/L, 0.1 Hz;

Time (h)	Optical reading (mV)			TSS (mg/L)			Average (mg/L)	SD
	1	2	3	1	2	3		
3	0.203	0.268	0.224	9.635	8.669	8.315	8.873	0.683
6	0.204	0.269	0.225	8.140	4.734	6.090	6.321	1.714
9	0.205	0.268	0.224	6.651	8.669	8.315	7.878	1.077
12	0.205	0.268	0.223	6.651	8.669	10.538	8.620	1.944
15	0.206	0.268	0.224	5.169	8.669	8.315	7.384	1.926
18	0.206	0.269	0.223	5.169	4.734	10.538	6.814	3.233
21	0.206	0.267	0.225	5.169	12.583	6.090	7.948	4.041
24	0.205	0.266	0.223	6.651	16.477	10.538	11.222	4.948
27	0.205	0.265	0.224	6.651	20.350	8.315	11.772	7.475
30	0.203	0.267	0.226	9.635	12.583	3.865	8.694	4.435
33	0.203	0.267	0.225	9.635	12.583	6.090	9.436	3.251
36	0.201	0.269	0.226	12.645	4.734	3.865	7.081	4.838
39	0.199	0.268	0.225	15.682	8.669	6.090	10.147	4.964
42	0.195	0.268	0.223	21.834	8.669	10.538	13.681	7.123
45	0.193	0.269	0.222	24.950	4.734	12.761	14.148	10.179
48	0.190	0.269	0.220	29.674	4.734	17.202	17.204	12.470
51	0.188	0.267	0.218	32.857	12.583	21.640	22.360	10.156
54	0.185	0.266	0.216	37.680	16.477	26.073	26.743	10.617
57	0.182	0.267	0.215	42.562	12.583	28.288	27.811	14.995
60	0.179	0.268	0.213	47.505	8.669	32.714	29.629	19.601
63	0.176	0.268	0.212	52.507	8.669	34.926	32.034	22.062
66	0.173	0.269	0.210	57.569	4.734	39.346	33.883	26.837
69	0.171	0.267	0.208	60.976	12.583	43.762	39.107	24.530
72	0.168	0.265	0.205	66.137	20.350	50.377	45.622	23.261
75	0.165	0.263	0.202	71.358	28.036	56.983	52.126	22.066
78	0.163	0.261	0.199	74.871	35.640	63.579	58.030	20.196
81	0.160	0.260	0.196	80.191	39.411	70.166	63.256	21.250
84	0.158	0.258	0.195	83.771	46.892	72.359	67.674	18.881
87	0.157	0.256	0.193	85.571	54.292	76.742	72.202	16.126
90	0.155	0.253	0.189	89.190	65.238	85.496	79.975	12.896
93	0.154	0.251	0.186	91.010	72.433	92.051	85.165	11.038
96	0.151	0.249	0.185	96.509	79.547	94.233	90.096	9.207
99	0.148	0.248	0.181	102.067	83.073	102.953	96.031	11.231
102	0.145	0.246	0.178	107.685	90.064	109.481	102.410	10.730
105	0.143	0.244	0.176	111.464	96.973	113.828	107.422	9.125
108	0.142	0.242	0.175	113.363	103.801	116.000	111.054	6.419
111	0.140	0.241	0.173	117.181	107.184	120.340	114.902	6.868
114	0.137	0.240	0.170	122.958	110.547	126.842	120.116	8.511
117	0.134	0.239	0.168	128.795	113.889	131.172	124.619	9.368

120	0.132	0.237	0.168	132.719	120.513	131.172	128.135	6.646
123	0.131	0.235	0.167	134.691	127.054	133.335	131.693	4.074
126	0.130	0.234	0.165	136.670	130.295	137.658	134.874	3.997
129	0.127	0.233	0.162	142.646	133.514	144.135	140.098	5.750
132	0.125	0.232	0.161	146.663	136.714	146.291	143.223	5.640
135	0.124	0.230	0.160	148.681	143.051	148.447	146.726	3.185
138	0.122	0.229	0.158	152.738	146.189	152.755	150.561	3.786
141	0.120	0.227	0.156	156.821	152.404	157.059	155.428	2.621
144	0.121	0.226	0.156	154.776	155.481	157.059	155.772	1.169
147	0.120	0.225	0.154	156.821	158.538	161.358	158.905	2.291
150	0.120	0.225	0.155	156.821	158.538	159.209	158.189	1.232
153	0.121	0.225	0.155	154.776	158.538	159.209		2.389

Table II.13. Data 25/1 D/L, 0.1 Hz;

Time (h)	Optical reading (mV)			TSS (mg/L)			Average (mg/L)	SD
	1	2	3	1	2	3		
3	0.249		0.205	9.472		8.515	8.994	0.677
6	0.248		0.204	12.563		10.297	11.430	1.602
9	0.248		0.204	12.563		10.297	11.430	1.602
12	0.249		0.204	9.472		10.297	9.885	0.583
15	0.250		0.203	6.370		12.087	9.229	4.043
18	0.249		0.201	9.472		15.687	12.580	4.395
21	0.250		0.202	6.370		13.884	10.127	5.313
24	0.250		0.200	6.370		17.498	11.934	7.869
27	0.250		0.201	6.370		15.687	11.029	6.588
30	0.248		0.200	12.563		17.498	15.031	3.489
33	0.247		0.200	15.644		17.498	16.571	1.311
36	0.246		0.200	18.713		17.498	18.105	0.859
39	0.245		0.199	21.771		19.316	20.543	1.736
42	0.245		0.198	21.771		21.141	21.456	0.446
45	0.244		0.197	24.818		22.972	23.895	1.305
48	0.243		0.196	27.854		24.811	26.333	2.151
51	0.242		0.196	30.879		24.811	27.845	4.290
54	0.240		0.194	36.895		28.510	32.703	5.929
57	0.240		0.192	36.895		32.237	34.566	3.294
60	0.238		0.191	42.868		34.111	38.490	6.192
63	0.236		0.191	48.796		34.111	41.454	10.384

66	0.235	0.190	51.744	35.992	43.868	11.138
69	0.235	0.190	51.744	35.992	43.868	11.138
72	0.234	0.189	54.680	37.880	46.280	11.879
75	0.233	0.188	57.606	39.776	48.691	12.608
78	0.233	0.187	57.606	41.678	49.642	11.263
81	0.232	0.186	60.520	43.587	52.054	11.973
84	0.232	0.184	60.520	47.427	53.973	9.258
87	0.230	0.183	66.316	49.357	57.836	11.992
90	0.239	0.182	39.887	51.295	45.591	8.066
93	0.238	0.180	42.868	55.190	49.029	8.713
96	0.237	0.182	45.838	51.295	48.566	3.859
99	0.236	0.180	48.796	55.190	51.993	4.521
102	0.236	0.179	48.796	57.149	52.973	5.906
105	0.235	0.177	51.744	61.087	56.415	6.607
108	0.235	0.175	51.744	65.054	58.399	9.412
111	0.234	0.174	54.680	67.047	60.864	8.745
114	0.233	0.173	57.606	69.048	63.327	8.091
117	0.232	0.173	60.520	69.048	64.784	6.030
120	0.231	0.172	63.423	71.056	67.240	5.397
123	0.231	0.172	63.423	71.056	67.240	5.397
126	0.230	0.171	66.316	73.071	69.693	4.777
129	0.230	0.170	66.316	75.093	70.704	6.206
132	0.229	0.170	69.197	75.093	72.145	4.169
135	0.226	0.168	77.774	79.158	78.466	0.978
138	0.224	0.167	83.437	81.201	82.319	1.582
141	0.221	0.166	91.849	83.251	87.550	6.080
144	0.221	0.165	91.849	85.308	88.579	4.625
147	0.220	0.165	94.631	85.308	89.969	6.592
150	0.220	0.165	94.631	85.308	89.969	6.592

Table II.14. Data 30/1 D/L , 0.1 Hz;

Time (h)	Optical reading (mV)			TSS (mg/L)			Average (mg/L)	SD
	1	2	3	1	2	3		
3	0.244	0.235	0.262	8.512	9.788	9.578	9.683	0.148
6	0.245	0.234	0.265	5.912	11.128	3.709	7.419	5.245
9	0.242	0.236	0.264	13.693	8.454	5.667	7.060	1.971
12	0.243	0.235	0.263	11.105	9.788	7.623	8.706	1.531
15	0.244	0.236	0.265	8.512	8.454	3.709	6.082	3.355
18	0.243	0.235	0.264	11.105	9.788	5.667	7.727	2.914

21	0.242	0.236	0.265	13.693	8.454	3.709	6.082	3.355
24	0.245	0.237	0.263	5.912	7.126	7.623	7.374	0.352
27	0.243	0.238	0.262	11.105	5.803	9.578	7.691	2.670
30	0.245	0.240	0.260	5.912	3.174	13.486	8.330	7.292
33	0.240	0.238	0.259	18.850	5.803	15.439	10.621	6.814
36	0.245	0.238	0.258	5.912	5.803	17.390	11.596	8.193
39	0.245	0.239	0.259	5.912	4.485	15.439	9.962	7.745
42	0.244	0.237	0.259	8.512	7.126	15.439	11.282	5.878
45	0.245	0.236	0.257	5.912	8.454	19.341	13.897	7.698
48	0.245	0.235	0.258	5.912	9.788	17.390	13.589	5.375
51	0.246	0.233	0.257	3.307	12.473	19.341	15.907	4.856
54	0.245	0.232	0.257	5.912	13.823	19.341	16.582	3.902
57	0.244	0.232	0.256	8.512	13.823	21.290	17.557	5.280
60	0.244	0.231	0.256	8.512	15.179	21.290	18.235	4.321
63	0.243	0.231	0.254	11.105	15.179	25.187	20.183	7.077
66	0.243	0.232	0.255	11.105	13.823	23.239	18.531	6.658
69	0.242	0.232	0.254	13.693	13.823	25.187	19.505	8.035
72	0.243	0.233	0.255	11.105	12.473	23.239	17.856	7.613
75	0.242	0.231	0.254	13.693	15.179	25.187	20.183	7.077
78	0.242	0.230	0.253	13.693	16.541	27.134	21.837	7.490
81	0.241	0.229	0.253	16.274	17.908	27.134	22.521	6.524
84	0.242	0.225	0.252	13.693	23.432	29.080	26.256	3.994
87	0.241	0.223	0.252	16.274	26.227	29.080	27.653	2.017
90	0.241	0.221	0.252	16.274	29.044	29.080	29.062	0.025
93	0.240	0.220	0.251	18.850	30.461	31.025	30.743	0.399
96	0.240	0.217	0.251	18.850	34.744	31.025	32.885	2.630
99	0.240	0.215	0.250	18.850	37.628	32.969	35.298	3.294
102	0.239	0.213	0.250	21.420	40.533	32.969	36.751	5.349
105	0.237	0.212	0.250	26.543	41.994	32.969	37.482	6.382
108	0.236	0.211	0.249	29.095	43.461	34.912	39.186	6.045
111	0.235	0.210	0.249	31.642	44.933	34.912	39.922	7.086
114	0.234	0.211	0.248	34.183	43.461	36.854	40.157	4.672
117	0.234	0.211	0.248	34.183	43.461	36.854	40.157	4.672
120	0.232	0.210	0.247	39.246	44.933	38.795	41.864	4.340
123	0.231	0.210	0.247	41.770	44.933	38.795	41.864	4.340
126	0.231	0.209	0.246	41.770	46.411	40.736	43.573	4.013
129	0.230	0.209	0.246	44.287	46.411	40.736	43.573	4.013
132	0.230	0.208	0.246	44.287	47.894	40.736	44.315	5.062
135	0.231	0.209	0.245	41.770	46.411	42.675	44.543	2.642
138	0.230	0.208	0.245	44.287	47.894	42.675	45.284	3.690
141	0.230	0.208	0.245	44.287	47.894	42.675	45.284	3.690

Table II.15. Growth rates at 1/1 -10/1 D/L and frequencies studied.

1|1	0.1	0.2	0.4	0.8	1.6	3.2	6.4	12.8	25.6
24	0.0053	0.0129	0.0166	0.0165	0.0196	0.0203	0.0225	0.0233	0.0235
48	0.0572	0.0648	0.0685	0.0684	0.0715	0.0722	0.0744	0.0752	0.0754
72	0.0508	0.0584	0.0621	0.0620	0.0651	0.0658	0.0680	0.0688	0.0690
96	0.0398	0.0474	0.0511	0.0510	0.0541	0.0548	0.0570	0.0578	0.0580
120	0.0285	0.0361	0.0398	0.0397	0.0428	0.0435	0.0457	0.0465	0.0467
144	0.0245	0.0321	0.0385	0.0357	0.0388	0.0395	0.0417	0.0425	0.0427
168	0.0170	0.0246	0.0283	0.0282	0.0313	0.0320	0.0342	0.0350	0.0352
192	0.0126	0.0202	0.0239	0.0238	0.0269	0.0276	0.0298	0.0306	0.0308
216	0.0061	0.0137	0.0174	0.0173	0.0204	0.0211	0.0233	0.0241	0.0243
240	0.0056	0.0132	0.0169	0.0168	0.0199	0.0206	0.0228		

2|1	0.1	0.2	0.4	0.8	1.6	3.2	6.4	12.8	25.6
24	0.0072	0.0094	0.0119	0.0151	0.0235	0.0255	0.0272	0.0281	0.0252
48	0.0235	0.0257	0.0282	0.0314	0.0398	0.0418	0.0435	0.0444	0.0415
72	0.0763	0.0785	0.0810	0.0842	0.0926	0.0946	0.0963	0.0972	0.0943
96	0.0759	0.0781	0.0806	0.0838	0.0922	0.0942	0.0959	0.0968	0.0939
120	0.0498	0.0520	0.0545	0.0577	0.0661	0.0681	0.0698	0.0707	0.0678
144	0.0376	0.0398	0.0423	0.0455	0.0539	0.0559	0.0576	0.0585	0.0556
168	0.0229	0.0251	0.0276	0.0308	0.0392	0.0412	0.0429	0.0438	0.0409
192	0.0170	0.0192	0.0217	0.0249	0.0333	0.0353	0.0370	0.0379	0.0350
216	0.0082	0.0104	0.0129	0.0161	0.0245	0.0265	0.0282	0.0291	0.0262
240	0.0076	0.0098	0.0123	0.0155	0.0239	0.0259	0.0276	0.0285	0.0256

3|1	0.1	0.2	0.4	0.8	1.6	3.2	6.4	12.8	25.6
24	0.0081	0.0085	0.0184	0.0339	0.0391	0.0418	0.0429	0.0471	0.0445
48	0.0152	0.0156	0.0255	0.0410	0.0462	0.0489	0.0500	0.0542	0.0516
72	0.0907	0.0911	0.1010	0.1165	0.1217	0.1244	0.1255	0.1297	0.1271

96	0.0875	0.0879	0.0978	0.1133	0.1185	0.1212	0.1223	0.1265	0.1239
120	0.0725	0.0729	0.0828	0.0983	0.1035	0.1062	0.1073	0.1115	0.1089
144	0.0423	0.0427	0.0526	0.0681	0.0733	0.0760	0.0771	0.0813	0.0787
168	0.0258	0.0262	0.0361	0.0516	0.0568	0.0595	0.0606	0.0648	0.0622
192	0.0191	0.0195	0.0294	0.0449	0.0501	0.0528	0.0539	0.0581	0.0555
216	0.0105	0.0109	0.0208	0.0363	0.0415	0.0442	0.0453	0.0495	0.0469
240	0.0101	0.0105	0.0204	0.0359	0.0411	0.0438	0.0449	0.0491	0.0465

4/1	0.1	0.2	0.4	0.8	1.6	3.2	6.4	12.8	25.6
24	0.009957	0.011957	0.014557	0.018057	0.020957438	0.024557	0.026257	0.021657	0.019557
48	0.01864	0.02064	0.02324	0.02674	0.02964	0.03324	0.03494	0.03034	0.02824
72	0.07256	0.07456	0.07716	0.08066	0.08356	0.08716	0.08886	0.08426	0.08216
96	0.1305	0.1325	0.1351	0.1386	0.1415	0.1451	0.1468	0.1422	0.1401
120	0.128135	0.130135	0.132735	0.136235	0.139135	0.142735	0.144435	0.139835	0.137735
144	0.0833	0.0853	0.0879	0.0914	0.0943	0.0979	0.0996	0.095	0.0929
168	0.05216	0.05416	0.05676	0.06026	0.063159922	0.06676	0.06846	0.06386	0.06176
192	0.023535	0.025535	0.028135	0.031635	0.034534728	0.038135	0.039835	0.035235	0.033135
216	0.012905	0.014905	0.017505	0.021005	0.023905449	0.027505	0.029205	0.024605	0.022505
240	0.01245	0.01445	0.01705	0.02055	0.02345	0.02705	0.02875	0.02415	0.02205

5/1	0.1	0.2	0.4	0.8	1.6	3.2	6.4	12.8	25.6
24	0.0090	0.0109	0.0124	0.0160	0.0203	0.0246	0.0238	0.0221	0.0197
48	0.0256	0.0275	0.0290	0.0326	0.0369	0.0412	0.0404	0.0387	0.0363
72	0.0603	0.0622	0.0637	0.0673	0.0716	0.0759	0.0751	0.0734	0.0710
96	0.1242	0.1261	0.1276	0.1312	0.1355	0.1398	0.1390	0.1373	0.1349
120	0.1271	0.1290	0.1305	0.1341	0.1384	0.1427	0.1419	0.1402	0.1378
144	0.0902	0.0921	0.0936	0.0972	0.1015	0.1058	0.1050	0.1033	0.1009
168	0.0582	0.0601	0.0616	0.0652	0.0695	0.0738	0.0730	0.0713	0.0689
192	0.0321	0.0340	0.0355	0.0391	0.0434	0.0477	0.0469	0.0452	0.0428

216	0.0236	0.0255	0.0270	0.0306	0.0349	0.0392	0.0384	0.0367	0.0343
240	0.0156	0.0175	0.0190	0.0226	0.0269	0.0312	0.0304	0.0287	0.0263

6/1	0.1	0.2	0.4	0.8	1.6	3.2	6.4	12.8	25.6
24	0.0090	0.0105	0.0118	0.0130	0.0182	0.0195	0.0204	0.0179	0.0134
48	0.0256	0.0271	0.0284	0.0296	0.0348	0.0361	0.0370	0.0345	0.0300
72	0.0626	0.0641	0.0654	0.0666	0.0718	0.0731	0.0740	0.0715	0.0670
96	0.1025	0.1040	0.1053	0.1065	0.1117	0.1130	0.1139	0.1114	0.1069
120	0.1270	0.1285	0.1298	0.1310	0.1362	0.1375	0.1384	0.1359	0.1314
144	0.1092	0.1107	0.1120	0.1132	0.1184	0.1197	0.1206	0.1181	0.1136
168	0.0682	0.0697	0.0710	0.0722	0.0774	0.0787	0.0796	0.0771	0.0726
192	0.0391	0.0406	0.0419	0.0431	0.0483	0.0496	0.0505	0.0480	0.0435
216	0.0127	0.0142	0.0155	0.0167	0.0219	0.0232	0.0241	0.0216	0.0171
240	0.0116	0.0131	0.0144	0.0156	0.0208	0.0221	0.0230	0.0205	0.0160

7/1	0.1	0.2	0.4	0.8	1.6	3.2	6.4	12.8	25.6
24	0.0160	0.0179	0.0191	0.0226	0.0259	0.0275	0.0224	0.0204	0.0164
48	0.0256	0.0275	0.0287	0.0322	0.0355	0.0371	0.0320	0.0300	0.0260
72	0.0453	0.0472	0.0484	0.0519	0.0552	0.0568	0.0517	0.0497	0.0457
96	0.0965	0.0984	0.0996	0.1031	0.1064	0.1080	0.1029	0.1009	0.0969
120	0.1250	0.1269	0.1281	0.1316	0.1349	0.1365	0.1314	0.1294	0.1254
144	0.1172	0.1191	0.1203	0.1238	0.1271	0.1287	0.1236	0.1216	0.1176
168	0.0782	0.0801	0.0813	0.0848	0.0881	0.0897	0.0846	0.0826	0.0786
192	0.0501	0.0520	0.0532	0.0567	0.0600	0.0616	0.0565	0.0545	0.0505
216	0.0327	0.0346	0.0358	0.0393	0.0426	0.0442	0.0391	0.0371	0.0331
240	0.0212	0.0231	0.0243	0.0278	0.0311	0.0327	0.0276	0.0256	0.0216
264	0.0219	0.0238	0.0250	0.0285	0.0318	0.0334	0.0283	0.0263	0.0223

8/1	0.1	0.2	0.4	0.8	1.6	3.2	6.4	12.8	25.6
24	0.0200	0.0260	0.0265	0.0288	0.0296	0.0320	0.0356	0.0269	0.0177
48	0.0356	0.0416	0.0421	0.0444	0.0452	0.0476	0.0512	0.0425	0.0333
72	0.0569	0.0629	0.0634	0.0657	0.0665	0.0689	0.0725	0.0638	0.0546
96	0.0915	0.0975	0.0980	0.1003	0.1011	0.1035	0.1071	0.0984	0.0892
120	0.1080	0.1140	0.1145	0.1168	0.1176	0.1200	0.1236	0.1149	0.1057
144	0.1203	0.1263	0.1268	0.1291	0.1299	0.1323	0.1359	0.1272	0.1180
168	0.0919	0.0979	0.0984	0.1007	0.1015	0.1039	0.1075	0.0988	0.0896
192	0.0591	0.0651	0.0656	0.0679	0.0687	0.0711	0.0747	0.0660	0.0568
216	0.0407	0.0467	0.0472	0.0495	0.0503	0.0527	0.0563	0.0476	0.0384
240	0.0301	0.0361	0.0366	0.0389	0.0397	0.0421	0.0457	0.0370	0.0278
264	0.0252	0.0312	0.0317	0.0340	0.0348	0.0372	0.0408	0.0321	0.0229

9/1	0.1	0.2	0.4	0.8	1.6	3.2	6.4	12.8	25.6
24	0.0189	0.0246	0.0270	0.0276	0.0297	0.0261	0.0261	0.0219	0.0207
48	0.0256	0.0313	0.0337	0.0343	0.0364	0.0328	0.0328	0.0286	0.0274
72	0.0454	0.0511	0.0535	0.0541	0.0562	0.0526	0.0526	0.0484	0.0472
96	0.0615	0.0672	0.0696	0.0702	0.0723	0.0687	0.0687	0.0645	0.0633
120	0.0903	0.0960	0.0984	0.0990	0.1011	0.0975	0.0975	0.0933	0.0921
144	0.1073	0.1130	0.1154	0.1160	0.1181	0.1145	0.1145	0.1103	0.1091
168	0.1121	0.1178	0.1202	0.1208	0.1229	0.1193	0.1193	0.1151	0.1139
192	0.0691	0.0748	0.0772	0.0778	0.0799	0.0763	0.0763	0.0721	0.0709
216	0.0407	0.0464	0.0488	0.0494	0.0515	0.0479	0.0479	0.0437	0.0425
240	0.0220	0.0277	0.0301	0.0307	0.0328	0.0292	0.0292	0.0250	0.0238
264	0.0202	0.0259	0.0283	0.0289	0.0310	0.0274	0.0274	0.0232	0.0220

10/1	0.1	0.2	0.4	0.8	1.6	3.2	6.4	12.8	25.6
24	0.0202	0.0228	0.0241	0.0299	0.0329	0.0320	0.0352	0.0295	0.0229
48	0.0356	0.0382	0.0395	0.0453	0.0483	0.0474	0.0506	0.0449	0.0383
72	0.0454	0.0480	0.0493	0.0551	0.0581	0.0572	0.0604	0.0547	0.0481
96	0.0515	0.0541	0.0554	0.0612	0.0642	0.0633	0.0665	0.0608	0.0542
120	0.0746	0.0772	0.0785	0.0843	0.0873	0.0864	0.0896	0.0839	0.0773
144	0.0973	0.0999	0.1012	0.1070	0.1100	0.1091	0.1123	0.1066	0.1000
168	0.1041	0.1067	0.1080	0.1138	0.1168	0.1159	0.1191	0.1134	0.1068
192	0.0901	0.0927	0.0940	0.0998	0.1028	0.1019	0.1051	0.0994	0.0928
216	0.0581	0.0607	0.0620	0.0678	0.0708	0.0699	0.0731	0.0674	0.0608
240	0.0241	0.0267	0.0280	0.0338	0.0368	0.0359	0.0391	0.0334	0.0268
264	0.0222	0.0248	0.0261	0.0319	0.0349	0.0340	0.0372	0.0315	0.0249

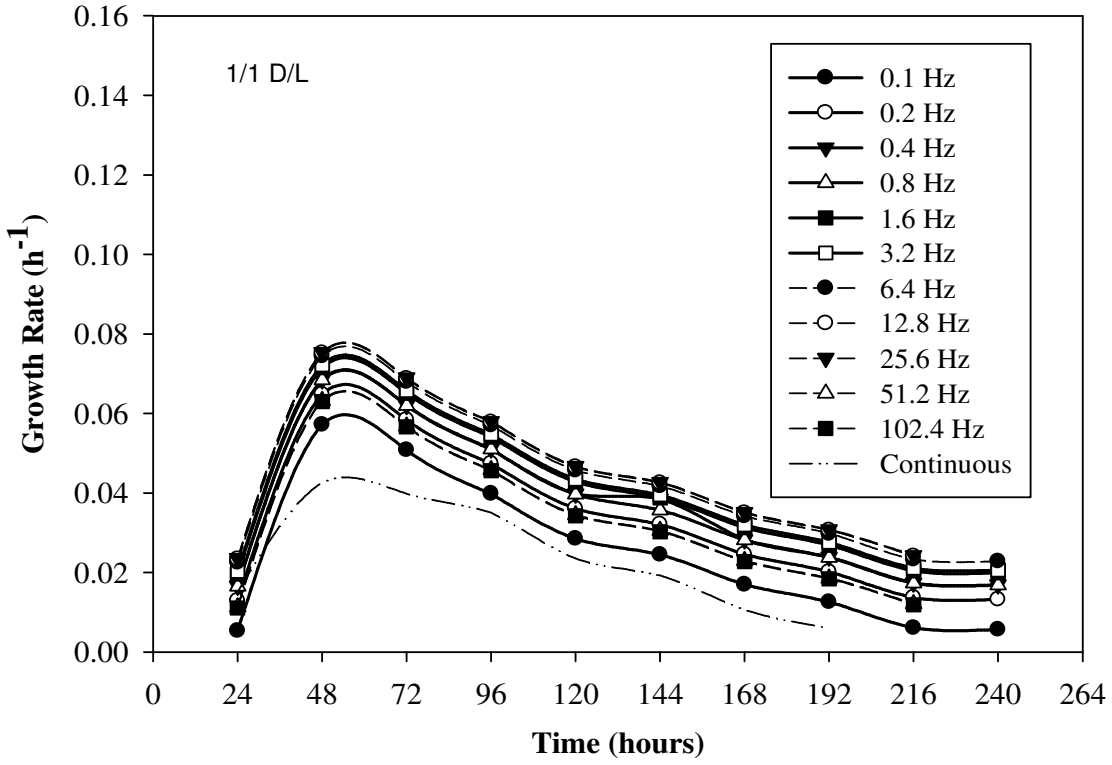
1/1 D/L
0.1 Hz
0.2 Hz
0.4 Hz
0.8 Hz
1.6 Hz
3.2 Hz
6.4 Hz
12.8 Hz
25.6 Hz
51.2 Hz
102.4 Hz
Continuous
Growth Rate (h-1)
Time (hours)
0.00
0.02
0.04
0.06
0.08
0.10
0.12
0.14
0.16
0
24
48
72
96
120
144
168
192
216
240
264

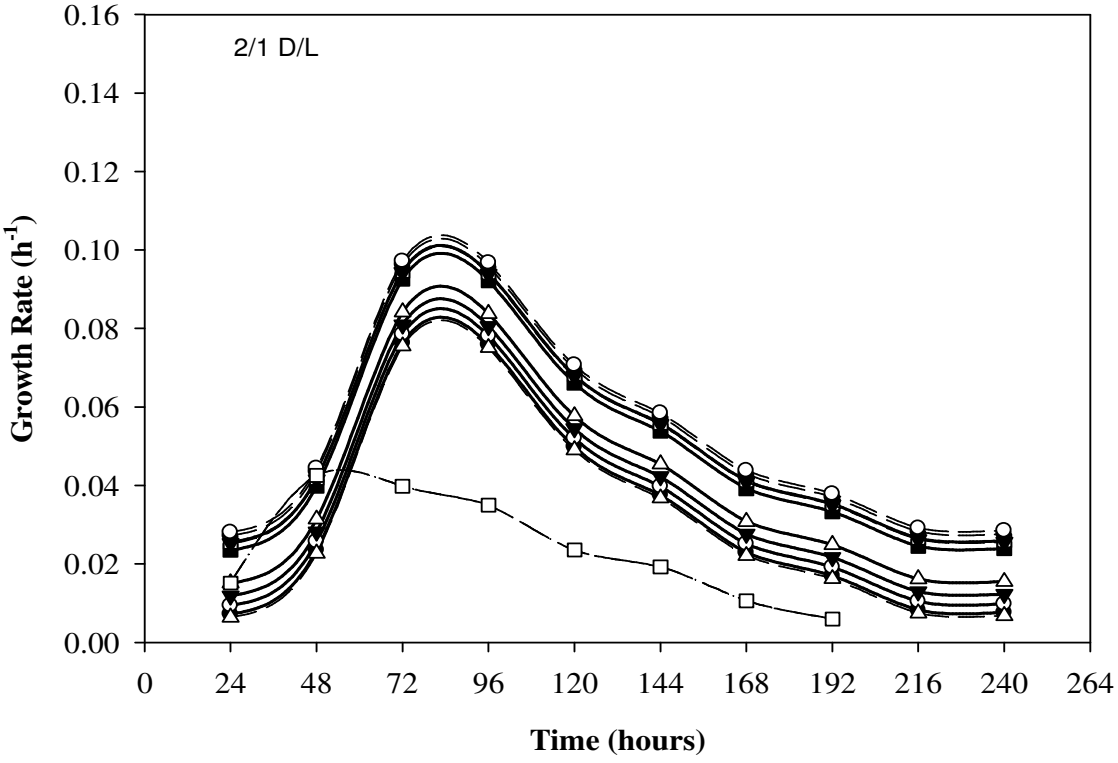
2/1 D/L
Growth Rate (h-1)
Time (hours)
0.00
0.02
0.04
0.06
0.08
0.10
0.12
0.14
0.16
0
24
48
72
96
120
144
168
192
216
240
264

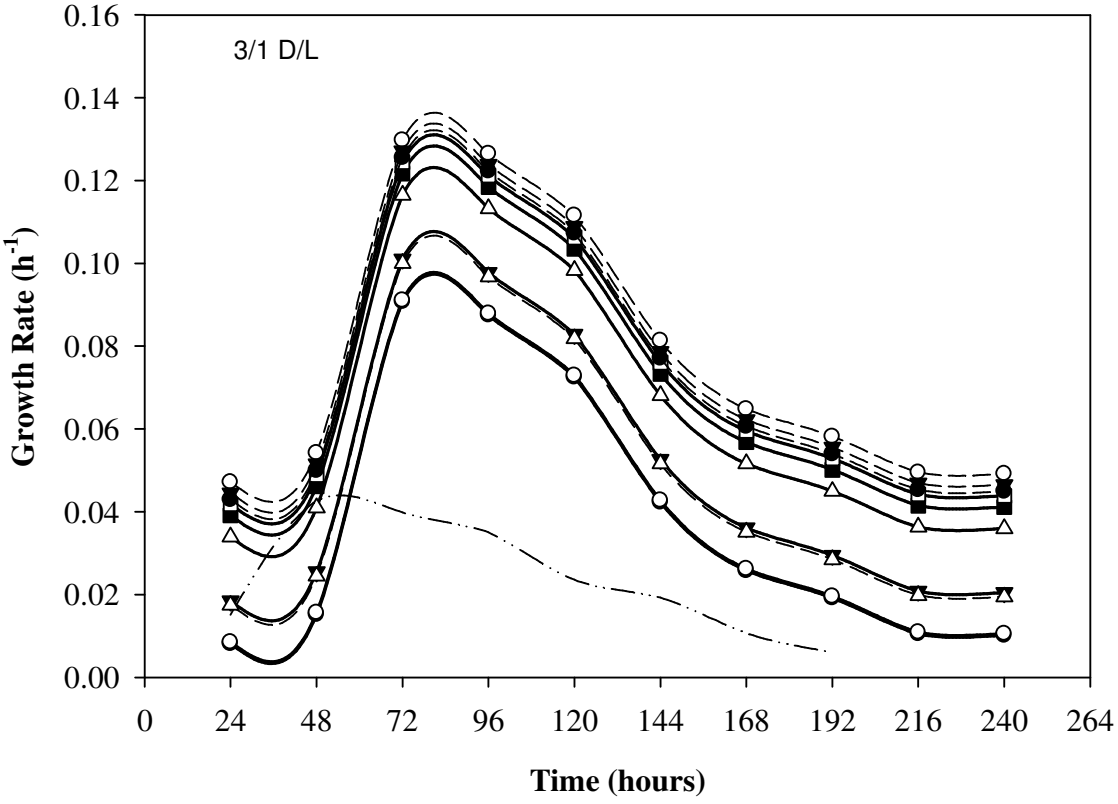
3/1 D/L
Growth Rate (h-1)
0.16
0.14
0.12
0.10
0.08
0.06
0.04
0.02
0.00
0
24
48
72
96
120
144
168
192
216
240
264
Time (hours)

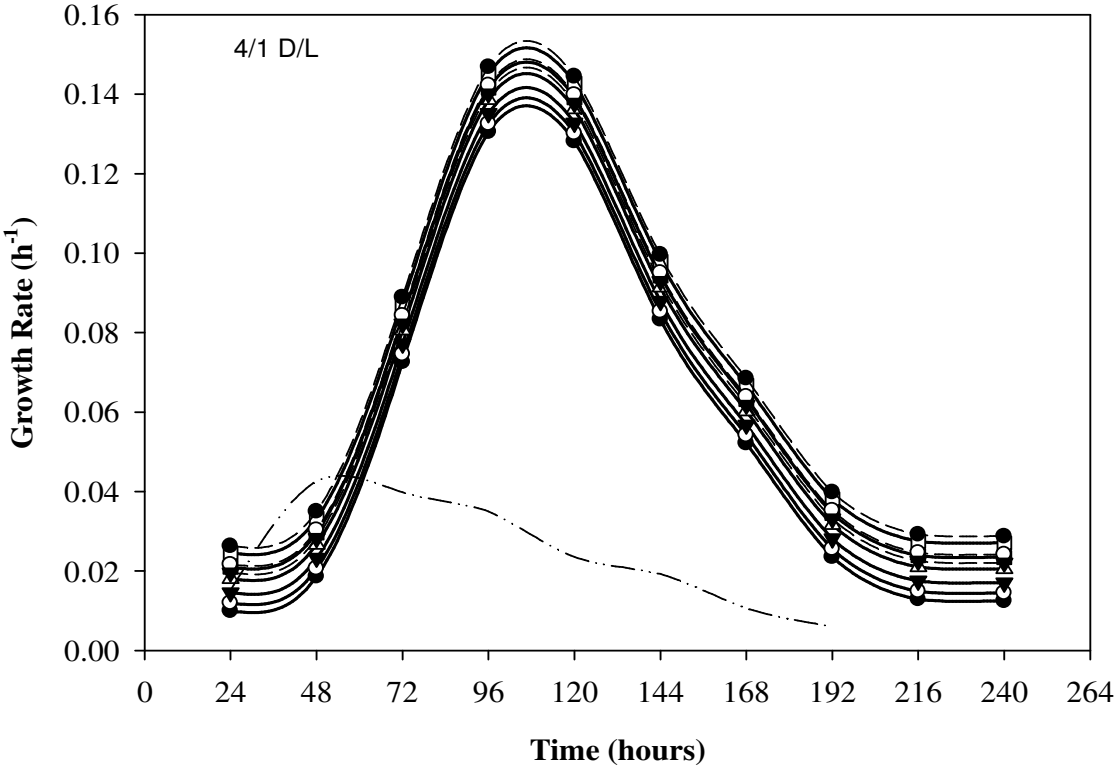
4/1 D/L
Growth Rate (h-1)
0.16
0.14
0.12
0.10
0.08
0.06
0.04
0.02
0.00
0
24
48
72
96
120
144
168
192
216
240
264
Time (hours)

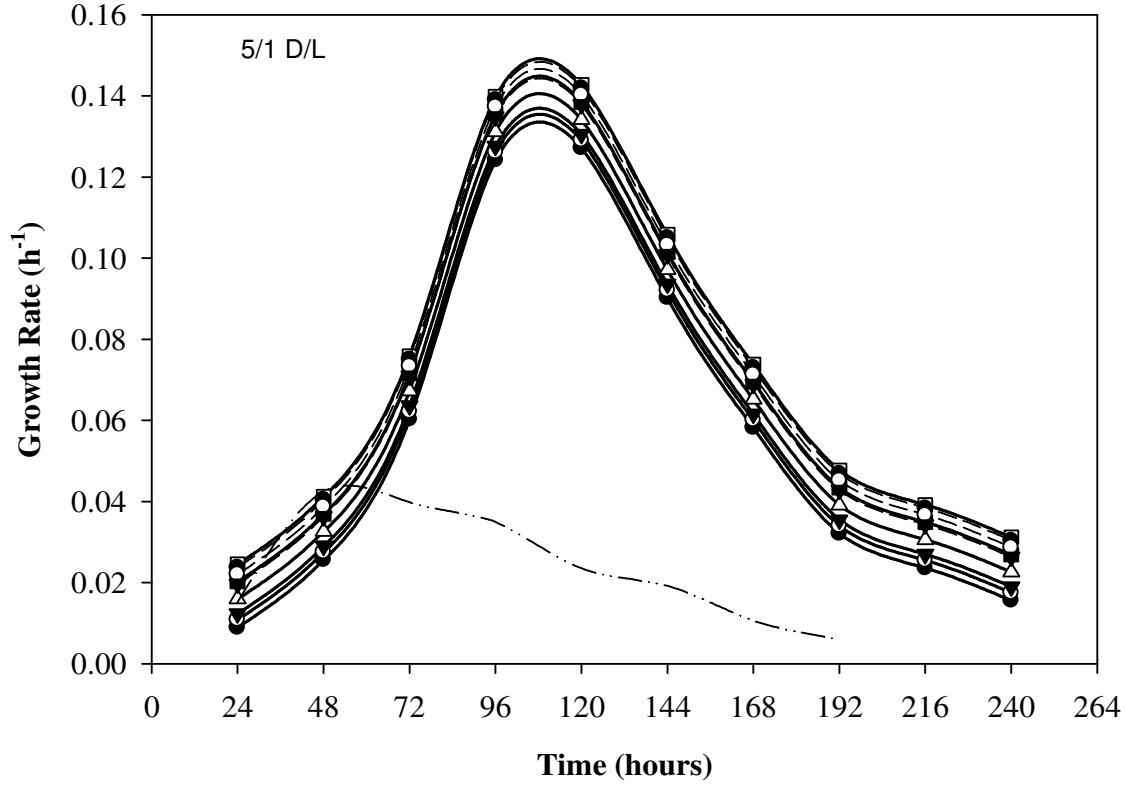
5/1 D/L
Growth Rate (h-1)
0.16
0.14
0.12
0.10
0.08
0.06
0.04
0.02
0.00
0
24
48
72
96
120
144
168
192
216
240
264
Time (hours)

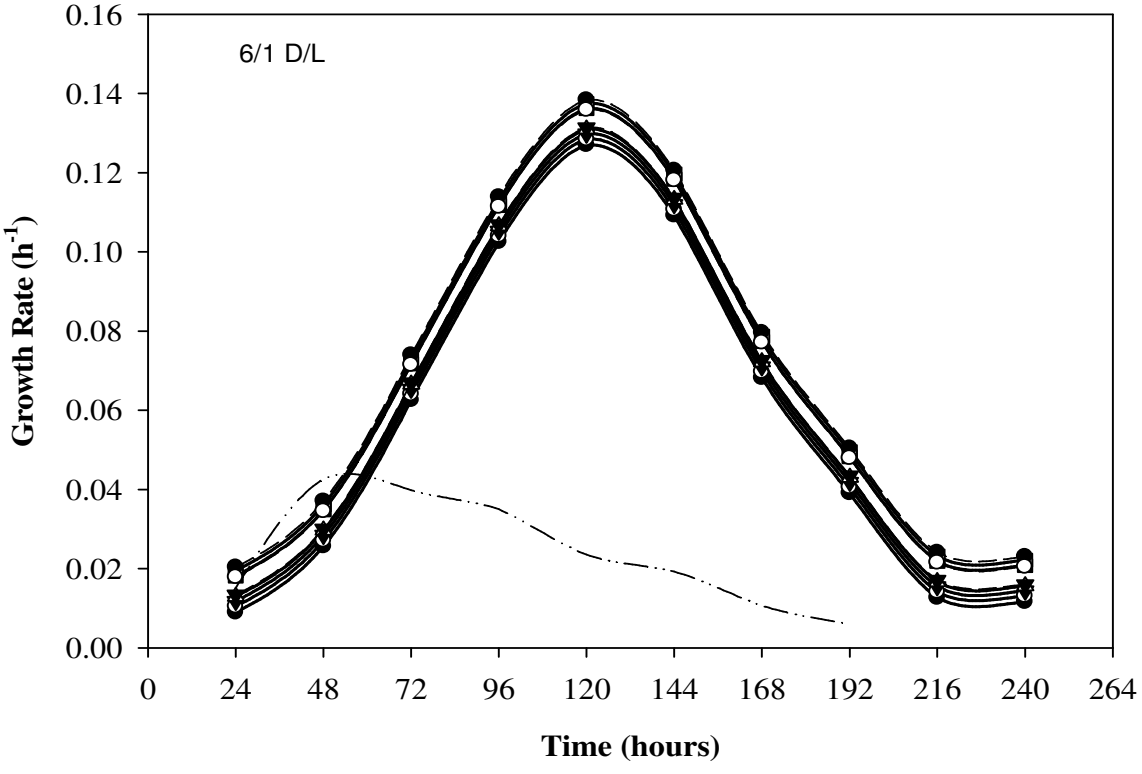
6/1 D/L
Growth Rate (h-1)
0.16
0.14
0.12
0.10
0.08
0.06
0.04
0.02
0.00
0
24
48
72
96
120
144
168
192
216
240
264
Time (hours)

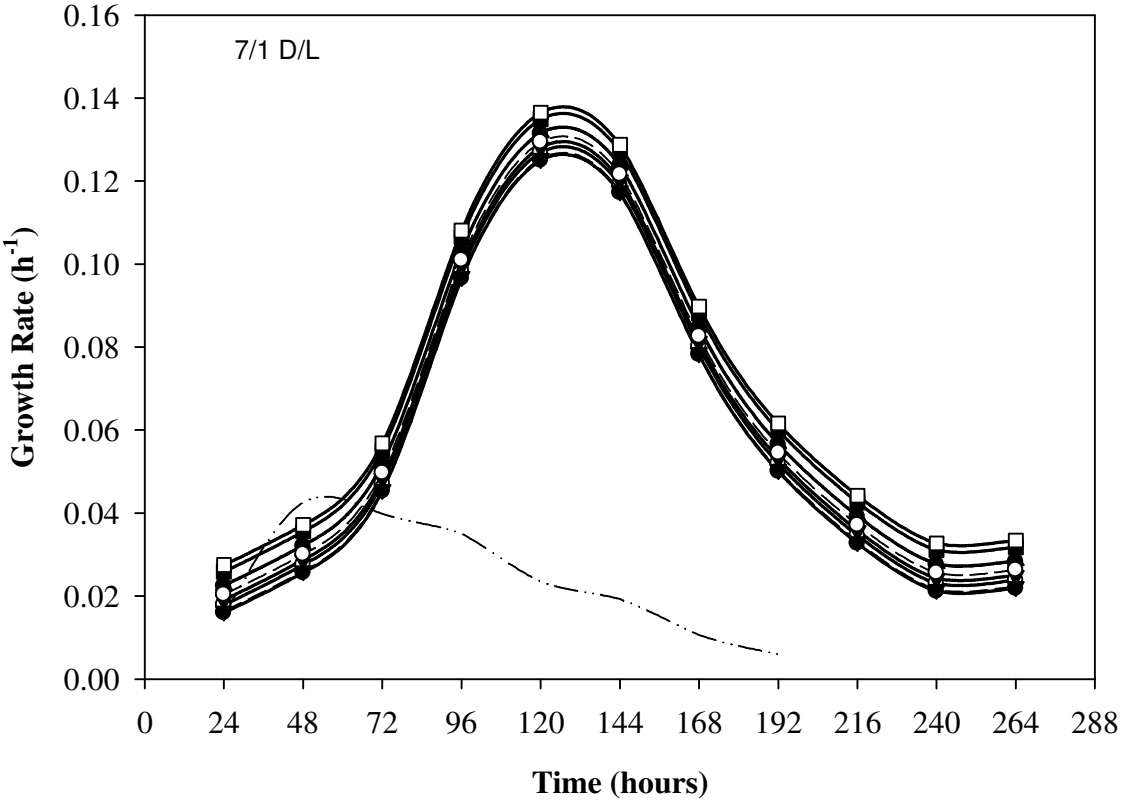
7/1 D/L
Growth Rate (h-1)
0.16
0.14
0.12
0.10
0.08
0.06
0.04
0.02
0.00
0
24
48
72
96
120
144
168
192
216
240
264
288
Time (hours)

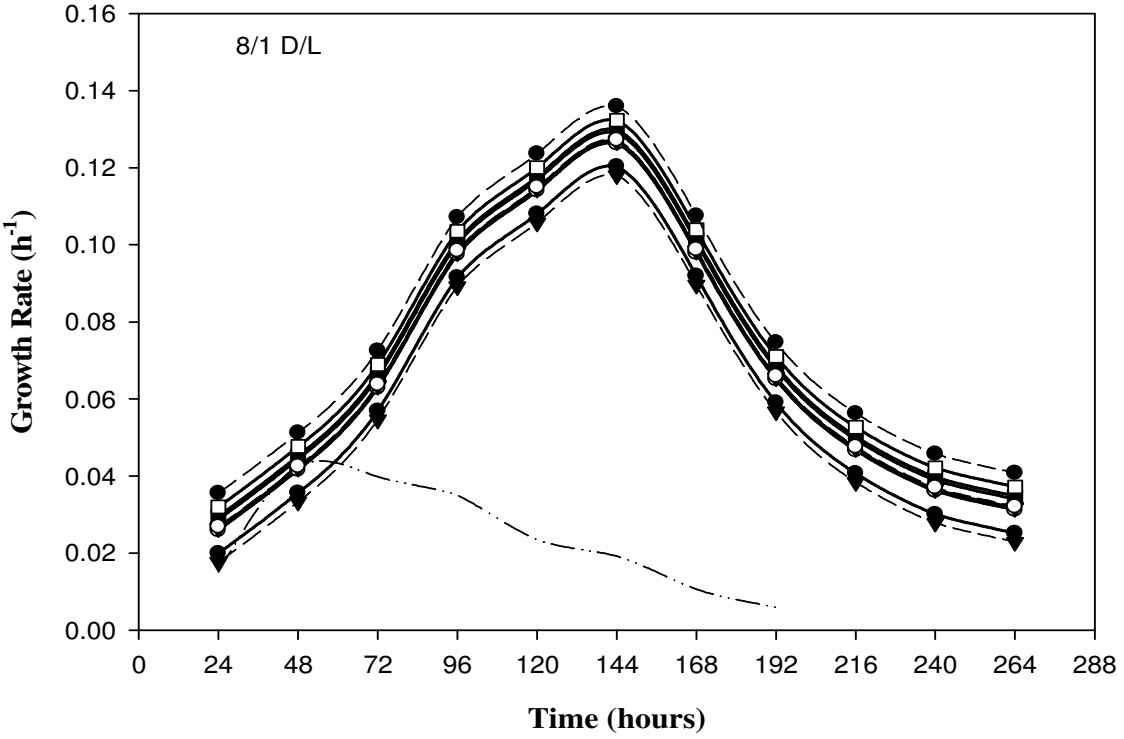
8/1 D/L
Growth Rate (h-1)
0.16
0.14
0.12
0.10
0.08
0.06
0.04
0.02
0.00
0
24
48
72
96
120
144
168
192
216
240
264
288
Time (hours)

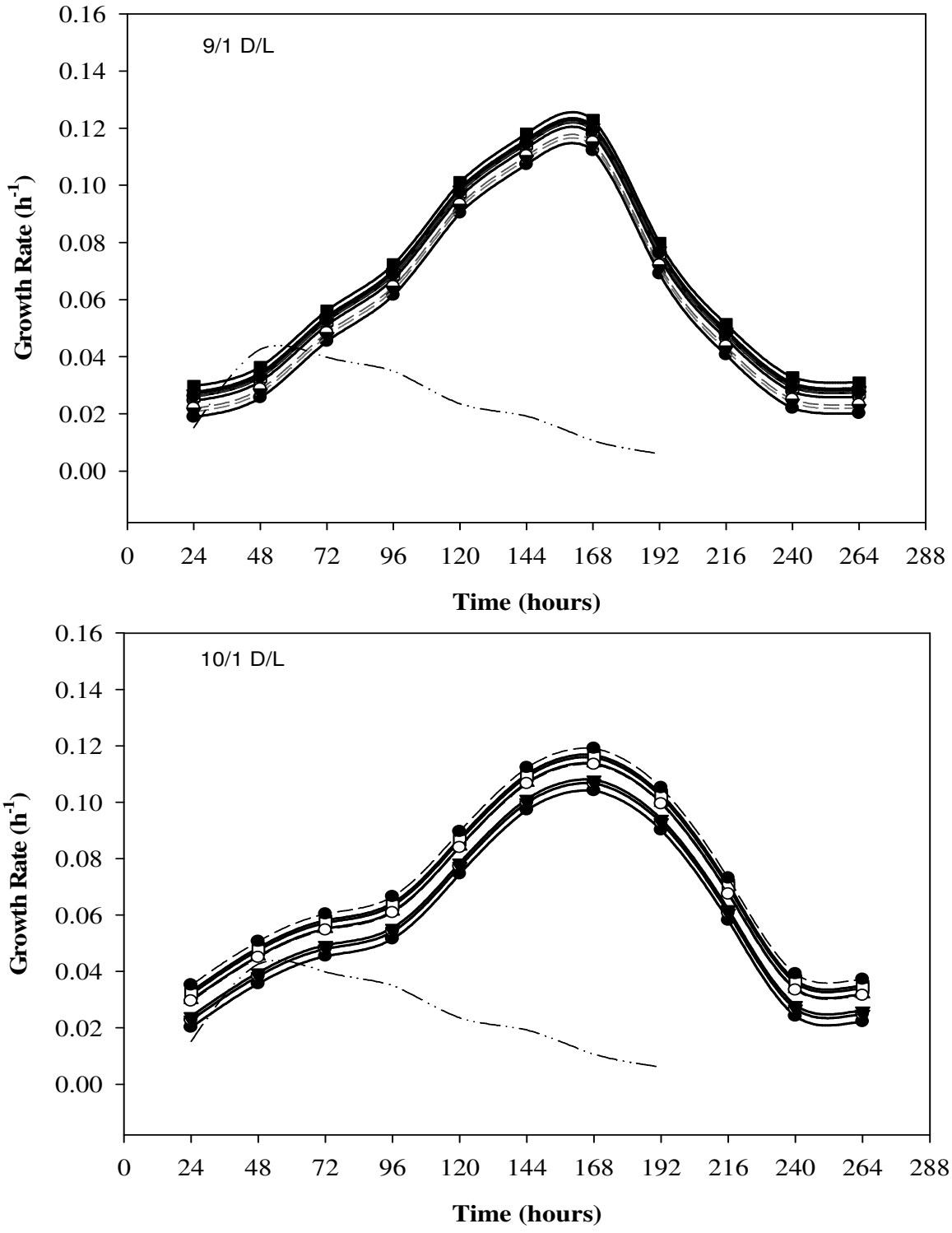

Figure II.1. Growth Rates for each D/L ratios (1/1-10/1) at frequencies used versus time. Legend is universal for all plots.

Table II. 16. Chlorophyll content of the algae at steady-state

Total Chl a+b,mg/g

	0.1	0.2	0.4	0.8	1.6	3.2	6.4	12.8	25.6	51.2	102.4
1	7.859264	8.229844	8.251811	7.861279	8.408279	8.160756	8.241601	8.267162	8.176996	7.706107	7.601325
2	9.628599	9.761334	9.716123	9.657082	10.10981	10.47954	10.51231	10.17204	9.842459	9.479777	
3	11.44903	11.76631	11.97697	12.89117	13.51123	13.51808	13.50773	13.42232	13.11772	12.673	
4	15.33239	15.44816	15.40753	15.37759	15.8112	15.88978	15.92223	15.14178	14.87701		
5	15.24652	15.36092	15.23051	15.20302	15.7578	15.88312	15.72384	15.17452	14.87959		
6	15.20696	15.28439	15.1391	14.92302	15.5438	15.43812	15.4118	14.79552	14.33576		
7	15.23701	15.35087	15.09871	15.16506	15.53289	15.5515	14.94391	14.50262	14.06229		
8	14.9282	15.41087	15.06232	15.02904	15.20047	15.28055	14.70046	14.39053	13.55799		
9	14.29749	14.70956	14.55195	14.38608	14.66367	14.27078	14.06876	13.4527	13.25463		
10	13.66611	13.83153	13.58669	13.56505	13.94522	14.07059	13.80524	12.79173			

Chl a, mg/g

	0.1	0.2	0.4	0.8	1.6	3.2	6.4	12.8	25.6	51.2	102.4
1	4.736188	5.132921	5.42258	5.418356	5.660741	5.717833	5.892678	5.95947	5.969304	5.618415	5.561325
2	6.018445	6.192411	6.392739	6.644006	6.886734	7.466465	7.599537	7.674348	7.444767	7.202085	
3	7.185657	7.544177	8.000373	9.224877	9.634934	9.851788	9.941745	10.27142	10.06682	9.742095	
4	10.33762	10.49462	10.69953	10.9799	11.20351	11.49209	11.62484	11.25947	11.0947		
5	10.15175	10.30738	10.42251	10.70533	11.0501	11.38543	11.32646	11.19221	10.99728		
6	10.0622	10.18086	10.2811	10.37533	10.7861	10.89043	10.96442	10.76321	10.40345		
7	9.89916	10.05425	10.14763	10.42429	10.68212	10.81073	10.40345	10.24878	9.908448		
8	9.530355	10.05425	10.05125	10.22827	10.2897	10.47978	10.1	10.07668	9.344148		
9	8.879641	9.332943	9.520873	9.565312	9.732903	9.450012	9.448296	9.118857	9.020781		
10	8.246261	8.452915	8.553611	8.742283	9.012454	9.247821	9.182778	8.455887			

Chl b, mg/g

	0.1	0.2	0.4	0.8	1.6	3.2	6.4	12.8	25.6	51.2	102.4
1	3.123077	3.096923	2.829231	2.442923077	2.747538	2.442923	2.348923	2.307692	2.207692	2.087692	2.04
2	3.610154	3.568923	3.323385	3.013076923	3.223077	3.013077	2.912769	2.497692	2.397692	2.277692	
3	4.263369	4.222138	3.9766	3.666292308	3.876292	3.666292	3.565985	3.150908	3.050908	2.930908	
4	4.994769	4.953538	4.708	4.397692308	4.607692	4.397692	4.297385	3.882308	3.782308		
5	5.094769	5.053538	4.808	4.497692308	4.707692	4.497692	4.397385	3.982308	3.882308		
6	5.144769	5.103538	4.858	4.547692308	4.757692	4.547692	4.447385	4.032308	3.932308		
7	5.337846	5.296615	4.951077	4.740769231	4.850769	4.740769	4.540462	4.253846	4.153846		
8	5.397846	5.356615	5.011077	4.800769231	4.910769	4.800769	4.600462	4.313846	4.213846		
9	5.417846	5.376615	5.031077	4.820769231	4.930769	4.820769	4.620462	4.333846	4.233846		
10	5.419846	5.378615	5.033077	4.822769231	4.932769	4.822769	4.622462	4.335846			

Chl a|b ratio

	0.1	0.2	0.4	0.8	1.6	3.2	6.4	12.8	25.6	51.2	102.4
1	1.516513	1.657426	1.916627	2.217980597	2.060295	2.34057	2.508672	2.582437	2.703866	2.691208	2.72614
2	1.667088	1.735092	1.923563	2.205056714	2.136695	2.47802	2.609042	3.072575	3.104972	3.16201	
3	1.685441	1.786814	2.011863	2.516132449	2.485606	2.687126	2.787938	3.259827	3.299613	3.323917	
4	2.06969	2.118611	2.272628	2.496741502	2.43148	2.613208	2.705097	2.9002	2.933315		
5	1.992582	2.039636	2.167744	2.380183289	2.347244	2.531393	2.575726	2.810484	2.832667		
6	1.955811	1.994862	2.116324	2.28144988	2.267087	2.394715	2.465362	2.669244	2.645634		
7	1.854523	1.898241	2.049581	2.198859597	2.20215	2.280374	2.291275	2.409297	2.385367		
8	1.765585	1.876978	2.005805	2.13054734	2.095333	2.182937	2.195432	2.04	2.217487		
9	1.638962	1.73584	1.892413	1.984187823	1.973912	1.960271	2.044881	2.104103	2.130635		
10	1.521494	1.571578	1.69948	1.812710281	1.827058	1.917533	1.986556	1.950228			

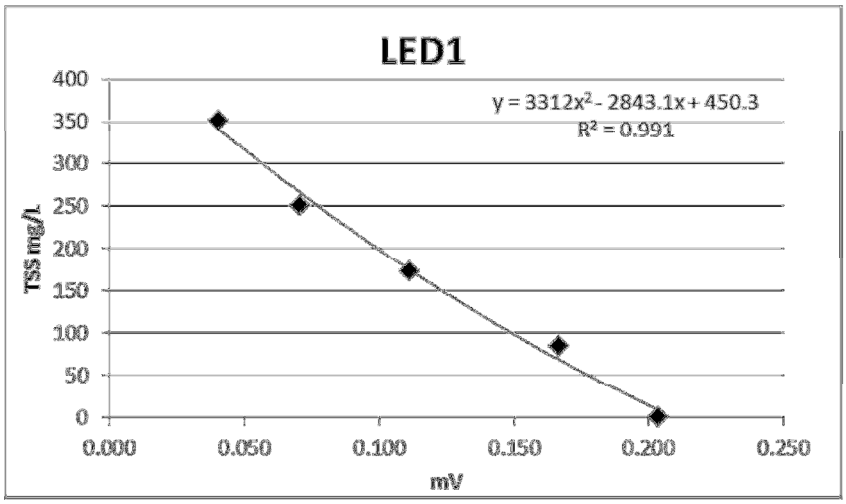
LED1
y = 3312x² - 2843.1x + 450.3
R² = 0.991
TSS mg/L
400
350
300
250
200
150
100
50
0
0.000
0.050
0.100
0.150
0.200
0.250
mV

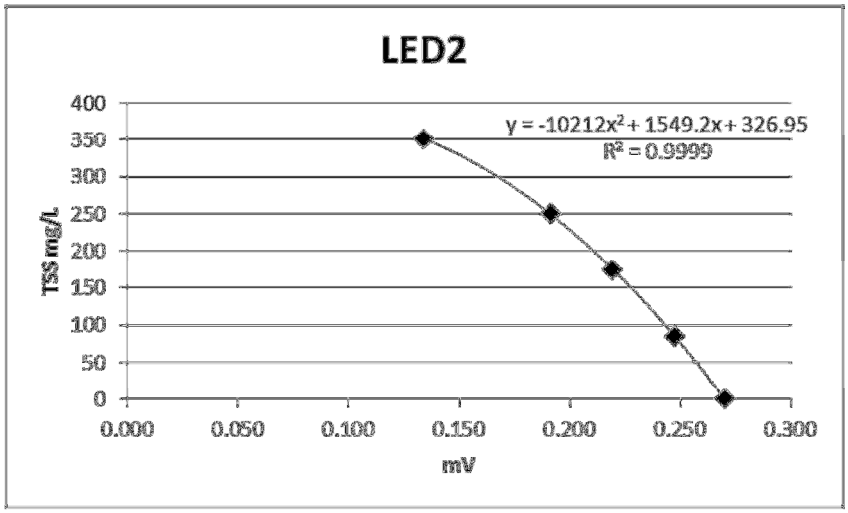
LED2
y = -10212x² + 1549.2x + 326.95
R² = 0.9999
TSS mg/L
400
350
300
250
200
150
100
50
0
0.000
0.050
0.100
0.150
0.200
0.250
0.300
mV

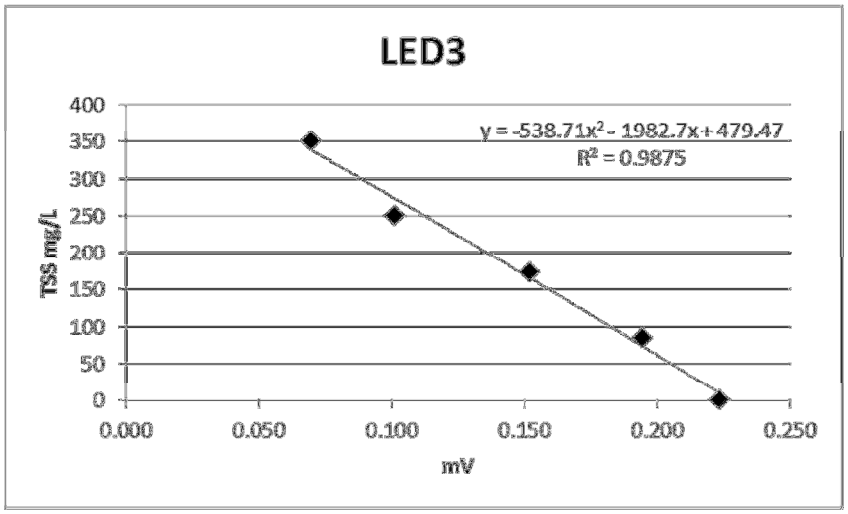
LED3
y = -538.71x² - 1982.7x + 479.47
R² = 0.9875
TSS mg/L
400
350
300
250
200
150
100
50
0
0.000
0.050
0.100
0.150
0.200
0.250
mV

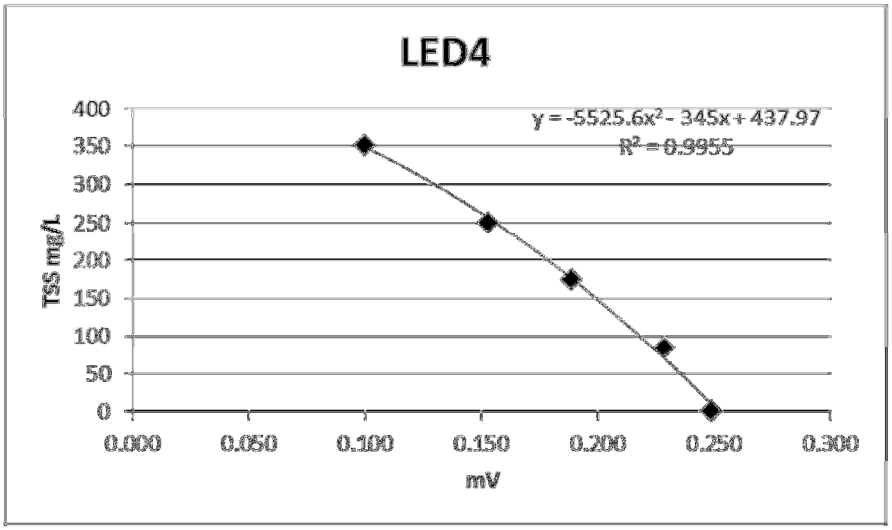
LED4
y = -5525.6x² - 345x + 437.97
R² = 0.9955
TSS mg/L
400
350
300
250
200
150
100
50
0
0.000
0.050
0.100
0.150
0.200
0.250
0.300
mV

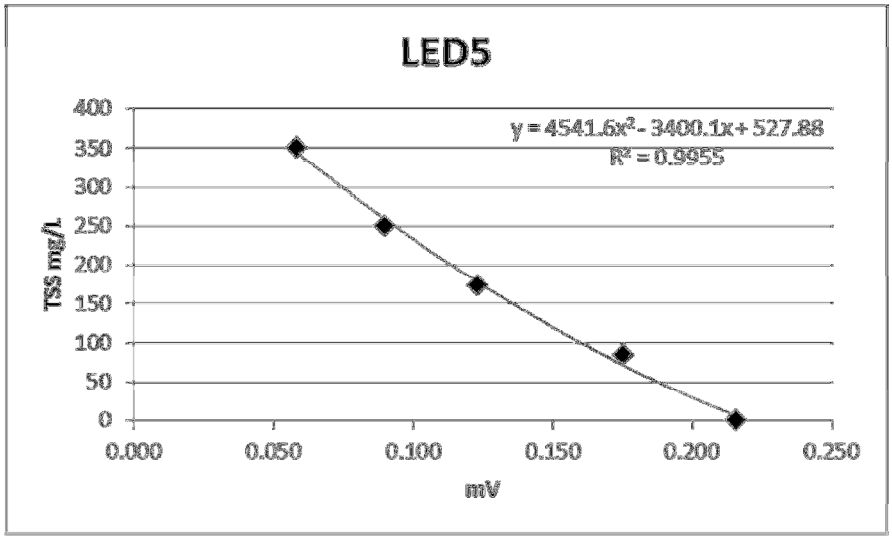
LED5
y = 4541.6x² - 3400.1x + 527.88
R² = 0.9955
TSS mg/L
400
350
300
250
200
150
100
50
0
0.000
0.050
0.100
0.150
0.200
0.250
mV

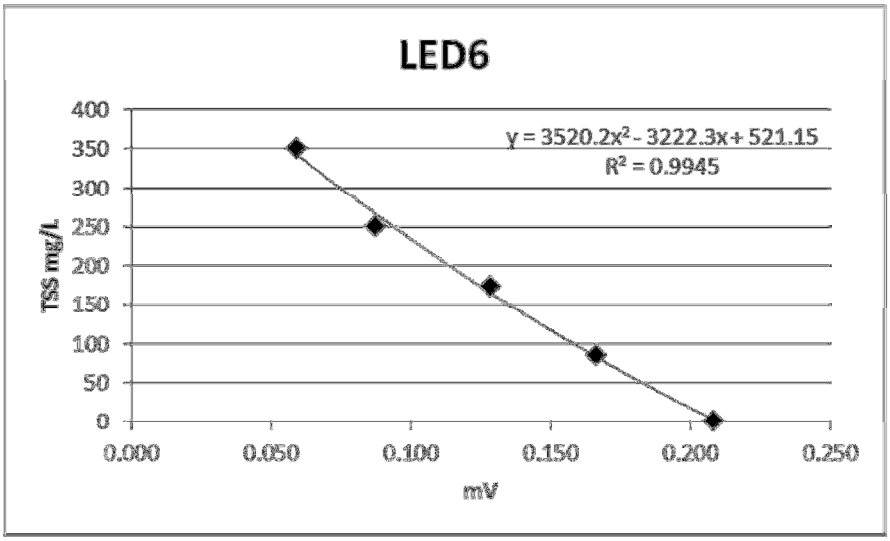
LED6
y = 3520.2x² - 3222.3x + 521.15
R² = 0.9945
TSS mg/L
400
350
300
250
200
150
100
50
0
0.000
0.050
0.100
0.150
0.200
0.250
mV

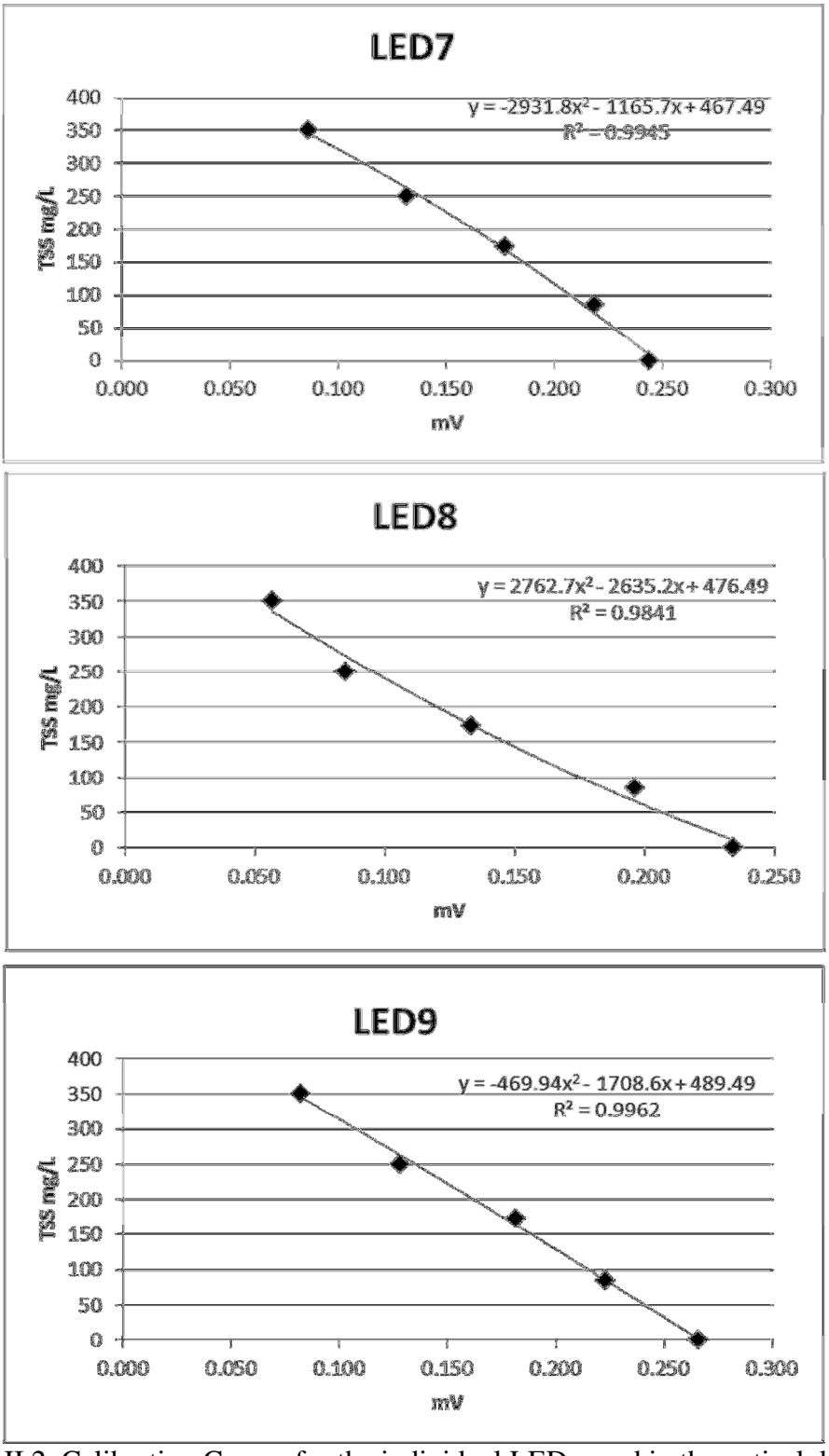

Figure II.2. Calibration Curves for the individual LEDs used in the optical devices.

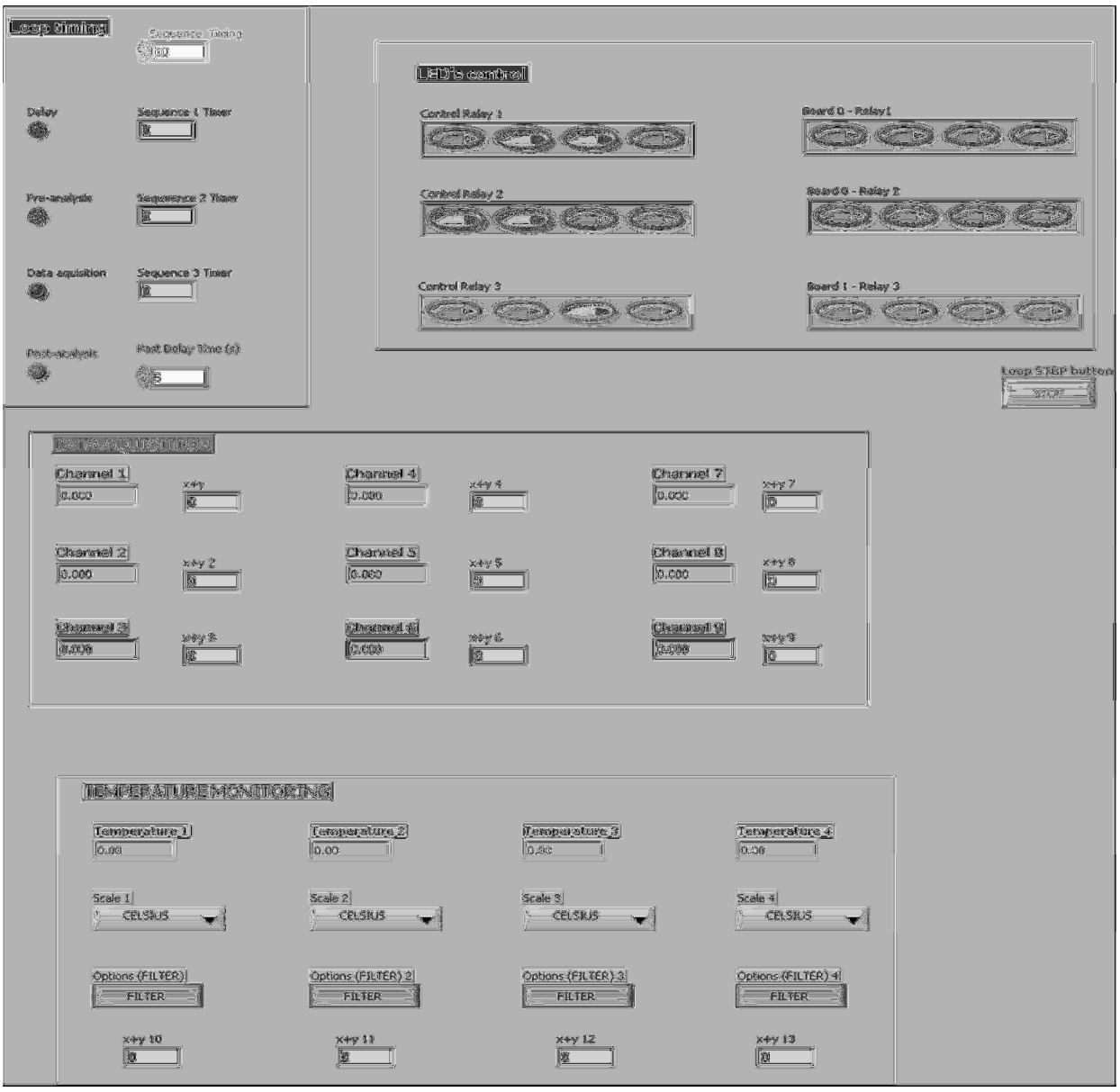

Figure. II.3. Immersible Device for Continuous Measurement of Biomass Concentration Data Control Panel

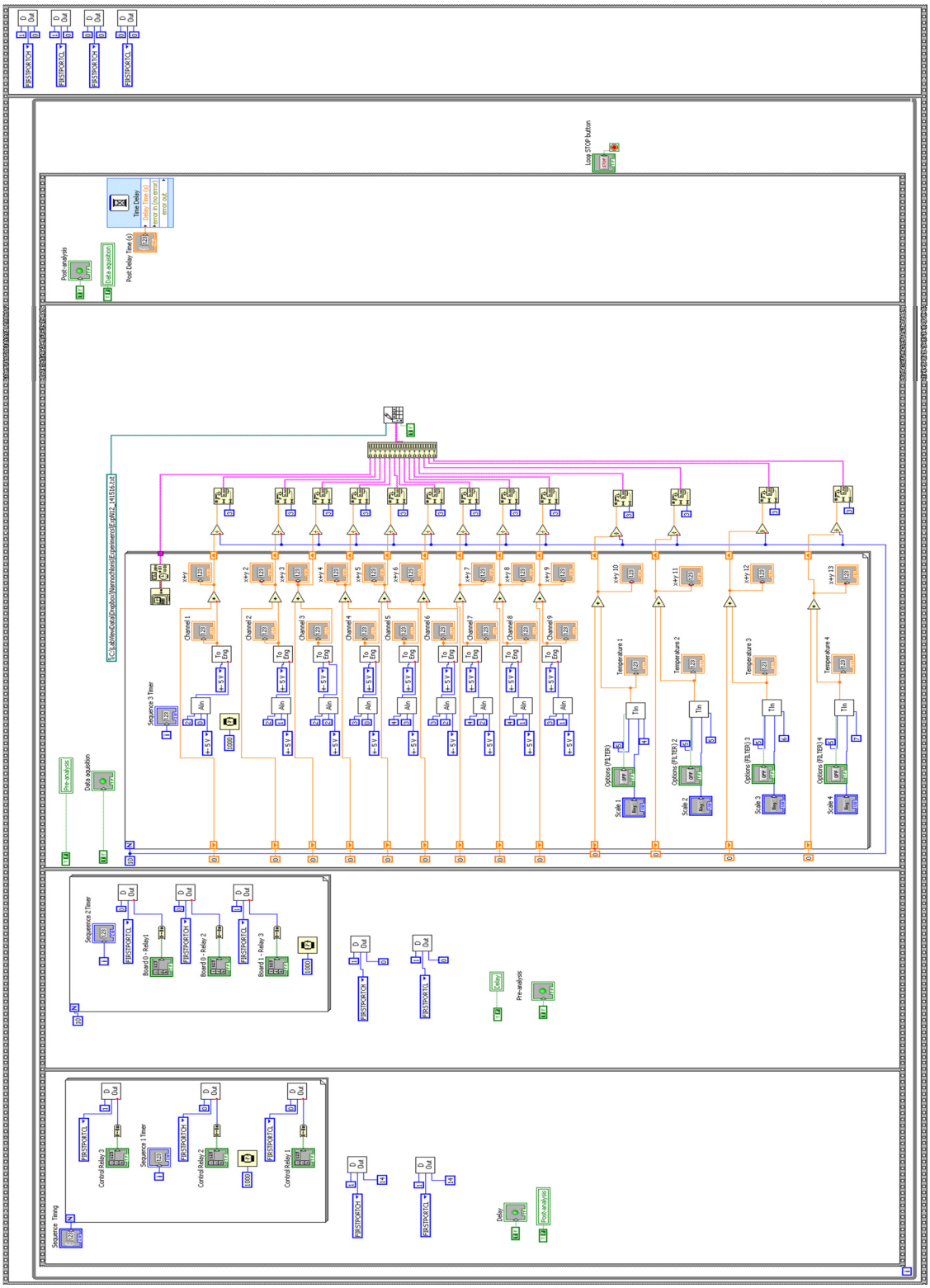

Figure II.4. Immersible Device for Continuous Measurement of Biomass Concentration Data; Block Diagram.

Figure. II.5. Pictures of the final set-up used for the indoor experiment. Front and back view of the final set-up.

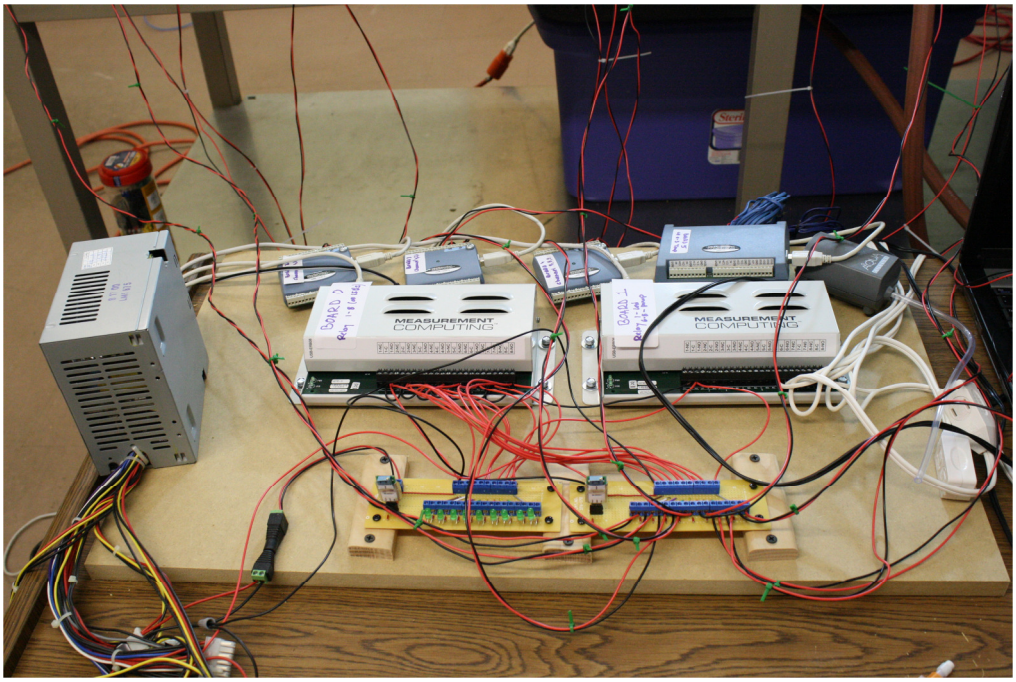

Figure. II.6. Electronics bench used to control the light, aeration pumps and immersible optical device.

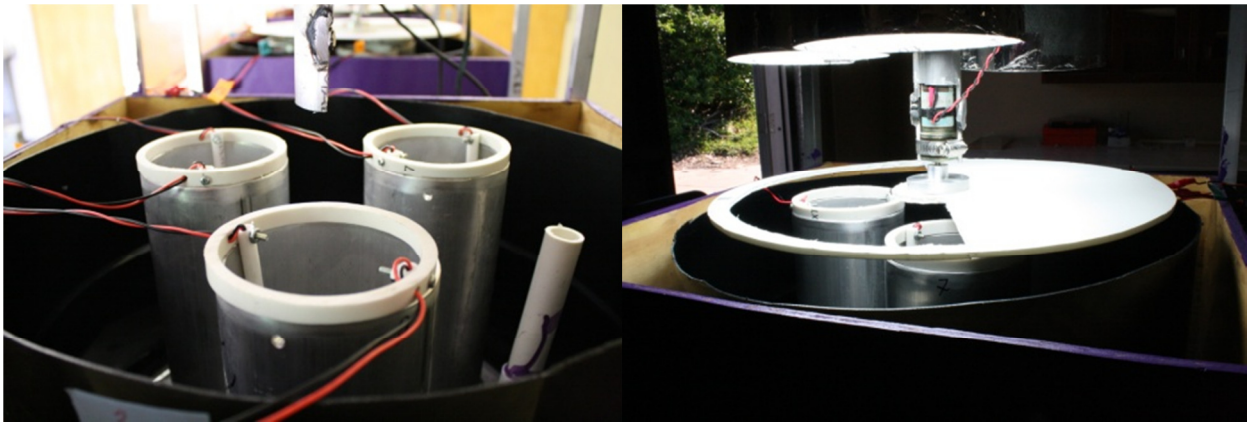

Figure II.7. Bioreactor set-up containing the immersible optical device (left), and rotating disk with lighting system (right).

Figure II.8. Pictures of the set-up used during outdoor experiments, before (top) and after (bottom) growth.

APPENDIX III: MODELING DATA

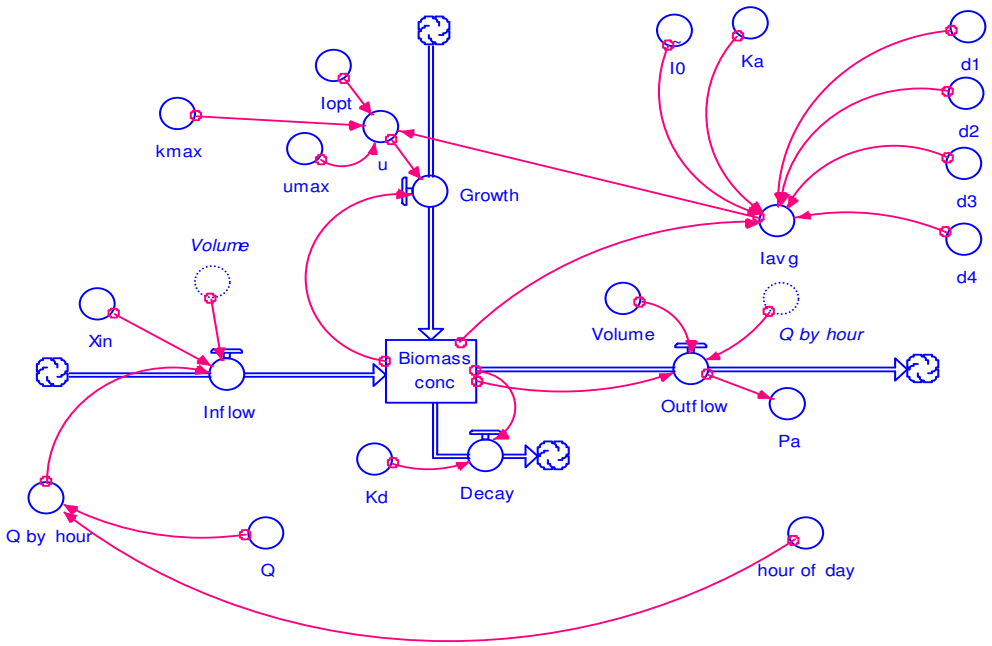

Figure III.1. Dynamic productivity model for *Selenastrum capricornutum* at 24, 18, 12 and 6 hr HRTs.

For the observed parameter model kmax=0 and kd is decay observed.
For the single parameter model kd=0 and kmax=0.025.

Stella equation output

Biomass_conc(t) = Biomass_conc(t - dt) + (Inflow + Growth - Outflow - Decay) * dtINIT
Biomass_conc = 11
UNITS: g/m^3

INFLOWS:
Inflow = (Q_by_hour*Xin)/Volume
UNITS: g/hr-m^3

Growth = Biomass_conc*u
UNITS: g/hr-m^3

OUTFLOWS:
Outflow = ((Biomass_conc*Q_by_hour)/Volume)
UNITS: g/hr-m^3

Decay = Biomass_conc*Kd
UNITS: g/hr-m^3

d1 = 7.6
UNITS: cm

d2 = 17.8
UNITS: cm

d3 = 28
UNITS: cm

d4 = 35.56
UNITS: cm

hour_of_day = (TIME/24-INT(TIME/24))*24

Iavg = ((((I0/(Ka*Biomass_conc*d1))-((I0*EXP(-
Ka*Biomass_conc*d1))/(Ka*Biomass_conc*d1)))+((I0/(Ka*Biomass_conc*d2))-((I0*EXP(-
Ka*Biomass_conc*d2))/(Ka*Biomass_conc*d2)))+((I0/(Ka*Biomass_conc*d3))-((I0*EXP(-
Ka*Biomass_conc*d3))/(Ka*Biomass_conc*d3)))+((I0/(Ka*Biomass_conc*d4))-((I0*EXP(-
Ka*Biomass_conc*d4))/(Ka*Biomass_conc*d4))))/4)
UNITS: umol/sec/m^2

Iopt = 1800
UNITS: umol/sec/m^2

Ka = 0.001113
UNITS: (m^3/g)/cm

Kd = 0
kmax = .025

Q = 0.0071
UNITS: m^3/hr

Q_by_hour = if hour_of_day>8-DT and hour_of_day<=20-dt then Q else 0
UNITS: m^3/hr

u = umax*((Iavg/Iopt)*EXP((-Iavg/Iopt)+1))-kmax*(Iopt-Iavg)/Iopt
UNITS: /day

umax = 0.24
UNITS: hr

Volume = 55/1000
UNITS: m^3

Xin = 0
UNITS: g/m^3

I0 = GRAPH(TIME)
(1.00, 0.00), (2.00, 0.00), (3.00, 0.00), (4.00, 0.00), (5.00, 0.00), (6.00, 0.00), (7.00, 80.0), (8.00, 596), (9.00, 1043), (10.0, 1421), (11.0, 1809), (12.0, 2110), (13.0, 2220), (14.0, 2150), (15.0, 1950), (16.0, 1700), (17.0, 1290), (18.0, 860), (19.0, 350), (20.0, 50.0), (21.0, 0.00), (22.0, 0.00), (23.0, 0.00), (24.0, 0.00), (25.0, 0.00), (26.0, 0.00), (27.0, 0.00), (28.0, 0.00), (29.0, 0.00), (30.0, 0.00), (31.0, 80.0), (32.0, 596), (33.0, 1045), (34.0, 1350), (35.0, 1730), (36.0, 2110), (37.0, 2220), (38.0, 2150), (39.0, 1950), (40.0, 1700), (41.0, 1290), (42.0, 860), (43.0, 350), (44.0, 50.0), (45.0, 0.00), (46.0, 0.00), (47.0, 0.00), (48.0, 0.00), (49.0, 0.00), (50.0, 0.00), (51.0, 0.00), (52.0, 0.00), (53.0, 0.00), (54.0, 0.00), (55.0, 80.0), (56.0, 596), (57.0, 1045), (58.0, 1350), (59.0, 1730), (60.0, 2110), (61.0, 2220), (62.0, 2150), (63.0, 1950), (64.0, 1700), (65.0, 1290), (66.0, 860), (67.0, 350), (68.0, 50.0), (69.0, 0.00), (70.0, 0.00), (71.0, 0.00), (72.0, 0.00), (73.0, 0.00), (74.0, 0.00), (75.0, 0.00), (76.0, 0.00), (77.0, 0.00), (78.0, 0.00), (79.0, 80.0), (80.0, 596), (81.0, 1045), (82.0, 1350), (83.0, 1730), (84.0, 2110), (85.0, 2220), (86.0, 2150), (87.0, 1950), (88.0, 1700), (89.0, 1290), (90.0, 860), (91.0, 350), (92.0, 50.0), (93.0, 0.00), (94.0, 0.00), (95.0, 0.00), (96.0, 0.00), (97.0, 0.00), (98.0, 0.00), (99.0, 0.00), (100, 0.00), (101, 0.00), (102, 0.00), (103, 80.0), (104, 596), (105, 1045), (106, 1350), (107, 1730), (108, 2110), (109, 2220), (110, 2150), (111, 1950), (112, 1700), (113, 1290), (114, 860), (115, 350), (116, 50.0), (117, 0.00), (118, 0.00), (119, 0.00), (120, 0.00), (121, 0.00), (122, 0.00), (123, 0.00), (124, 0.00), (125, 0.00), (126, 0.00), (127, 80.0), (128, 596), (129, 1045), (130, 1350), (131, 1730), (132, 2110), (133, 2220), (134, 2150), (135, 1950), (136, 1700), (137, 1290), (138, 860), (139, 350), (140, 50.0), (141, 0.00), (142, 0.00), (143, 0.00), (144, 0.00), (145, 0.00), (146, 0.00), (147, 0.00), (148, 0.00), (149, 0.00), (150, 0.00), (151, 80.0), (152, 596), (153, 1045), (154, 1350), (155, 1730), (156, 2110), (157, 2220), (158, 2150), (159, 1950), (160, 1700), (161, 1290), (162, 860), (163, 350), (164, 50.0), (165, 0.00), (166, 0.00), (167, 0.00), (168, 0.00), (169, 0.00), (170, 0.00), (171, 0.00), (172, 0.00), (173, 0.00), (174, 0.00), (175, 80.0), (176, 596), (177, 1045), (178, 1350), (179, 1730), (180, 2110), (181, 2220), (182, 2150), (183, 1950), (184, 1700), (185, 1290), (186, 860), (187, 350), (188, 50.0), (189, 0.00), (190, 0.00), (191, 0.00), (192, 0.00), (193, 0.00), (194, 0.00), (195, 0.00), (196, 0.00), (197, 0.00), (198, 0.00), (199, 80.0), (200, 596), (201, 1045), (202, 1350), (203, 1730), (204, 2110), (205, 2220), (206, 2150), (207, 1950), (208, 1700), (209, 1290), (210, 860), (211, 350), (212, 50.0), (213, 0.00), (214, 0.00), (215, 0.00), (216, 0.00), (217, 0.00), (218, 0.00), (219, 0.00), (220, 0.00), (221, 0.00), (222, 0.00), (223, 80.0), (224, 596), (225, 1045), (226, 1350), (227, 1730), (228, 2110), (229, 2220), (230, 2150), (231, 1950), (232, 1700), (233, 1290), (234, 860), (235, 350), (236, 50.0), (237, 0.00), (238, 0.00), (239, 0.00), (240, 0.00), (241, 0.00), (242, 0.00), (243, 0.00), (244, 0.00), (245, 0.00), (246, 0.00), (247, 80.0), (248, 596), (249, 1045), (250, 1350), (251, 1730), (252, 2110), (253, 2220), (254, 2150), (255, 1950), (256, 1700), (257, 1290), (258, 860), (259, 350), (260, 50.0), (261, 0.00), (262, 0.00), (263, 0.00), (264, 0.00), (265, 0.00), (266, 0.00), (267, 0.00), (268, 0.00), (269, 0.00), (270, 0.00), (271, 80.0), (272, 596), (273, 1045), (274, 1350), (275, 1730), (276, 2110), (277, 2220), (278, 2150),

(279, 1950), (280, 1700), (281, 1290), (282, 860), (283, 350), (284, 50.0), (285, 0.00), (286, 0.00), (287, 0.00), (288, 0.00), (289, 0.00), (290, 0.00), (291, 0.00), (292, 0.00), (293, 0.00), (294, 0.00), (295, 80.0), (296, 596), (297, 1045), (298, 1350), (299, 1730), (300, 2110), (301, 2220), (302, 2150), (303, 1950), (304, 1700), (305, 1290), (306, 860), (307, 350), (308, 50.0), (309, 0.00), (310, 0.00), (311, 0.00), (312, 0.00), (313, 0.00), (314, 0.00), (315, 0.00), (316, 0.00), (317, 0.00), (318, 0.00), (319, 80.0), (320, 596), (321, 1045), (322, 1350), (323, 1730), (324, 2110), (325, 2220), (326, 2150), (327, 1950), (328, 1700), (329, 1290), (330, 860), (331, 350), (332, 50.0), (333, 0.00), (334, 0.00), (335, 0.00), (336, 0.00), (337, 0.00), (338, 0.00), (339, 0.00), (340, 0.00), (341, 0.00), (342, 0.00), (343, 80.0), (344, 596), (345, 1045), (346, 1350), (347, 1730), (348, 2110), (349, 2220), (350, 2150), (351, 1950), (352, 1700), (353, 1290), (354, 860), (355, 350), (356, 50.0), (357, 0.00), (358, 0.00), (359, 0.00), (360, 0.00), (361, 0.00), (362, 0.00), (363, 0.00), (364, 0.00), (365, 0.00), (366, 0.00), (367, 80.0), (368, 596), (369, 1045), (370, 1350), (371, 1730), (372, 2110), (373, 2220), (374, 2150), (375, 1950), (376, 1700), (377, 1290), (378, 860), (379, 350), (380, 50.0), (381, 0.00), (382, 0.00), (383, 0.00), (384, 0.00), (385, 0.00), (386, 0.00), (387, 0.00), (388, 0.00), (389, 0.00), (390, 0.00), (391, 80.0), (392, 596), (393, 1045), (394, 1350), (395, 1730), (396, 2110), (397, 2220), (398, 2150), (399, 1950), (400, 1700), (401, 1290), (402, 860), (403, 350), (404, 50.0), (405, 0.00), (406, 0.00), (407, 0.00), (408, 0.00), (409, 0.00), (410, 0.00), (411, 0.00), (412, 0.00), (413, 0.00), (414, 0.00), (415, 80.0), (416, 596), (417, 1045), (418, 1350), (419, 1730), (420, 2110), (421, 2220), (422, 2150), (423, 1950), (424, 1700), (425, 1290), (426, 860), (427, 350), (428, 50.0), (429, 0.00), (430, 0.00), (431, 0.00), (432, 0.00), (433, 0.00), (434, 0.00), (435, 0.00), (436, 0.00), (437, 0.00), (438, 0.00), (439, 80.0), (440, 596), (441, 1045), (442, 1350), (443, 1730), (444, 2110), (445, 2220), (446, 2150), (447, 1950), (448, 1700), (449, 1290), (450, 860), (451, 350), (452, 50.0), (453, 0.00), (454, 0.00), (455, 0.00), (456, 0.00), (457, 0.00), (458, 0.00), (459, 0.00), (460, 0.00), (461, 0.00), (462, 0.00), (463, 80.0), (464, 596), (465, 1045), (466, 1350), (467, 1730), (468, 2110), (469, 2220), (470, 2150), (471, 1950), (472, 1700), (473, 1290), (474, 860), (475, 350), (476, 50.0), (477, 0.00), (478, 0.00), (479, 0.00), (480, 0.00)
UNITS: umol/sec/m^2

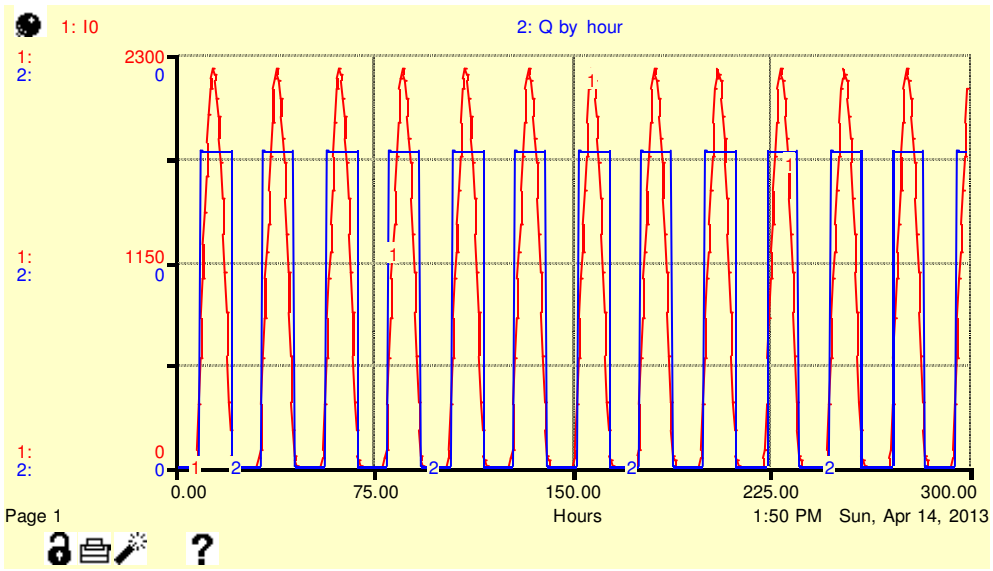

Figure III.2. Surface intensity and flow rate during the night and day period.

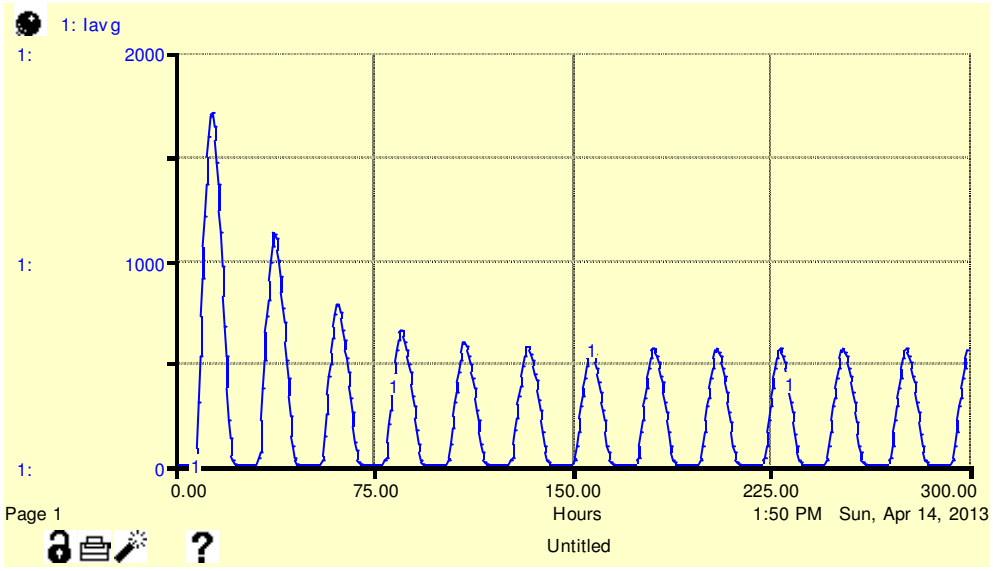

Figure III.3. Average intensity during the night and day period vs time..

VITA

Beatrice Gabriela Terigar was born in Arad, Romania, in 1984. She received her Bachelor of Science degree in Food Engineering Control and Food Expertise in June 2007 from Aurel Vlaicu University of Arad, Romania. Beatrice began a master's program in Fall 2007 in Biological and Agricultural Engineering at Louisiana State University with a concentration in microwave oil extraction and biodiesel production. She further attended LSU after her M.S. graduation to pursue Doctor of Philosophy degree in the Engineering Science Department.